A PARAMETRIC STUDY AIMED AT ASSESSING FATIGUE PERFORMANCE OF BOLTED CONNECTIONS

By

Cheng Chen

Submitted to the graduate degree program in Civil, Architectural, and Environmental Engineering and the Graduate Faculty of the University of Kansas in partial fulfillment of the requirements for the degree of Master of Science.

Committee members: ________________________________
Chairperson Dr. Caroline Bennett

____
Dr. Adolfo Matamoros

____
Dr. Jian Li

____
Dr. William Collins

____
Dr. Matthew Fadden

Date Defended: June 9, 2016

The Thesis Committee for Cheng Chen

certifies that this is the approved Version of the following thesis:

A PARAMETRIC STUDY AIMED AT ASSESSING FATIGUE PERFORMANCE OF BOLTED CONNECTIONS

Committee members: ______________________________

Chairperson Dr. Caroline Bennett

____

Dr. Adolfo Matamoros

____

Dr. Jian Li

____

Dr. William Collins

____

Dr. Matthew Fadden

Date approved: ____________________

Acknowledgements

I would like to express my sincere thanks to Drs. Caroline Bennett and Adolfo Matamoros for their constant guidance and encouragement, without which this work would not have been possible. In addition, I would like to thank Drs. Jian Li, William Collins, and Matthew Fadden for their support towards the successful completion of my studies at KU. Thanks also go to my fellow graduate students, especially to Danqing Yu, James Zhou and Xiangxiong Kong.

Finally, I would like to thank my parents and my husband for their continuous support and encouragement.

Table of Contents

LIST OF FIGURES

List of Tables

APPENDIX A LIST OF CURRENT SPECIFICATIONS

APPENDIX B: TEST MATRIX

APPENDIX C COMPLETED MODELS

APPENDIX D STRESS DISTRIBUTIONS

APPENDIX E COMPARISON OF STRESS DISTRIBUTIONS OF EDGE DISTANCES AND BOLT SPACING

APPENDIX F CHANG IN STRESS VS. VARIABLES

Appendix G SPSS Output

A PARAMETRIC STUDY AIMED AT ASSESSING FATIGUE PERFORMANCE OF BOLTED CONNECTIONS

ABSTRACT

The fatigue design provisions in the AASHTO-LRFD Bridge Design Specifications (2012) state that steel components with open holes should be classified as Fatigue Category D details, while bolted connections with pretensioned bolts are Category B details. The two-category difference in fatigue performance between holes with and without bolts is based on experimental evidence which showed that compressive stresses imposed by pretensioned bolts in the region around the bolt holes reduce the effective net tensile stresses. Fatigue category classification is based solely on the presence or absence of pretensioned bolts, without consideration to the influence of connection geometry, including bolt spacing and plate thickness.

A numerical study was undertaken to determine the fatigue performance of connections with pretensioned bolts and various geometric configurations. Approximately 150 high-resolution finite element models were analyzed using the finite element software Abaqus 6.13-3. Models consisted of single steel plates with unfilled bolt holes and connections with pretensioned bolts. The parameters of the study were bolt diameter, bolt spacing, plate thickness, bolt pattern, edge distance, and ratio of nominal stress to pretensioned bolt load.

The effect of these parameters on fatigue initiation life was evaluated by comparing calculated stress fields of bolted and unbolted plates. The change in stress ($\Delta\sigma_{local}$) between the two configurations was used as a means to estimate the level of improvement in terms of AASHTO fatigue categories. A linear regression analysis was performed to investigate the sensitivity of the change in stress to the parameters of the study. It was found that the plate thickness was the dominant parameter, and that the change in stress decreased with increasing plate thickness. Results from this investigation suggest that there is a size effect associated with the thickness of plate that should be considered in the AASHTO fatigue category classification for bolted connections.

Background

High Strength Bolted Connections

There are two types of high-strength bolted connections: bearing-type and slip-critical. Bearing-type connections are installed using bolts installed to the snug-tight condition, such that loads are transferred through the bolts bearing against the connected elements. Once a load is applied to a plate in a bearing-type connection, it will slip until the plies contact the bolt shanks. The load in a slip-critical connection is transferred through friction between the connected parts. The pretensioned bolt in a slip-critical connection applies a clamping force between the connected parts. In slip-critical joints, since no slip occurs, the bolt shanks should not move relative to the bolt holes when loading is applied. This research was focused on slip-critical bolted connections.

Current Specifications

According to the Research Council on Structural Connections Specifications (RCSC 2014), bolt pretension is required in pretensioned and slip-critical joints. The American Institute of Steel Construction (AISC 2011) Steel Construction Manual 14th Edition requires that bolt tension in pretensioned or slip-critical joints should not be less than the value listed in Table J3.1 in the AISC Specification (AISC 2011). It is the same as presented in RCSC Specifications (RCSC 2014) Table 8.1 and in the 6th Edition of the American Association of State Highway and Transportation Officials LRFD 2012 Bridge Design Specifications (AASHTO 2012). For slip-critical joints, the slip coefficient, μ, for Class A surfaces is 0.3 (RCSC 2014) and the minimum edge distance for joints is listed in Appendix A, which is in RCSC Section 5.4.

The 2014 RCSC Specification requires that the minimum bolt spacing (center to center) should be not less than the three times the bolt diameter. Table 3.1 in the 2014 RCSC Specification shows the hole dimensions for high-strength bolts. The minimum allowable thickness of structural steel provided by AASHTO (2012) is 3/16 in.

Fatigue Categorization of Bolted Connections

Fatigue categories for load-induced fatigue are provided in AASHTO Specifications (2012). "Base metal at the gross section of high-strength bolted joints designed as slip-critical connections with pretensioned high-strength bolts installed in holes drilled full size or sub punched and reamed to size" is assigned as Category B. However, no specific limitations on plate thickness or other connection variables are described. A detail that includes "open holes in members" is assigned Category D. An illustrative example of each category is presented in Appendix A of this thesis. Based on this, AASHTO (2012) implies that a two-category increase in fatigue performance of plate with drilled holes can be achieved by adding pretensioned bolts. For this reason, it is important to quantify the influence of geometric variables on the effectiveness of pretensioned on fatigue performance of the connected parts. Hence, the influence of plate thickness and other variables were investigated in this project.

PROBLEM STATEMENT AND OBJECTIVE

From Category D to Category B, the improvement of fatigue category is based solely on the pretensioned bolts, without consideration to the influence of connection geometry. The objective of this study was to investigate the fatigue performance of steel connections with pretensioned bolts by changing geometric variables (plate thickness, bolt diameter, edge distance, bolt spacing and bolt pattern) and compare the relative importance of variables. This study was also focused on answering the following questions:

- How to compare between models to determine the effect of addition of pretensioned bolt(s) on change in fatigue performance? And where was the right place to look at stresses to make that comparison?
- How can existing results from the literature which are experimentally derived be used?
- How to put the analytical results in the contest of the AASHTO S-N diagrams?

LITERATURE REVIEW

Brown et al. (2006) performed a series of tests conducted on steel specimens with punched and drilled holes. 118 of tension tests were conducted to determine the influence of punched holes on fatigue life. The recommendation from Brown et al. (2007) that "members with open holes should be classified as Category D" was adopted by AASHTO (2010). However, a few results from fatigue tests of slip-critical connection with drilled holes were also conducted to investigate the influence of geometric variables on the fatigue performance. The fatigue performance of unbolted plates are highlighted in Figure 1, showing that the nine tests (with drilled hole) fell above the AASHTO Category D curve.

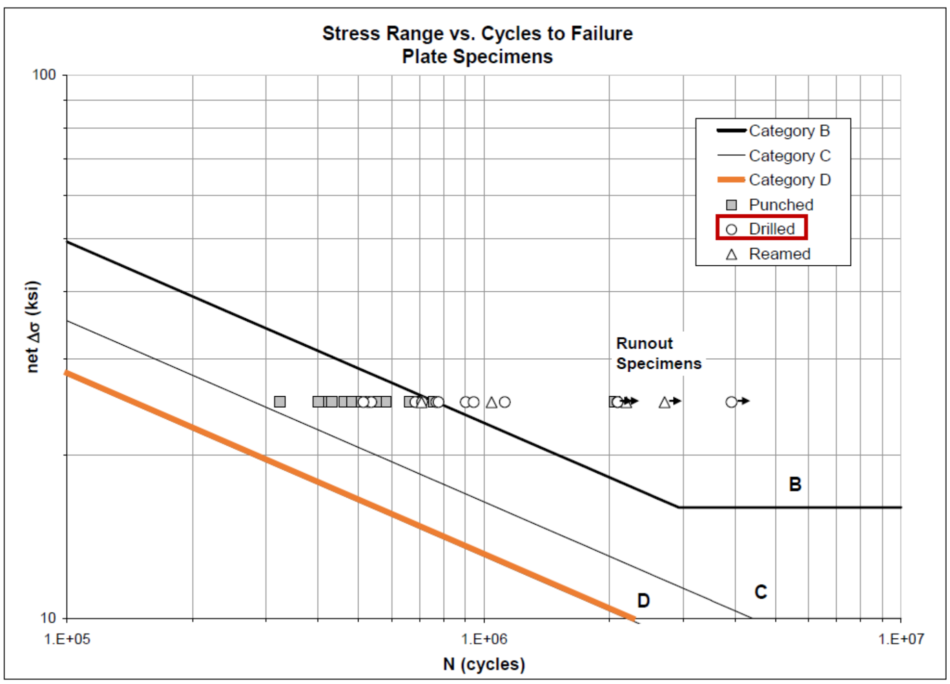

Figure 1: Unbolted plate fatigue test results (Brown et al. 2006)

Two tests quantified the fatigue performance of connections with pretensioned bolts in drilled holes, showing that these connections performed above Category B. The data is shown in Figure 2. Conclusions reported in Brown et al. (2006) included that the slip-critical connections met the Fatigue Category B critia regardless the hole type.

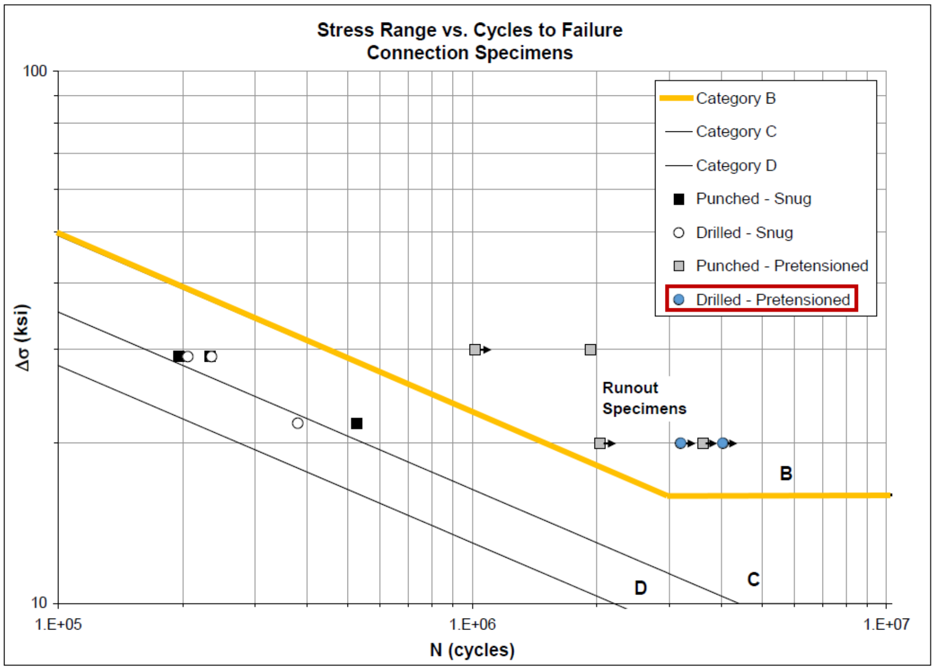

Figure 2: Bolted plate fatigue test results (Brown et al. 2006)

Frank et al. (1981) performed a study which was focused on the behavior of bolted shear connection with coated contact surfaces. In this study, five fatigue tests were conducted on 3/8 in. thick bolted plates (slip-critical) with no paint on the faying surface. All five specimens performed above Category B, however, no examination on the effect of geometric variables was made from Frank et al. (1981).

A study was performed by Bennett et al. (2007) in which a series of fatigue tests were conducted on high-performance steel (HPS) regarding on the influence of specimen thickness, hole diameter, and hole fabrication method. In the HPS fatigue tests, Bennett et al. (2007) concluded that "A trend exists which suggests that fatigue resistance increases with increasing diameter to thickness ratio." While the study was conducted on the high-performance steel, a point of interest is the influence of geometric variables on the bolted plates.

Research was performed by Georg et al. (2004) for bearing-type connections with staggered holes. Georg et al. (2004) concluded that a slight effect on fatigue life while changing geometric parameters, such as edge distance. However, the study did not appear to include slip-critical connections.

FINITE ELEMENT ANALYSIS METHOD

NOMINAL STRESS METHOD

The AASHTO Specification (2012) relies on a nominal stress approach for fatigue analysis. The approach taken by AASHTO relies on a large database of empirical evidence from physical tests, presenting the number of cycles to failure on S-N diagram organized by fatigue categories. The AASHTO nominal stress approach to fatigue design is direct, and does not require advanced analysis for most connections. However, there is little guidance for translating results from an FE analysis to the AASHTO S-N diagrams.

HOT SPOT STRESS

The nominal stress approach has clear limitations, including difficulty defining nominal stress in a complex welded structures (Kim and Kang 2008) and a lack of consideration of localized geometry of the specimens (Poutiainen et al. 2004). Another method that takes localized geometry into account is the structural hot spot stress approach (HSS). This method is widely used in welded structures to extract realistic values for stress from a finite element model that includes high stress gradients in regions of geometric discontinuity. However, the HSS technique was developed and validated specifically for welded connections, and it is unlikely that it is valid for bolted connections.

The local stress approach is a Finite Element Analysis method also used to analyze welded structures. As mentioned, the nominal stress method relies on nominal stress used in the context of an S-N curve, where it ignores the variation of structural dimensions. In the Standard Specifications for Structural Supports for Highway Signs, Luminaires, and Traffic Signals 2013, Appendix D, a numerical approach was introduced based on local stress for welded structures. This methodology established a location to extract maximum (tensile) principle stress from finite element model with linear elastic material. The location of the extracting stress is on the surface at $0.1\sqrt{(r \times t)}$ ahead of weld toe. The number of cycles $\boldsymbol{N}$ for fatigue life is obtained from the Equation 1, where N is number of cycles for fatigue life and $(\Delta F)_l$ is the local stress:

$$(\Delta \boldsymbol{F})_l = (\frac{\mathbf{44 \times 10^8}}{\boldsymbol{N}})^{\frac{1}{3}} \times \boldsymbol{ksi} \qquad \textbf{Equation 1}$$

STRUCTURAL STRESS APPROACH AND MASTER S-N CURVE

The structural stress approach is another technique that was developed for welded structure finite element analysis. The Master S-N curve was first reported by Dong and has since been adopted by ASME (ASME, 2007) and API A579 (API 2007). The Master S-N curve was developed from physical fatigue tests performed on welded structures. In Figure 3, the horizontal axis is the number of cycles on a logarithmic scale and the vertical axis is the equivalent structural stress range converted from welded structure fatigue tests. The structural stress (σ_s) is defined as the sum of the membrane stress (σ_m) and the bending stress (σ_b) at a structural discontinuity, where the membrane and bending components were extracted from finite element models. Studies (Marin et al. 2009, Selvakumar et al. 2013), have shown that the structural stress approach and Master S-N curve were well-matched to physical fatigue tests. A case study was reported by Selvakumar et al. (2013) that investigated the accuracy of this method compared with actual fatigue test results. The conclusion was:

- "This method can adequately capture the failure location and provide a good life prediction for welded components regardless of their joint geometry, loading mode, and plate thickness. Further, the structural stress method can simplify fatigue analysis procedures for welded components and significantly reduce testing requirements."

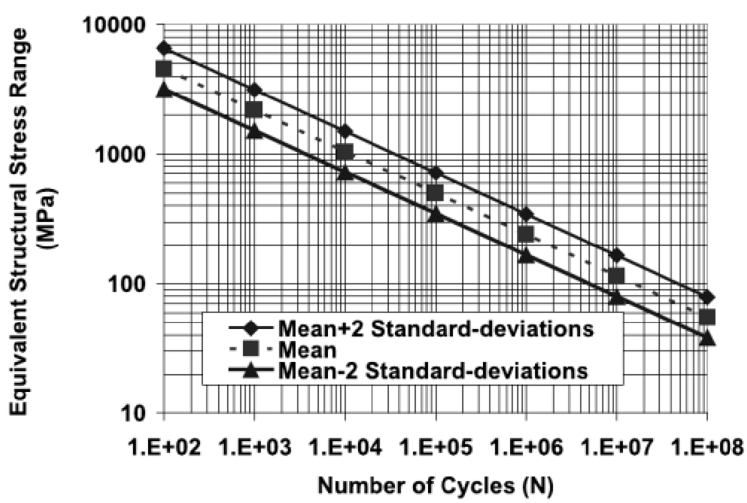

Figure 3: Master S-N curve (Dong et al. 2005)

MODELING METHODOLOGY

Every specimen was modeled using the commercially-available finite element software Abaqus 6.13-3 (Simulia 2013). Two types of models were created: Figure 4(a) shows single plates with unfilled bolt holes (Unbolted Plates) and Figure 4(b) plates in connections that included pretensioned bolts (Bolted Plates).

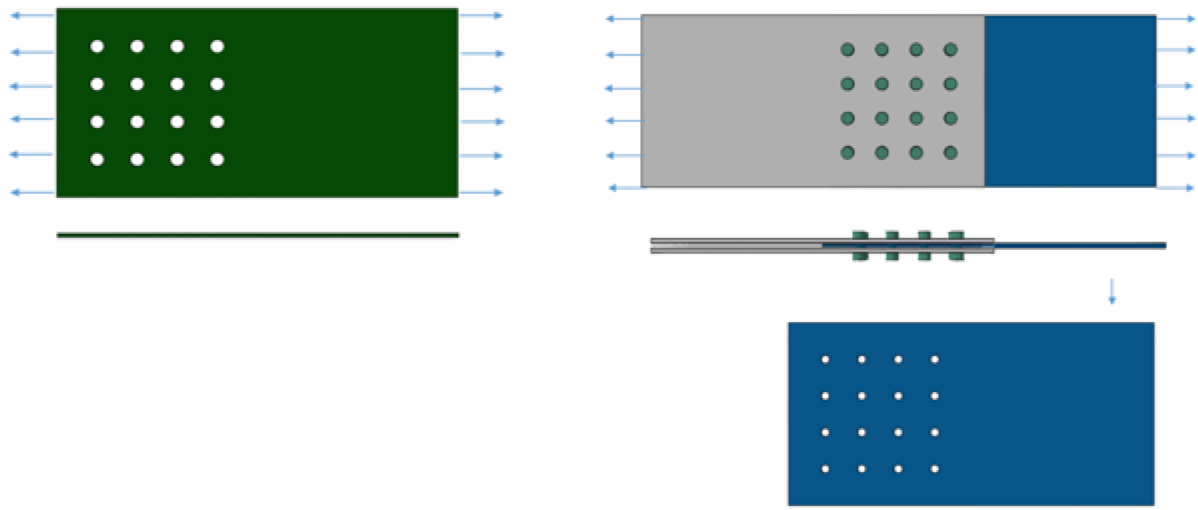

(a)Unbolted Plate (b)Bolted Plate

Figure 4: Unbolted and Bolted Plates

PARAMETERS CONSIDERED

Five parameters were considered: bolt pattern, plate thickness ***t***, bolt diameter ***d***, edge distance ***e***, and bolt spacing ***s***. Table 1 lists the selected values for each parameter, which are also described in more detail in Figure 5.

Table 1: Parameter considered

Parameters	
Bolt Pattern	4×4 Rectangular, 3×3 Rectangular, 5-bolt staggered
Plate Thickness ***t*** mm [in.]	6.4[1/4], 12.7 [1/2], 25.4[1]
Bolt Diameter ***d*** mm [in]	15.9[5/8], 25.4[1]
Edge Distance ***e*** mm [in.]	50.8[2], 76.2[3]
Bolt Spacing ***s*** mm [in.]	50.8[2], 76.2[3]

The model matrix is shown in Appendix B, with a total number of 144 models included in this study. 72 models were plates without bolts, while 72 models were three plate lap splice connections with the same dimensions as for the plates without bolts, but with pretensioned bolts.

MATERIAL PROPERTIES

All the models included linear-elastic material. The Young's Modulus was 29,000 ksi and the Poisson's Ratio was defined to be 0.3. Since Abaqus does not carry units, to keep the simulations consistent, the geometry unit was "inch", the unit of stress was "ksi" and the unit for force was "kip" during modeling process.

GEOMETRY

There were three types of connection geometries included in the study: 4 x 4 rectangular (Figure 5a), 3 x 3 rectangular (Figure 5b) and 5 bolt-staggered (Figure 5c), respectively. The parameters of plate thickness, ***t***, edge distance, ***e***, bolt spacing, ***s***, and bolt diameter, ***d***, are shown in Figure 5. The parameters forced variations in the height and length of the models such that the minimum and maximum heights were 8 in. and 15 in., respectively. The minimum and maximum lengths were 16 in. and 30 in., respectively.

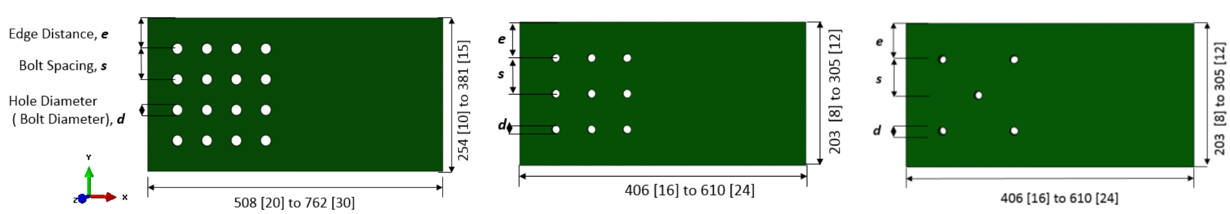

(a) 4 x 4 rectangular (b) 3 x 3 rectangular (c) 5 bolt-staggered

Figure 5: Model Geometry (mm [in.])

BOUNDARY CONDITIONS

To save model running time, the boundary conditions were restricted at both ends of models. For the unbolted plates, the end with holes was restricted by a center point through-thickness in both the y and z directions; the other end was restricted by a center point through-thickness in the x, y and z directions. For the bolted plates, the end with one plate was restricted by a center point through-thickness in the x, y and z directions; the other end with two plates were restricted by two points on both plates through thickness in the y and z directions. For all the models, the load was applied in the x direction.

A tensile stress was applied to both ends of the plate. The magnitude of tensile stress was 25 ksi based on gross area.

According to the AISC Steel Construction Manual prescription for minimum bolt pretension for Group A bolts, bolt loads were modeled as 202 ksi (62 kip) for the bolts with 5/8 in. bolt diameter, and 82 ksi (65 kip) for the bolts with 1 in. bolt diameter.

MESH

A mesh sensitivity analysis was performed, and the results are shown in Figure 6. A 1/4 in. thick plate was used to test mesh sensitivity. The horizontal axis represents mesh size, and the mesh sizes used in this sensitivity analysis were 1/64 in., 1/32 in., 1/16 in., 1/8 in., and 1/4 in., respectively. Values on the vertical axis represent the maximum principal stress extracted from the red point that shows in Figure 6. From the curve, the stresses were found to be sensitive to mesh density. Mesh sizes of 1/64 in. and 1/32 in. showed similar maximum principal stress. However, for computational efficiency, 1/16 in was chosen as the mesh size for all models in the matrix.

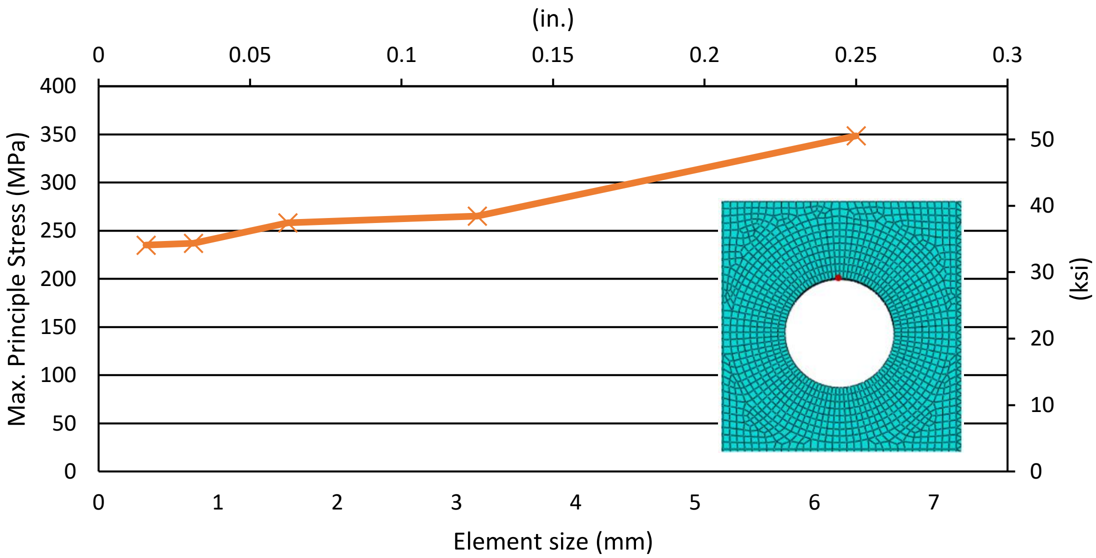

Figure 6: Mesh Sensitivity

MESH TRANSITION

Since the focus of the study was on stresses directly around the holes, smaller mesh size was used in those regions. Thus, larger element sizes were used in regions away from holes. To accommodate the mesh difference, a mesh transition zone was developed. About 3 in. away from the last zone of the holes, a transition zone was developed. Wedge element shapes were used to translate small elements to large elements through longitudinal and transverse directions, respectively. The translation zone translated the mesh sizes from 1/16 in. to 3/10 in. and kept the mesh remaining cubic.

Figure 7 shows details of the partition and mesh. Elements shown as green were hex-elements in a structured mesh; elements shown as yellow were hex elements in a swept mesh.

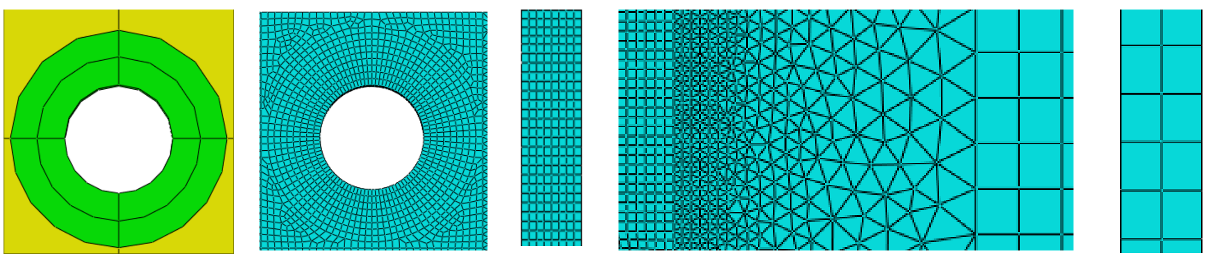

(a) (b) (c) (d) (e)

Figure 7: Mesh detail (a)**Partition around hole** (b)**Mesh around hole** (c)**Mesh through thickness around hole** (d) **Element size translated from 1/16 in to 3/10 in** (e) **Mesh through thickness after transition zone**

INTERACTIONS BETWEEN MODEL PARTS

Interactions were defined between the bolt head and plate, as well as between plates in models that included bolts. To make the contact accurately, all pairs were found automatically using the command Find Contact Pairs. Interaction between bolt heads and plate was accomplished using tie constraints, and plate-plate interaction was defined by tangential behavior with a 0.35 friction coefficient. Since bolt diameters were less than the hole diameters by 1/16 in., there was no contact between bolts and inside of the holes.

Model Steps

There were two steps for single plate (unbolted plate) models and three steps for connection (bolted plates) models because bolt loads must be applied in Step-1. Except for the Initial Step, other steps were in automatic incrementation type with that maximum number of increments: (10,000). The increment size was taken as 0.1 with a minimum of 1E-20 and a maximum: 1.

Results

One hundred and twenty one models were completed successfully, the completed models is listed in Appendix C. The investigated models were unbolted and bolted plates that had the same geometry. The number of investigated models for 4 x 4 rectangular, 3 x 3 rectangular and 5-bolt staggered bolt patterns were 32, 38 and 28, respectively. Stresses were extracted from FE models using a path oriented perpendicular to the direction of the applied load (Figure 8b). The location from which maximum principle stress were extracted in each model was at the hole, where the hole was in the first row and the last column in the bolt pattern (Figure 8a).

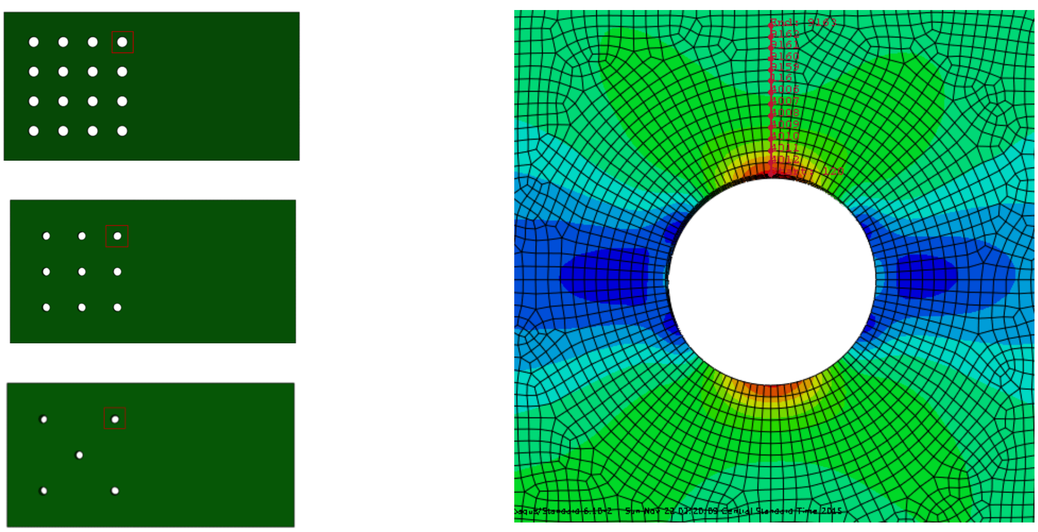

(a) (b)

Figure 8: (a) Location of holes (b) Stress path

Stress data extracted from the models in this way were examined in different manners. First, local stresses, σ_{local}, (maximum principal stresses directly extracted from the model) were considered.

Changes in local stress between models with and without pretensioned bolts ($\Delta\sigma_{local}$) were also considered as an indicator of connection stress demand.

The following topics will be discussed briefly:

- Local stresses (σ_{local}) versus model parameters
- Change in local stresses between models with and without pretensioned bolts ($\Delta\sigma_{local}$) versus model parameters
- Statistical consideration of the model parameters

LOCAL STRESS VERSUS MODEL PARAMETERS

Figure 9 shows an example of the stress distribution along the path that was perpendicular to the load direction. The title of each figure represents the values of variables (in US Customary units): *t* represents plate thickness, *d* represents bolt diameter, *e* represents edge distance, *s* represents bolt spacing, α represents the stress ratio of nominal stress against the pretensioned bolt load, and the last parameter is bolt pattern. For example, *1/4t_5/8d_3e_3s_0.15α_3x3* represents a plate or connection with 1/4 in. plate thickness, 5/8 in. bolt diameter, 3 in. edge distance, 3 in. bolt spacing, a ratio of 0.15 for the nominal stress against the pretensioned bolt load, and 3x3 bolt pattern.

The objective of this investigation was to examine the influence of variables on the state of stress bolted plates with reference to the state of stress in an unbolted plate. Hence, the comparison was focused on the overall stress distributions and the distributions of $\Delta\sigma_{local}$. Figure 9 shows the stress distributions for 1/4 in., 1/2 in., and 1 in. thick plates, respectively. In Figure 9, the yellow and dark blue lines represent stresses extracted from mid-thickness and at the surface, respectively, for plates with bolt holes but no bolts. The orange and blue lines represent stresses extracted from the bolted plates at mid-thickness and at the surface, respectively. The green and gray dashed lines represent the difference ($\Delta\sigma_{local}$) in local stresses between the unbolted plate and the bolted plates at mid-thickness and surface, respectively.

Results showed that $\Delta\sigma_{local}$ varied from 34 ksi to -6 ksi for the 1/4 in. thick plate, from 28 ksi to 0 ksi for the 1/2 in. thick plate, and from 12 ksi to 4 ksi for the 1 in. thick plate. Therefore, from the 1/4 in. thick plate to the 1 in. thick plate, a 80% decrease in amplitude of $\Delta\sigma_{local}$ was observed.

Comparing the yellow and dark blue lines in three graphs, local stress distributions in unbolted plates with different thicknesses showed only slight differences. However, the stress distributions in bolted plates with different thicknesses varied significantly (orange and blue lines in Figure 9). A comparison of stress distributions for the 1 in. thick unbolted and bolted plates showed that the stresses were more similar than for stress distributions between unbolted and bolted plates for both 1/4 in. and 1/2 in. plate thicknesses. Appendix D includes results for all model variations included in the study.

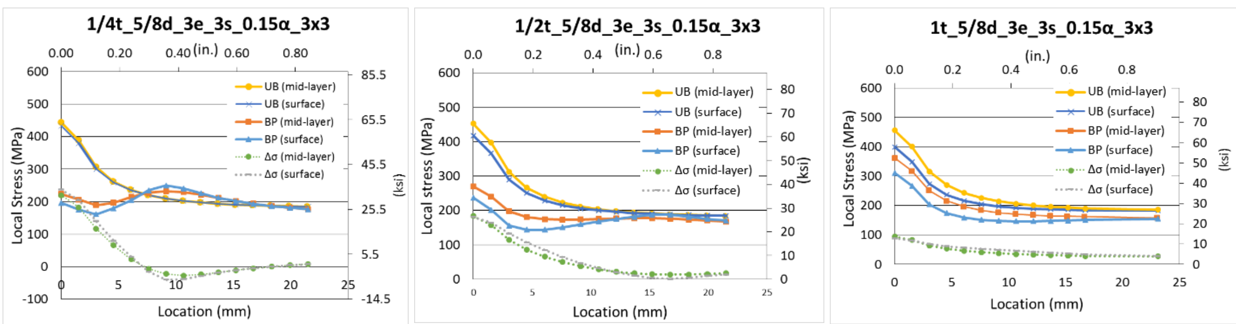

(a) (b) (c)

Figure 9: Comparison of stress distribution with different thicknesses

Figure 10 shows a comparison between stress distributions for plates with 5/8 in. and 1 in. bolt diameters. In Figure 10 (a), (b) and (c) the stress distributions of plates with 1/4 in., 1/2 in., and 1 in. plate thicknesses and 5/8 in. bolt diameter are shown. Figure 10 (d), (e), (f) shows the stress distributions of 1 in. bolt diameter plates with 1/4 in., 1/2 in. and 1 in. plate thicknesses, respectively. Each column in Figure 10 shows a comparison between bolt diameters on plates with the same thickness. In other words, a comparison of data for 1/4 in. thick plates (Figure 10a and Figure 10d) shows that $\Delta\sigma_{local}$ varied from 36 ksi to -8 ksi for 5/8 in. bolt diameters and 52 ksi to 4 ksi for 1 in. bolt diameters. For 1/2 in. thick plates (Figure 10b and Figure 10e), $\Delta\sigma_{local}$ varied from 26 ksi to 0 ksi for 5/8 in. bolt diameter and 30 ksi to 4 ksi for the 1 in. bolt diameter. For 1 in. thick plates (Figure 10c and Figure 10f) $\Delta\sigma_{local}$ varied from 12 ksi to 4 ksi for the 5/8 in. bolt diameter and 12 ksi to 4 ksi for the 1 in. bolt diameter plates. Therefore, from 5/8 in. bolt diameter to 1 in. bolt diameter, less than 10% increase in amplitude of $\Delta\sigma_{local}$ was observed. The stress distributions had slightly changed.

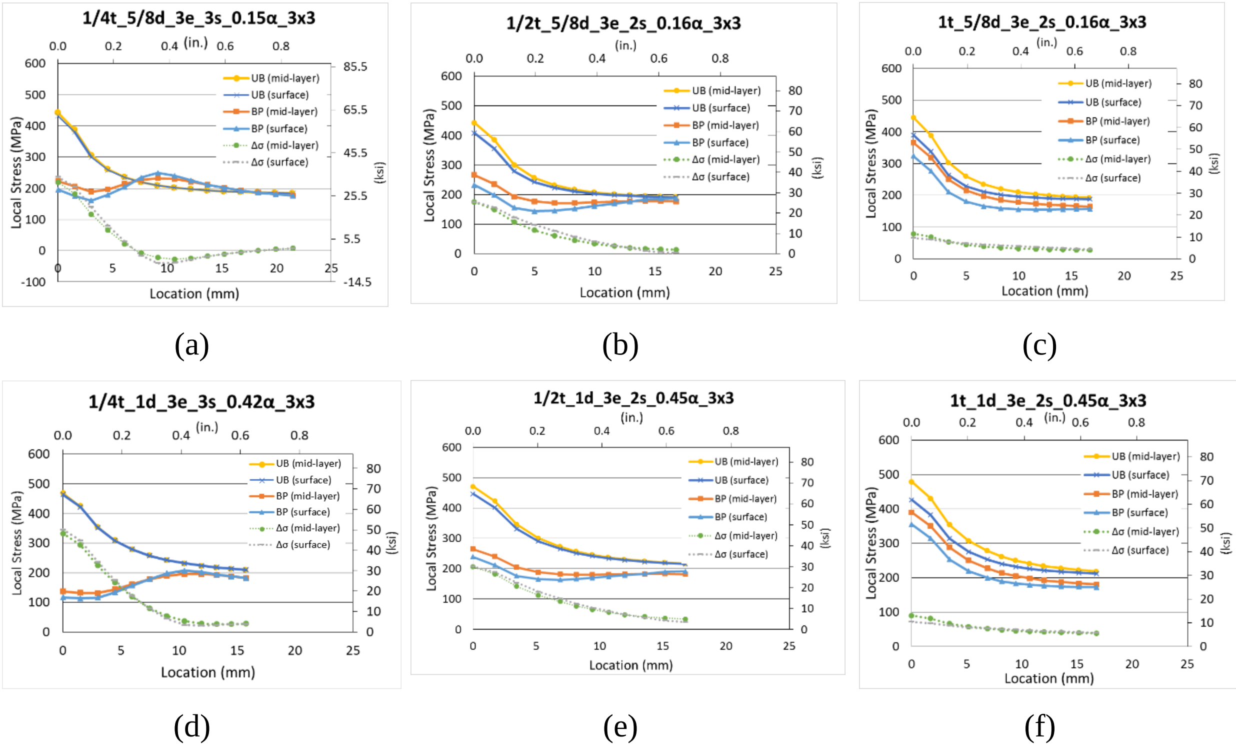

Figure 10: Comparison of stress distributions with different bolt diameters

Comparing the stress distributions and $\Delta\sigma_{local}$ magnitudes for different edge distance and bolt spacing, it is apparent that these two parameters have little effect on the stress distributions. A further comparison of edge distance and bolt spacing is presented in Appendix E. The FE results for unbolted plates indicated that edge distance and hole size had little influence on fatigue life. This is consistent with the conclusions that Brown et al. 2006 made regarding unbolted plates, however, work done by Brown et al. (2006) included only limited examination on the effect of geometric variables on bolted connections.

BOLT LOAD STRESS PATTERNS

Stresses induced in the bolted plates from the pretensioned bolts are shown in Figure 11, which presents cross-section views of connections made up of ¼ in. thick plates, ½ in. thick plates, and 1 in. thick plates. The minimum principal stresses show the compressive stresses that occurred in the bolted plates from the bolt clamping forces. It is apparent that as plate thickness increased, compressive stresses imparted in the steel plates decreased in the center plate.

The plots shown in Figure 12 represent minimum principal stress extracted along a path from edge to edge of the middle plate at the surface.

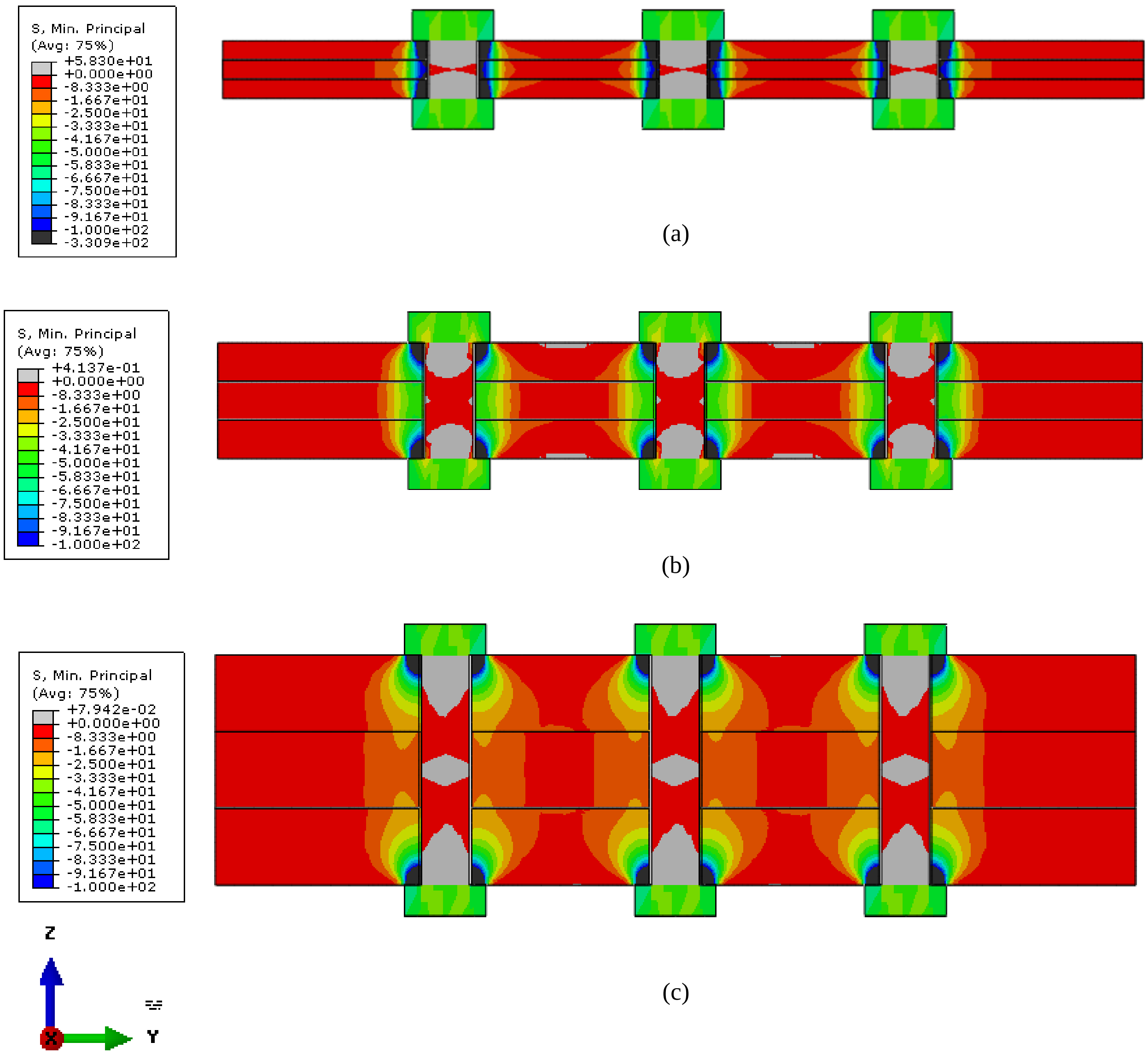

Figure 11: Cross sections of bolted plates, all shown with 5/8 in. diameter bolts: (a) cross section of 1/4 in. thick plate; (b) cross section of 1/2 in. thick plate; (c) cross section of 1 in. thick plate

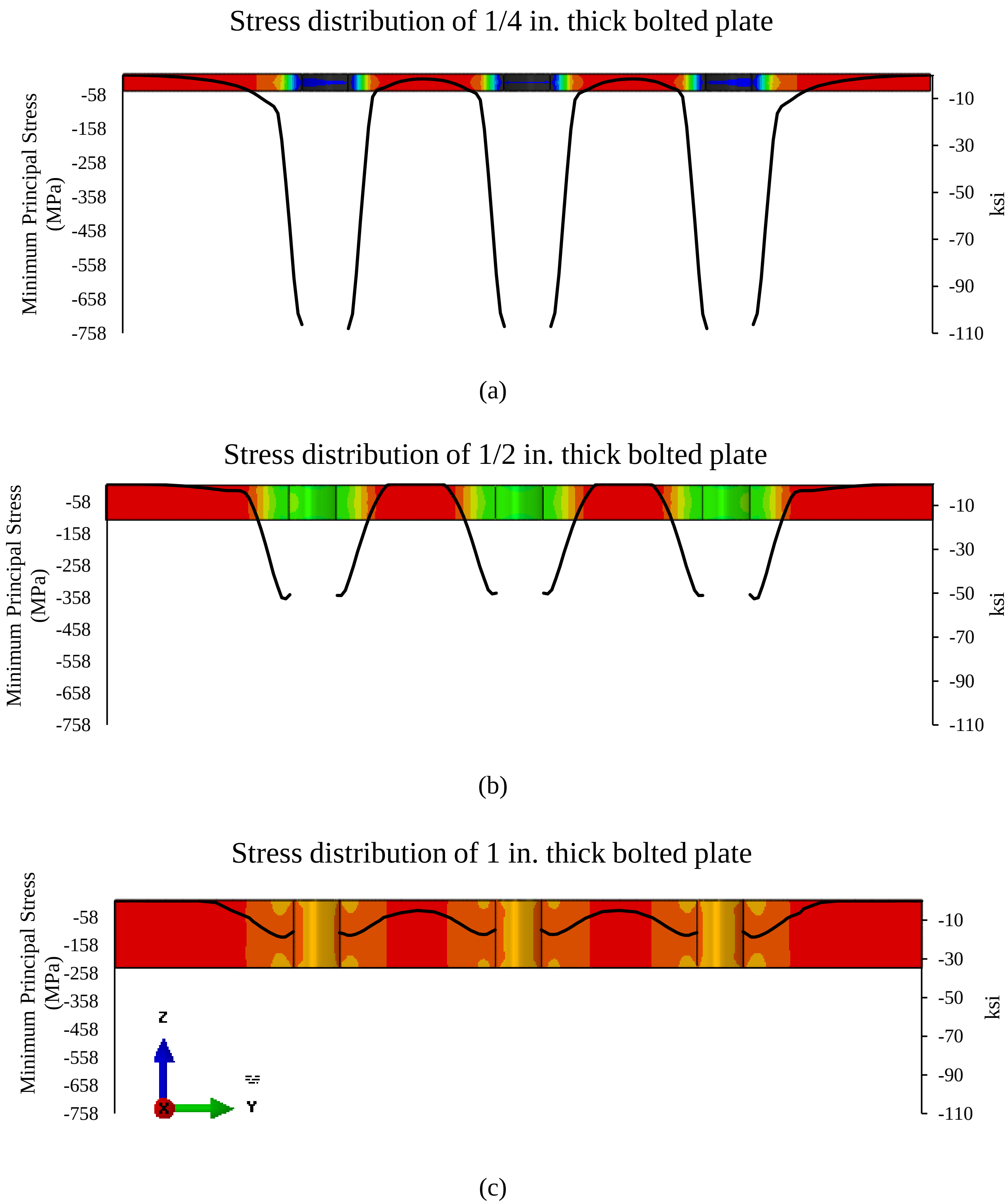

Figure 12 : Stress distributions of bottled center plates: (a) 1/4 in thick bolted center plate; (b) 1/2 in thick bolted plate; (c) 1 in. thick bolted center plate

PRESENTING DATA IN AN S-N DIAGRAM

As discussed, there is little guidance for translating results from a finite element analysis to the AASHTO S-N diagram, which is based on empirical evidence that includes realistic geometric effects and residual stresses. To account for the fatigue performance based on the local stress in the context of AASHTO fatigue design, the following procedure was developed and followed. First, in the y-direction of the unbolted plate model, locate the point from the hole edge to where the nominal stress occurred (nominal stress was computed based on net cross-sectional area), as shown in Figure 13.

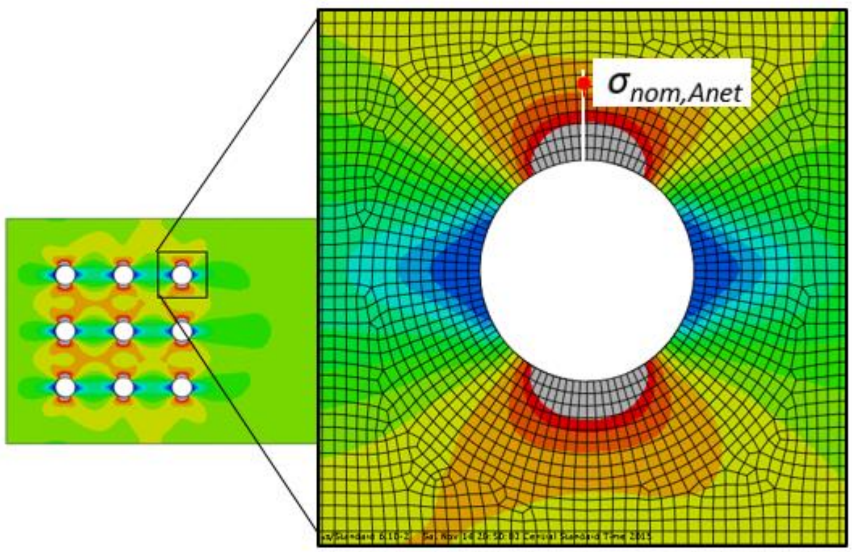

Figure 13: Location of stress in unbolted model

Next, in the bolted plate model, local stress was extracted at the same element as identified in the unbolted plate models (Figure 13), as shown in Figure 14.

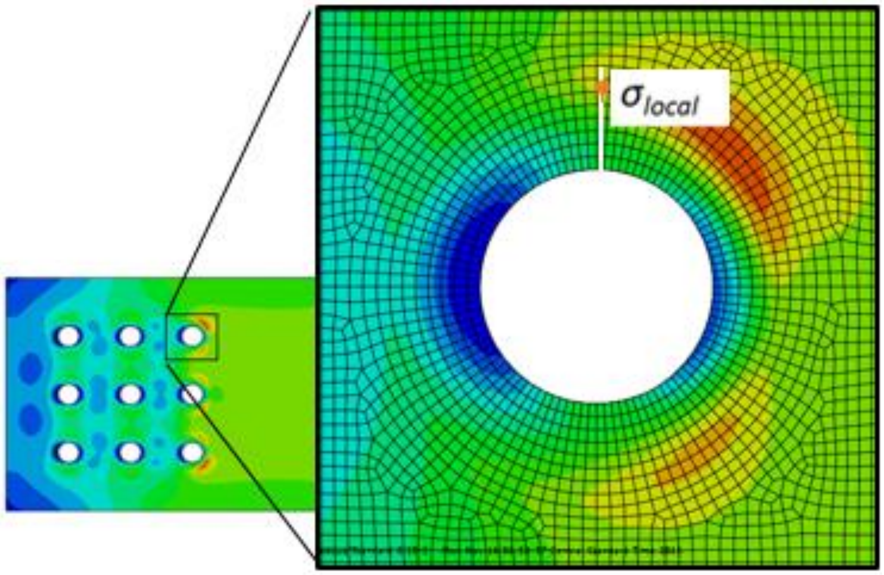

Figure 14: Location of stress in bolted model

The difference ($\Delta\sigma_{local}$) between the nominal stress (from unbolted plates) and local stress (from the bolted plate) was used to quantify the *change* in fatigue category performance in the finite-life portion of the S-N diagram. As mentioned in the background section, the unbolted plate has Fatigue Cateogy D detail. In this approach, the data point representative of the unbolted plate was plotted on the S-N diagram based on the nominal stress (based on net area) and the AASHTO fatigue Category D curve, as shown in Figure 15.

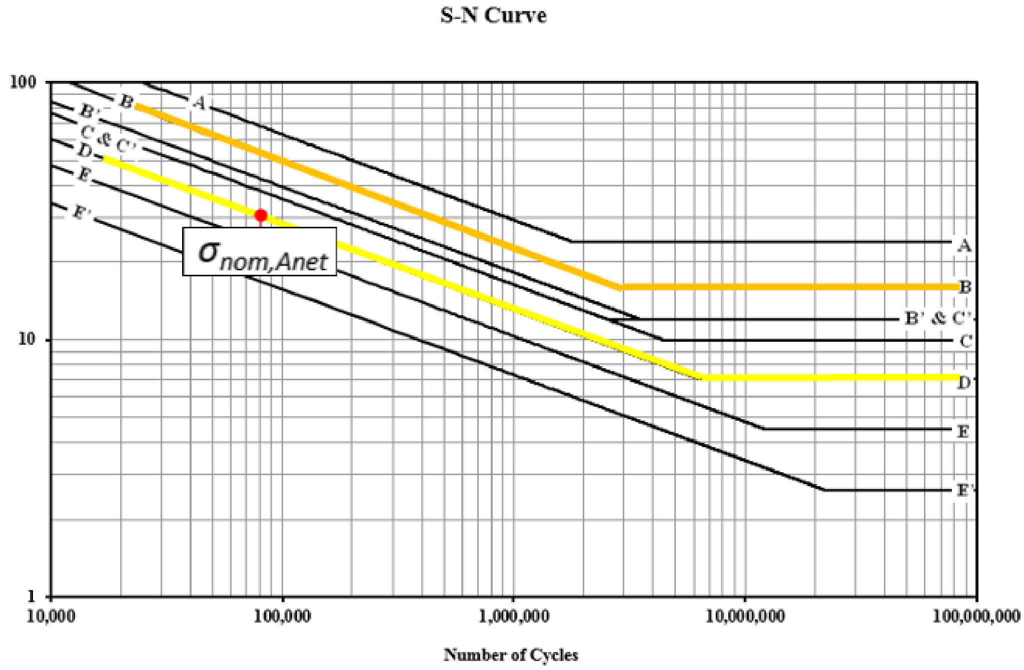

Figure 15: The Category D data point for unbolted plate

The location of bolted plate was defined by moving the point of unbolted plate vertically by the magnitude of $\Delta\sigma_{local}$, as shown in Figure 16.

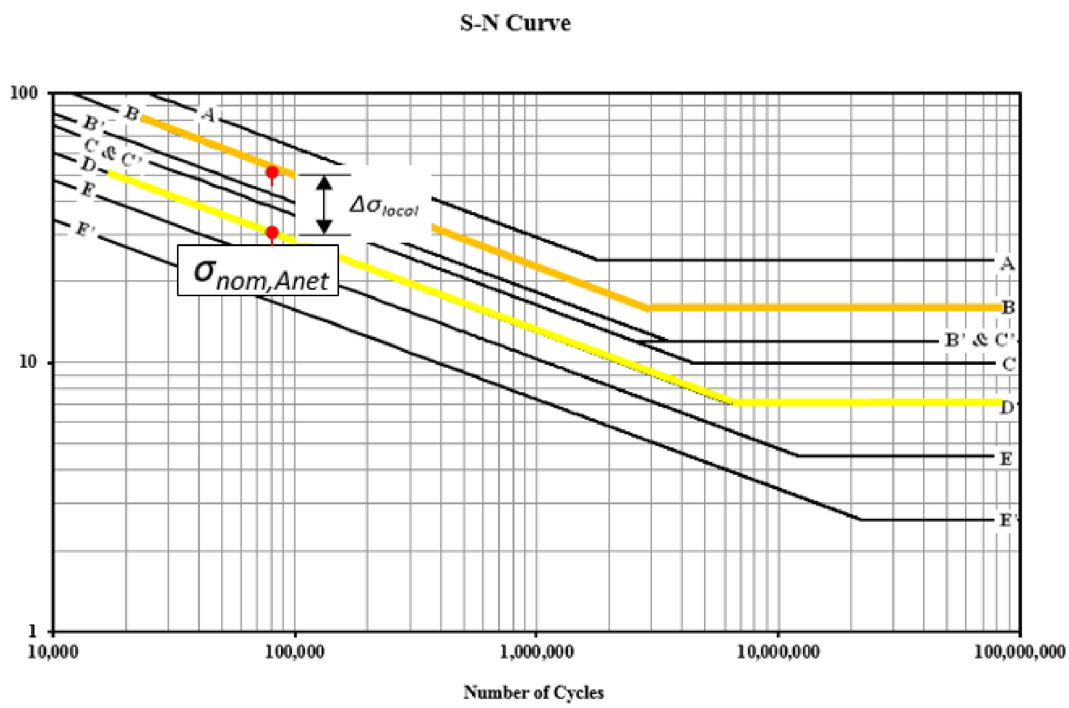

Figure 16: The new data point for the bolted plate

It is noted that this approach should be expected to be sensitive to the location of stress extraction, and only one location of stress extraction has been presented here. It is hoped that this procedure provides a methodology that can be used later in a rigorous investigation examining the effects of distance from the hole edge on use of this procedure.

The following example is presented to show how this procedure may be applied. Again, it is emphasized that this example only utilized stresses extracted from one location away from the hole (the location in the unbolted model where local stress was found to equal nominal stress based on the net area) and future research should be performed to consider the appropriateness of this choice.

To apply the general procedure described, a double lap splice model was created that represented connections tested by Brown et al. (2006). According to the physical test data from Brown et al. (2006), this bolted connection performed as an AASHTO Category B detail when it included pretensioned bolts. A variation of this model was also examined – an unbolted plate from the connection -- which according to AASHTO 2012 is a Category D fatigue detail. Figure 17 shows the FE model of the bolted plate (Figure 17a) from the Brown et al. (2006) investigation and the corresponding unbolted plate (Figure 17b). It should be made clear that the corresponding single plate was not physically tested in Brown et al. (2006)'s study, but was modeled here to provide context to the model of the bolted connection that was tested by Brown et al. (2006).

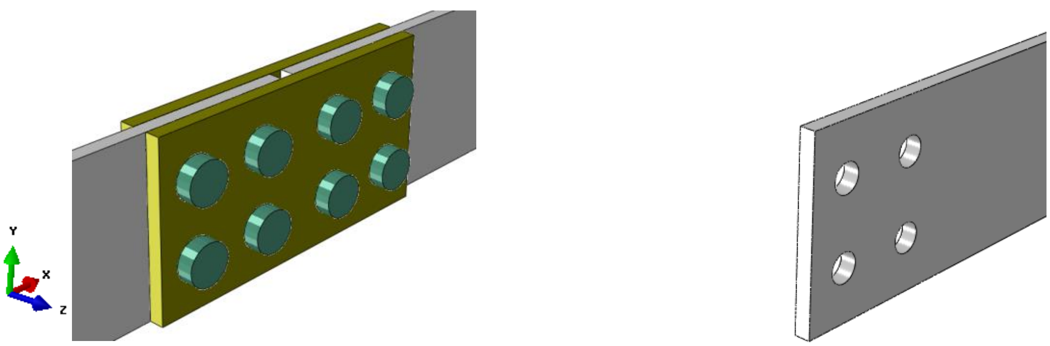

(a) (b)

Figure 17: FE model of bolted plate and unbolted plate

The nominal stress computed based on the net section ($\sigma_{nom,Anet}$) was equal to 29.1 ksi (Brown et al. 2006) and the location that local stress was equal to nominal stress was at 3/10 in. (Figure 18a). away from hole edge on unbolted plate. The local stress (σ_{local}) on the bolted plate at the same location was found to be 9.5 ksi (Figure 18b). $\Delta\sigma_{local}$ was defined as the difference between the nominal stress ($\sigma_{nom,Anet}$) and the local stress (σ_{local}) on the bolted plate.

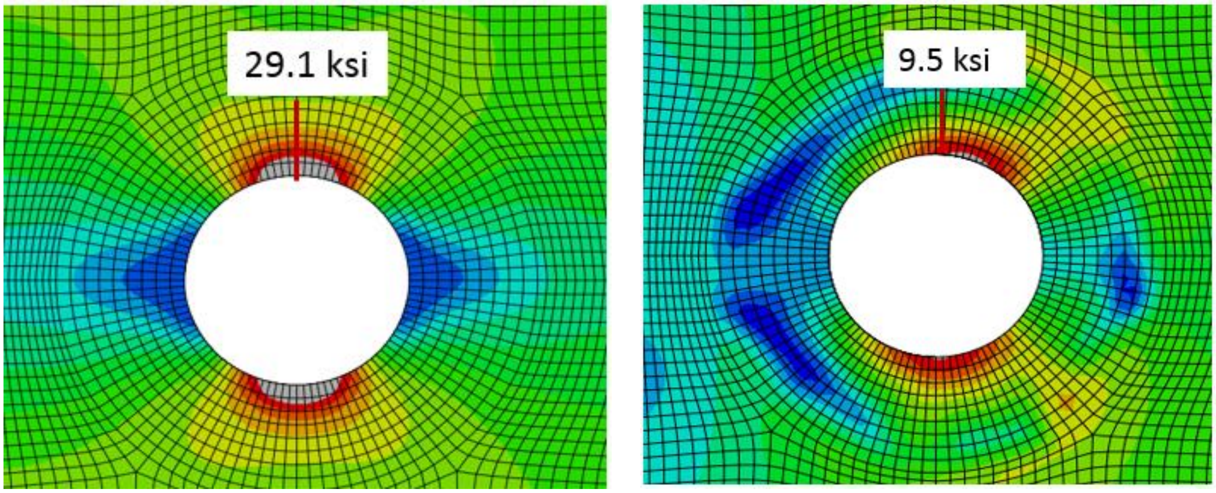

(a) (b)

Figure 18: (a) the nominal stress on unbolted plate; (b) local stress on bolted plate

The data point for the unbolted plate was located on the S-N diagram by plotting the nominal stress (29.1 ksi) on the Category D curve. The data point for the bolted plate (48.7 ksi) was located by adding $\Delta\sigma_{local}$ (19.7 ksi) to the nominal stress value (29.1 ksi) for the unbolted plate. On the S-N diagram, the resulting data point for the bolted plate ocurred on the Category B curve, matching the physical test done by Brown et al. (2006). However, it is again noted that more investigation should be done regarding where best to extract $\Delta\sigma_{local}$ from the FE models, and it is noted that this procedure will not have the same result if fatigue behavior in the constant-amplitude fatigue life region is being investigated.

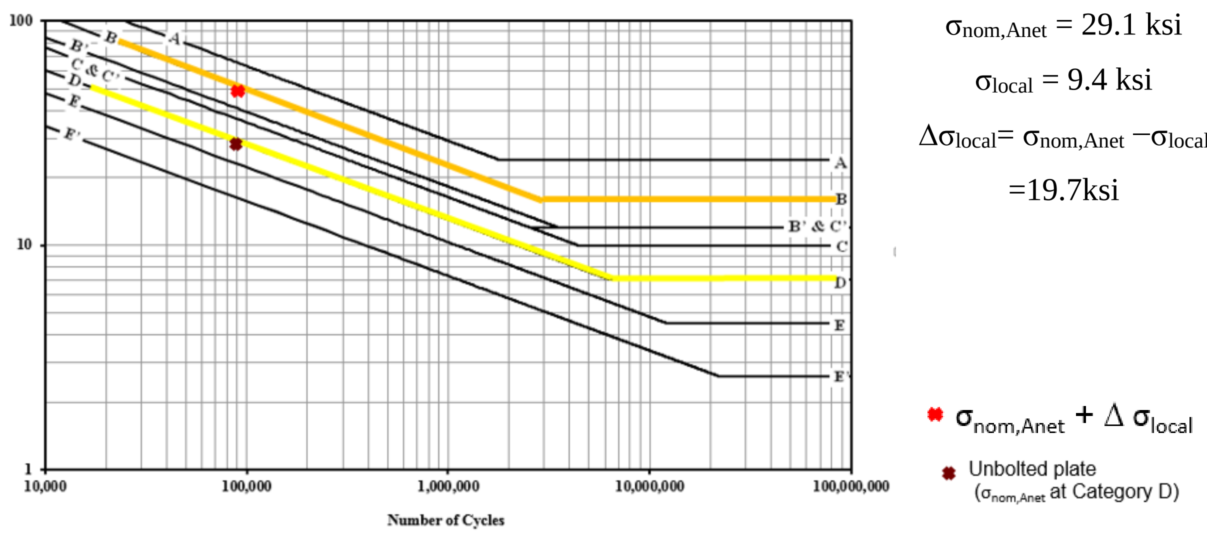

Figure 19: FEA Data on S-N diagram

CHANGE IN STRESS VERSUS MODEL PARAMETERS

A significant challenge associated with examining finite element results in the context of fatigue susceptibility is choosing an appropriate location within the FE model from which to extract stress data. Many studies have been performed around this topic for welded details, but bolted details have not received the same attention.

As mentioned in the previous section, the first location in the model considered was where local stress was found to be equal to nominal stress computed based on net cross-sectional area. This location was unique to each model. To examine whether this location was a reasonable place at which to investigate the stress comparison, the variables *d/t*, *d*, *t*, *e*, *s*, and α were examined against $\Delta\sigma_{local}$ and a normalized stress, $\Delta\sigma_{local}/\sigma_{nom}$, at different distances away from the bolt hole.

Table 2 shows the variables and the distances examined in this investigation. $\Delta\sigma_{local}$ was the difference in local stress between unbolted plates and bolted plates extracted from the same location. $\Delta\sigma_{local}/\sigma_{nom}$ was the $\Delta\sigma_{local}$ value normalized against the net-section nominal stress. As discussed, the mesh size in all models was identical, hence, distance has been represented here by the number of elements. $\Delta\sigma_{local}$ was extracted at the edge of hole, one element away from hole, two elements away from hole and the location where local stress equals nominal stress, respectively.

Table 2: List of variables

Vertical Axis Variable	Horizontal AxisVariable	Distance
$\Delta\sigma_{local}$	Bolt Diameter to Thickness ***d/t***	At the edge of hole (0 mm [0 in.])
$\Delta\sigma_{local}/\sigma_{nom}$	Thickness ***t***	At one element (1.6 mm [1/16 in.])
	Bolt Diameter ***d***	At two elements (3.2 mm [2/16 in.])
	Edge Distance ***e***	At $\sigma_{local}=\sigma_{nom}$
	Bolt Spacing ***s***	
	Stress Ratio ***α***	

EFFECT OF BOLT DIAMETER-TO-THICKNESS RATIO:

The bolt diameter to plate thickness ratio (*d/t*) was calculated for each specimen to investigate the effect of *d/t* on normalized $\Delta\sigma_{local}/\sigma_{nom}$ at different distances away from the hole. $\Delta\sigma_{local}/\sigma_{nom}$ versus *d/t* at different distances is shown in Figure 20, where the data were sorted by bolt pattern. From the left hand side to the right hand side, it is apparent that as distance away from the hole increased, the correlation between $\Delta\sigma_{local}/\sigma_{nom}$ and *d/t* decreased. However, a very clear trend was observed between $\Delta\sigma_{local}/\sigma_{nom}$ and *d/t* near the edge of the hole. It was found that the $\Delta\sigma_{local}$ increased with increasing bolt diameter to thickness ratio.

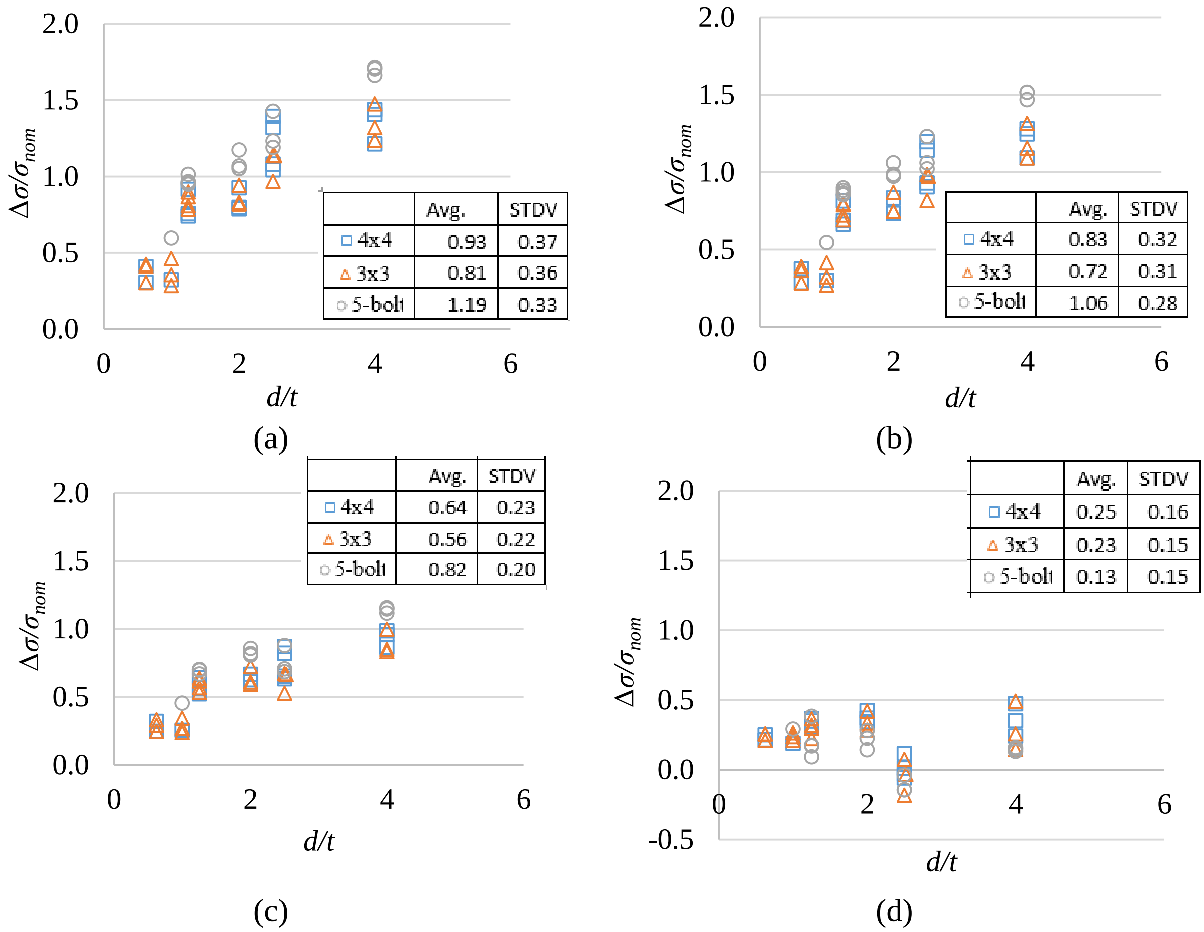

Figure 20: The $\Delta\sigma_{local}/\sigma_{nom}$ versus *d/t* at different distances away from bolt hole: (a) distance = at hole edge; (b) distance = one element from hole edge; (c) distance = two elements from hole edge; (d) σ_{local} = σ_{nom}

Similarly, Figure 21 presents a comparison of $\Delta\sigma_{local}/\sigma_{nom}$ versus t at different distances away from the hole. A trend showing that $\Delta\sigma_{local}$ decreased with decreasing thickness was obvious at the edge of the hole.

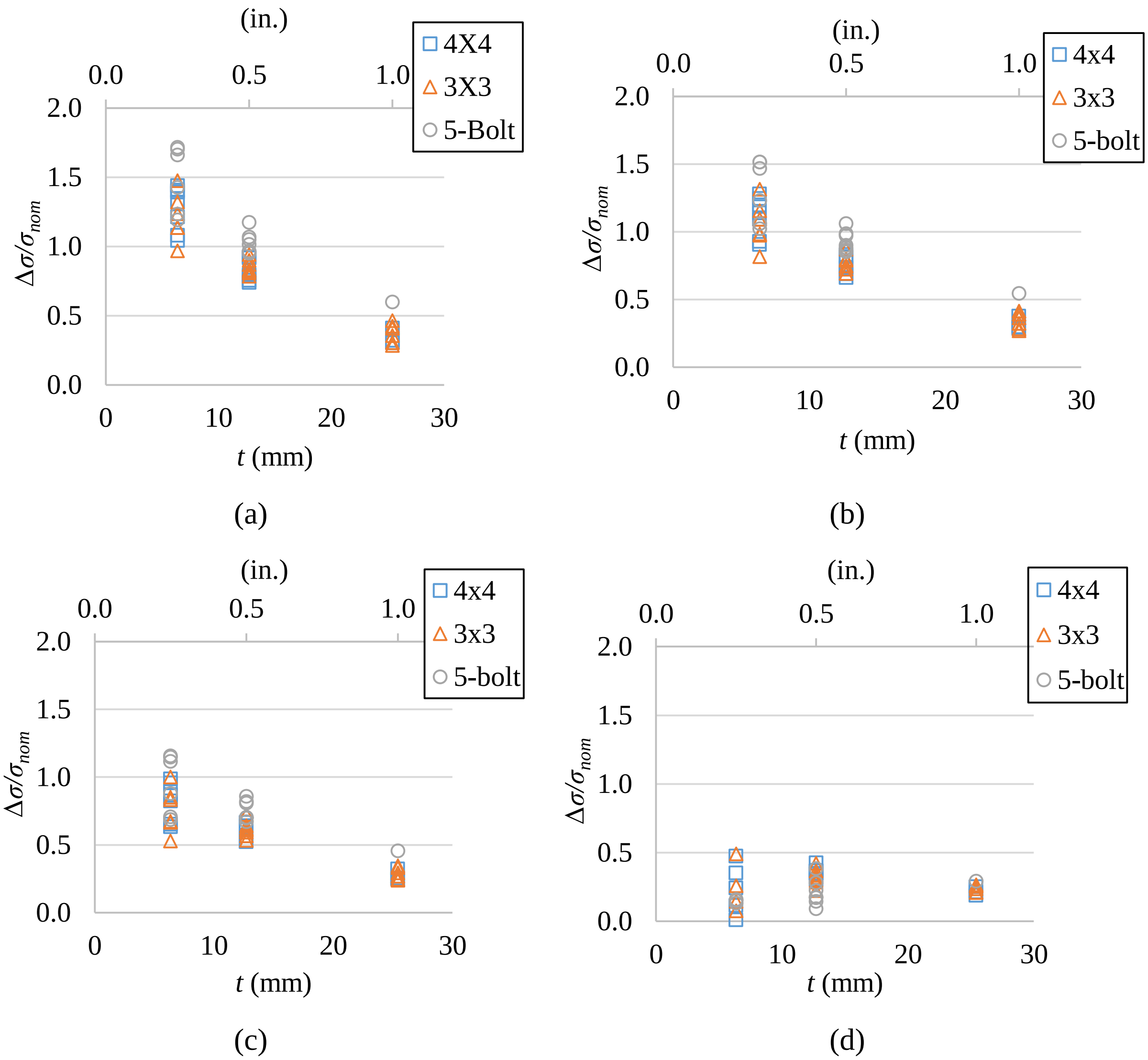

Figure 21: The $\Delta\sigma_{local}/\sigma_{nom}$ versus *t* at different distances away from bolt hole: (a) distance = at hole edge; (b) distance = one element from hole edge; (c) distance = two elements from hole edge; (d) $\sigma_{local} = \sigma_{nom}$

Comparisons between $\Delta\sigma_{local}/\sigma_{nom}$ and *d* are shown in Figure 22. A weak trend is observed at the edge of the hole.

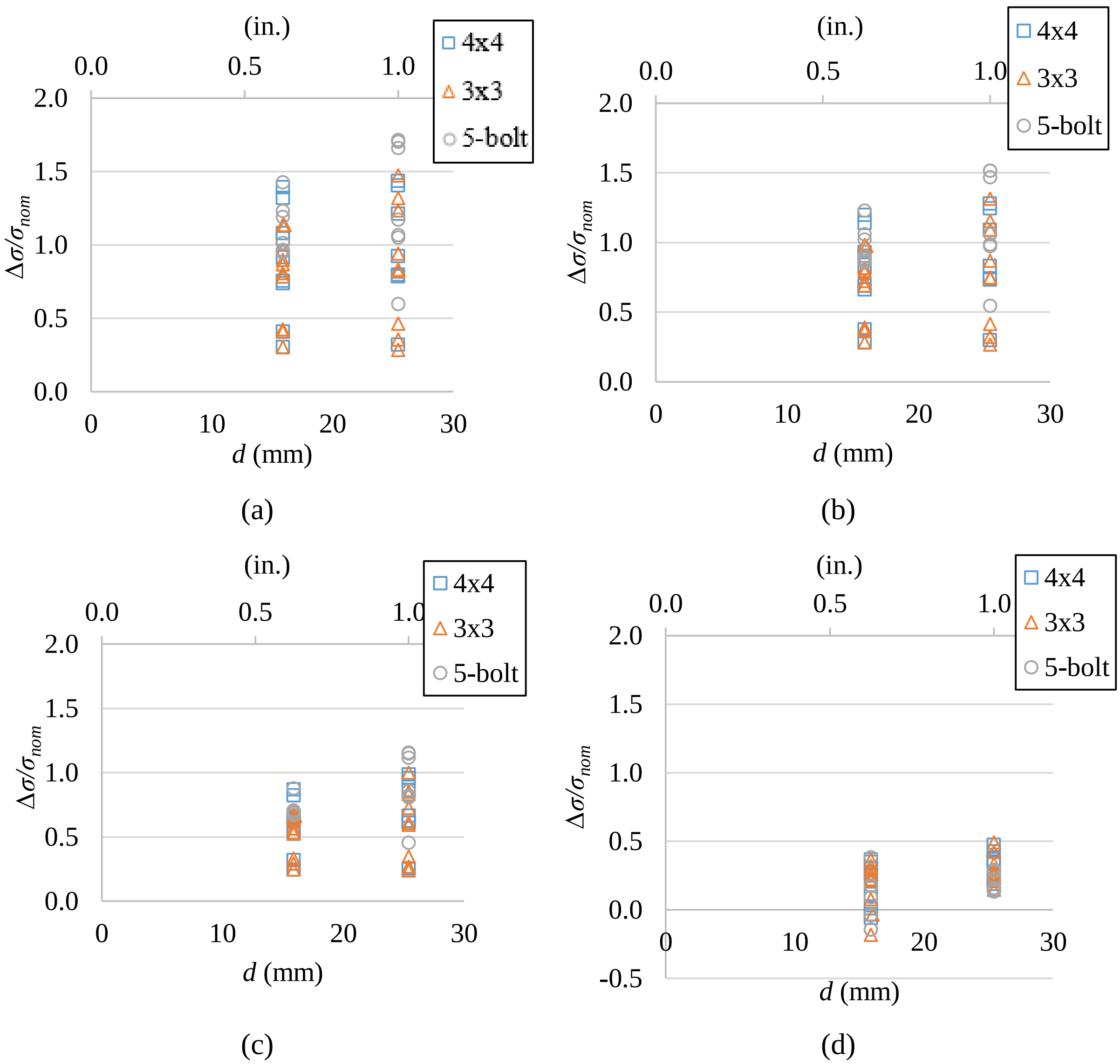

Figure 22: The $\Delta\sigma_{local}/\sigma_{nom}$ versus *d* at different distances away from bolt hole: (a) distance = at hole edge; (b) distance = one element from hole edge; (c) distance = two elements from hole edge; (d) σ_{local} = σ_{nom}

Comparisons between $\Delta\sigma_{local}/\sigma_{nom}$ and *e* as well as $\Delta\sigma_{local}/\sigma_{nom}$ vs. s, at different distances away from the hole are shown in Figure 23 and Figure 24, respectively. The data points presented randomly, and little correlation was found to exist at any distance from the hole.

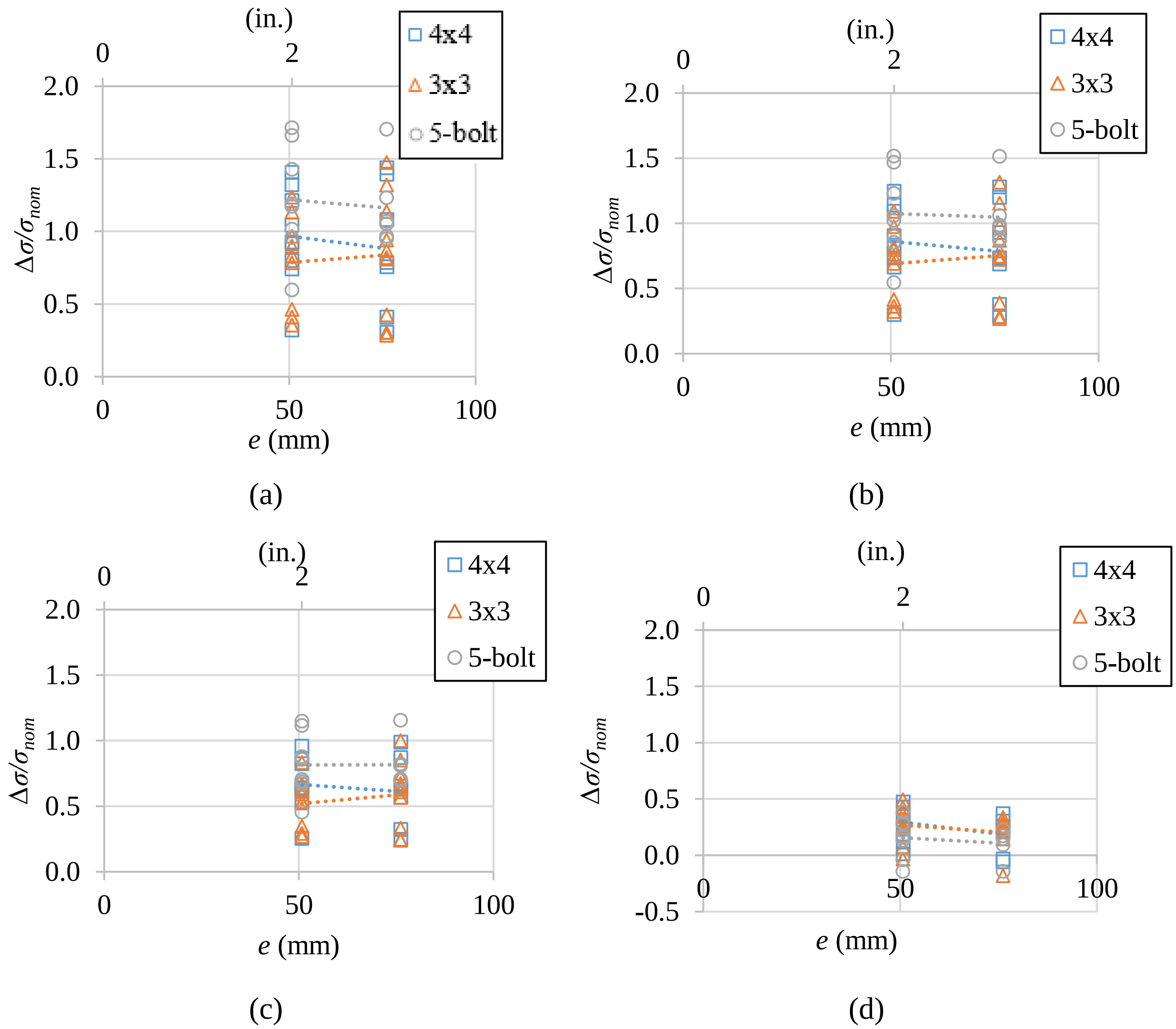

Figure 23: The Δσ_{local}/σ_{nom} versus *e* at different distances away from bolt hole: (a) distance = at hole edge; (b) distance = one element from hole edge; (c) distance = two elements from hole edge; (d) σ_{local} = σ_{nom}

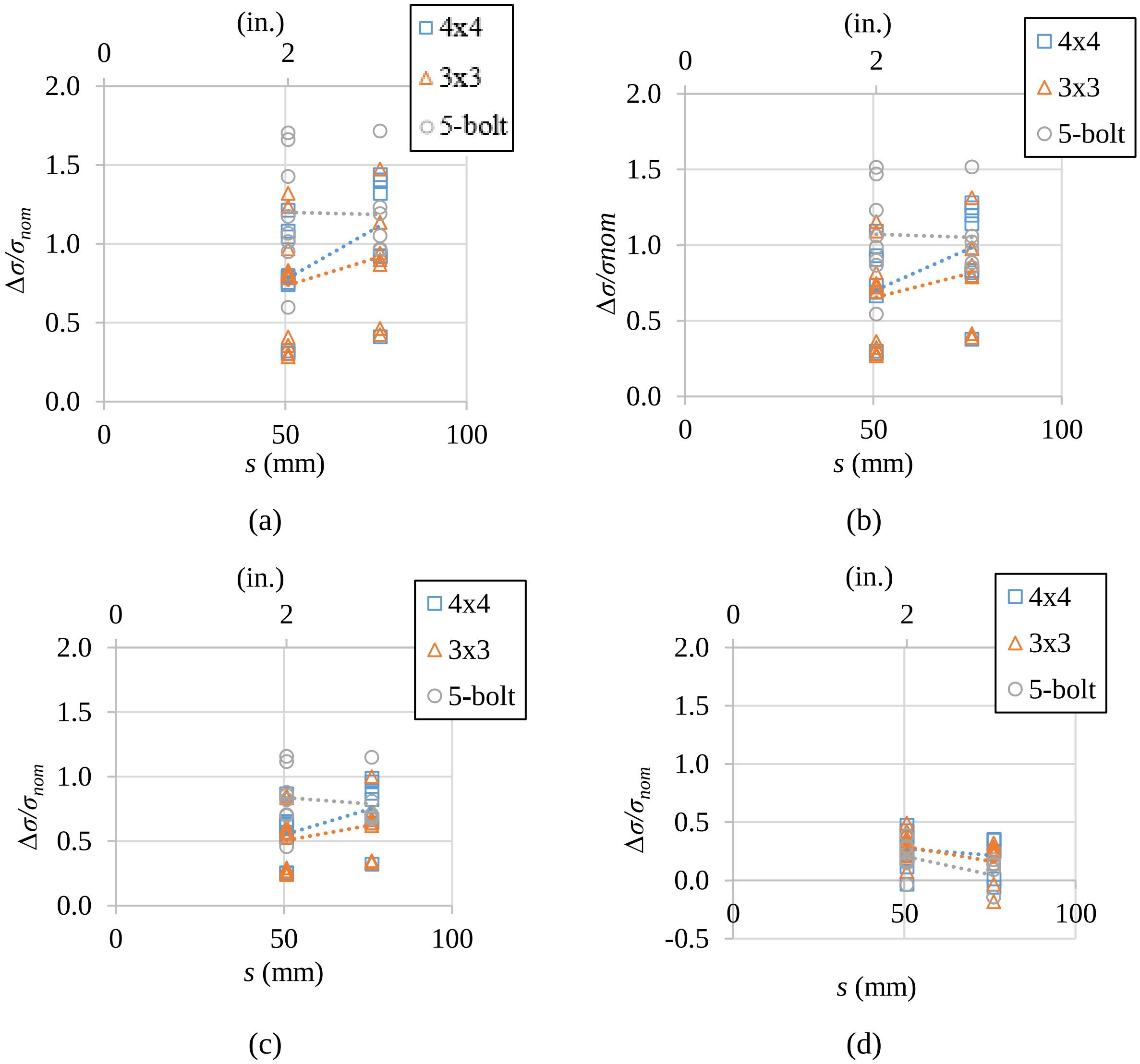

Figure 24: The $\Delta\sigma_{local}/\sigma_{nom}$ versus *s* at different distance away from bolt hole: (a) distance = at hole edge; (b) distance = one element from hole edge; (c) distance = two elements from hole edge; (d) $\sigma_{local} = \sigma_{nom}$

In general, comparisons between $\Delta\sigma_{local}$ and each variable at different distances from the hole showed similar results as the comparisons presented on the basis of $\Delta\sigma_{local}/\sigma_{nom}$. The comparisons presented in terms of $\Delta\sigma_{local}$ vs. each variable at different distances from the hole are included in Appendix E.

STATISTICAL CONSIDERATION OF THE MODEL PARAMETERS

A linear regression analysis was performed to assess the relative importance between variables included in the parametric finite element analysis. A statistical analysis software called SPSS (IBM Corp. 2015) was used to analyze the linear regression between variables. Two slightly different methods for examining the relative influence of the variables were considered in SPSS output: ***standardized coefficient (β)*** and ***partial correlations***. These methods are introduced briefly here.

STANDARDIZED COEFFICIENT (BETA)

This coefficient can be used to determine which independent variable has a greater effect on the dependent variable by comparing the absolute value of *Beta*. The higher the absolute value of *Beta*, the greater effect the variable has relative to other dependent variables included in the regression analysis.

To understand the standardized coefficient (β), it is necessary to introduce the unstandardized coefficient (B) first. The unstandardized coefficients (B) follow the regression equation (where t, d, e, s represent independent variables and $\Delta\sigma_{local}/\sigma_{nom}$ represents the dependent variable), as shown in Equation 2:

$$\frac{\Delta\sigma}{\sigma_{nom}} = B_0 + (B_1 * t) + (B_2 * d) + (B_3 * e) + (B_4 * s) + Std.Error \qquad \text{Equation 2}$$

Where B is the unstandardized coefficient of each independent variable. For example: B_1 is the unstandardized coefficient of t (thickness), and B_0 is the constant unstandardized coefficient. That is, the value of the dependent variable equals the summation of the product of unstandardized coefficients and independent variables plus the constant unstandardized coefficient and standard error.

To obtain the value of standardized coefficients, *Beta*, divide dependent variable (DV) values and independent variable (IV) values by their standard deviations to obtain standardized values for DV and IV. Then, re-performing the regression, *Beta* (β) was obtained and the new standardized regression equation is shown in Equation 3:

$$\frac{\Delta\sigma}{\sigma_{nom}} = (\beta_1 * t) + (\beta_2 * d) + (\beta_3 * e) + (\beta_4 * s) + Std.Error \qquad \text{Equation 3}$$

Where β is the standardized coefficient of each IV, and β is a standardized form of the original coefficient, *B*. This standardized regression equation removes the constant coefficient. The value of the dependent variable equals the summation of the product of standardized coefficients and independent variables plus the standard error.

Part Correlations

The square of the part correlation of a variable is the change in the coefficient of determination (R^2) when this variable is dropped from the analysis. In other words, the part correlation describes the influence of dropping a variable from the regression analysis. The larger the square of the part correlation, the greater the effect of the variable.

Variables Included in the Parametric Finite Element Study and Linear Regression Analyses:

As mentioned, the variables in parametric finite element study were thickness (*t*), bolt diameter (*d*), edge distance (*e*), and bolt spacing (*s*). Table 3 shows the variables included in linear regression analysis, where the dependent variables were $\Delta\sigma_{local}$, $\Delta\sigma_{local}/\sigma_{nom}$ (where nominal stress was calculated based on the net section), and $\Delta\sigma_{local}/(\sigma_{nom\_Agro})$ (where the nominal stress was calculated based on the gross section). $\Delta\sigma_{local}$ was the difference in local stress at a zero distance away from the hole on the unbolted plates and the bolted plates, and $\Delta\sigma_{local}/\sigma_{nom}$ was $\Delta\sigma_{local}$ normalized against the nominal net section stress. The independent variables in the linear regression analysis were thickness (*t*), bolt diameter (*d*), edge distance (*e*), bolt spacing (*s*), and each of the variables normalized by *d, t, e, and s*, respectively.

Table 3: List of dependent variables and indpendent variables

Dependent Variable	Independent Variable
$\Delta\sigma_{local}$	*t, d, e, s*
$\Delta\sigma_{local}/\sigma_{nom}$	*t/d, e/d, s/d*
$\Delta\sigma_{local}/(\sigma_{nom\_Agro})$	*d/t, e/t, s/t*
	t/e, d/e, s/e
	t/s, d/s, e/s

QUANTIFYING THE RELATIVE IMPORTANCE BETWEEN INDEPENDENT VARIABLES IN THE PARAMETRIC ANALYSES:

Dependent variables extracted from the Abaqus analyses, as well as independent variables shown in Table 3, were input into the SPSS analysis engine. Output from the SPSS analysis is shown in Appendix G. Figure 25 shows the relative influence in terms of *Beta* and squared part correlations, respectively. The horizontal axis of the figure shows the independent variables: *t* (plate thickness), *d* (bolt diameter), *e* (edge distance) and *s* (bolt spacing), and the dependent stress variable, $\Delta\sigma_{local}/\sigma_{nom}$. The goal of the statistical analysis was to determine which independent variables had the greatest influence on $\Delta\sigma_{local}/\sigma_{nom}$. Comparing the *Beta* and squared part correlation in Figure 25 (a) and (b), it is apparent that *t* (thickness) had the largest value, meaning that *t* has the greatest relative effect on $\Delta\sigma_{local}/\sigma_{nom}$.

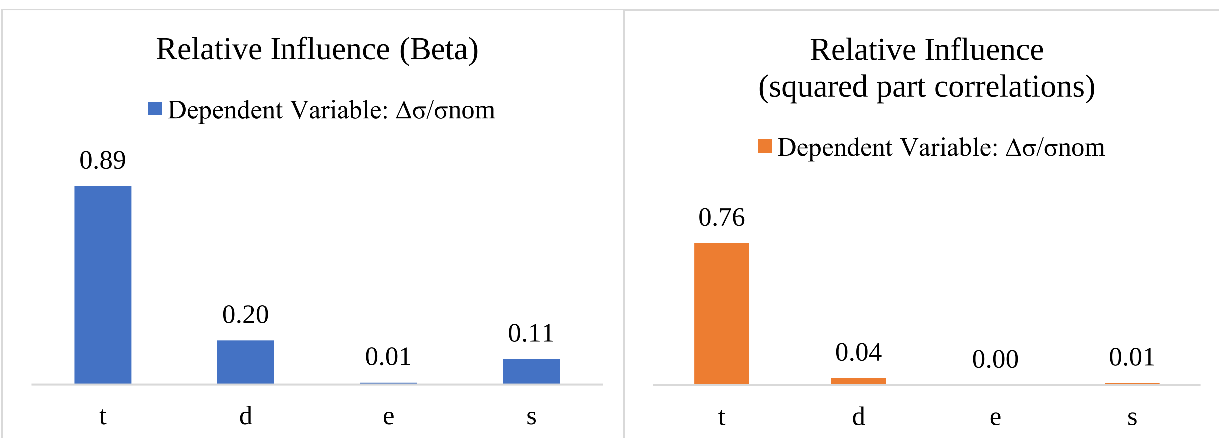

(a) (b)

Figure 25: Relative influence (geometric variables): (a) relative influence (Beta); (b) relative influence (squared part correlation)

Similarly, Figure 26 shows the relative influence of independent variables on $\Delta\sigma_{loca}/\sigma_{nom}$, where $\Delta\sigma_{local}$ is the difference in local stress between the unbolted plates and bolted plates. It is apparent that *d/t* has the greatest relative effect on the $\Delta\sigma_{local}$ by comparing the standardized coefficient (*Beta*) and the square of part correlations, respectively.

Figure 26: Relative Influence of geometric variables normalized by thickness: (a) relative influence (Beta); (b) relative influence (squared part correlation)

Figure 27 shows the relative influence of variables normalized by *d* where the dependent variable was $\Delta\sigma_{local}/\sigma_{nom}$. Comparing either *Beta* or the square of part correlations, *t/d* has the highest relative influence on the $\Delta\sigma_{local}/\sigma_{nom}$. The relative influence of variables that were normalized by *t*, *e*, and *s* indicated that the variables included *t* or *d* have greater effect on the dependent variable. The relative influence for all normalized variables has been presented in Appendix G.

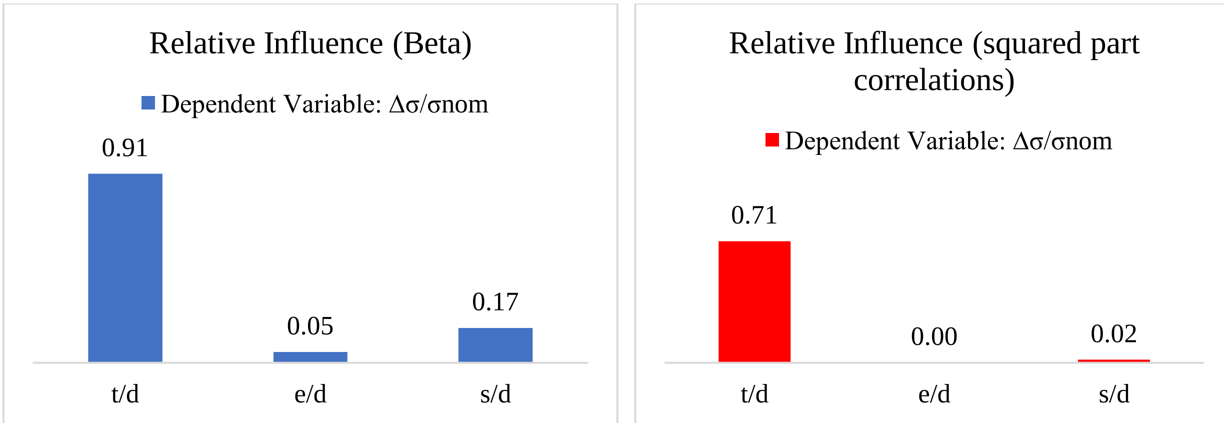

(a) (b)

Figure 27: Relative influence of geometric variables normalized by bolt diameter: (a) relative influence (Beta); (b) relative influence (squared part correlation)

CONCLUSIONS

The parametric study performed in this investigation was aimed at determining the influence of geometric variables on the fatigue performance of bolted connections. The study focused on comparisons of stress distribution in bolted and unbolted plates, the stress difference ($\Delta\sigma_{local}$) in bolted and unbolted plates (to quantify the level of fatigue improvement when a pretensioned bolt was added), and a linear regression analysis quantifying the relative importance between the variables. Based on the results of this parametric study, the following conclusions can be drawn:

- The thicker the plates, the less effect pretensioned bolts had in reducing tensile stress at the hole. In other words, the stress difference between unbolted plates and bolted connections decreased with the increasing plate thickness. This finding implies that the fatigue resistance of thick bolted connections (where plates are greater than 1 in. thick) may not meet the criteria for Category B performance.
- Of the geometric variables investigated in this study, thickness had the greatest influence on stresses around the bolt holes, when bolted and unbolted plates were compared. The linear regression analysis showed that hole/bolt diameter had less effect on stresses around bolt holes. Hole/bolt spacing and edge distance had negligible influence on stresses around bolt holes.

- The stress difference between unbolted plates and bolted connections decreased as *t* increased, implying that the fatigue resistance of the plates should decreased with increasing *t*.
- From linear regression analysis, the normalized variables that included *t* and *d* had the greatest relative influence on $\Delta\sigma_{local}$.

The findings from this study show that the improvement of fatigue performance from Cat. D (unbolted plates) to Cat. B (bolted plates) can be expected to be influenced by plate thickness (and to a lesser extent, bolt diameter). Therefore, plate thickness should be taken into consideration in the fatigue design of pretensioned bolted connections.

Future work should be conducted to further investigate the phenomena described in this study. Physical fatigue tests should be performed on bolted and unbolted plates to discern whether thick bolted connections meet the AASHTO (2012) Category B criteria. Additional finite element analysis should be performed to determine the behavior of plates thicker than 1 in. Future studies should also be performed to further develop a procedure for translating finite element analysis results to the AASHTO S-N diagram for bolted connections, including examining the influence of the location of stress extraction in the models in predicting the level of fatigue improvement on the S-N diagrams.

REFERENCES

AASHTO (2012). *LRFD Bridge Design Specifications, 6th Ed*. American Association of State Highway and Transportation Officials, Washington, D.C.

AISC (2011). *Steel Construction Manual, 14th Ed.* American Institute of Steel Construction, Chicago, IL.

RCSC (2014). *Specification for Structural Joints Using High-Strength Bolts,* Research Council on Structural Connections, Chicago, IL.

Brown, J. D. (2006). *Punched Holes in Structural Connections*. Master of Science Thesis, The University of Texas at Austin.

Brown, J. D., Lubitz, D. J., Cekov, Y. C., Frank, K. H., & Keating, P. B. (2007). *Evaluation of influence of hole making upon the performance of structural steel plates and connections*. CTR Technical Report 0-4624-1. Center for Transportation Research, Austin, Texas

Frank, K. H., & Yura, J. A. (1981). *An experimental study of bolted shear connections* (No. FHWA-RD-81-148 Final Rpt.).

Kulak, G. L., Fisher, J. W., & Struik, J. H. (2001). Guide to Design Criteria for Bolted and Riveted Joints Second Edition.

Bennett, C. R., Swanson, J. A., & Linzell, D. G. (2007). Fatigue Resistance of HPS-485W (70 W) Continuous Plate with Punched Holes. *Journal of Bridge Engineering*, *12*(1), 98-104.

Josi, G., Grondin, G. Y., & Kulak, G. L. (2004). Fatigue of joints with staggered holes. *Journal of Bridge Engineering*, *9*(6), 614-622.

Kim, H. J. (1996). *The effect of end distance on the bearing strength of bolted connections*. (Master of Science Thesis, The University of Texas at Austin).

Kim, M. H., & Kang, S. W. (2008). Testing and analysis of fatigue behaviour in edge details: a comparative study using hot spot and structural stresses.*Proceedings of the Institution of Mechanical Engineers, Part C: Journal of Mechanical Engineering Science*, *222*(12), 2351-2363.

Poutiainen, I., Tanskanen, P., & Marquis, G. (2004). Finite element methods for structural hot spot stress determination—a comparison of procedures.*International journal of fatigue*, *26*(11), 1147-1157.

Marin, T., & Nicoletto, G. (2009). Fatigue design of welded joints using the finite element method and the 2007 ASME Div. 2 Master curve. *Frattura ed Integritá Strutturale*, (9), 76.

Selvakumar, P., & Hong, J. K. (2013). Robust mesh insensitive structural stress method for fatigue analysis of welded structures. *Procedia Engineering*, *55*, 374-379.

Simulia (2013). Abaqus, Version 6.13-3. http://www.simulia.com

Grondin, G. Y., Jin, M., & Josi, G. (2007). *Slip Critical Bolted Connections: A Reliability Analysis for Design at the Ultimate Limit State*. Department of Civil & Environmental Engineering, University of Alberta. *Structural Engineering Report No. 274.*

Dong, P. (2001). A structural stress definition and numerical implementation for fatigue analysis of welded joints. *International Journal of Fatigue*, *23*(10), 865-876.

Adams, C. A. (2010). *Finite element study on bridge details susceptible to distortion-induced fatigue* (Master of Science Thesis, University of Kansas).

Mashiri, F., Zhao, X., & Dong, P. (2008). Approaches for fatigue design of tubular structures. *Tubular Structures XII: Proceedings of Tubular Structures XII, Shanghai, China, 8-10 October 2008*, 153.

Marquis, G., & Samuelsson, J. (2005). Modelling and fatigue life assessment of complex structures. *Materialwissenschaft und Werkstofftechnik*, *36*(11), 678-684.

Heshmati, M., & Al-Emrani, M. (2012). Fatigue design of plated structures using structural hot spot stress approach. In *Proceedings of the Sixth International Conference on Bridge Maintenance, Safety and Management, IABMAS 2012, Stresa, Lake Maggiore, 8-12 July 2012* (pp. 3146-3153).

Niemi, E., & Marquis, G. (2002). Introduction to the structural stress approach to fatigue analysis of plate structures. In *Proceedings of the IIW Fatigue Seminar, Tokyo Institute of Technology* (pp. 73-90).

Dong, P., Hong, J. K., Osage, D. A., & Prager, M. (2002). Master SN curve method for fatigue evaluation of welded components. *Welding Research Council Bulletin*, (474).

Moon, J. E., Perrett, B. H., & Edwards, P. R. (1976). *A study of local stress histories in loaded and unloaded holes and their implications to fatigue life estimation* (No. ARC-CP-1374). Aeronautical Research Council, London, UK.

Rex, C. O., & Easterling, W. S. (2003). Behavior and modeling of a bolt bearing on a single plate. *Journal of Structural Engineering*, *129*(6), 792-800.

IBM Corp. (2015). IBM SPSS Statistics, Version 23. http://www.ibm.com

Shewhart, W. A. and Wilks, S. S. (2014). Applied Linear Regression (Fourth ed.). *Minneapolis, MN: University of Minnesota* (pp.119)

APPENDIX A: LIST OF CURRENT SPECIFICATIONS

Table A. 1: Minimum Bolt Pretension, Pretensioned and Slip-Critical Joints (AISC 14th Ed.)

Nominal Bolt Diameter, d_b, in.	Specified Minimum Bolt Pretension, T_m, kips [a]	
	ASTM A325 and F1852	ASTM A490 and F2280
½	12	15
⅝	19	24
¾	28	35
⅞	39	49
1	51	64
1⅛	56	80
1¼	71	102
1⅜	85	121
1½	103	148

[a] Equal to 70 percent of the specified minimum tensile strength of bolts as specified in ASTM Specifications for tests of full-size ASTM A325 and A490 bolts with UNC threads loaded in axial tension, rounded to the nearest kip.

Table A. 2: Minimum Edge Distance (RCSC 2014)

Bolt Diameter	Sheared Edges	Rolled Edges of Plates or Shapes, or Gas Cut Edges
in.	in.	in.
5/8	1-1/8	7/8
3/4	1-1/4	1
7/8	1-1/2	1-1/8
1	1-3/4	1-1/4
1-1/8	2	1-1/2
1-1/4	2-1/4	1-5/8
1-3/8	2-3/8	1-3/4

Table A. 3: Nominal Bolt Hole Dimensions (RCSC 2014)

Nominal Bolt Diameter, d_b, in.	Nominal Bolt Hole Dimensions [a,b], in.			
	Standard (diameter)	Oversized (diameter)	Short-slotted (width × length)	Long-slotted (width × length)
½	9/16	5/8	9/16 × 11/16	9/16 × 1¼
5/8	11/16	13/16	11/16 × 7/8	11/16 × 1 9/16
¾	13/16	15/16	13/16 × 1	13/16 × 1 7/8
7/8	15/16	1 1/16	15/16 × 1 1/8	15/16 × 2 3/16
1	1 1/16	1¼	1 1/16 × 1 5/16	1 1/16 × 2½
≥1 1/8	d_b + 1/16	d_b + 5/16	(d_b + 1/16) × (d_b + 3/8)	(d_b + 1/16) × (2.5d_b)

[a] The upper tolerance on the tabulated nominal dimensions shall not exceed 1/32 in. Exception: In the width of slotted holes, gouges not more than 1/16 in. deep are permitted.

[b] The slightly conical hole that naturally results from punching operations with properly matched punches and dies is acceptable.

Table A. 4: AASHTO Fatigue Design Parameters (AASHTO 2012)

Description	Category	Constant A (ksi^3)	Threshold $(\Delta F)_{TH}$ ksi	Potential Crack Initiation Point	Illustrative Examples
Section 1—Plain Material away from Any Welding					
1.1 Base metal, except noncoated weathering steel, with rolled or cleaned surfaces. Flame-cut edges with surface roughness value of 1,000 μ-in. or less, but without re-entrant corners.	A	250×10^8	24	Away from all welds or structural connections	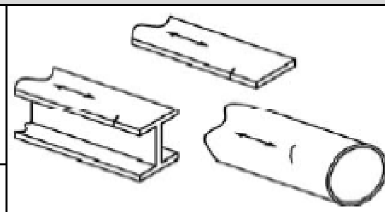
1.2 Noncoated weathering steel base metal with rolled or cleaned surfaces designed and detailed in accordance with FHWA (1989). Flame-cut edges with surface roughness value of 1,000 μ-in. or less, but without re-entrant corners.	B	120×10^8	16	Away from all welds or structural connections	
1.3 Member with re-entrant corners at copes, cuts, block-outs or other geometrical discontinuities made to the requirements of AASHTO/AWS D1.5, except weld access holes.	C	44×10^8	10	At any external edge	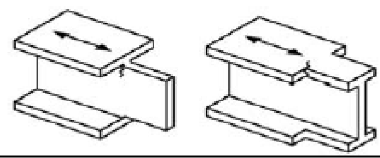
1.4 Rolled cross sections with weld access holes made to the requirements of AASHTO/AWS D1.5, Article 3.2.4.	C	$44 \text{ x } 10^8$	10	In the base metal at the re-entrant corner of the weld access hole	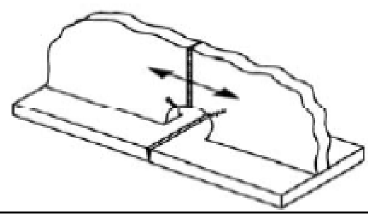
1.5 Open holes in members (Brown et al., 2007).	D	22×10^8	7	In the net section originating at the side of the hole	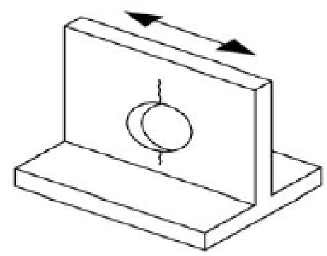
Section 2—Connected Material in Mechanically Fastened Joints					
2.1 Base metal at the gross section of high-strength bolted joints designed as slip-critical connections with pretensioned high-strength bolts installed in holes drilled full size or subpunched and reamed to size—e.g., bolted flange and web splices and bolted stiffeners. (Note: see Condition 2.3 for bolt holes punched full size; see Condition 2.5 for bolted angle or tee section member connections to gusset or connection plates.)	B	120×10^8	16	Through the gross section near the hole	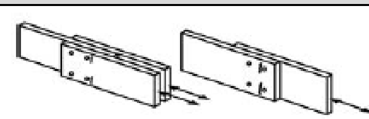

APPENDIX B: TEST MATRIX

Table B. 1: 4X4 Rectangular Bolt Pattern Model Matrix

Model Name	Model Name	Bolt Pattern	Bolt Spacing *s*		Plate Thickness *t*		Bolt Diameter *d*		Edge Distance *e*	
Bolted Plate	Unbolted Plate		mm	[in]	mm	[in]	mm	[in]	mm	[in]
1/4t_5/8d_3e_3s_0.15α_4x4_BP	1/4t_5/8d_3e_3s_0.15α_4x4_UP	4 x 4 Rectangular	76.2	[3]	6.4	[1/4]	15.9	[5/8]	76.2	[3]
1/4t_1d_3e_3s_0.43α_4x4_BP	1/4t_1d_3e_3s_0.43α_4x4_UP	4 x 4 Rectangular	76.2	[3]	6.4	[1/4]	25.4	[1]	76.2	[3]
1/4t_5/8d_2e_3s_0.16α_4x4_BP	1/4t_5/8d_2e_3s_0.16α_4x4_UP	4 x 4 Rectangular	76.2	[3]	6.4	[1/4]	15.9	[5/8]	50.8	[2]
1/4t_1d_2e_3s_0.45α_4x4_BP	1/4t_1d_2e_3s_0.45α_4x4_UP	4 x 4 Rectangular	76.2	[3]	6.4	[1/4]	25.4	[1]	50.8	[2]
1/2t_5/8d_3e_3s_0.15α_4x4_BP	1/2t_5/8d_3e_3s_0.15α_4x4_UP	4 x 4 Rectangular	76.2	[3]	12.7	[1/2]	15.9	[5/8]	76.2	[3]
1/2t_1d_3e_3s_0.43α_4x4_BP	1/2t_1d_3e_3s_0.43α_4x4_UP	4 x 4 Rectangular	76.2	[3]	12.7	[1/2]	25.4	[1]	76.2	[3]
1/2t_5/8d_2e_3s_0.16α_4x4_BP	1/2t_5/8d_2e_3s_0.16α_4x4_UP	4 x 4 Rectangular	76.2	[3]	12.7	[1/2]	15.9	[5/8]	50.8	[2]
1/2t_1d_2e_3s_0.45α_4x4_BP	1/2t_1d_2e_3s_0.45α_4x4_UP	4 x 4 Rectangular	76.2	[3]	12.7	[1/2]	25.4	[1]	50.8	[2]
1t_5/8d_3e_3s_0.15α_4x4_BP	1t_5/8d_3e_3s_0.15α_4x4_UP	4 x 4 Rectangular	76.2	[3]	25.4	[1]	15.9	[5/8]	76.2	[3]
1t_1d_3e_3s_0.43α_4x4_BP	1t_1d_3e_3s_0.43α_4x4_UP	4 x 4 Rectangular	76.2	[3]	25.4	[1]	25.4	[1]	76.2	[3]
1t_5/8d_2e_3s_0.16α_4x4_BP	1t_5/8d_2e_3s_0.16α_4x4_UP	4 x 4 Rectangular	76.2	[3]	25.4	[1]	15.9	[5/8]	50.8	[2]
1t_1d_2e_3s_0.45α_4x4_BP	1t_1d_2e_3s_0.45α_4x4_UP	4 x 4 Rectangular	76.2	[3]	25.4	[1]	25.4	[1]	50.8	[2]
1/4t_5/8d_3e_2s_0.16α_4x4_BP	1/4t_5/8d_3e_2s_0.16α_4x4_UP	4 x 4 Rectangular	50.8	[2]	6.4	[1/4]	15.9	[5/8]	76.2	[3]
1/4t_1d_3e_2s_0.47α_4x4_BP	1/4t_1d_3e_2s_0.47α_4x4_UP	4 x 4 Rectangular	50.8	[2]	6.4	[1/4]	25.4	[1]	76.2	[3]
1/4t_5/8d_2e_2s_0.17α_4x4_BP	1/4t_5/8d_2e_2s_0.17α_4x4_UP	4 x 4 Rectangular	50.8	[2]	6.4	[1/4]	15.9	[5/8]	50.8	[2]
1/4t_1d_2e_2s_0.53α_4x4_BP	1/4t_1d_2e_2s_0.53α_4x4_UP	4 x 4 Rectangular	50.8	[2]	6.4	[1/4]	25.4	[1]	50.8	[2]
1/2t_5/8d_3e_2s_0.16α_4x4_BP	1/2t_5/8d_3e_2s_0.16α_4x4_UP	4 x 4 Rectangular	50.8	[2]	12.7	[1/2]	15.9	[5/8]	76.2	[3]
1/2t_1d_3e_2s_0.47α_4x4_BP	1/2t_1d_3e_2s_0.47α_4x4_UP	4 x 4 Rectangular	50.8	[2]	12.7	[1/2]	25.4	[1]	76.2	[3]
1/2t_5/8d_2e_2s_0.17α_4x4_BP	1/2t_5/8d_2e_2s_0.17α_4x4_UP	4 x 4 Rectangular	50.8	[2]	12.7	[1/2]	15.9	[5/8]	50.8	[2]
1/2t_1d_2e_2s_0.53α_4x4_BP	1/2t_1d_2e_2s_0.53α_4x4_UP	4 x 4 Rectangular	50.8	[2]	12.7	[1/2]	25.4	[1]	50.8	[2]
1t_5/8d_3e_2s_0.16α_4x4_BP	1t_5/8d_3e_2s_0.16α_4x4_UP	4 x 4 Rectangular	50.8	[2]	25.4	[1]	15.9	[5/8]	76.2	[3]
1t_1d_3e_2s_0.47α_4x4_BP	1t_1d_3e_2s_0.47α_4x4_UP	4 x 4 Rectangular	50.8	[2]	25.4	[1]	25.4	[1]	76.2	[3]
1t_5/8d_2e_2s_0.17α_4x4_BP	1t_5/8d_2e_2s_0.17α_4x4_UP	4 x 4 Rectangular	50.8	[2]	25.4	[1]	15.9	[5/8]	50.8	[2]
1t_1d_2e_2s_0.53α_4x4_BP	1t_1d_2e_2s_0.53α_4x4_UP	4 x 4 Rectangular	50.8	[2]	25.4	[1]	25.4	[1]	50.8	[2]

Table B. 2: 3X3 Rectangular Bolt Pattern Model Matrix

Model Name	Model Name	Bolt Pattern	Bolt Spacing *s*		Plate Thickness *t*		Bolt Diameter *d*		Edge Distance *e*	
Bolted Plate	Unbolted Plate		mm	[in]	mm	[in]	mm	[in]	mm	[in]
1/4t_5/8d_3e_3s_0.15α_3x3_BP	1/4t_5/8d_3e_3s_0.15α_3x3_UP	3 x 3 Rectangular	76.2	[3]	6.4	[1/4]	15.9	[5/8]	76.2	[3]
1/4t_1d_3e_3s_0.42α_3x3_BP	1/4t_1d_3e_3s_0.42α_3x3_UP	3 x 3 Rectangular	76.2	[3]	6.4	[1/4]	25.4	[1]	76.2	[3]
1/4t_5/8d_2e_3s_0.16α_3x3_BP	1/4t_5/8d_2e_3s_0.16α_3x3_UP	3 x 3 Rectangular	76.2	[3]	6.4	[1/4]	15.9	[5/8]	50.8	[2]
1/4t_1d_2e_3s_0.45α_3x3_BP	1/4t_1d_2e_3s_0.45α_3x3_UP	3 x 3 Rectangular	76.2	[3]	6.4	[1/4]	25.4	[1]	50.8	[2]
1/2t_5/8d_3e_3s_0.15α_3x3_BP	1/2t_5/8d_3e_3s_0.15α_3x3_UP	3 x 3 Rectangular	76.2	[3]	12.7	[1/2]	15.9	[5/8]	76.2	[3]
1/2t_1d_3e_3s_0.42α_3x3_BP	1/2t_1d_3e_3s_0.42α_3x3_UP	3 x 3 Rectangular	76.2	[3]	12.7	[1/2]	25.4	[1]	76.2	[3]
1/2t_5/8d_2e_3s_0.16α_3x3_BP	1/2t_5/8d_2e_3s_0.16α_3x3_UP	3 x 3 Rectangular	76.2	[3]	12.7	[1/2]	15.9	[5/8]	50.8	[2]
1/2t_1d_2e_3s_0.45α_3x3_BP	1/2t_1d_2e_3s_0.45α_3x3_UP	3 x 3 Rectangular	76.2	[3]	12.7	[1/2]	25.4	[1]	50.8	[2]
1t_5/8d_3e_3s_0.15α_3x3_BP	1t_5/8d_3e_3s_0.15α_3x3_UP	3 x 3 Rectangular	76.2	[3]	25.4	[1]	15.9	[5/8]	76.2	[3]
1t_1d_3e_3s_0.42α_3x3_BP	1t_1d_3e_3s_0.42α_3x3_UP	3 x 3 Rectangular	76.2	[3]	25.4	[1]	25.4	[1]	76.2	[3]
1t_5/8d_2e_3s_0.16α_3x3_BP	1t_5/8d_2e_3s_0.16α_3x3_UP	3 x 3 Rectangular	76.2	[3]	25.4	[1]	15.9	[5/8]	50.8	[2]
1t_1d_2e_3s_0.45α_3x3_BP	1t_1d_2e_3s_0.45α_3x3_UP	3 x 3 Rectangular	76.2	[3]	25.4	[1]	25.4	[1]	50.8	[2]
1/4t_5/8d_3e_2s_0.16α_3x3_BP	1/4t_5/8d_3e_2s_0.16α_3x3_UP	3 x 3 Rectangular	50.8	[2]	6.4	[1/4]	15.9	[5/8]	76.2	[3]
1/4t_1d_3e_2s_0.45α_3x3_BP	1/4t_1d_3e_2s_0.45α_3x3_UP	3 x 3 Rectangular	50.8	[2]	6.4	[1/4]	25.4	[1]	76.2	[3]
1/4t_5/8d_2e_2s_0.17α_3x3_BP	1/4t_5/8d_2e_2s_0.17α_3x3_UP	3 x 3 Rectangular	50.8	[2]	6.4	[1/4]	15.9	[5/8]	50.8	[2]
1/4t_1d_2e_2s_0.51α_3x3_BP	1/4t_1d_2e_2s_0.51α_3x3_UP	3 x 3 Rectangular	50.8	[2]	6.4	[1/4]	25.4	[1]	50.8	[2]
1/2t_5/8d_3e_2s_0.16α_3x3_BP	1/2t_5/8d_3e_2s_0.16α_3x3_UP	3 x 3 Rectangular	50.8	[2]	12.7	[1/2]	15.9	[5/8]	76.2	[3]
1/2t_1d_3e_2s_0.45α_3x3_BP	1/2t_1d_3e_2s_0.45α_3x3_UP	3 x 3 Rectangular	50.8	[2]	12.7	[1/2]	25.4	[1]	76.2	[3]
1/2t_5/8d_2e_2s_0.17α_3x3_BP	1/2t_5/8d_2e_2s_0.17α_3x3_UP	3 x 3 Rectangular	50.8	[2]	12.7	[1/2]	15.9	[5/8]	50.8	[2]
1/2t_1d_2e_2s_0.51α_3x3_BP	1/2t_1d_2e_2s_0.51α_3x3_UP	3 x 3 Rectangular	50.8	[2]	12.7	[1/2]	25.4	[1]	50.8	[2]
1t_5/8d_3e_2s_0.16α_3x3_BP	1t_5/8d_3e_2s_0.16α_3x3_UP	3 x 3 Rectangular	50.8	[2]	25.4	[1]	15.9	[5/8]	76.2	[3]
1t_1d_3e_2s_0.45α_3x3_BP	1t_1d_3e_2s_0.45α_3x3_UP	3 x 3 Rectangular	50.8	[2]	25.4	[1]	25.4	[1]	76.2	[3]
1t_5/8d_2e_2s_0.17α_3x3_BP	1t_5/8d_2e_2s_0.17α_3x3_UP	3 x 3 Rectangular	50.8	[2]	25.4	[1]	15.9	[5/8]	50.8	[2]
1t_1d_2e_2s_0.51α_3x3_BP	1t_1d_2e_2s_0.51α_3x3_UP	3 x 3 Rectangular	50.8	[2]	25.4	[1]	25.4	[1]	50.8	[2]

Table B. 3: 5-bolt Staggered Bolt Pattern Model Matrix

Model Name	Model Name	Bolt Pattern	Bolt Spacing *s*		Plate Thickness *t*		Bolt Diameter *d*		Edge Distance *e*	
Bolted Plate	Unbolted Plate		mm	[in]	mm	[in]	mm	[in]	mm	[in]
1/4t_5/8d_3e_3s_0.15α_5_BP	1/4t_5/8d_3e_3s_0.15α_5_UP	5-bolt staggered	76.2	[3]	6.4	[1/4]	15.9	[5/8]	76.2	[3]
1/4t_1d_3e_3s_0.37α_5_BP	1/4t_1d_3e_3s_0.37α_5_UP	5-bolt staggered	76.2	[3]	6.4	[1/4]	25.4	[1]	76.2	[3]
1/4t_5/8d_2e_3s_0.14α_5_BP	1/4t_5/8d_2e_3s_0.14α_5_UP	5-bolt staggered	76.2	[3]	6.4	[1/4]	15.9	[5/8]	50.8	[2]
1/4t_1d_2e_3s_0.39α_5_BP	1/4t_1d_2e_3s_0.39α_5_UP	5-bolt staggered	76.2	[3]	6.4	[1/4]	25.4	[1]	50.8	[2]
1/2t_5/8d_3e_3s_0.14α_5_BP	1/2t_5/8d_3e_3s_0.14α_5_UP	5-bolt staggered	76.2	[3]	12.7	[1/2]	15.9	[5/8]	76.2	[3]
1/2t_1d_3e_3s_0.37α_5_BP	1/2t_1d_3e_3s_0.37α_5_UP	5-bolt staggered	76.2	[3]	12.7	[1/2]	25.4	[1]	76.2	[3]
1/2t_5/8d_2e_3s_0.14α_5_BP	1/2t_5/8d_2e_3s_0.14α_5_UP	5-bolt staggered	76.2	[3]	12.7	[1/2]	15.9	[5/8]	50.8	[2]
1/2t_1d_2e_3s_0.39α_5_BP	1/2t_1d_2e_3s_0.39α_5_UP	5-bolt staggered	76.2	[3]	12.7	[1/2]	25.4	[1]	50.8	[2]
1t_5/8d_3e_3s_0.14α_5_BP	1t_5/8d_3e_3s_0.14α_5_UP	5-bolt staggered	76.2	[3]	25.4	[1]	15.9	[5/8]	76.2	[3]
1t_1d_3e_3s_0.37α_5_BP	1t_1d_3e_3s_0.37α_5_UP	5-bolt staggered	76.2	[3]	25.4	[1]	25.4	[1]	76.2	[3]
1t_5/8d_2e_3s_0.14α_5_BP	1t_5/8d_2e_3s_0.14α_5_UP	5-bolt staggered	76.2	[3]	25.4	[1]	15.9	[5/8]	50.8	[2]
1t_1d_2e_3s_0.39α_5_BP	1t_1d_2e_3s_0.39α_5_UP	5-bolt staggered	76.2	[3]	25.4	[1]	25.4	[1]	50.8	[2]
1/4t_5/8d_3e_2s_0.14α_5_BP	1/4t_5/8d_3e_2s_0.14α_5_UP	5-bolt staggered	50.8	[2]	6.4	[1/4]	15.9	[5/8]	76.2	[3]
1/4t_1d_3e_2s_0.39α_5_BP	1/4t_1d_3e_2s_0.39α_5_UP	5-bolt staggered	50.8	[2]	6.4	[1/4]	25.4	[1]	76.2	[3]
1/4t_5/8d_2e_2s_0.15α_5_BP	1/4t_5/8d_2e_2s_0.15α_5_UP	5-bolt staggered	50.8	[2]	6.4	[1/4]	15.9	[5/8]	50.8	[2]
1/4t_1d_2e_2s_0.42α_5_BP	1/4t_1d_2e_2s_0.42α_5_UP	5-bolt staggered	50.8	[2]	6.4	[1/4]	25.4	[1]	50.8	[2]
1/2t_5/8d_3e_2s_0.14α_5_BP	1/2t_5/8d_3e_2s_0.14α_5_UP	5-bolt staggered	50.8	[2]	12.7	[1/2]	15.9	[5/8]	76.2	[3]
1/2t_1d_3e_2s_0.39α_5_BP	1/2t_1d_3e_2s_0.39α_5_UP	5-bolt staggered	50.8	[2]	12.7	[1/2]	25.4	[1]	76.2	[3]
1/2t_5/8d_2e_2s_0.15α_5_BP	1/2t_5/8d_2e_2s_0.15α_5_UP	5-bolt staggered	50.8	[2]	12.7	[1/2]	15.9	[5/8]	50.8	[2]
1/2t_1d_2e_2s_0.42α_5_BP	1/2t_1d_2e_2s_0.42α_5_UP	5-bolt staggered	50.8	[2]	12.7	[1/2]	25.4	[1]	50.8	[2]
1t_5/8d_3e_2s_0.14α_5_BP	1t_5/8d_3e_2s_0.14α_5_UP	5-bolt staggered	50.8	[2]	25.4	[1]	15.9	[5/8]	76.2	[3]
1t_1d_3e_2s_0.39α_5_BP	1t_1d_3e_2s_0.39α_5_UP	5-bolt staggered	50.8	[2]	25.4	[1]	25.4	[1]	76.2	[3]
1t_5/8d_2e_2s_0.15α_5_BP	1t_5/8d_2e_2s_0.15α_5_UP	5-bolt staggered	50.8	[2]	25.4	[1]	15.9	[5/8]	50.8	[2]
1t_1d_2e_2s_0.42α_5_BP	1t_1d_2e_2s_0.42α_5_UP	5-bolt staggered	50.8	[2]	25.4	[1]	25.4	[1]	50.8	[2]

APPENDIX C COMPLETED MODELS

Table C. 1: List of Completed Models (4x4)

Model Name	Model Name	Bolt Pattern	Bolt Spacing *s*		Plate Thickness *t*		Bolt Diameter *d*		Edge Distance *e*	
Bolted Plate	Unbolted Plate		mm	[in]	mm	[in]	mm	[in]	mm	[in]
1/4t_5/8d_3e_3s_0.15α_4x4_BP	1/4t_5/8d_3e_3s_0.15α_4x4_UP	4 x 4 Rectangular	76.2	[3]	6.4	[1/4]	15.9	[5/8]	76.2	[3]
1/4t_1d_3e_3s_0.43α_4x4_BP	1/4t_1d_3e_3s_0.43α_4x4_UP	4 x 4 Rectangular	76.2	[3]	6.4	[1/4]	25.4	[1]	76.2	[3]
1/4t_5/8d_2e_3s_0.16α_4x4_BP	1/4t_5/8d_2e_3s_0.16α_4x4_UP	4 x 4 Rectangular	76.2	[3]	6.4	[1/4]	15.9	[5/8]	50.8	[2]
1/4t_1d_2e_3s_0.45α_4x4_BP	1/4t_1d_2e_3s_0.45α_4x4_UP	4 x 4 Rectangular	76.2	[3]	6.4	[1/4]	25.4	[1]	50.8	[2]
1/2t_5/8d_3e_3s_0.15α_4x4_BP	1/2t_5/8d_3e_3s_0.15α_4x4_UP	4 x 4 Rectangular	76.2	[3]	12.7	[1/2]	15.9	[5/8]	76.2	[3]
1/2t_1d_3e_3s_0.43α_4x4_BP	1/2t_1d_3e_3s_0.43α_4x4_UP	4 x 4 Rectangular	76.2	[3]	12.7	[1/2]	25.4	[1]	76.2	[3]
1/2t_5/8d_2e_3s_0.16α_4x4_BP	1/2t_5/8d_2e_3s_0.16α_4x4_UP	4 x 4 Rectangular	76.2	[3]	12.7	[1/2]	15.9	[5/8]	50.8	[2]
1/2t_1d_2e_3s_0.45α_4x4_BP	1/2t_1d_2e_3s_0.45α_4x4_UP	4 x 4 Rectangular	76.2	[3]	12.7	[1/2]	25.4	[1]	50.8	[2]
1t_5/8d_3e_3s_0.15α_4x4_BP	1t_5/8d_3e_3s_0.15α_4x4_UP	4 x 4 Rectangular	76.2	[3]	25.4	[1]	15.9	[5/8]	76.2	[3]
1t_1d_3e_3s_0.43α_4x4_BP	1t_1d_3e_3s_0.43α_4x4_UP	4 x 4 Rectangular	76.2	[3]	25.4	[1]	25.4	[1]	76.2	[3]
1t_5/8d_2e_3s_0.16α_4x4_BP	1t_5/8d_2e_3s_0.16α_4x4_UP	4 x 4 Rectangular	76.2	[3]	25.4	[1]	15.9	[5/8]	50.8	[2]
1t_1d_2e_3s_0.45α_4x4_BP	1t_1d_2e_3s_0.45α_4x4_UP	4 x 4 Rectangular	76.2	[3]	25.4	[1]	25.4	[1]	50.8	[2]
1/4t_5/8d_3e_2s_0.16α_4x4_BP	1/4t_5/8d_3e_2s_0.16α_4x4_UP	4 x 4 Rectangular	50.8	[2]	6.4	[1/4]	15.9	[5/8]	76.2	[3]
1/4t_1d_3e_2s_0.47α_4x4_BP	1/4t_1d_3e_2s_0.47α_4x4_UP	4 x 4 Rectangular	50.8	[2]	6.4	[1/4]	25.4	[1]	76.2	[3]
1/4t_5/8d_2e_2s_0.17α_4x4_BP	1/4t_5/8d_2e_2s_0.17α_4x4_UP	4 x 4 Rectangular	50.8	[2]	6.4	[1/4]	15.9	[5/8]	50.8	[2]
1/4t_1d_2e_2s_0.53α_4x4_BP	1/4t_1d_2e_2s_0.53α_4x4_UP	4 x 4 Rectangular	50.8	[2]	6.4	[1/4]	25.4	[1]	50.8	[2]
1/2t_5/8d_3e_2s_0.16α_4x4_BP	1/2t_5/8d_3e_2s_0.16α_4x4_UP	4 x 4 Rectangular	50.8	[2]	12.7	[1/2]	15.9	[5/8]	76.2	[3]
1/2t_1d_3e_2s_0.47α_4x4_BP	1/2t_1d_3e_2s_0.47α_4x4_UP	4 x 4 Rectangular	50.8	[2]	12.7	[1/2]	25.4	[1]	76.2	[3]
1/2t_5/8d_2e_2s_0.17α_4x4_BP	1/2t_5/8d_2e_2s_0.17α_4x4_UP	4 x 4 Rectangular	50.8	[2]	12.7	[1/2]	15.9	[5/8]	50.8	[2]
1/2t_1d_2e_2s_0.53α_4x4_BP	1/2t_1d_2e_2s_0.53α_4x4_UP	4 x 4 Rectangular	50.8	[2]	12.7	[1/2]	25.4	[1]	50.8	[2]
1t_5/8d_3e_2s_0.16α_4x4_BP	1t_5/8d_3e_2s_0.16α_4x4_UP	4 x 4 Rectangular	50.8	[2]	25.4	[1]	15.9	[5/8]	76.2	[3]
1t_1d_3e_2s_0.47α_4x4_BP	1t_1d_3e_2s_0.47α_4x4_UP	4 x 4 Rectangular	50.8	[2]	25.4	[1]	25.4	[1]	76.2	[3]
1t_5/8d_2e_2s_0.17α_4x4_BP	1t_5/8d_2e_2s_0.17α_4x4_UP	4 x 4 Rectangular	50.8	[2]	25.4	[1]	15.9	[5/8]	50.8	[2]
1t_1d_2e_2s_0.53α_4x4_BP	1t_1d_2e_2s_0.53α_4x4_UP	4 x 4 Rectangular	50.8	[2]	25.4	[1]	25.4	[1]	50.8	[2]
Note: highlighted in green: completed models										

Table C. 2: List of Completed Models (3x3)

Model Name	Model Name	Bolt Pattern	Bolt Spacing *s*		Plate Thickness *t*		Bolt Diameter *d*		Edge Distance *e*	
Bolted Plate	Unbolted Plate		mm	[in]	mm	[in]	mm	[in]	mm	[in]
1/4t_5/8d_3e_3s_0.15α_3x3_BP	1/4t_5/8d_3e_3s_0.15α_3x3_UP	3 x 3 Rectangular	76.2	[3]	6.4	[1/4]	15.9	[5/8]	76.2	[3]
1/4t_1d_3e_3s_0.42α_3x3_BP	1/4t_1d_3e_3s_0.42α_3x3_UP	3 x 3 Rectangular	76.2	[3]	6.4	[1/4]	25.4	[1]	76.2	[3]
1/4t_5/8d_2e_3s_0.16α_3x3_BP	1/4t_5/8d_2e_3s_0.16α_3x3_UP	3 x 3 Rectangular	76.2	[3]	6.4	[1/4]	15.9	[5/8]	50.8	[2]
1/4t_1d_2e_3s_0.45α_3x3_BP	1/4t_1d_2e_3s_0.45α_3x3_UP	3 x 3 Rectangular	76.2	[3]	6.4	[1/4]	25.4	[1]	50.8	[2]
1/2t_5/8d_3e_3s_0.15α_3x3_BP	1/2t_5/8d_3e_3s_0.15α_3x3_UP	3 x 3 Rectangular	76.2	[3]	12.7	[1/2]	15.9	[5/8]	76.2	[3]
1/2t_1d_3e_3s_0.42α_3x3_BP	1/2t_1d_3e_3s_0.42α_3x3_UP	3 x 3 Rectangular	76.2	[3]	12.7	[1/2]	25.4	[1]	76.2	[3]
1/2t_5/8d_2e_3s_0.16α_3x3_BP	1/2t_5/8d_2e_3s_0.16α_3x3_UP	3 x 3 Rectangular	76.2	[3]	12.7	[1/2]	15.9	[5/8]	50.8	[2]
1/2t_1d_2e_3s_0.45α_3x3_BP	1/2t_1d_2e_3s_0.45α_3x3_UP	3 x 3 Rectangular	76.2	[3]	12.7	[1/2]	25.4	[1]	50.8	[2]
1t_5/8d_3e_3s_0.15α_3x3_BP	1t_5/8d_3e_3s_0.15α_3x3_UP	3 x 3 Rectangular	76.2	[3]	25.4	[1]	15.9	[5/8]	76.2	[3]
1t_1d_3e_3s_0.42α_3x3_BP	1t_1d_3e_3s_0.42α_3x3_UP	3 x 3 Rectangular	76.2	[3]	25.4	[1]	25.4	[1]	76.2	[3]
1t_5/8d_2e_3s_0.16α_3x3_BP	1t_5/8d_2e_3s_0.16α_3x3_UP	3 x 3 Rectangular	76.2	[3]	25.4	[1]	15.9	[5/8]	50.8	[2]
1t_1d_2e_3s_0.45α_3x3_BP	1t_1d_2e_3s_0.45α_3x3_UP	3 x 3 Rectangular	76.2	[3]	25.4	[1]	25.4	[1]	50.8	[2]
1/4t_5/8d_3e_2s_0.16α_3x3_BP	1/4t_5/8d_3e_2s_0.16α_3x3_UP	3 x 3 Rectangular	50.8	[2]	6.4	[1/4]	15.9	[5/8]	76.2	[3]
1/4t_1d_3e_2s_0.45α_3x3_BP	1/4t_1d_3e_2s_0.45α_3x3_UP	3 x 3 Rectangular	50.8	[2]	6.4	[1/4]	25.4	[1]	76.2	[3]
1/4t_5/8d_2e_2s_0.17α_3x3_BP	1/4t_5/8d_2e_2s_0.17α_3x3_UP	3 x 3 Rectangular	50.8	[2]	6.4	[1/4]	15.9	[5/8]	50.8	[2]
1/4t_1d_2e_2s_0.51α_3x3_BP	1/4t_1d_2e_2s_0.51α_3x3_UP	3 x 3 Rectangular	50.8	[2]	6.4	[1/4]	25.4	[1]	50.8	[2]
1/2t_5/8d_3e_2s_0.16α_3x3_BP	1/2t_5/8d_3e_2s_0.16α_3x3_UP	3 x 3 Rectangular	50.8	[2]	12.7	[1/2]	15.9	[5/8]	76.2	[3]
1/2t_1d_3e_2s_0.45α_3x3_BP	1/2t_1d_3e_2s_0.45α_3x3_UP	3 x 3 Rectangular	50.8	[2]	12.7	[1/2]	25.4	[1]	76.2	[3]
1/2t_5/8d_2e_2s_0.17α_3x3_BP	1/2t_5/8d_2e_2s_0.17α_3x3_UP	3 x 3 Rectangular	50.8	[2]	12.7	[1/2]	15.9	[5/8]	50.8	[2]
1/2t_1d_2e_2s_0.51α_3x3_BP	1/2t_1d_2e_2s_0.51α_3x3_UP	3 x 3 Rectangular	50.8	[2]	12.7	[1/2]	25.4	[1]	50.8	[2]
1t_5/8d_3e_2s_0.16α_3x3_BP	1t_5/8d_3e_2s_0.16α_3x3_UP	3 x 3 Rectangular	50.8	[2]	25.4	[1]	15.9	[5/8]	76.2	[3]
1t_1d_3e_2s_0.45α_3x3_BP	1t_1d_3e_2s_0.45α_3x3_UP	3 x 3 Rectangular	50.8	[2]	25.4	[1]	25.4	[1]	76.2	[3]
1t_5/8d_2e_2s_0.17α_3x3_BP	1t_5/8d_2e_2s_0.17α_3x3_UP	3 x 3 Rectangular	50.8	[2]	25.4	[1]	15.9	[5/8]	50.8	[2]
1t_1d_2e_2s_0.51α_3x3_BP	1t_1d_2e_2s_0.51α_3x3_UP	3 x 3 Rectangular	50.8	[2]	25.4	[1]	25.4	[1]	50.8	[2]

Note: highlighted in green: completed models

Table C. 3: List of Completed Models (5-bolt staggered)

Model Name	**Model Name**	**Bolt Pattern**	**Bolt Spacing** *s*		**Plate Thickness** *t*		**Bolt Diameter** *d*		**Edge Distance** *e*	
Bolted Plate	Unbolted Plate		mm	[in]	mm	[in]	mm	[in]	mm	[in]
1/4t_5/8d_3e_3s_0.15α_5_BP	1/4t_5/8d_3e_3s_0.15α_5_UP	5-bolt staggered	76.2	[3]	6.4	[1/4]	15.9	[5/8]	76.2	[3]
1/4t_1d_3e_3s_0.37α_5_BP	1/4t_1d_3e_3s_0.37α_5_UP	5-bolt staggered	76.2	[3]	6.4	[1/4]	25.4	[1]	76.2	[3]
1/4t_5/8d_2e_3s_0.14α_5_BP	1/4t_5/8d_2e_3s_0.14α_5_UP	5-bolt staggered	76.2	[3]	6.4	[1/4]	15.9	[5/8]	50.8	[2]
1/4t_1d_2e_3s_0.39α_5_BP	1/4t_1d_2e_3s_0.39α_5_UP	5-bolt staggered	76.2	[3]	6.4	[1/4]	25.4	[1]	50.8	[2]
1/2t_5/8d_3e_3s_0.14α_5_BP	1/2t_5/8d_3e_3s_0.14α_5_UP	5-bolt staggered	76.2	[3]	12.7	[1/2]	15.9	[5/8]	76.2	[3]
1/2t_1d_3e_3s_0.37α_5_BP	1/2t_1d_3e_3s_0.37α_5_UP	5-bolt staggered	76.2	[3]	12.7	[1/2]	25.4	[1]	76.2	[3]
1/2t_5/8d_2e_3s_0.14α_5_BP	1/2t_5/8d_2e_3s_0.14α_5_UP	5-bolt staggered	76.2	[3]	12.7	[1/2]	15.9	[5/8]	50.8	[2]
1/2t_1d_2e_3s_0.39α_5_BP	1/2t_1d_2e_3s_0.39α_5_UP	5-bolt staggered	76.2	[3]	12.7	[1/2]	25.4	[1]	50.8	[2]
1t_5/8d_3e_3s_0.14α_5_BP	1t_5/8d_3e_3s_0.14α_5_UP	5-bolt staggered	76.2	[3]	25.4	[1]	15.9	[5/8]	76.2	[3]
1t_1d_3e_3s_0.37α_5_BP	1t_1d_3e_3s_0.37α_5_UP	5-bolt staggered	76.2	[3]	25.4	[1]	25.4	[1]	76.2	[3]
1t_5/8d_2e_3s_0.14α_5_BP	1t_5/8d_2e_3s_0.14α_5_UP	5-bolt staggered	76.2	[3]	25.4	[1]	15.9	[5/8]	50.8	[2]
1t_1d_2e_3s_0.39α_5_BP	1t_1d_2e_3s_0.39α_5_UP	5-bolt staggered	76.2	[3]	25.4	[1]	25.4	[1]	50.8	[2]
1/4t_5/8d_3e_2s_0.14α_5_BP	1/4t_5/8d_3e_2s_0.14α_5_UP	5-bolt staggered	50.8	[2]	6.4	[1/4]	15.9	[5/8]	76.2	[3]
1/4t_1d_3e_2s_0.39α_5_BP	1/4t_1d_3e_2s_0.39α_5_UP	5-bolt staggered	50.8	[2]	6.4	[1/4]	25.4	[1]	76.2	[3]
1/4t_5/8d_2e_2s_0.15α_5_BP	1/4t_5/8d_2e_2s_0.15α_5_UP	5-bolt staggered	50.8	[2]	6.4	[1/4]	15.9	[5/8]	50.8	[2]
1/4t_1d_2e_2s_0.42α_5_BP	1/4t_1d_2e_2s_0.42α_5_UP	5-bolt staggered	50.8	[2]	6.4	[1/4]	25.4	[1]	50.8	[2]
1/2t_5/8d_3e_2s_0.14α_5_BP	1/2t_5/8d_3e_2s_0.14α_5_UP	5-bolt staggered	50.8	[2]	12.7	[1/2]	15.9	[5/8]	76.2	[3]
1/2t_1d_3e_2s_0.39α_5_BP	1/2t_1d_3e_2s_0.39α_5_UP	5-bolt staggered	50.8	[2]	12.7	[1/2]	25.4	[1]	76.2	[3]
1/2t_5/8d_2e_2s_0.15α_5_BP	1/2t_5/8d_2e_2s_0.15α_5_UP	5-bolt staggered	50.8	[2]	12.7	[1/2]	15.9	[5/8]	50.8	[2]
1/2t_1d_2e_2s_0.42α_5_BP	1/2t_1d_2e_2s_0.42α_5_UP	5-bolt staggered	50.8	[2]	12.7	[1/2]	25.4	[1]	50.8	[2]
1t_5/8d_3e_2s_0.14α_5_BP	1t_5/8d_3e_2s_0.14α_5_UP	5-bolt staggered	50.8	[2]	25.4	[1]	15.9	[5/8]	76.2	[3]
1t_1d_3e_2s_0.39α_5_BP	1t_1d_3e_2s_0.39α_5_UP	5-bolt staggered	50.8	[2]	25.4	[1]	25.4	[1]	76.2	[3]
1t_5/8d_2e_2s_0.15α_5_BP	1t_5/8d_2e_2s_0.15α_5_UP	5-bolt staggered	50.8	[2]	25.4	[1]	15.9	[5/8]	50.8	[2]
1t_1d_2e_2s_0.42α_5_BP	1t_1d_2e_2s_0.42α_5_UP	5-bolt staggered	50.8	[2]	25.4	[1]	25.4	[1]	50.8	[2]
Note: highlighted in green: completed models										

APPENDIX D STRESS DISTRIBUTIONS

This appendix section represents the stress distributions of all investigated models. In each figure, the stress distributions are shown in (a), and screenshots from FE models are provided in (b).

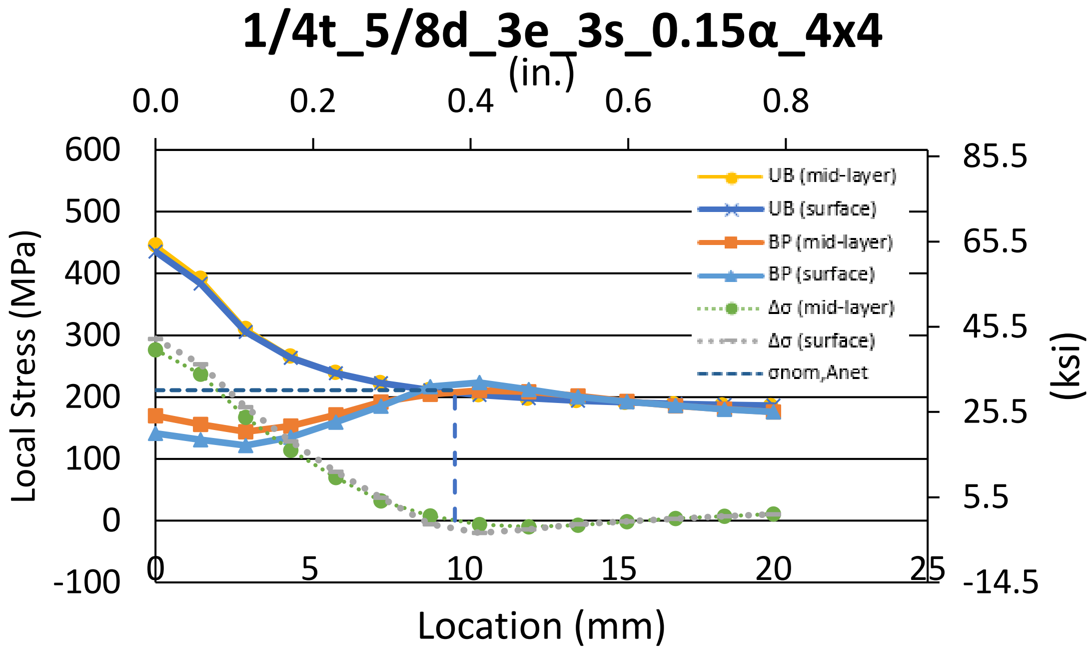

(a)Stress Distributions

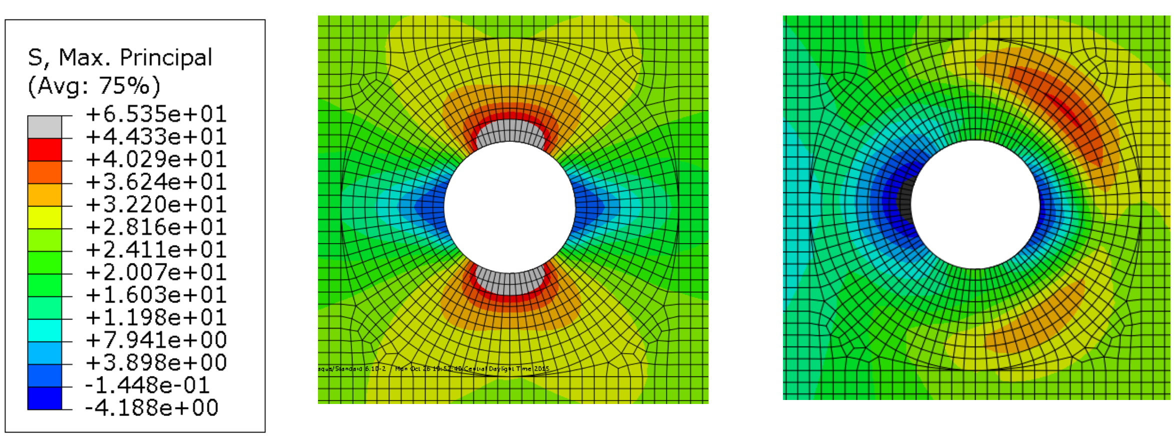

Unbolted Plate

Bolted Plate

$\sigma_{nom,Anet}$ = 30.61 ksi

(b) FEM screenshots

Figure D. 1: 1/4t_5/8d_3e_3s_0.15α_4x4

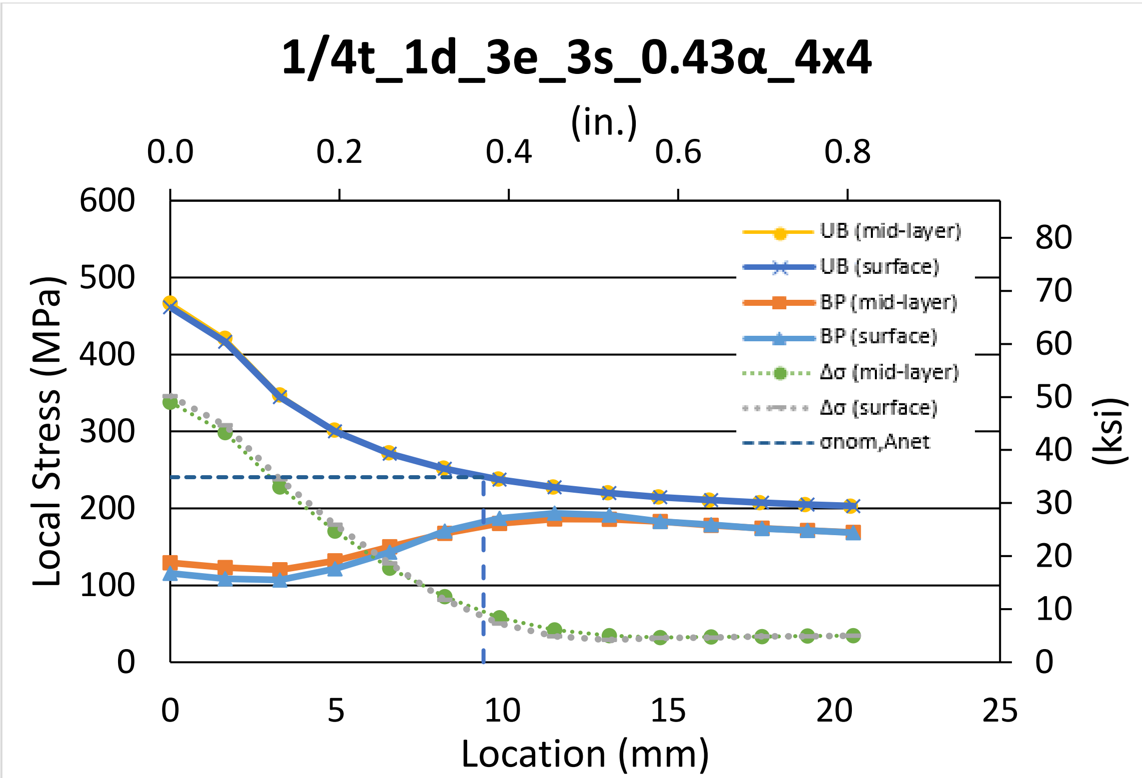

(a)Stress Distributions

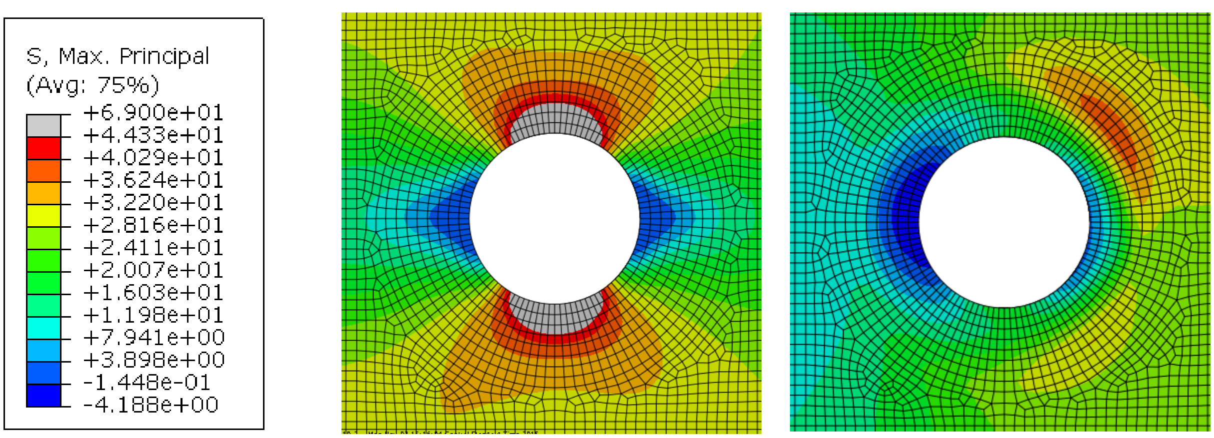

Unbolted Plate

Bolted Plate

$\sigma_{nom,Anet}$ = 34.88 ksi

(b) FEM screenshots

Figure D. 2: 1/4t_1d_3e_3s_0.43α_4x4

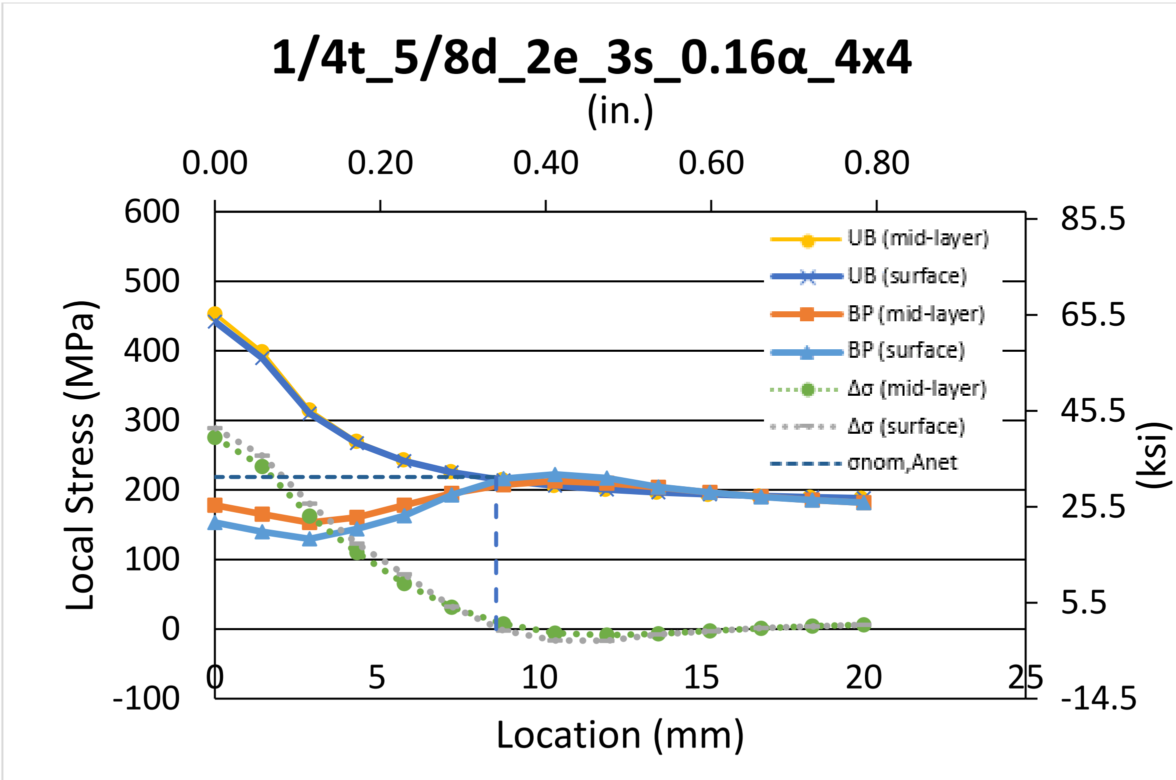

(a)Stress Distributions

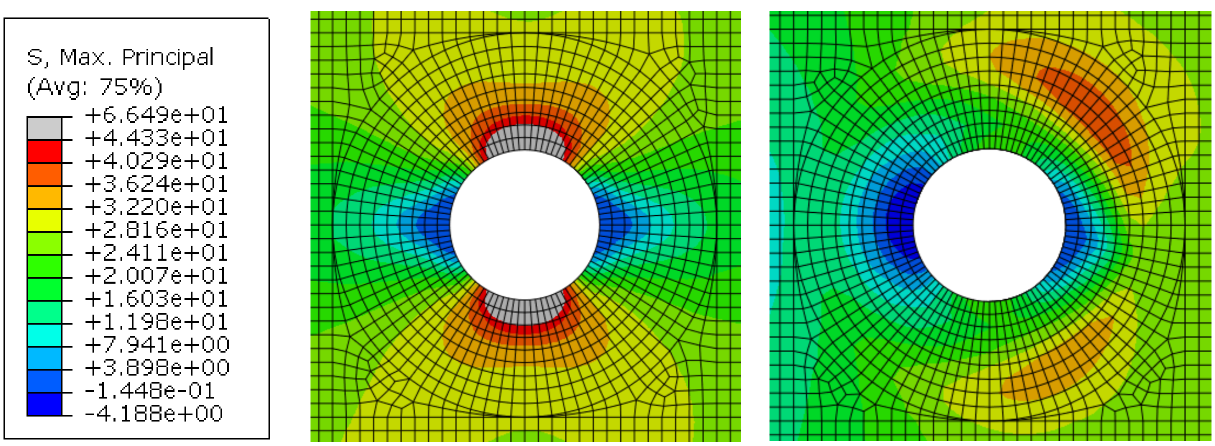

Unbolted Plate

Bolted Plate

$\sigma_{nom,Anet}$ = 31.71 ksi

(b) FEM screenshots

Figure D. 3: 1/4t_5/8d_2e_3s_0.16α_4x4

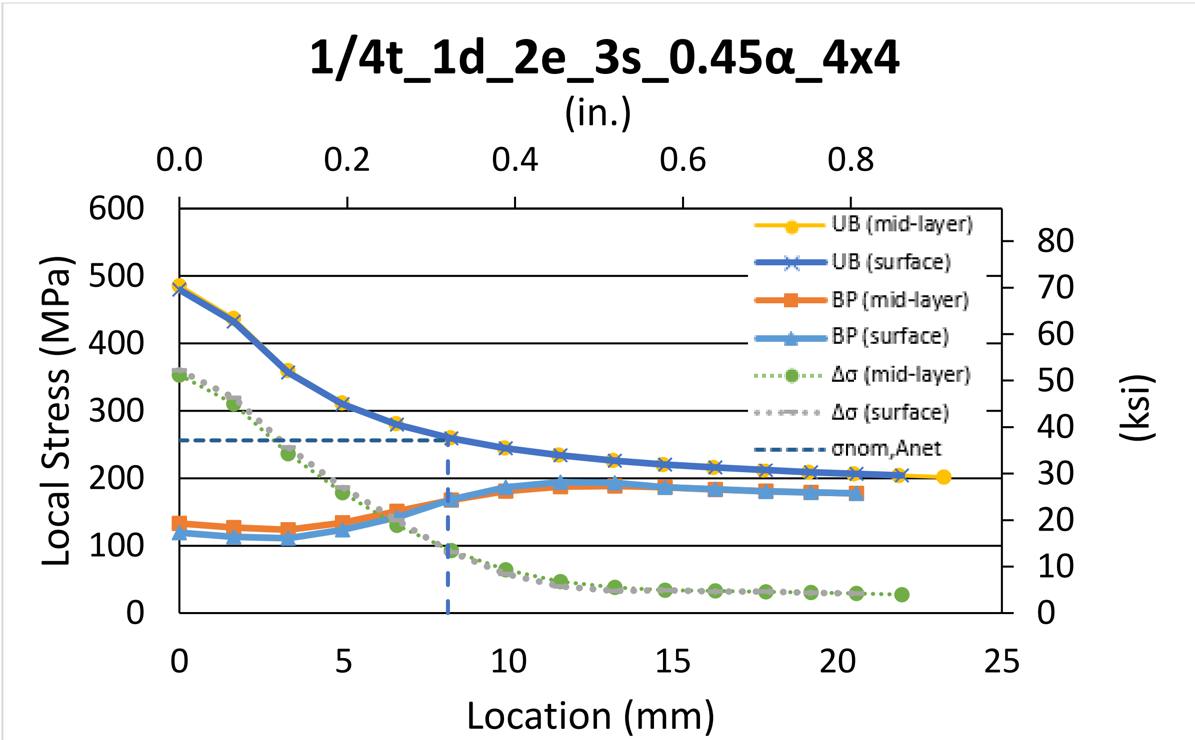

(a)Stress Distributions

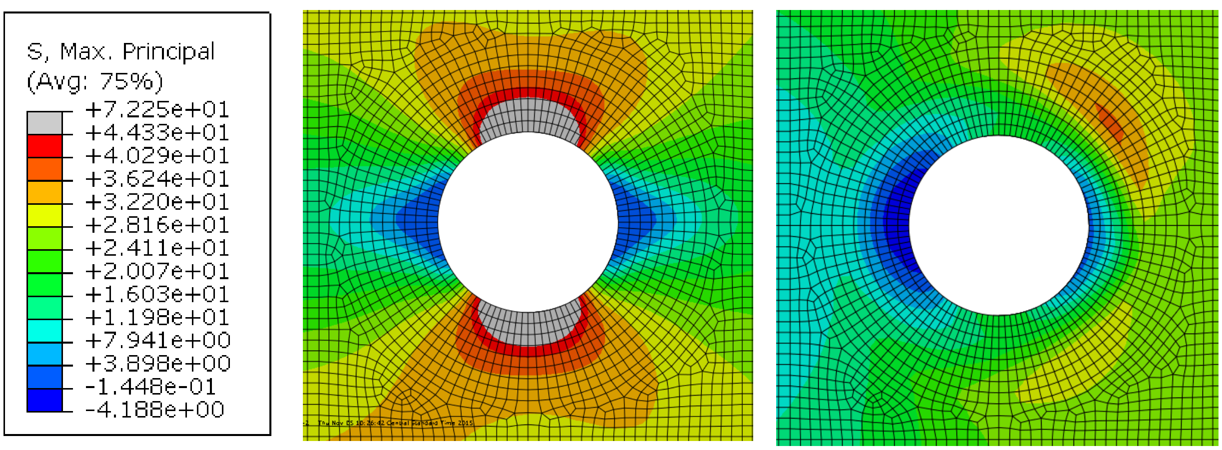

Unbolted Plate

Bolted Plate

$\sigma_{nom,Anet}$ = 37.14 ksi

(b) FEM screenshots

Figure D. 4: 1/4t_1d_2e_3s_0.45α_4x4

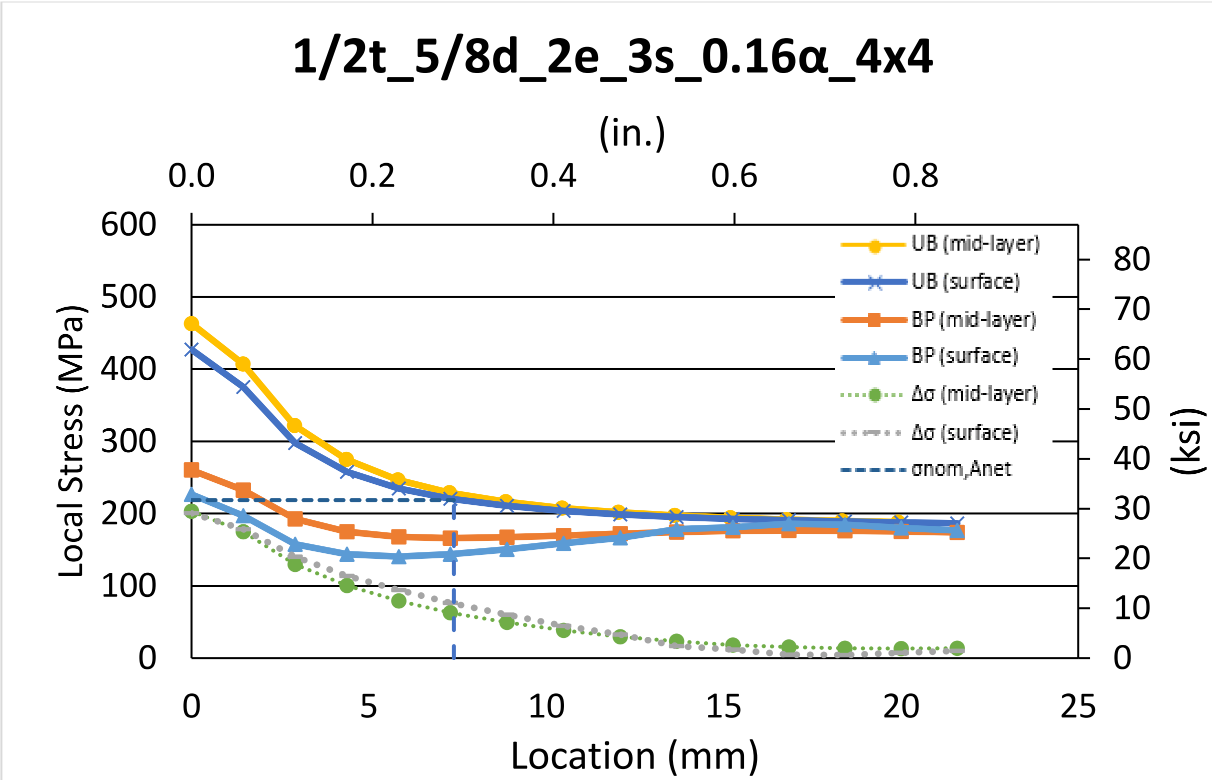

(a)Stress Distributions

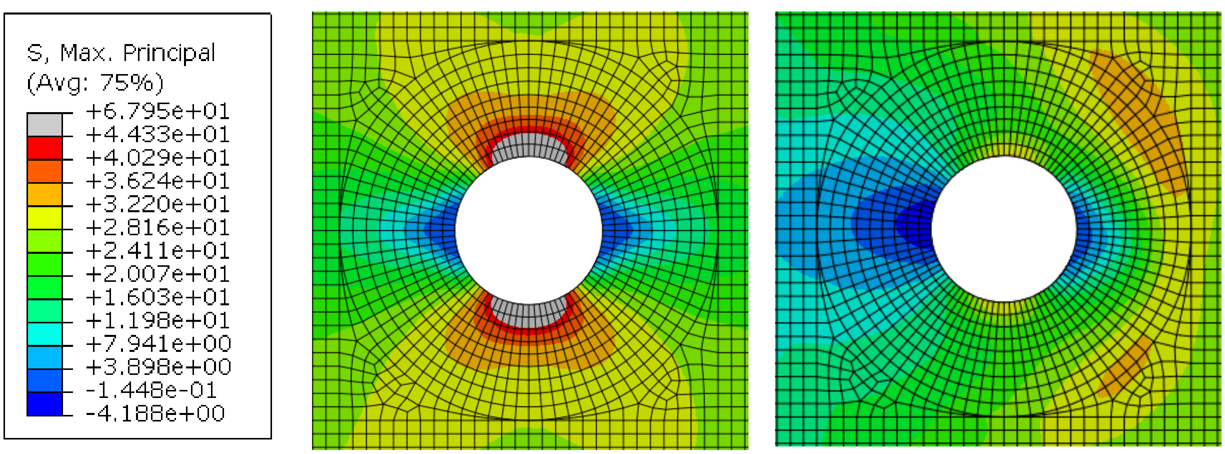

Unbolted Plate

Bolted Plate

$\sigma_{nom,Anet}$ = 31.71 ksi

(b) FEM screenshots

Figure D. 5: 1/2t_5/8d_2e_3s_0.16α_4x4

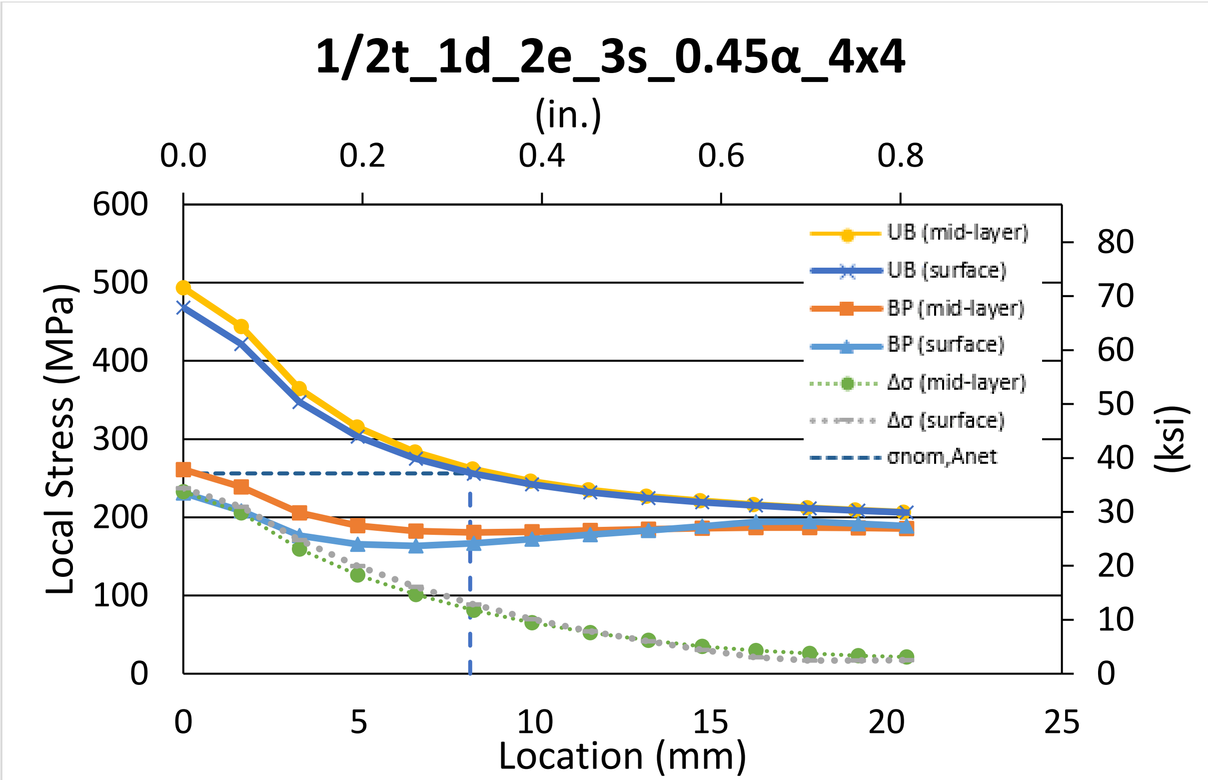

(a)Stress Distributions

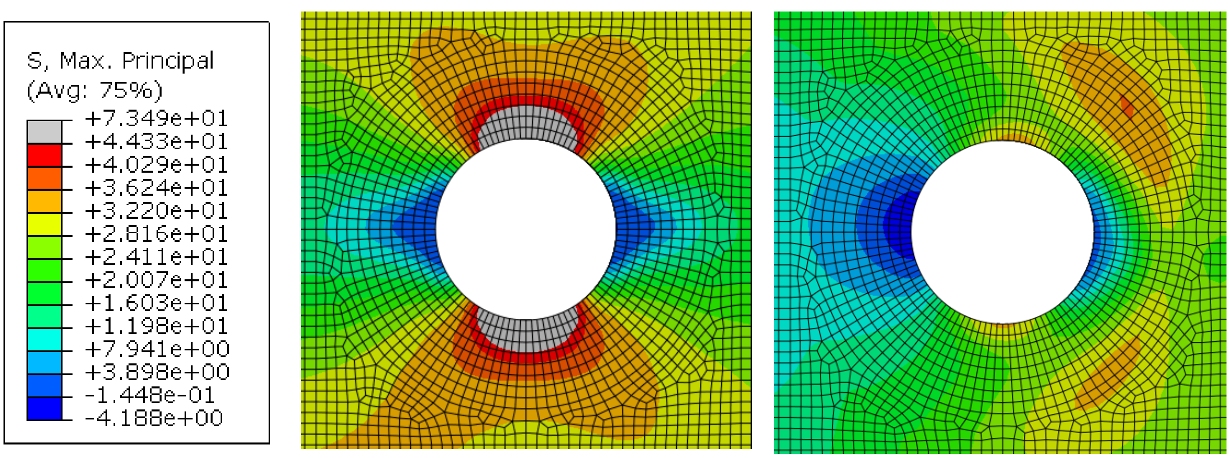

Unbolted Plate

Bolted Plate

$\sigma_{nom,Anet}$ = 37.14 ksi

(b) FEM screenshots

Figure D. 6: 1/2t_1d_2e_3s_0.45α_4x4

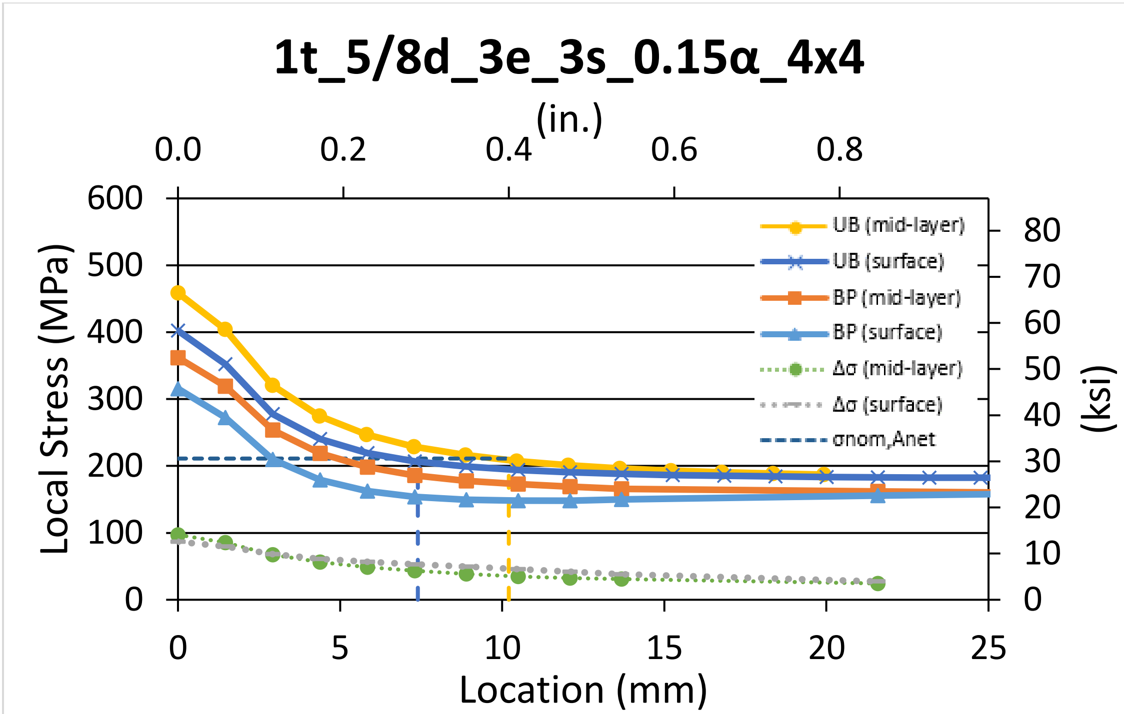

(a)Stress Distributions

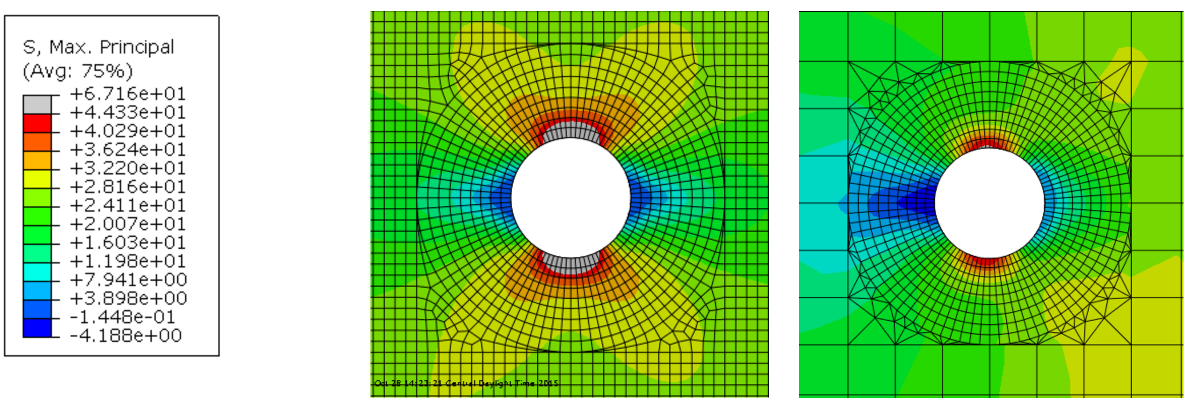

Unbolted Plate

Bolted Plate

$\sigma_{nom,Anet}$ = 30.61 ksi

(b) FEM screenshots

Figure D. 7: 1t_5/8d_3e_3s_0.15α_4x4

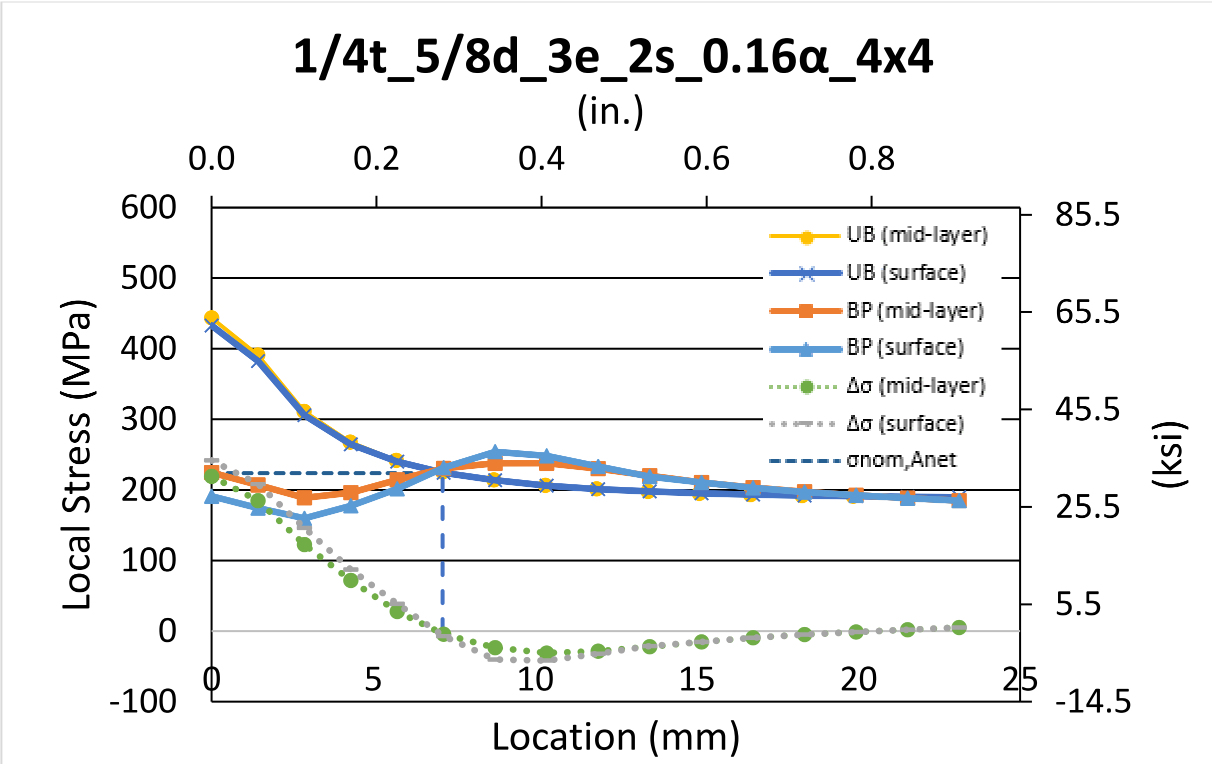

(a)Stress Distributions

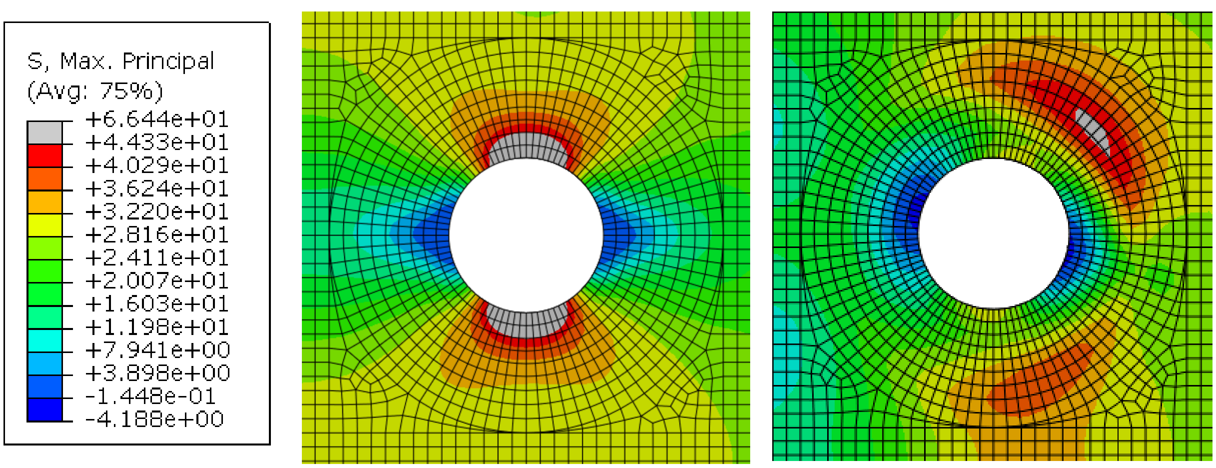

Unbolted Plate

Bolted Plate

$\sigma_{nom,Anet}$ = 32.43 ksi

(b) FEM screenshots

Figure D. 8: 1/4t_5/8d_3e_2s_0.16α_4x4

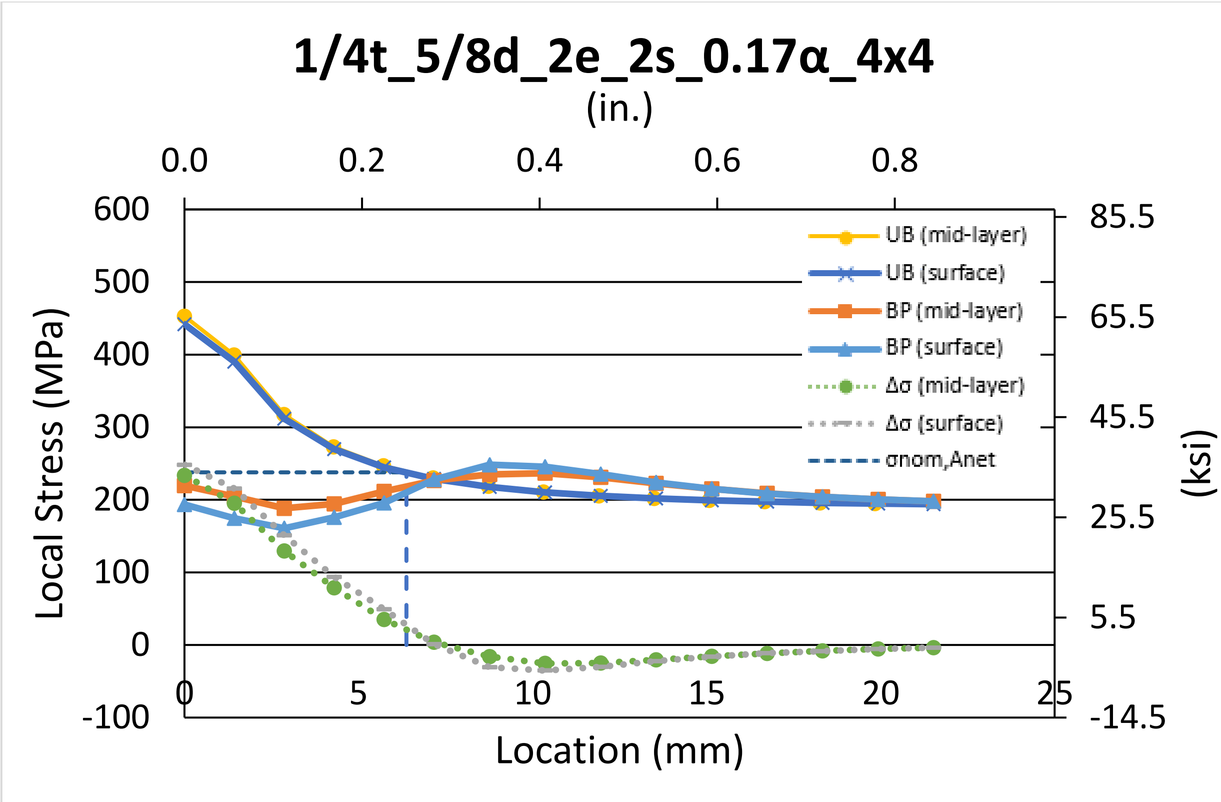

(a)Stress Distributions

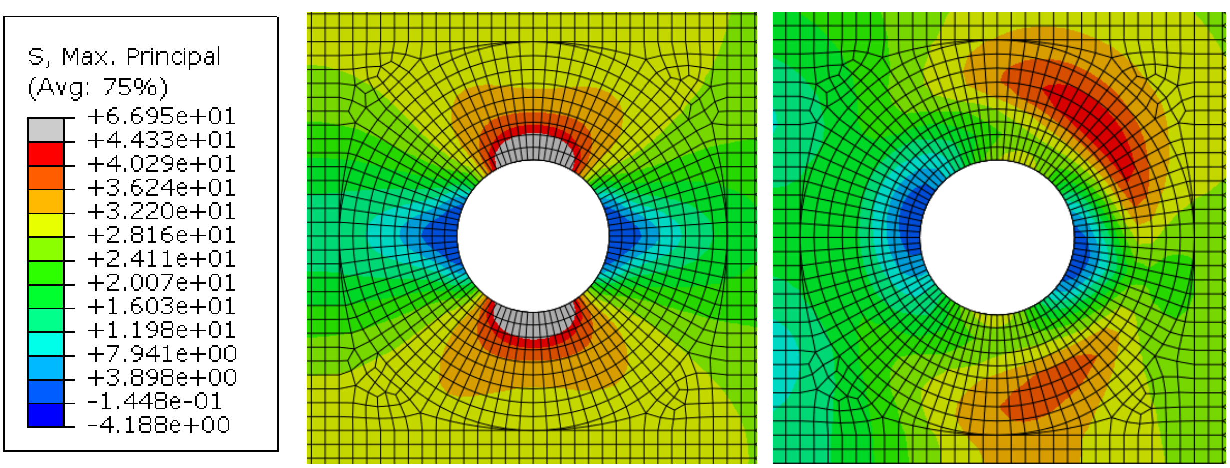

Unbolted Plate

Bolted Plate

$\sigma_{nom,Anet}$ = 34.48 ksi

(b) FEM screenshots

Figure D. 9: 1/4t_5/8d_2e_2s_0.17α_4x4

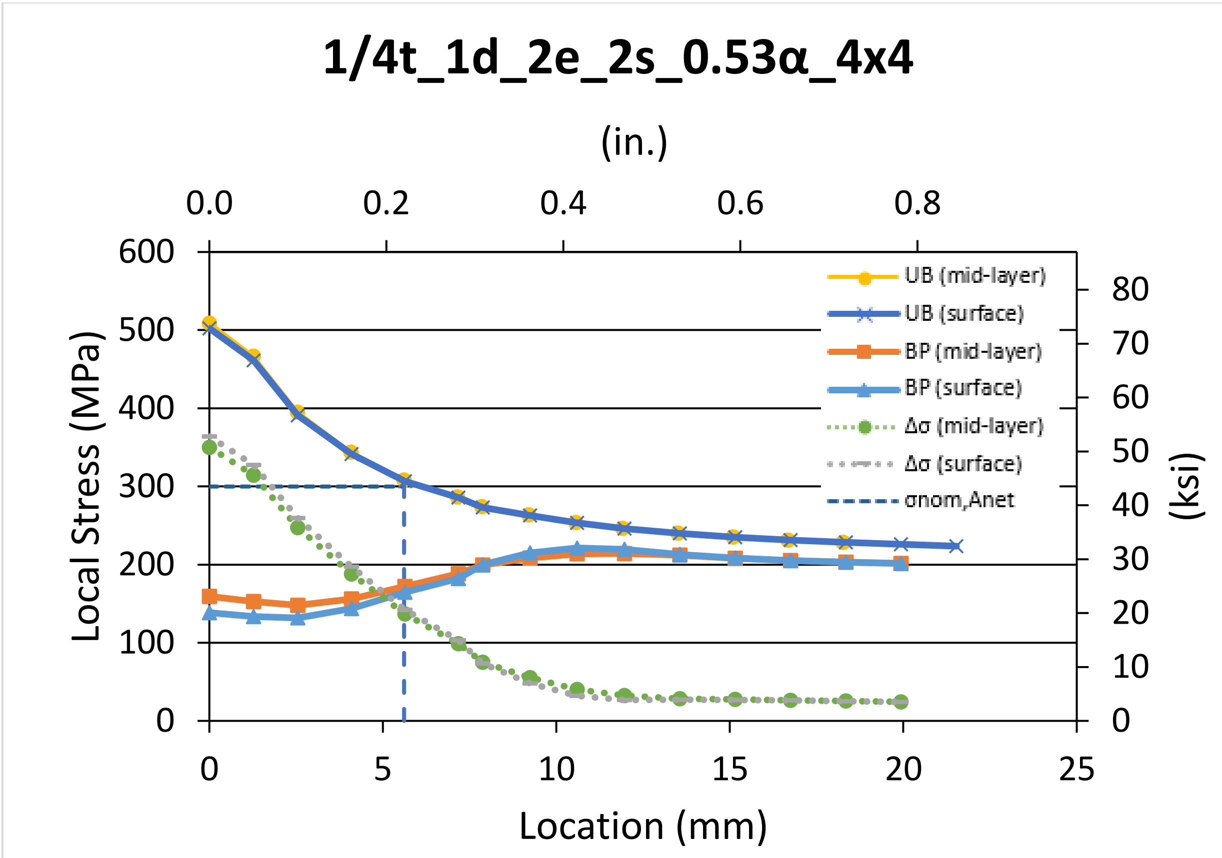

(a)Stress Distributions

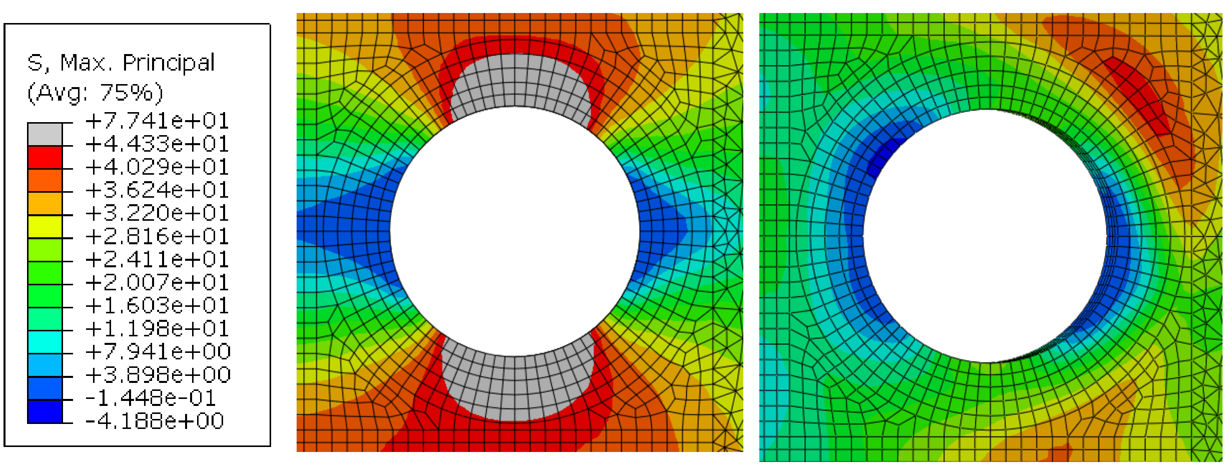

Unbolted Plate Bolted Plate

$\sigma_{nom,Anet}$ = 43.48 ksi

(b) FEM screenshots

Figure D. 10: 1/4t_1d_2e_2s_0.53α_4x4

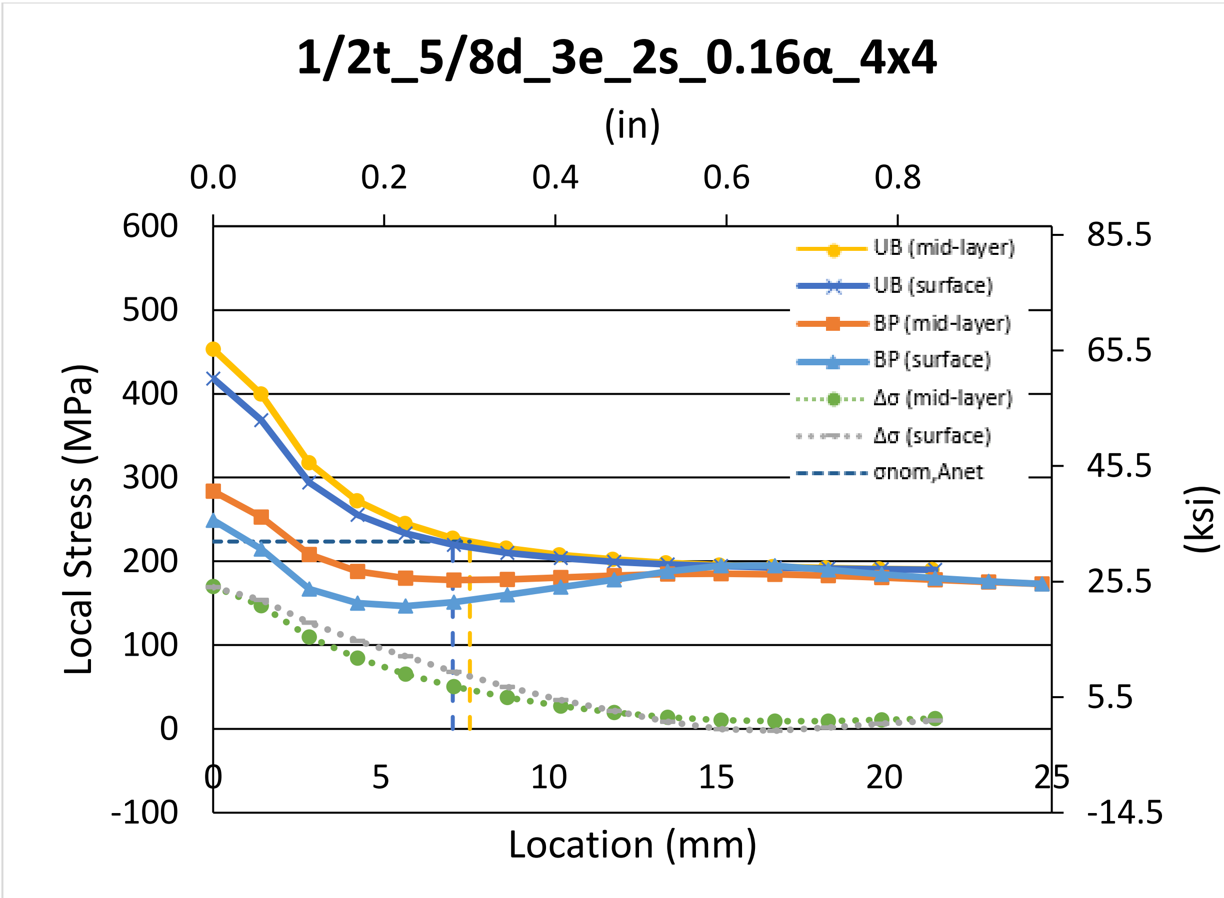

(a)Stress Distributions

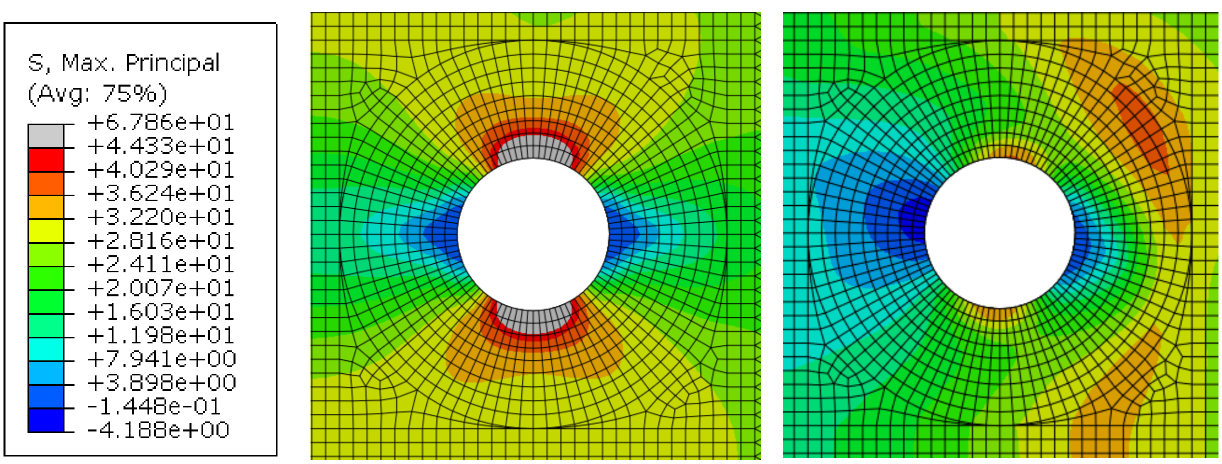

Unbolted Plate

Bolted Plate

$\sigma_{nom,Anet}$ = 32.43 ksi

(b) FEM screenshots

Figure D. 11: 1/2t_5/8d_3e_2s_0.16α_4x4

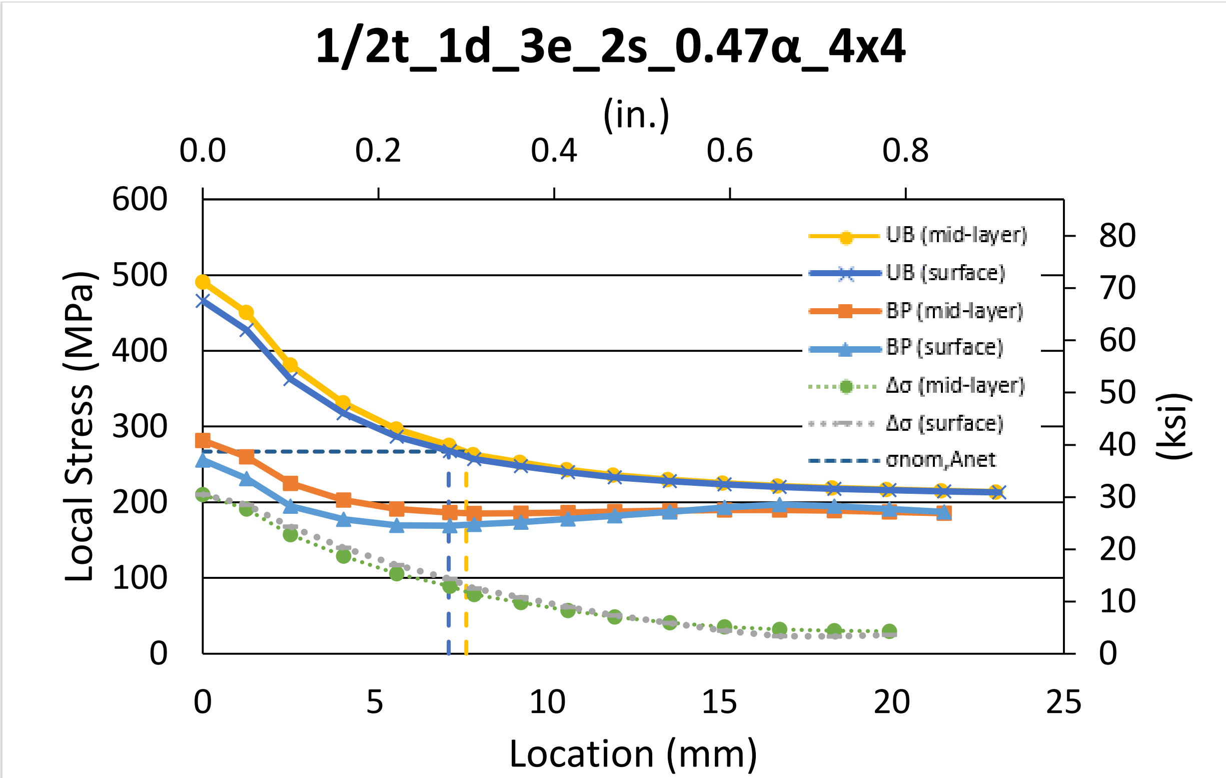

(a)Stress Distributions

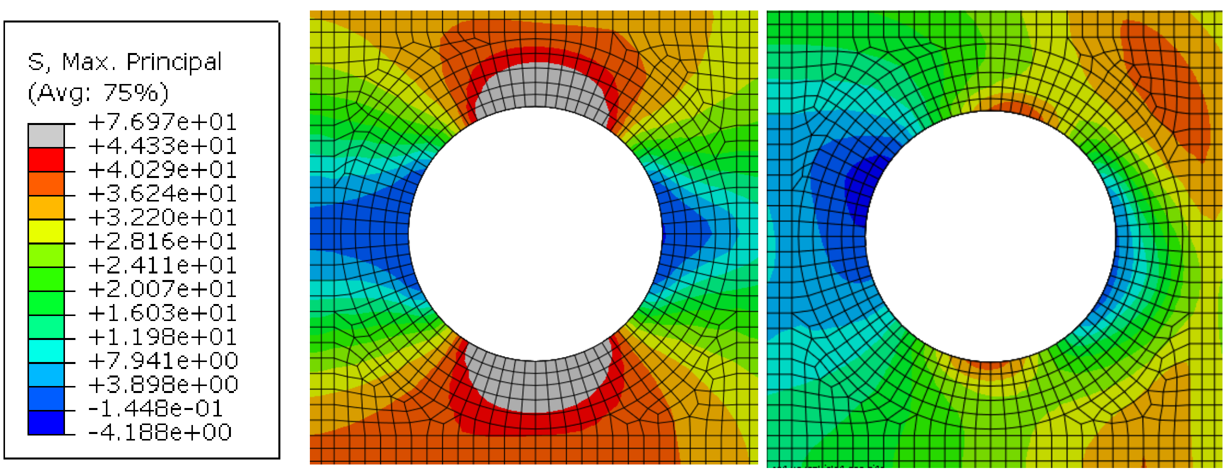

Unbolted Plate

Bolted Plate

$\sigma_{nom,Anet}$ = 38.71 ksi

(b) FEM screenshots

Figure D. 12: 1/2t_1d_3e_2s_0.47α_4x4

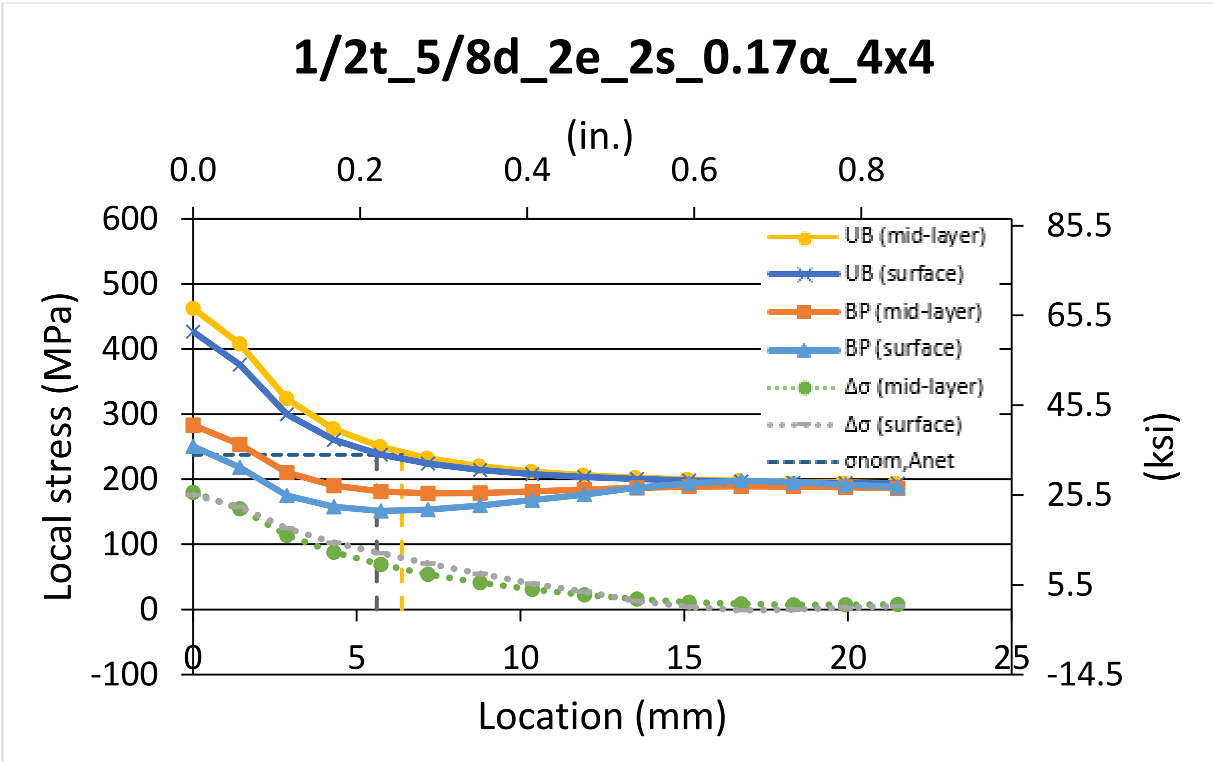

(a)Stress Distributions

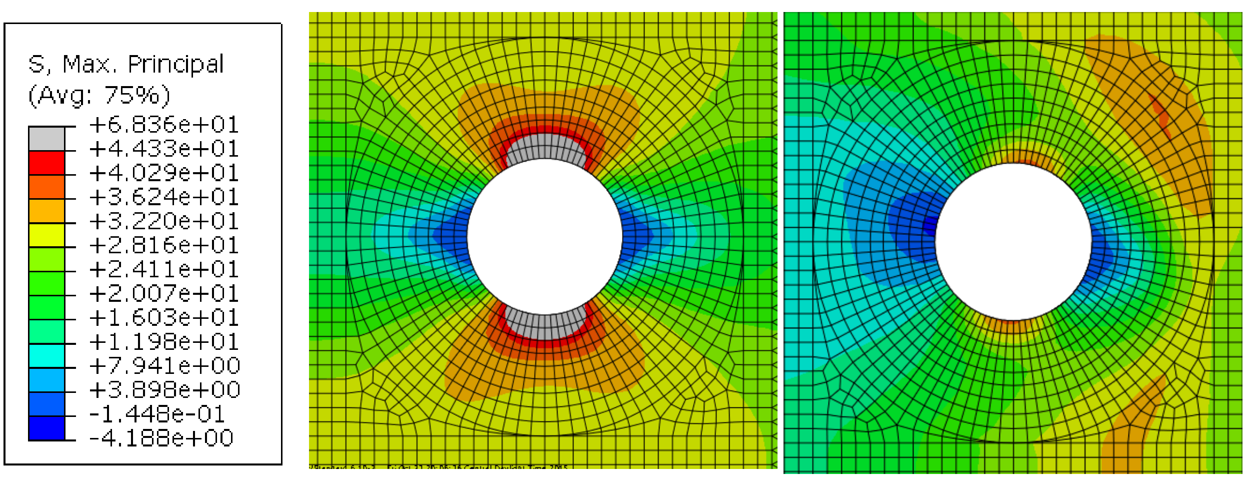

Unbolted Plate

Bolted Plate

$\sigma_{nom,Anet}$ = 34.48 ksi

(b) FEM screenshots

Figure D. 13: 1/2t_5/8d_2e_2s_0.17α_4x4

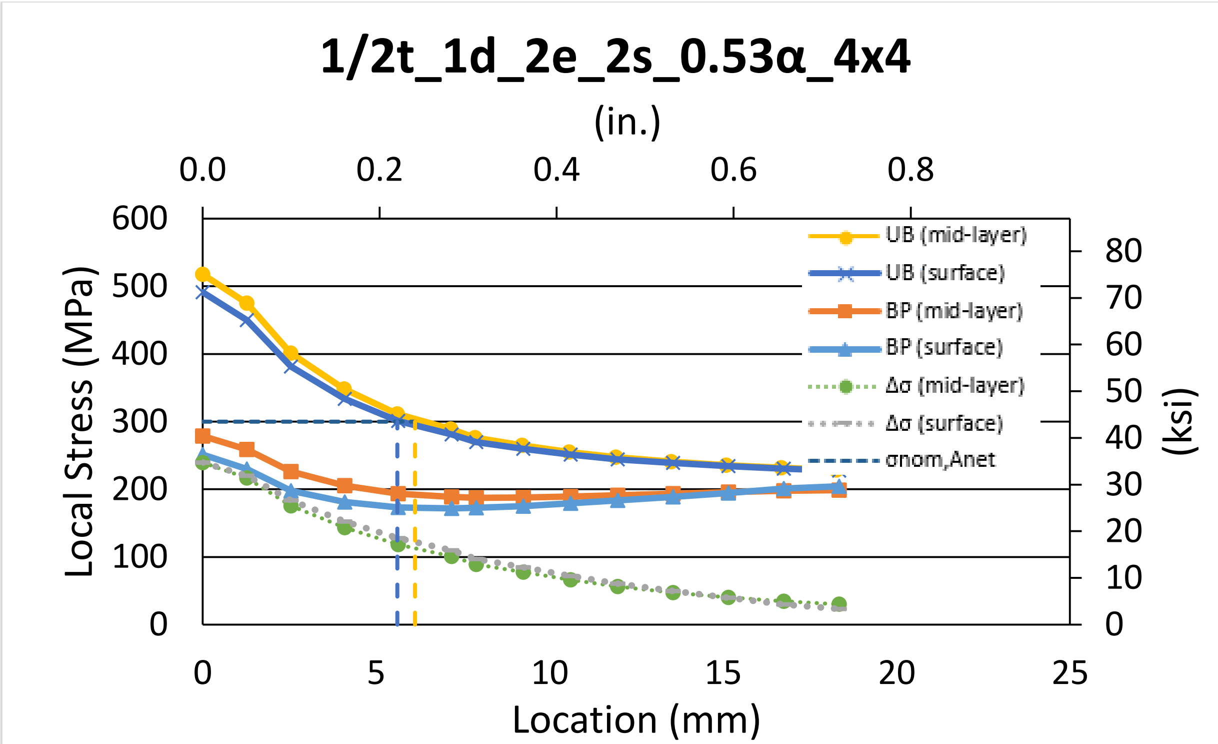

(a)Stress Distributions

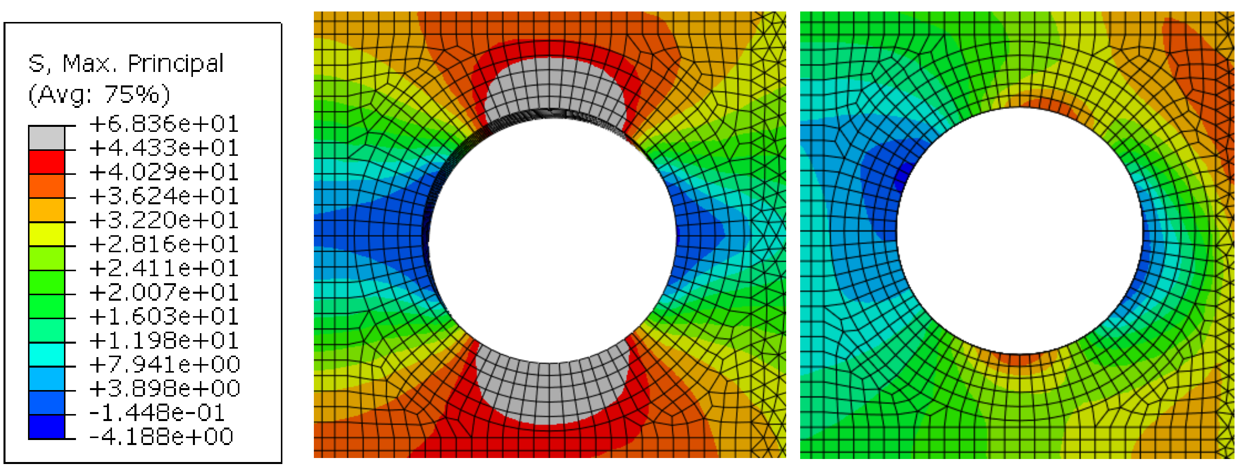

Unbolted Plate

Bolted Plate

$\sigma_{nom,Anet}$ = 43.48 ksi

(b) FEM screenshots

Figure D. 14: 1/2t_1d_2e_2s_0.53α_4x4

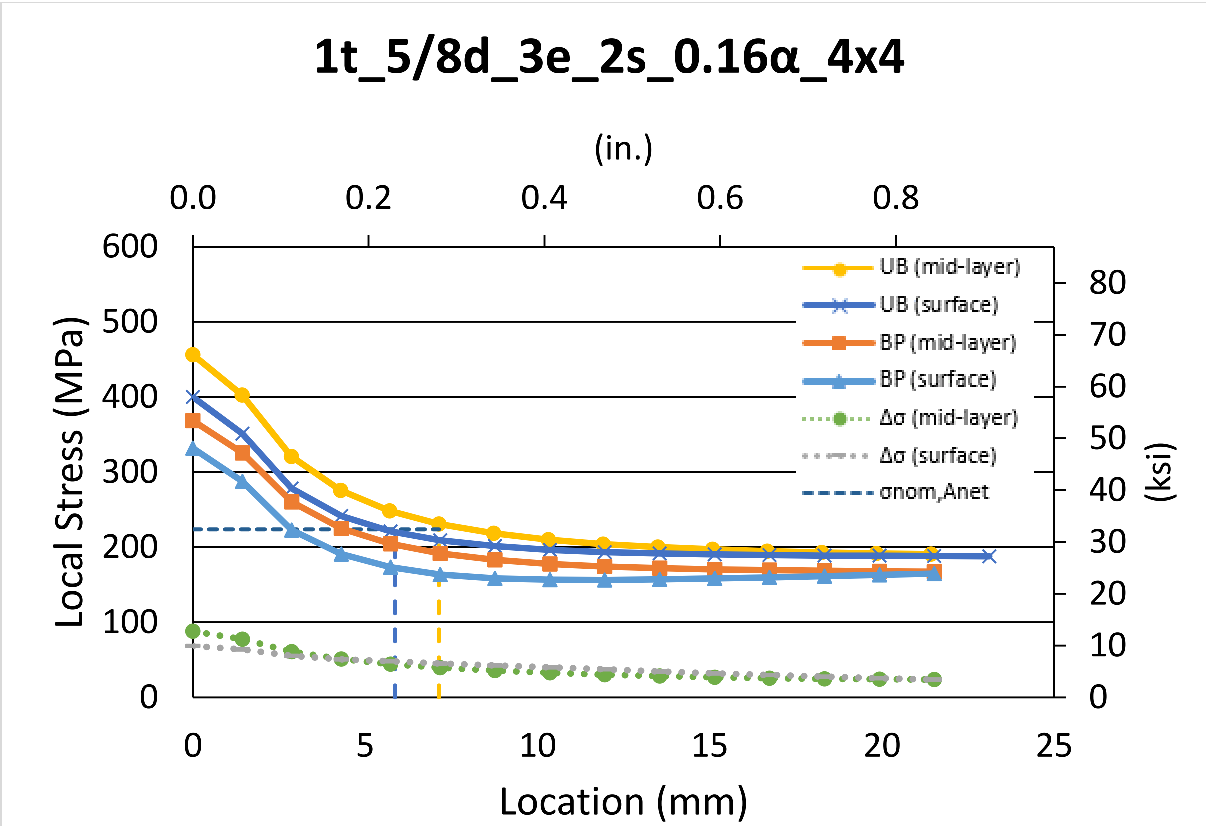

(a)Stress Distributions

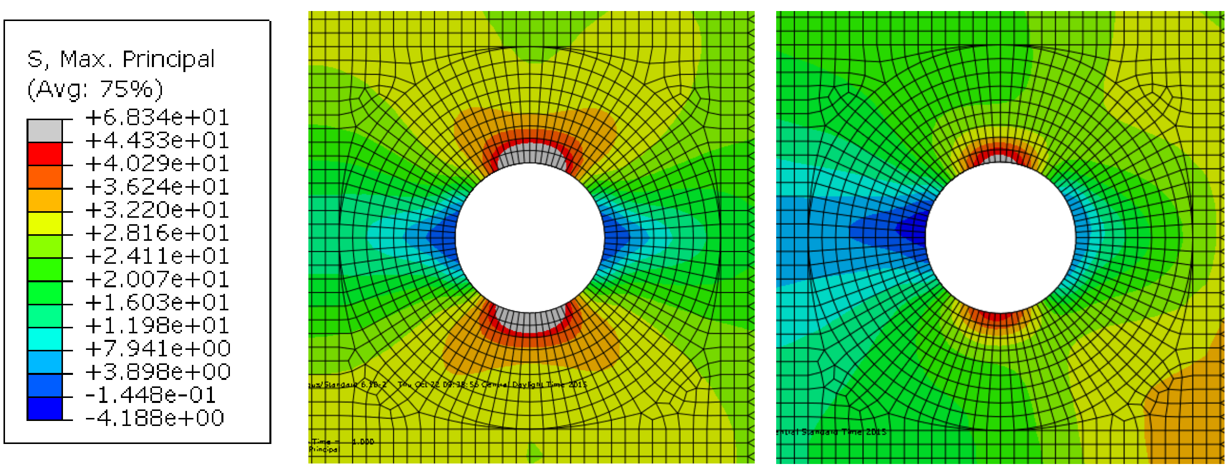

Unbolted Plate

Bolted Plate

$\sigma_{nom,Anet}$ = 32.43 ksi

(b) FEM screenshots

Figure D. 15: 1t_5/8d_3e_2s_0.16α_4x4

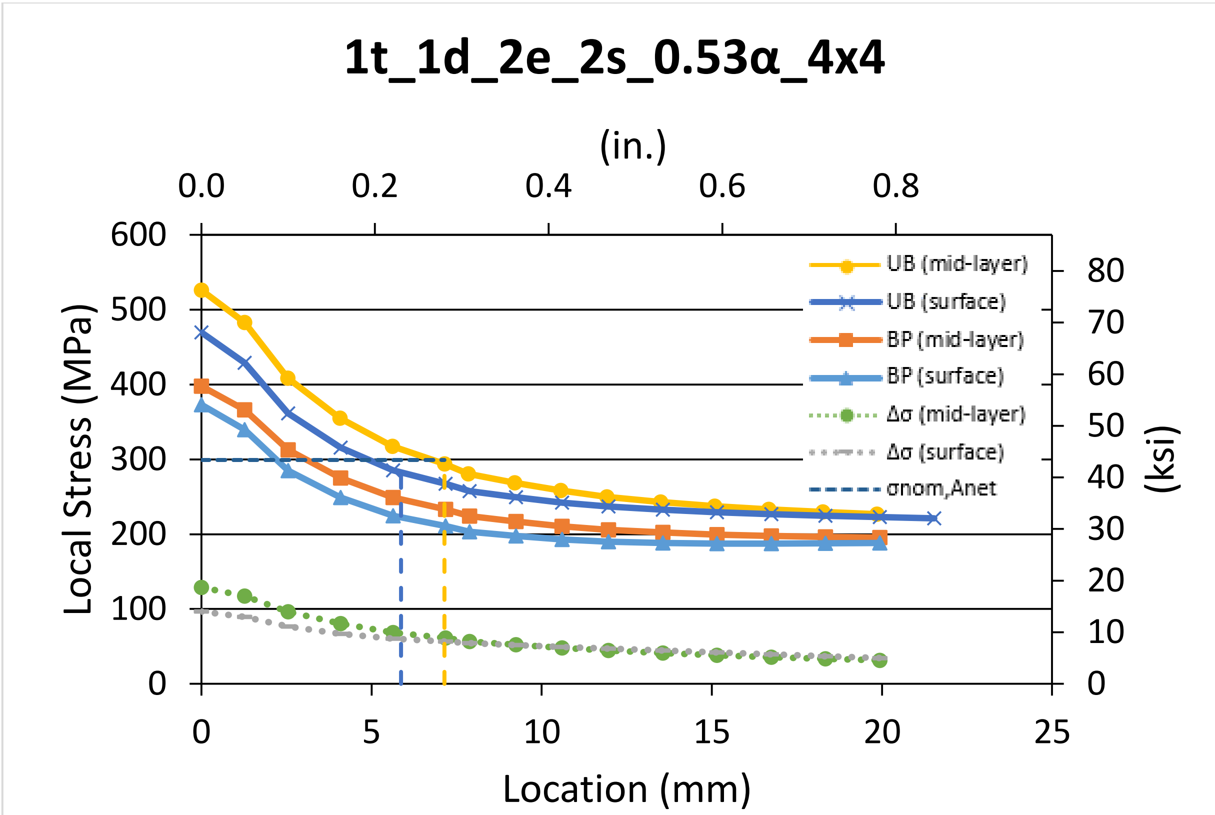

(a)Stress Distributions

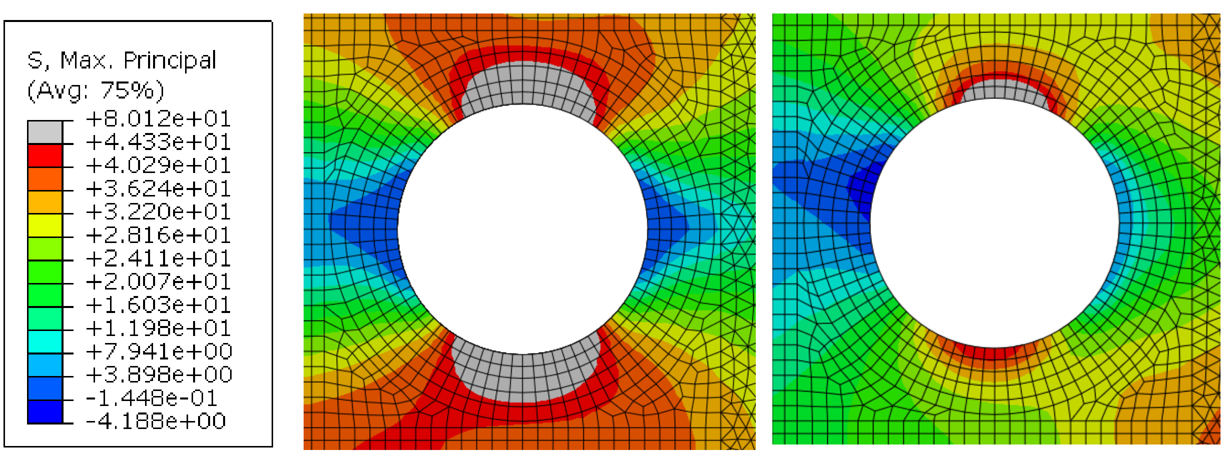

Unbolted Plate

Bolted Plate

$\sigma_{nom,Anet}$ = 43.48 ksi

(b) FEM screenshots

Figure D. 16: 1t_1d_2e_2s_0.53α_4x4

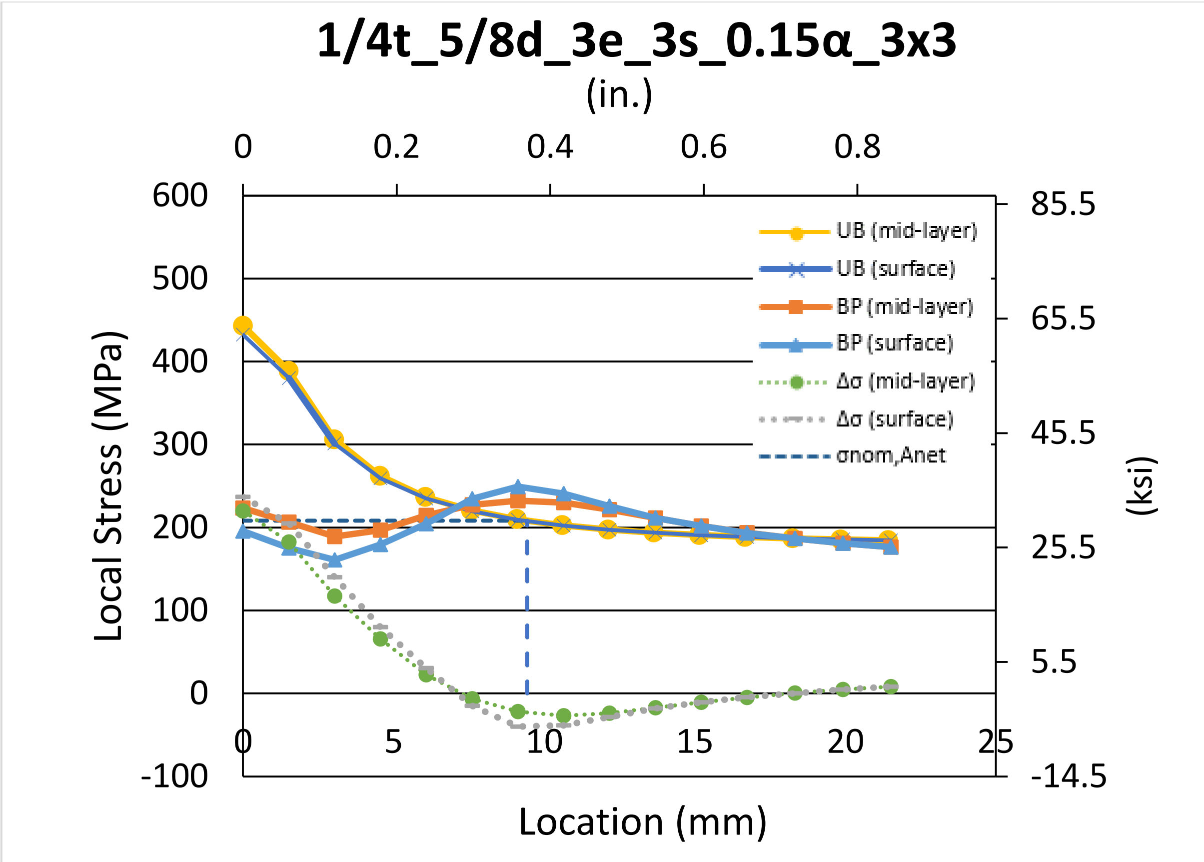

(a)Stress Distributions

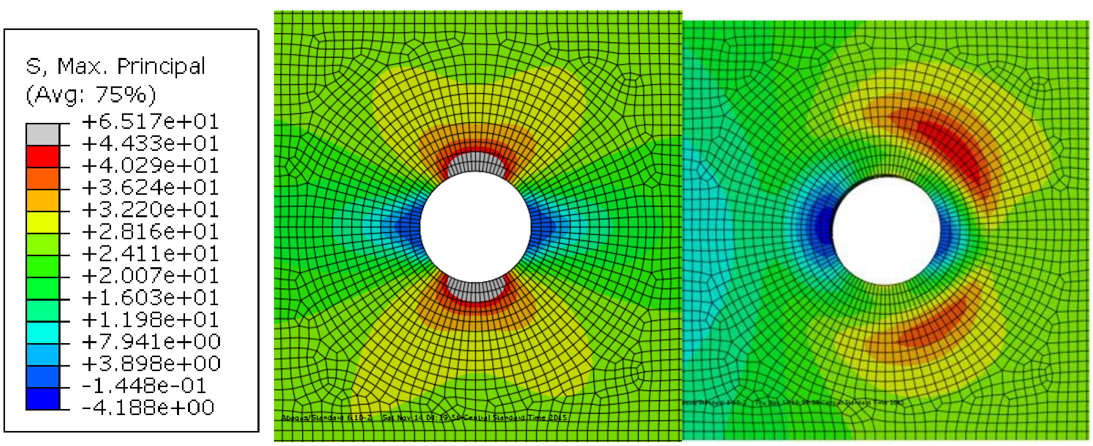

Unbolted Plate Bolted Plate

$\sigma_{nom,Anet}$ = 30.19 ksi

(b) FEM screenshots

Figure D. 17: 1/4t_5/8d_3e_3s_0.15α_3x3

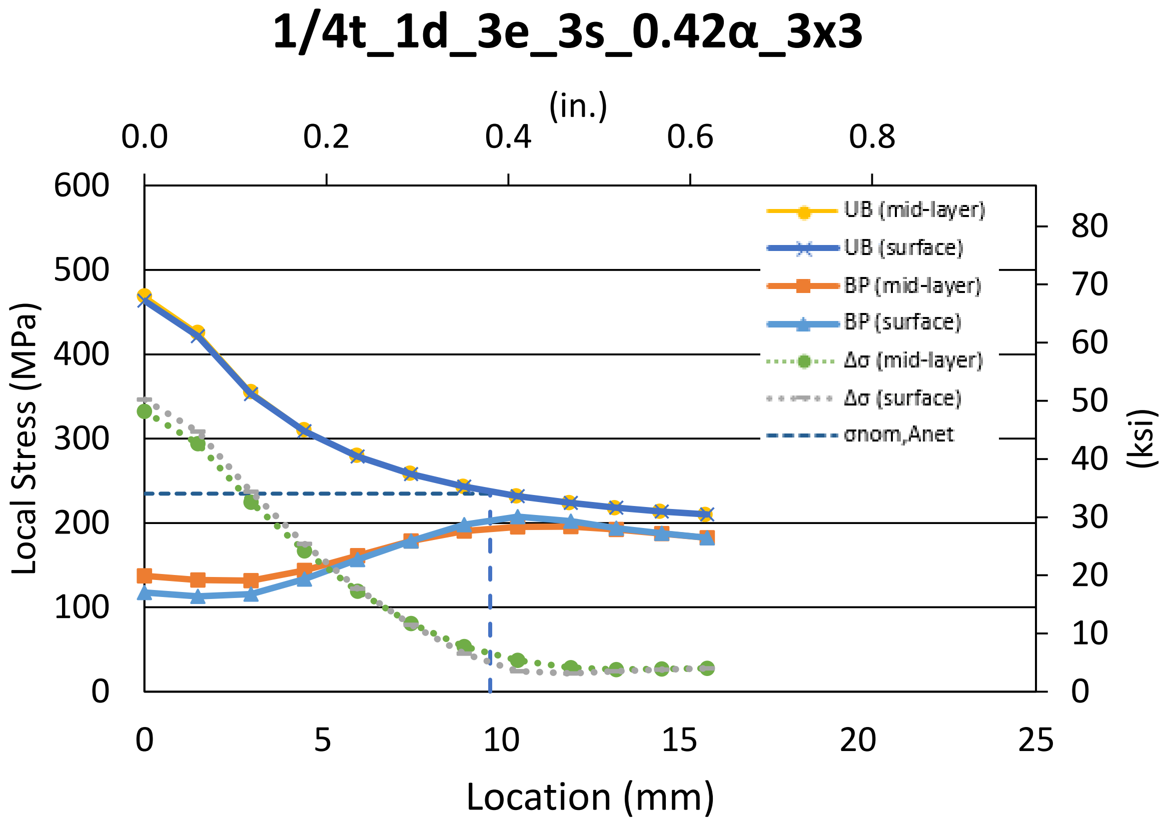

(a)Stress Distributions

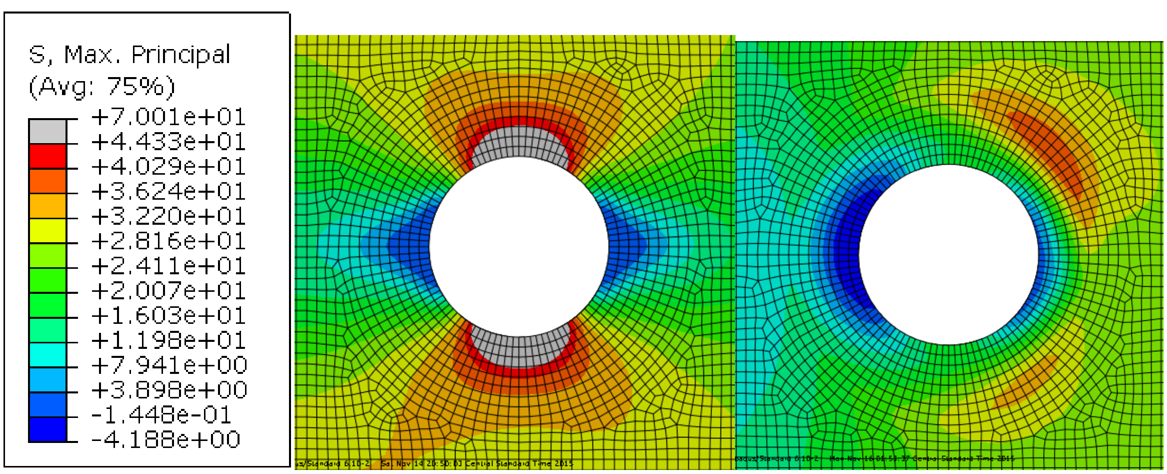

Unbolted Plate Bolted Plate

$\sigma_{nom,Anet}$ = 34.04 ksi

(b) FEM screenshots

Figure D. 18: 1/4t_1d_3e_3s_0.42α_3x3

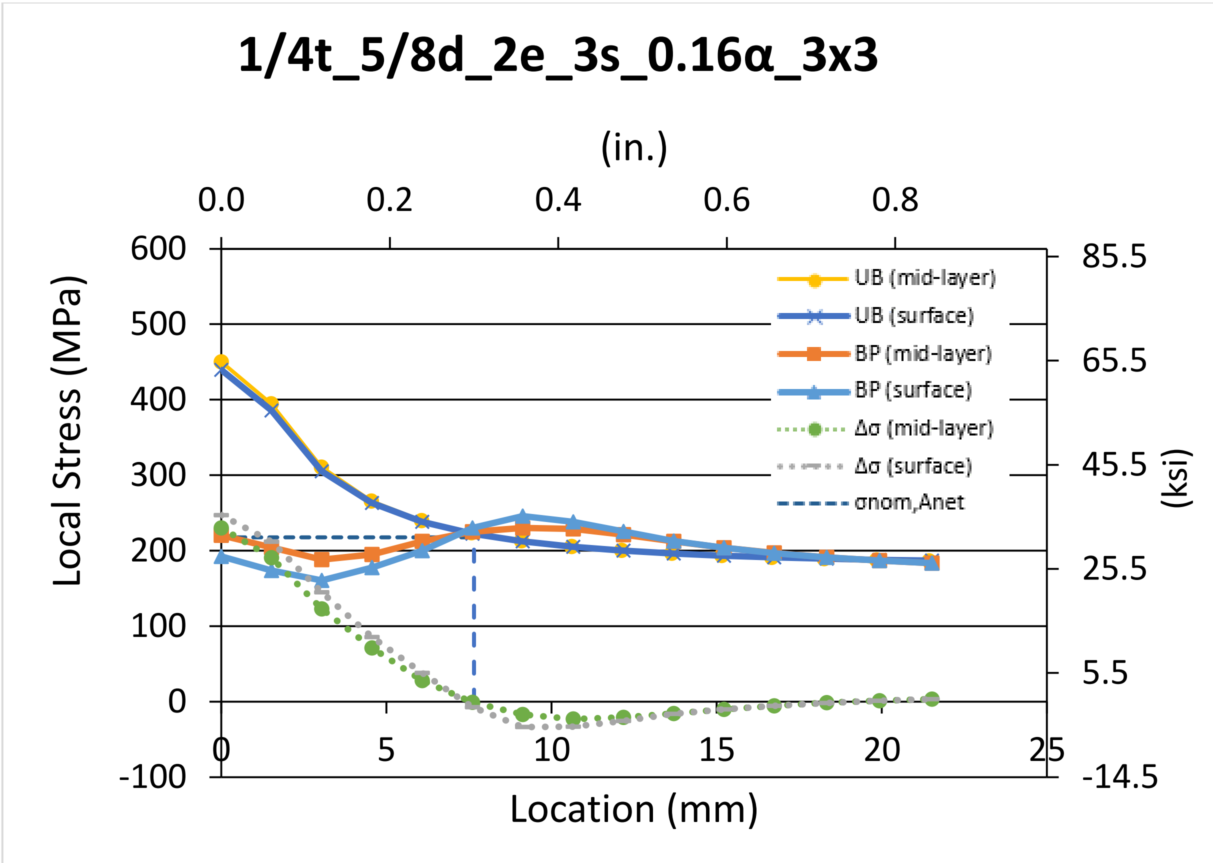

(a)Stress Distributions

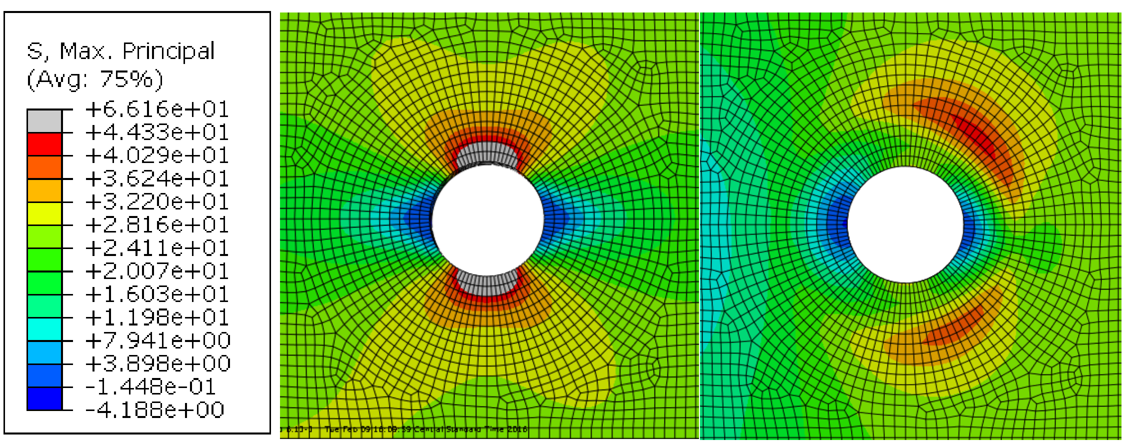

Unbolted Plate   Bolted Plate

$\sigma_{nom,Anet}$ = 31.56 ksi

(b) FEM screenshots

Figure D. 19: 1/4t_5/8d_2e_3s_0.16α_3x3

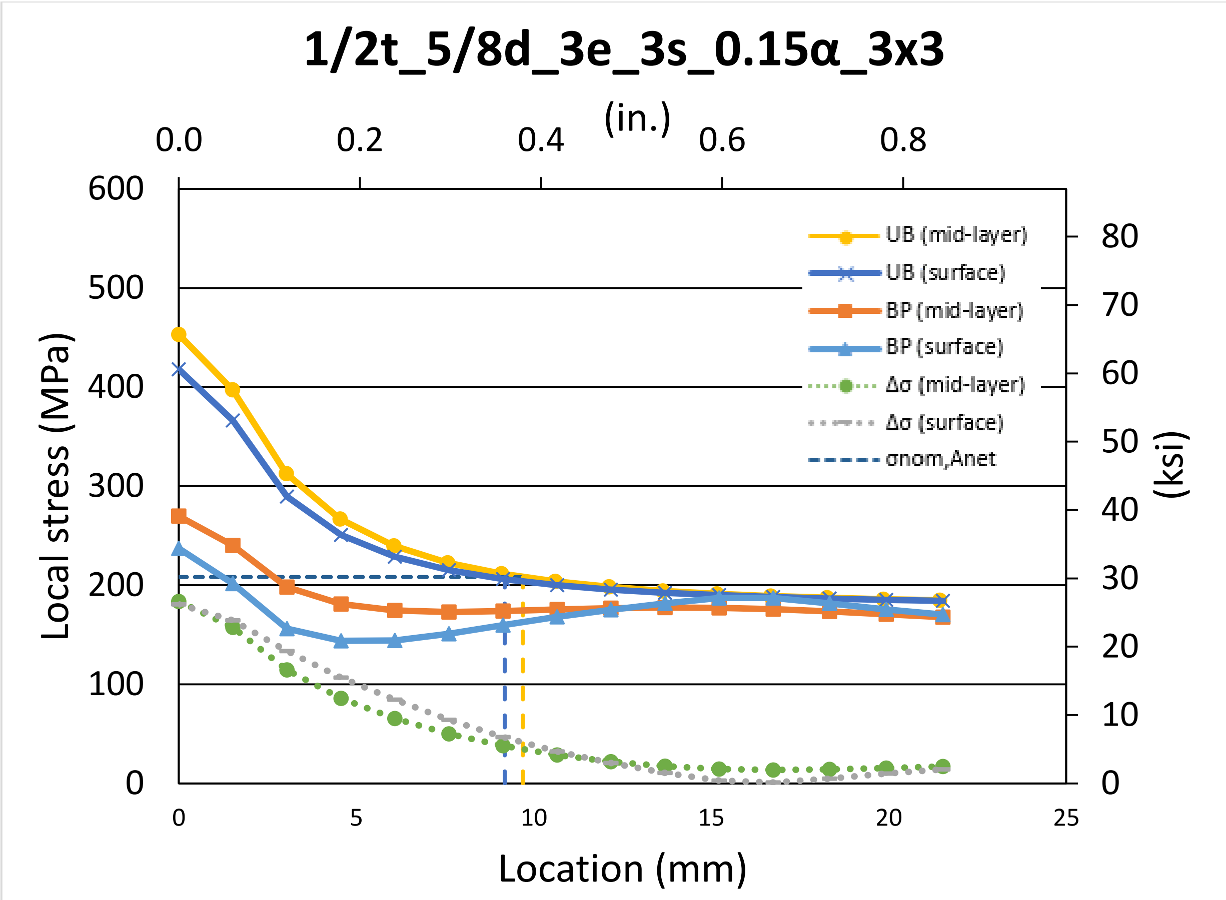

(a)Stress Distributions

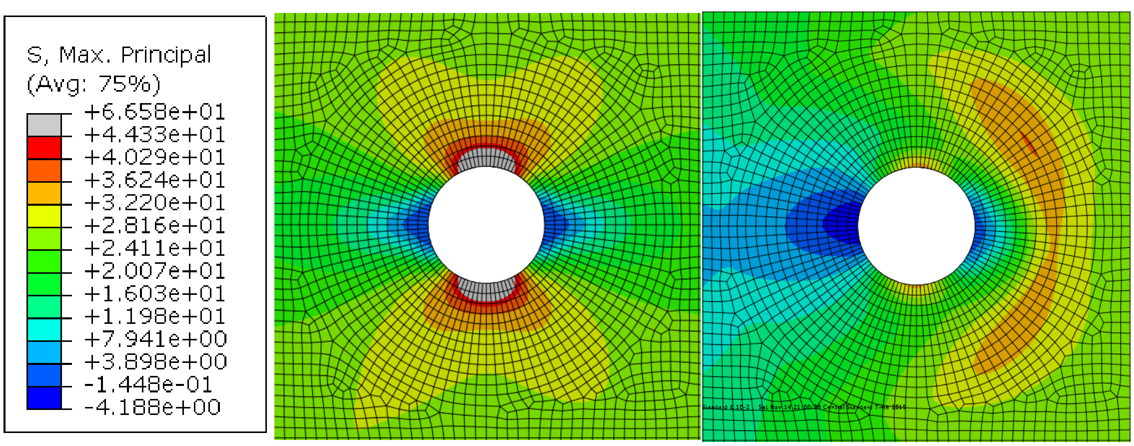

Unbolted Plate Bolted Plate

$\sigma_{nom,Anet}$ = 30.19 ksi

(b) FEM screenshots

Figure D. 20: 1/2t_5/8d_3e_3s_0.15α_3x3

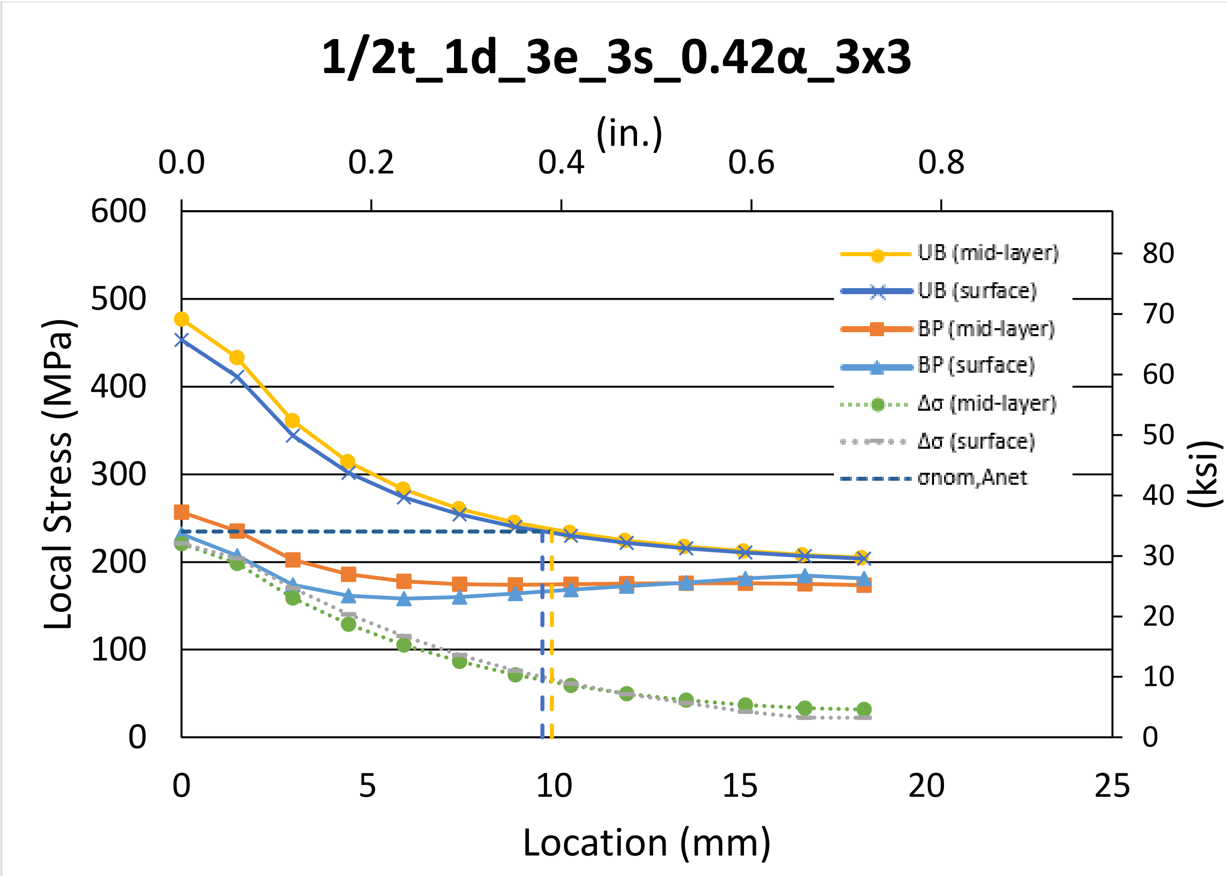

(a)Stress Distributions

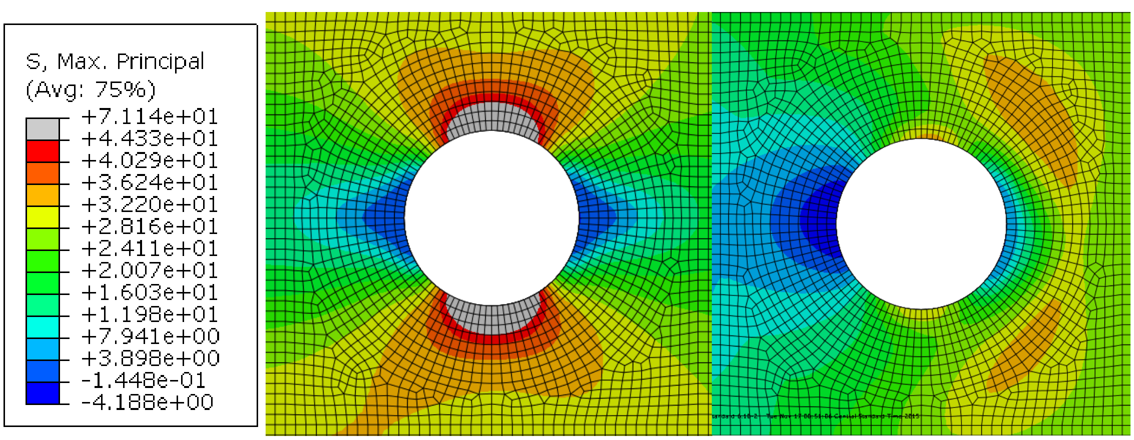

Unbolted Plate Bolted Plate

$\sigma_{nom,Anet}$ = 34.04 ksi

(b) FEM screenshots

Figure D. 21: 1/2t_1d_3e_3s_0.42α_3x3

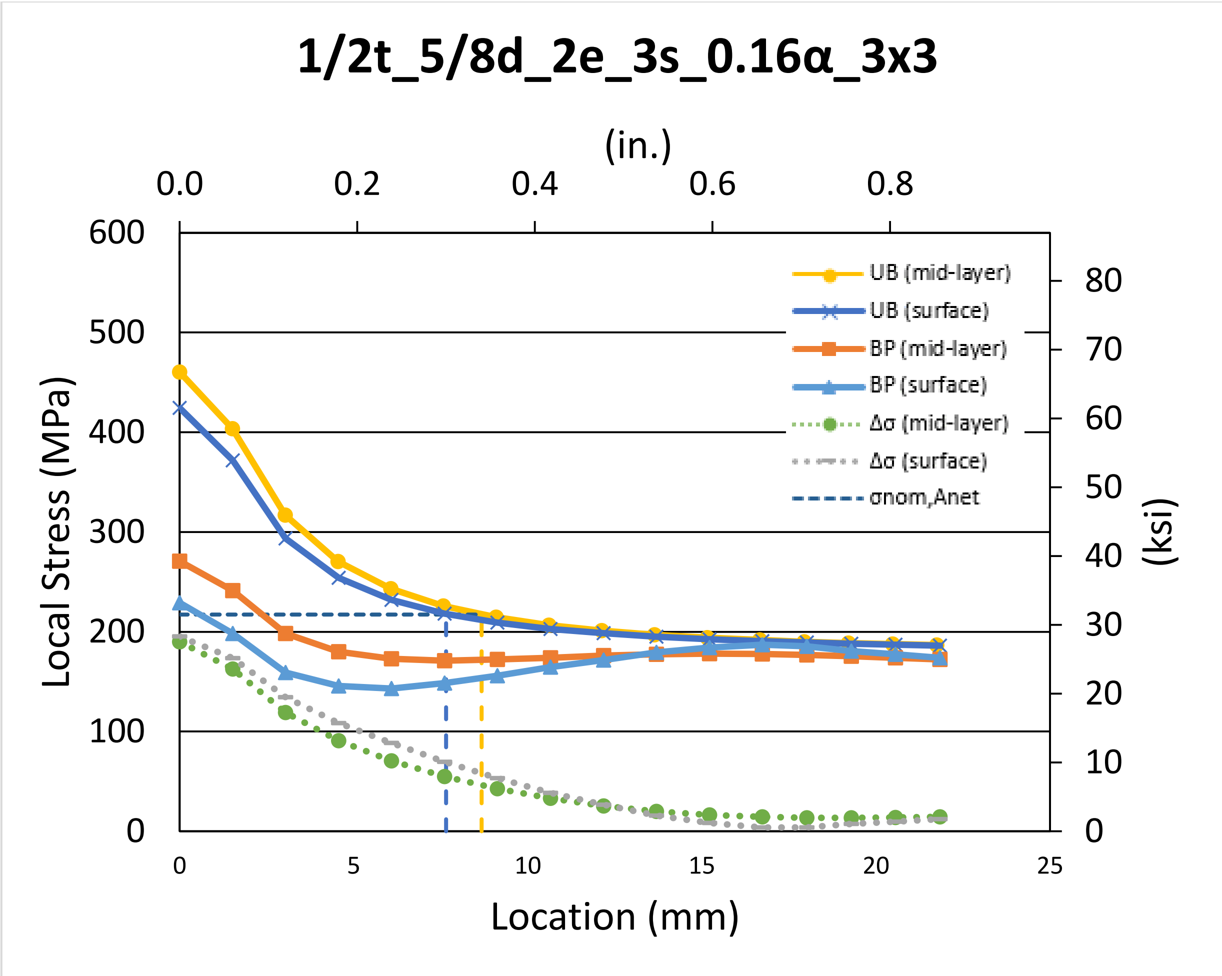

(a)Stress Distributions

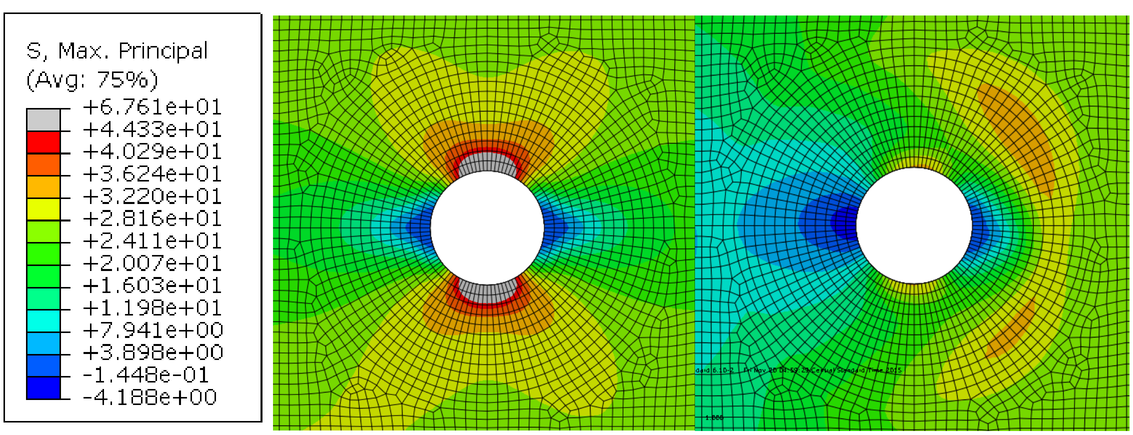

Unbolted Plate Bolted Plate

$\sigma_{nom,Anet}$ = 31.5 ksi

(b) FEM screenshots

Figure D. 22: 1/2t_5/8d_2e_3s_0.16α_3x3

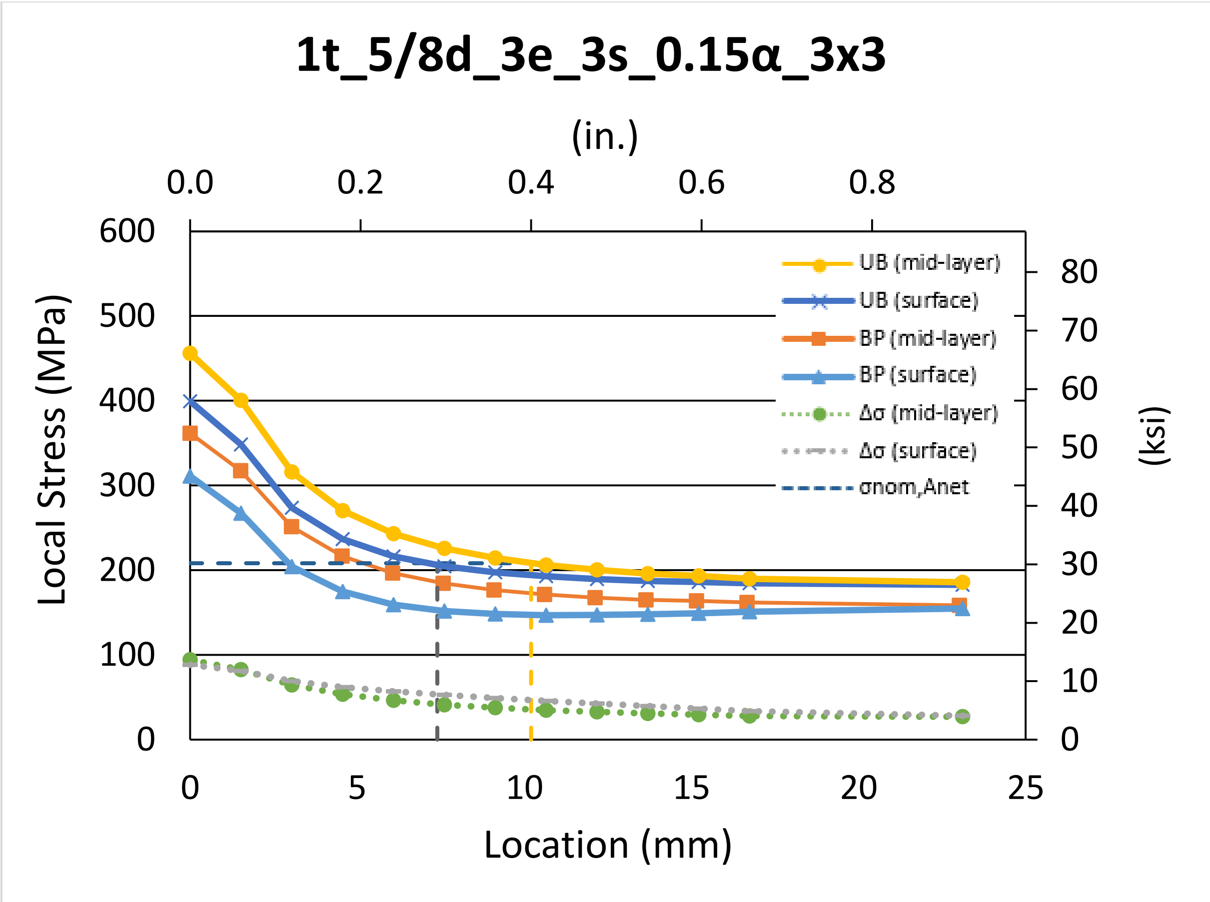

(a)Stress Distributions

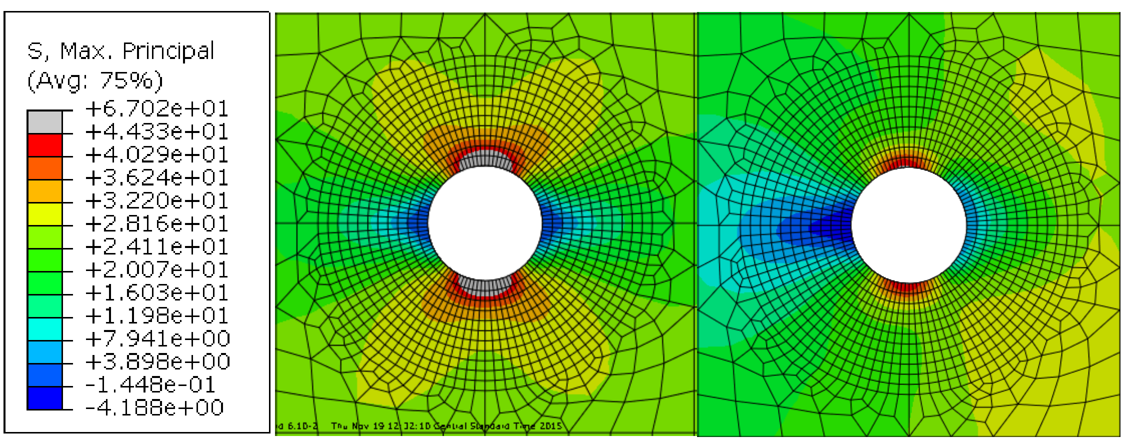

Unbolted Plate   Bolted Plate

$\sigma_{nom,Anet}$ = 30.19 ksi

(b) FEM screenshots

Figure D. 23: 1t_5/8d_3e_3s_0.15α_3x3

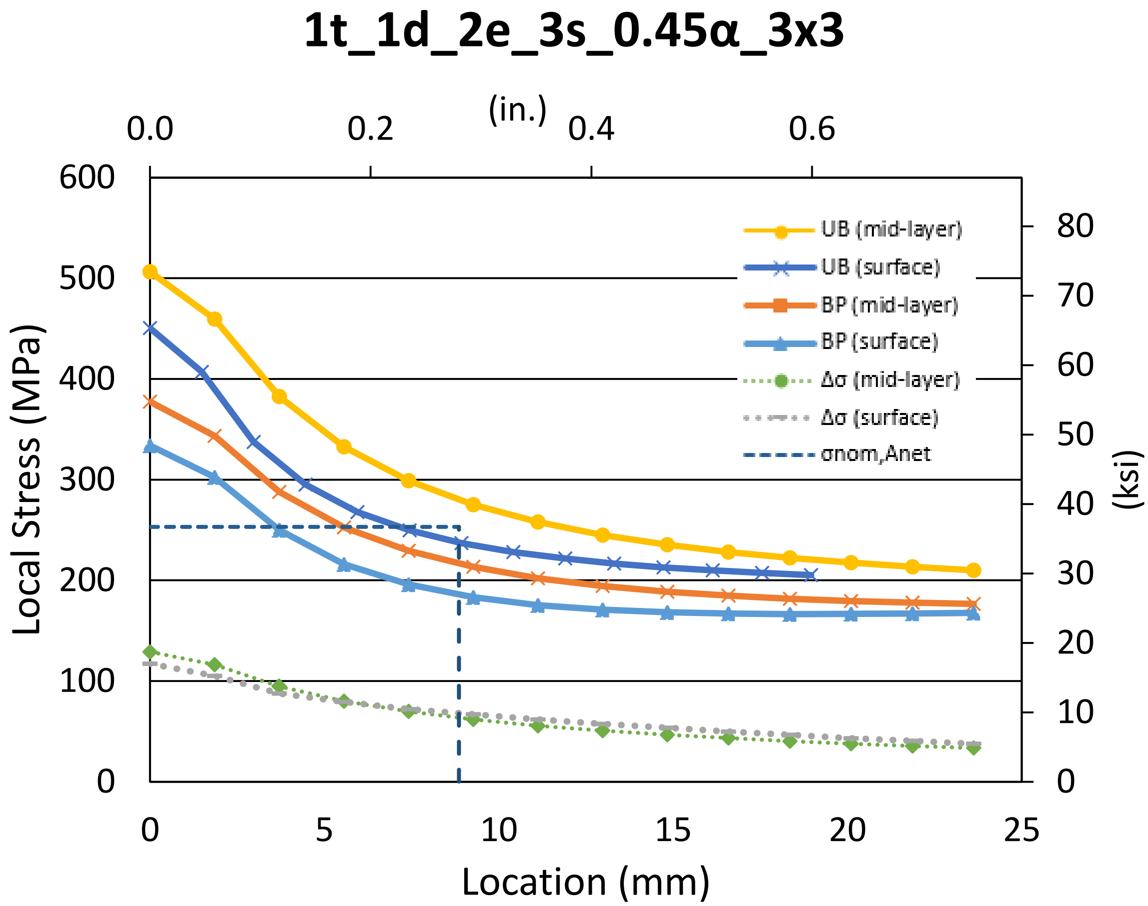

(a)Stress Distributions

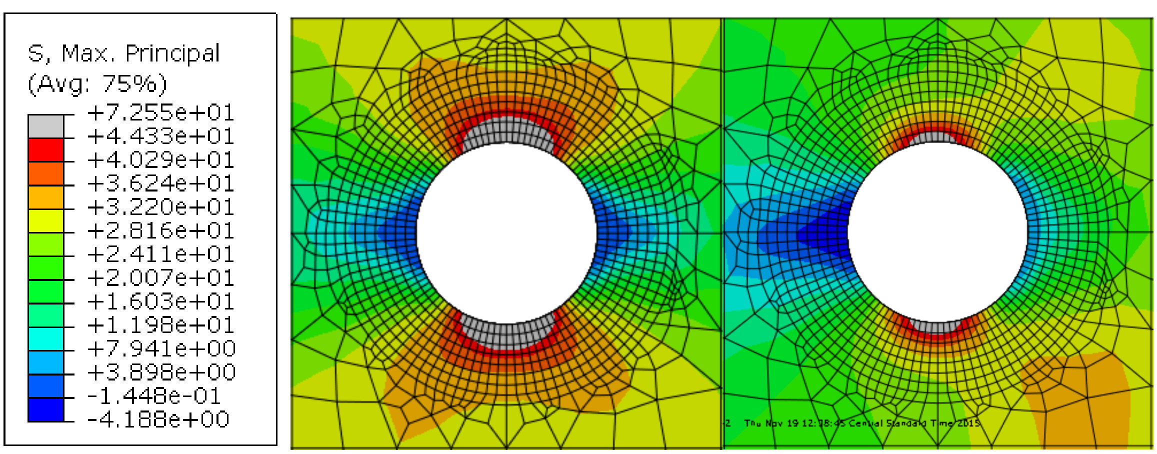

Unbolted Plate Bolted Plate

$\sigma_{nom,Anet}$ = 34.04 ksi

(b) FEM screenshots

Figure D. 24: 1t_1d_2e_3s_0.45α_3x3

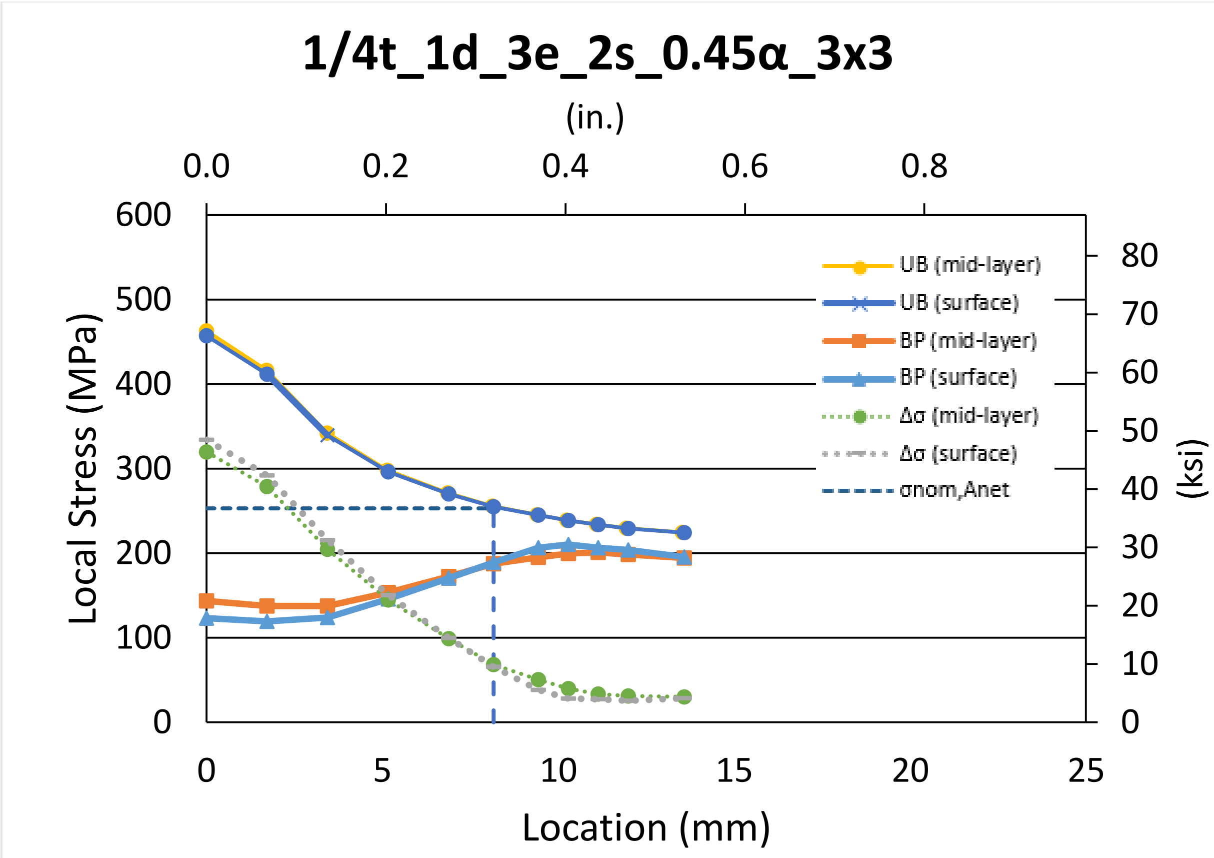

(a)Stress Distributions

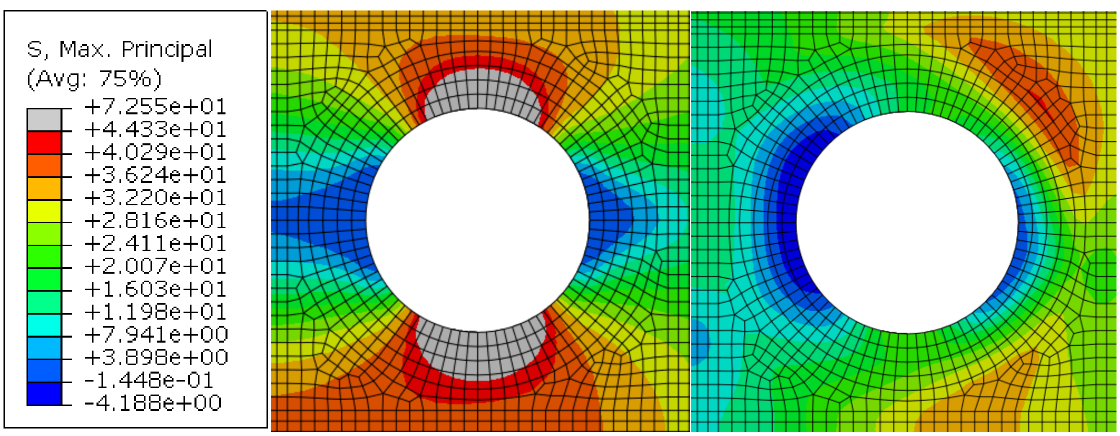

Unbolted Plate Bolted Plate

$\sigma_{nom,Anet}$ = 36.7 ksi

(b) FEM screenshots

Figure D. 25: 1/4t_1d_3e_2s_0.45α_3x3

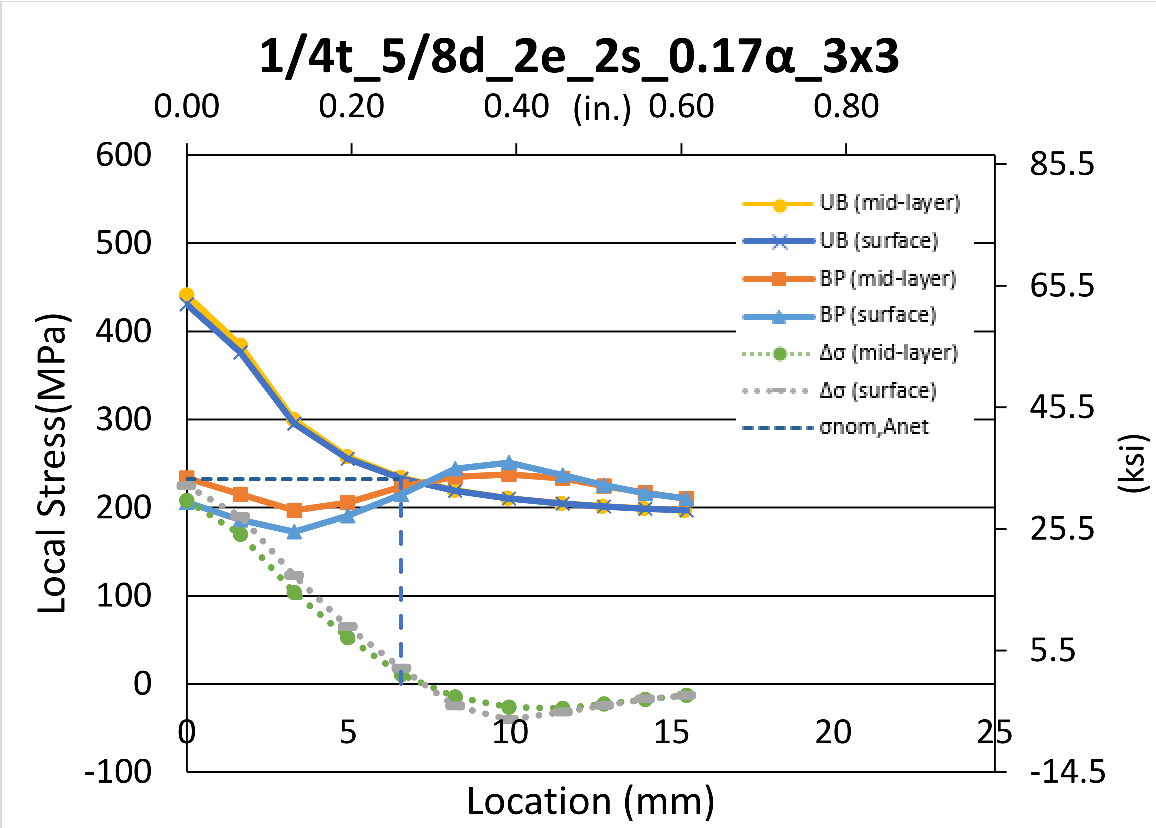

(a)Stress Distributions

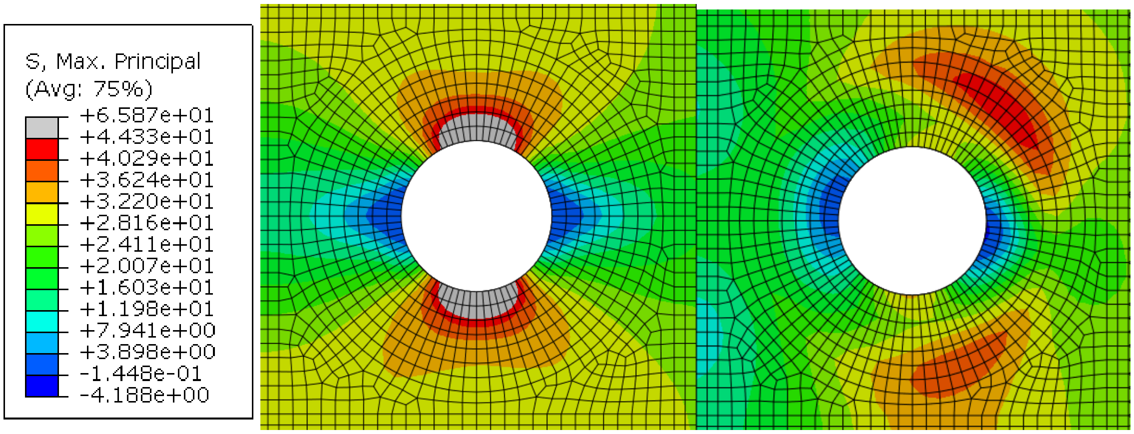

Unbolted Plate Bolted Plate

$\sigma_{nom,Anet}$ = 33.68 ksi

(b) FEM screenshots

Figure D. 26: 1/4t_5/8d_2e_2s_0.17α_3x3

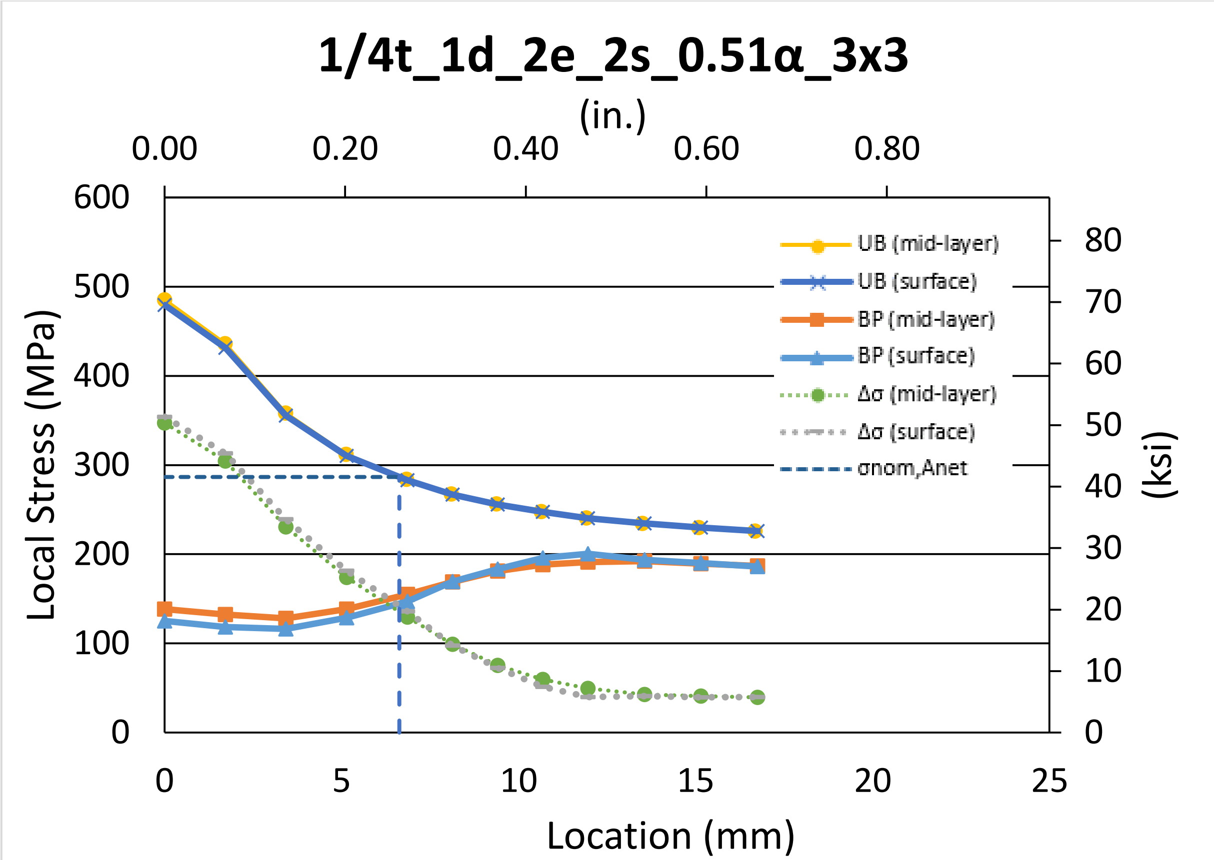

(a)Stress Distributions

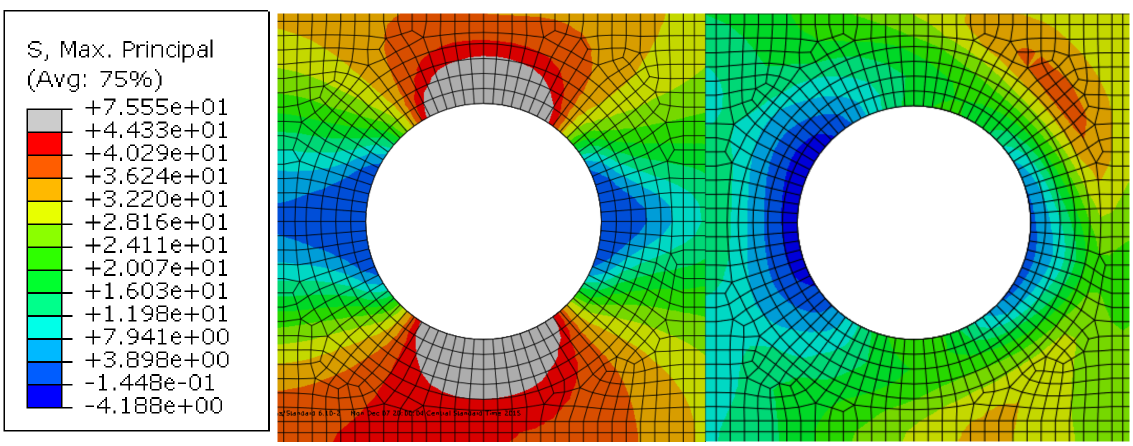

Unbolted Plate　　　　　Bolted Plate

$\sigma_{nom,Anet}$ = 41.56 ksi

(b) FEM screenshots

Figure D. 27: 1/4t_1d_2e_2s_0.51α_3x3

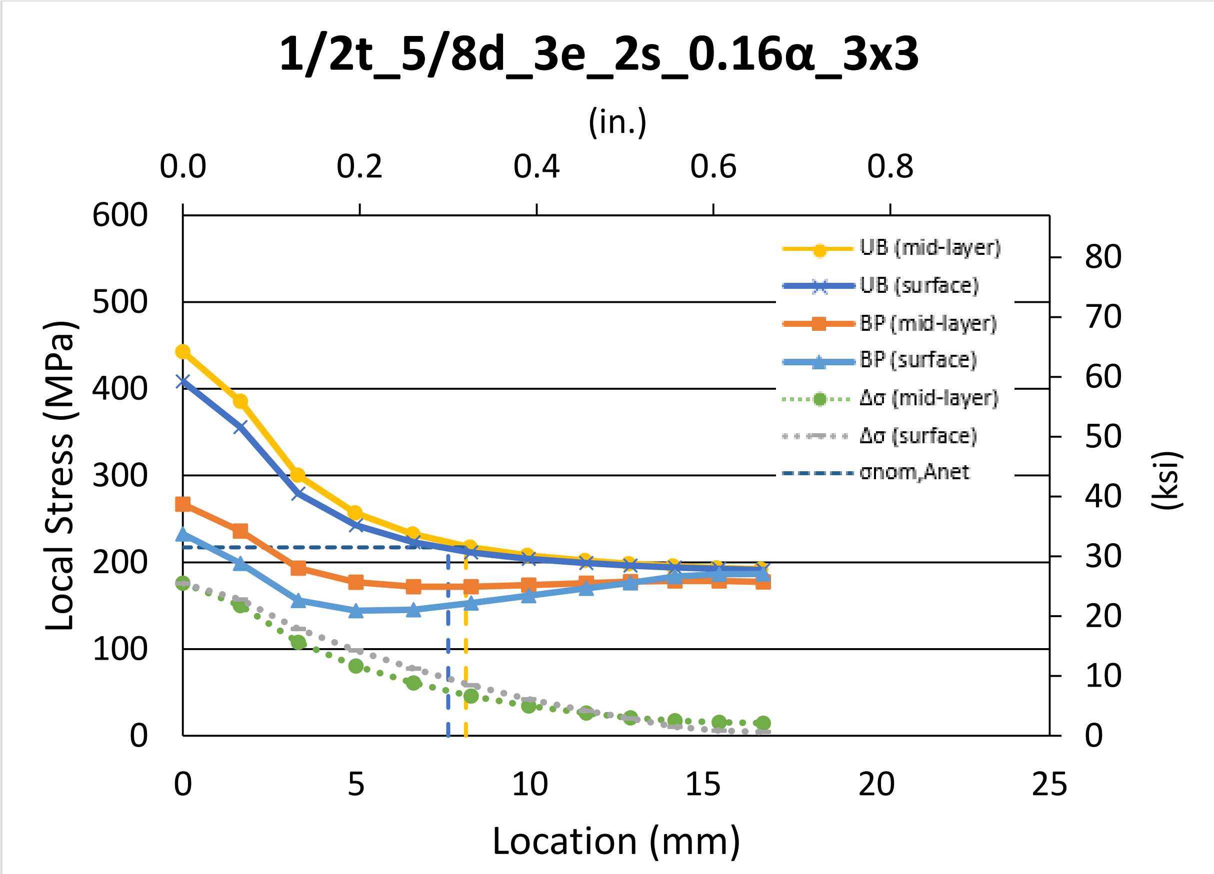

(a)Stress Distributions

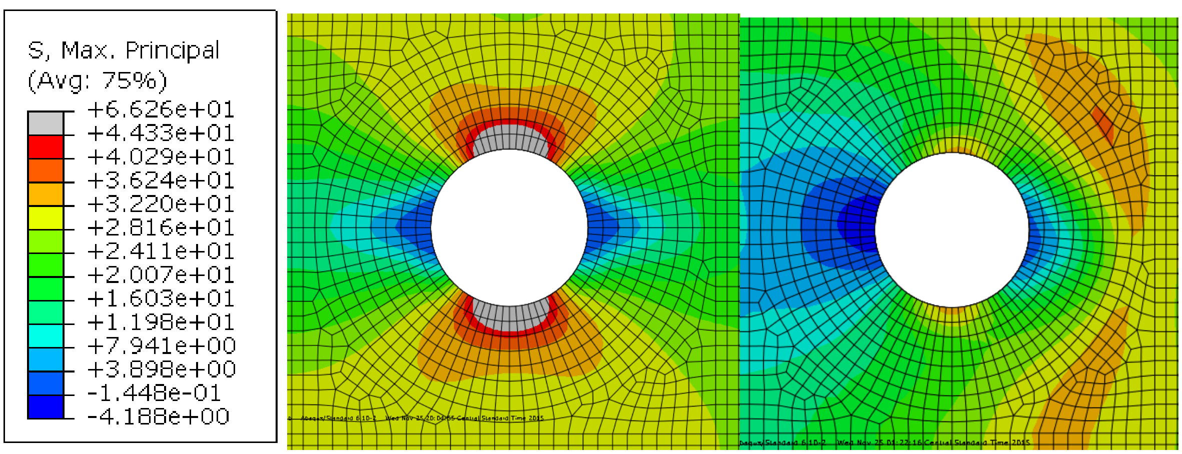

Unbolted Plate Bolted Plate

$\sigma_{nom,Anet}$ = 31.50 ksi

(b) FEM screenshots

Figure D. 28: 1/2t_5/8d_3e_2s_0.16α_3x3

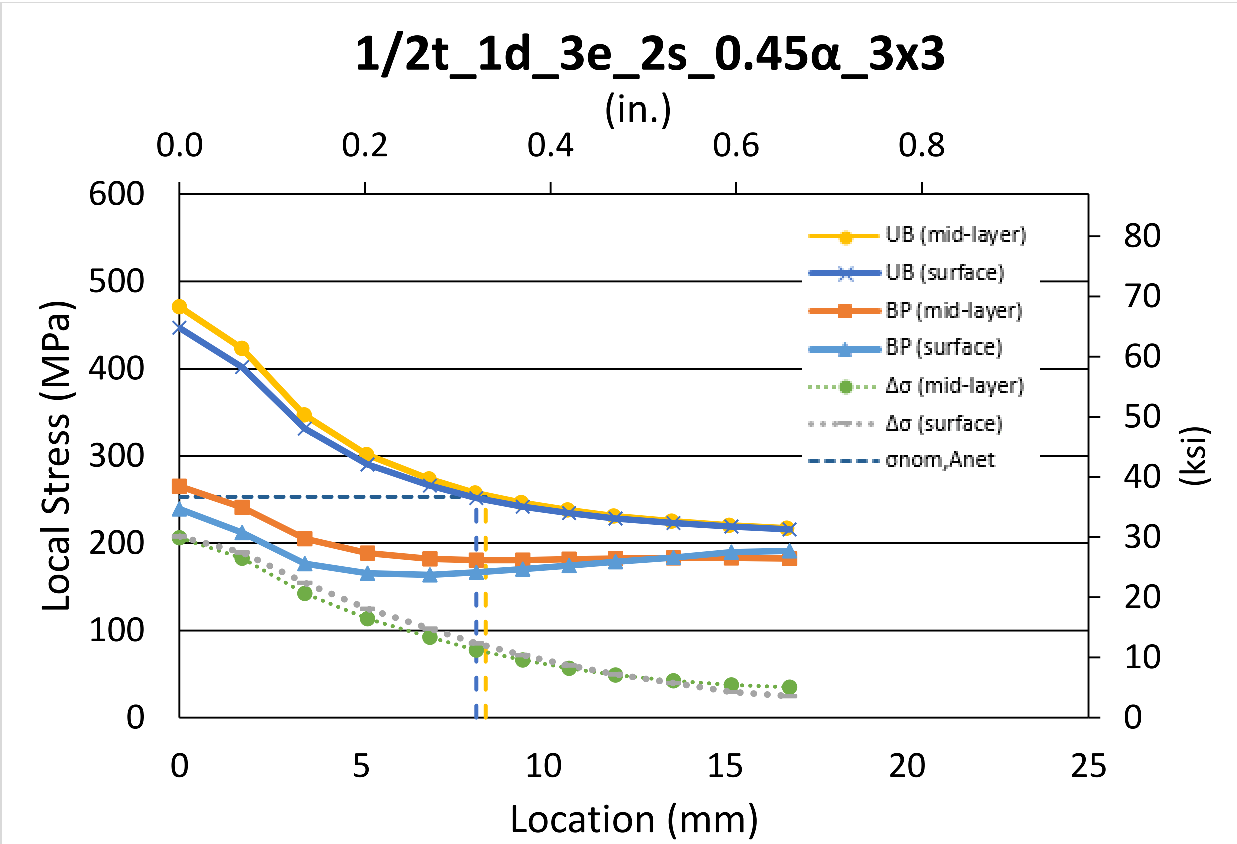

(a)Stress Distributions

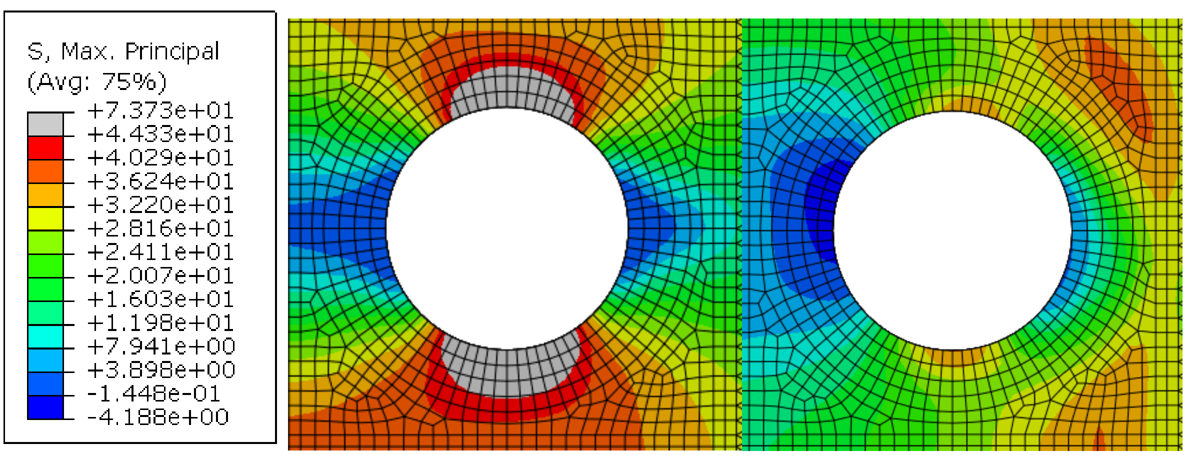

Unbolted Plate Bolted Plate

$\sigma_{nom,Anet}$ = 36.7 ksi

(b) FEM screenshots

Figure D. 29: 1/2t_1d_3e_2s_0.45α_3x3

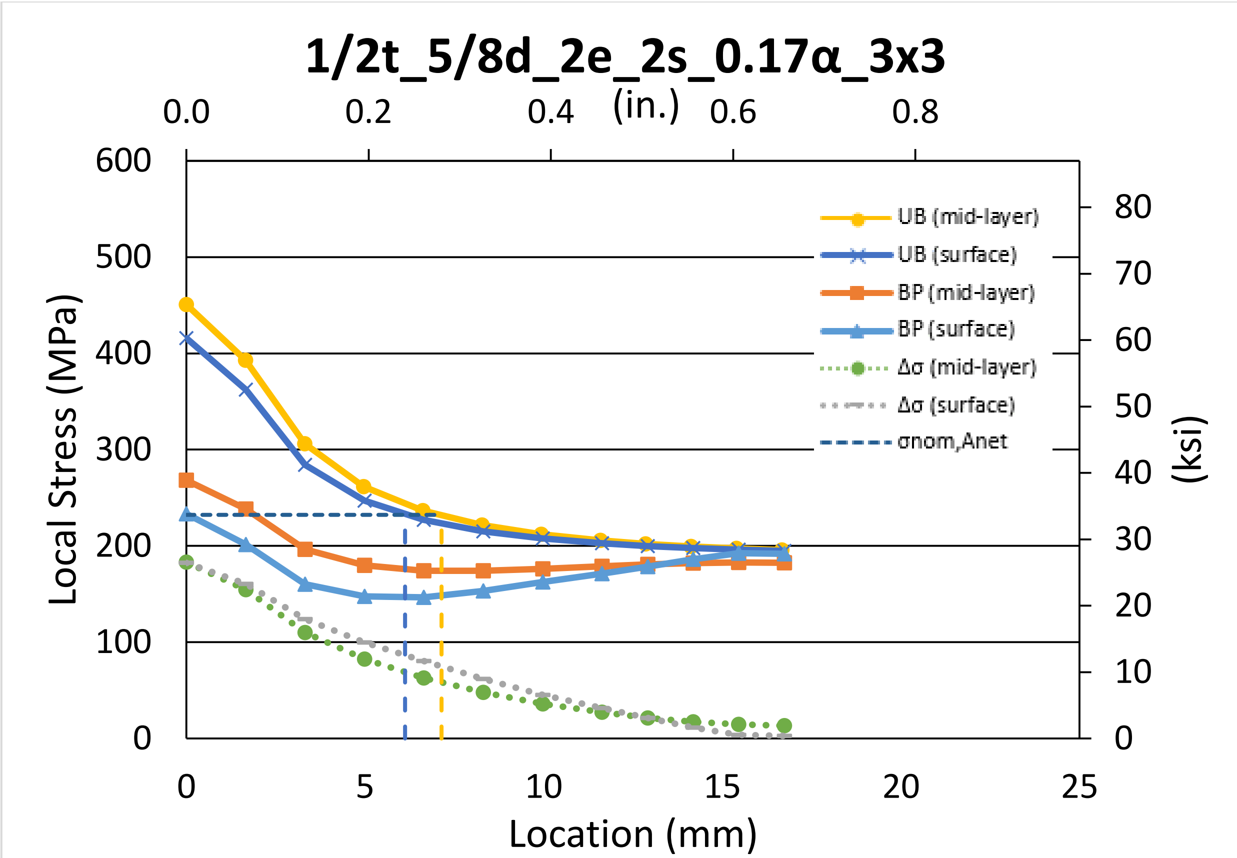

(a)Stress Distributions

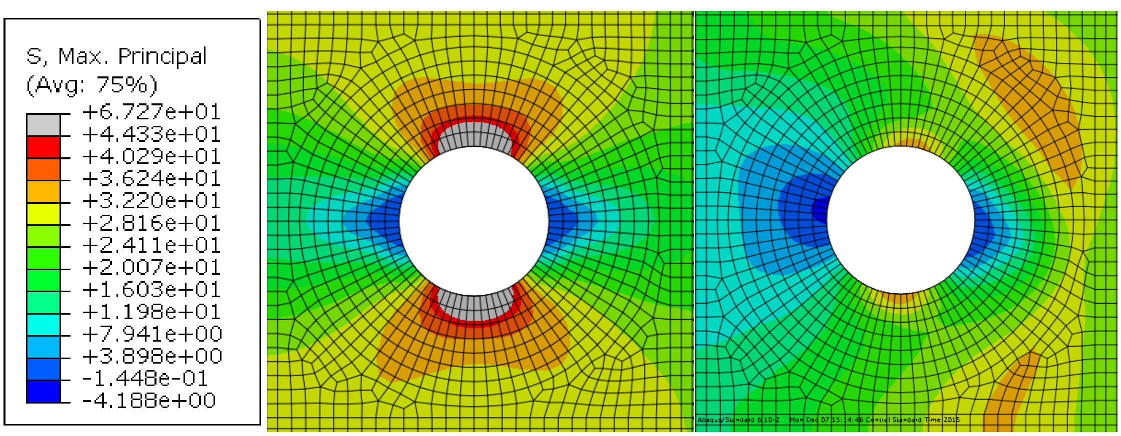

Unbolted Plate Bolted Plate

$\sigma_{nom,Anet}$ = 33.68 ksi

(b) FEM screenshots

Figure D. 30: 1/2t_5/8d_2e_2s_0.17α_3x3

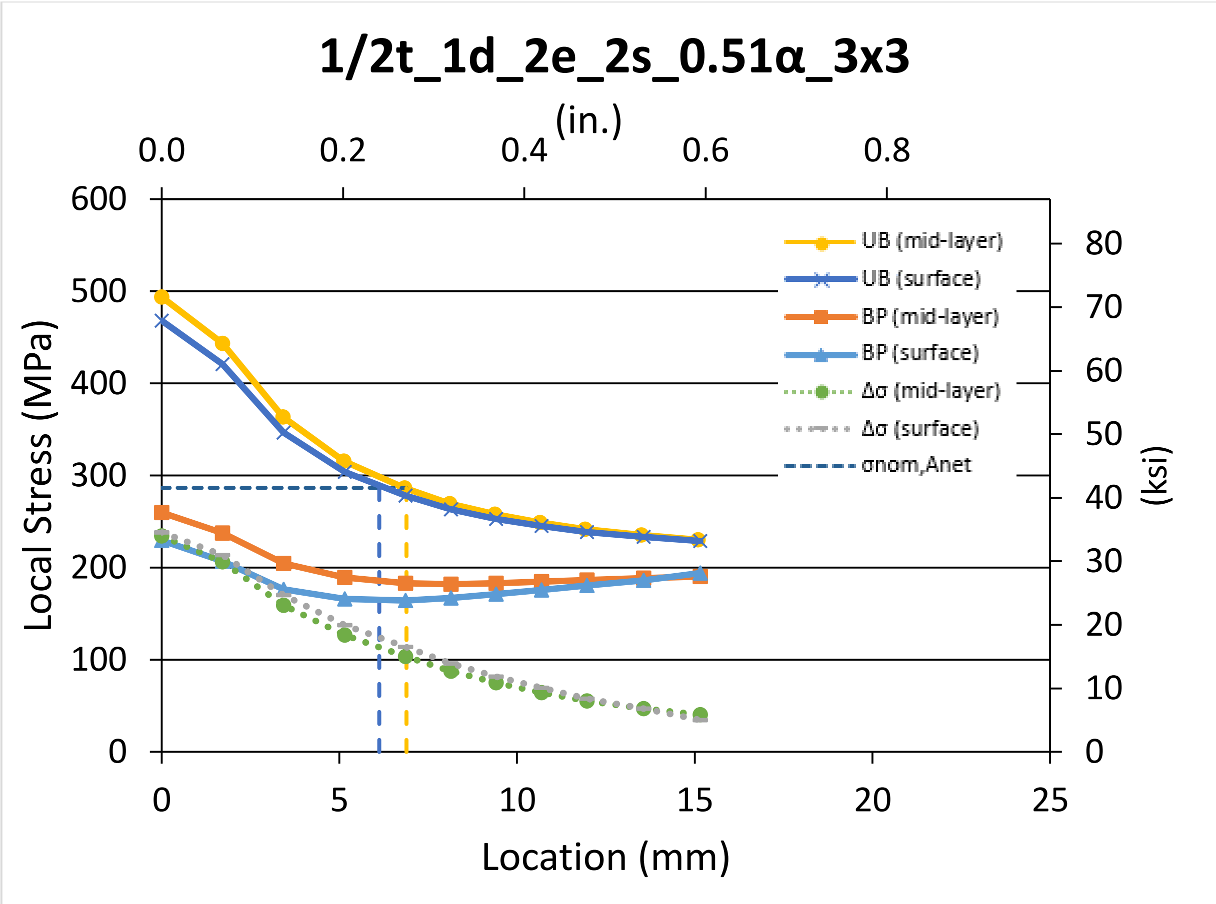

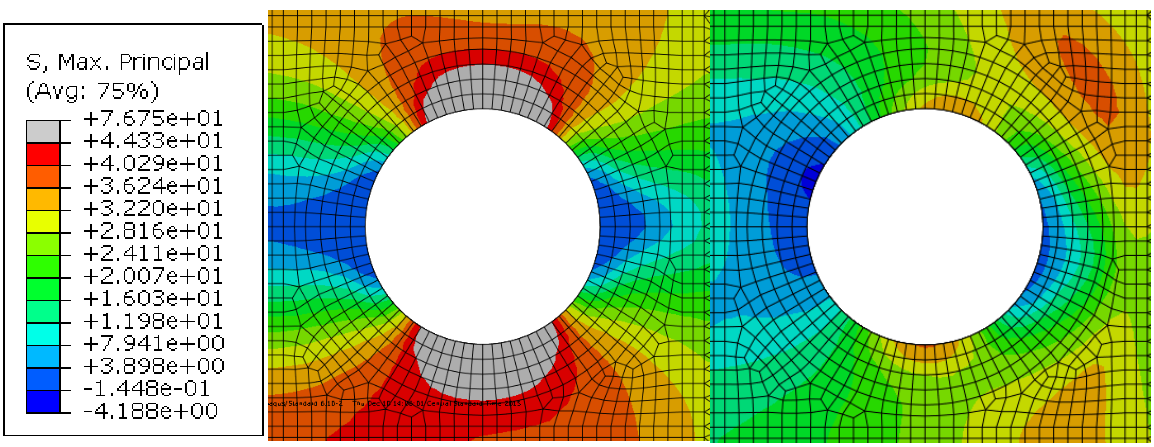

Unbolted Plate

Bolted Plate

$\sigma_{nom,Anet}$ = 41.56 ksi

(b) FEM screenshots

Figure D. 31: 1/2t_1d_2e_2s_0.51α_3x3

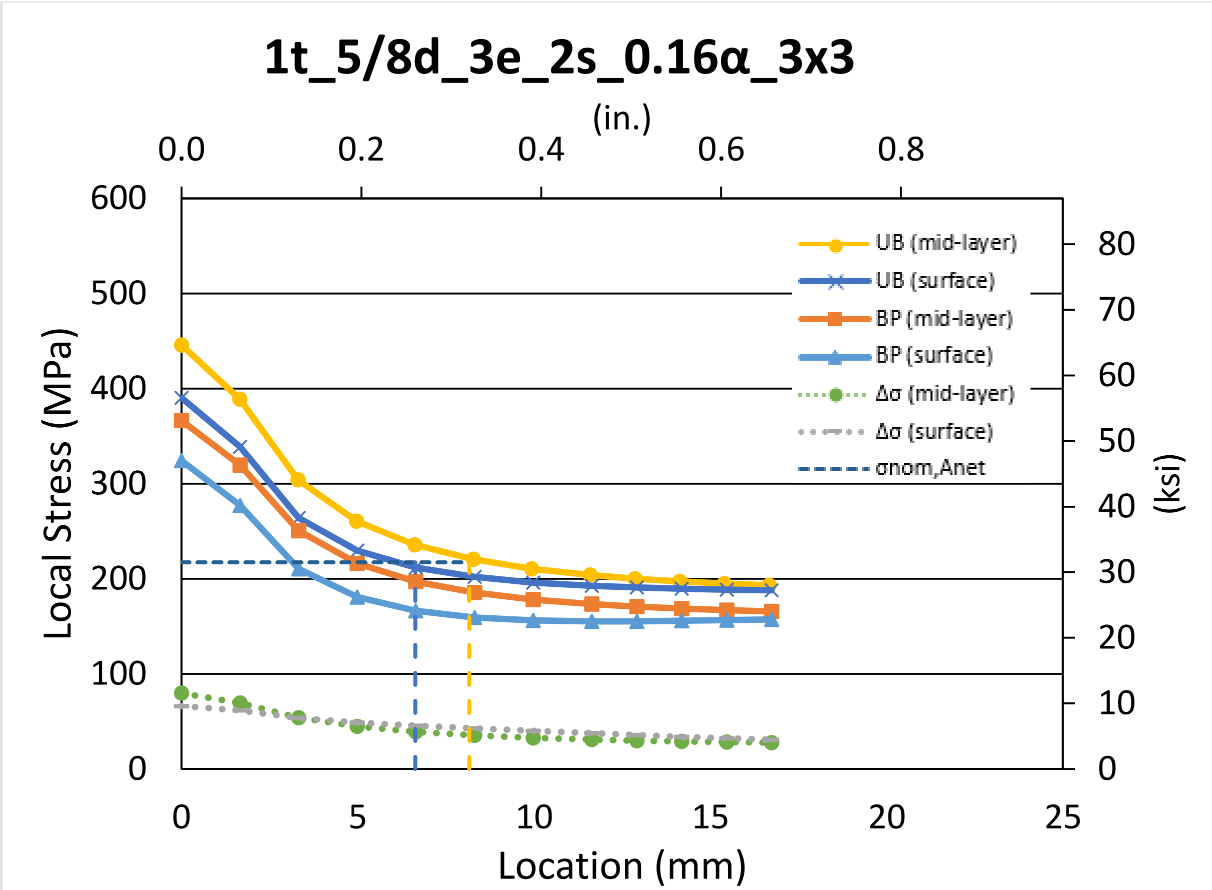

(a)Stress Distributions

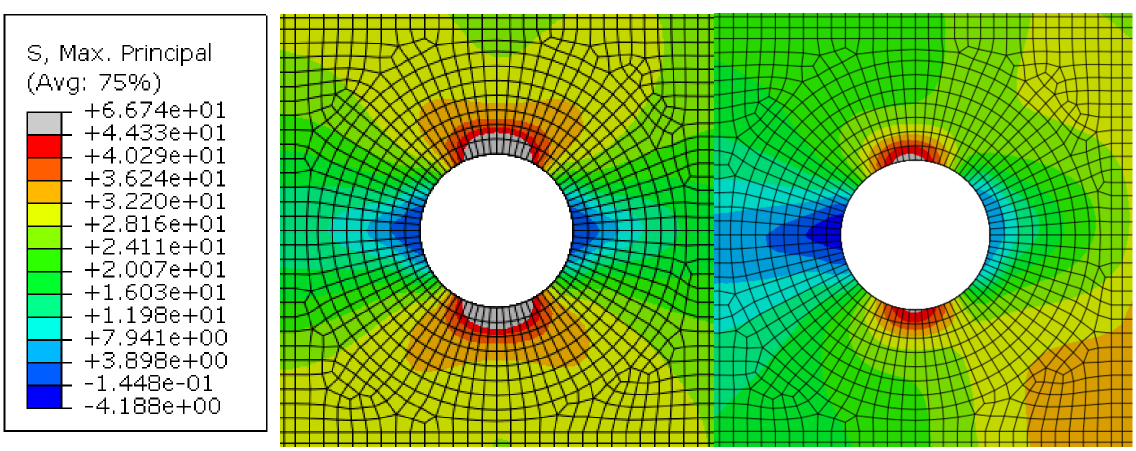

Unbolted Plate Bolted Plate

$\sigma_{nom,Anet}$ = 31.5 ksi

(b) FEM screenshots

Figure D. 32: 1t_5/8d_3e_2s_0.16α_3x3

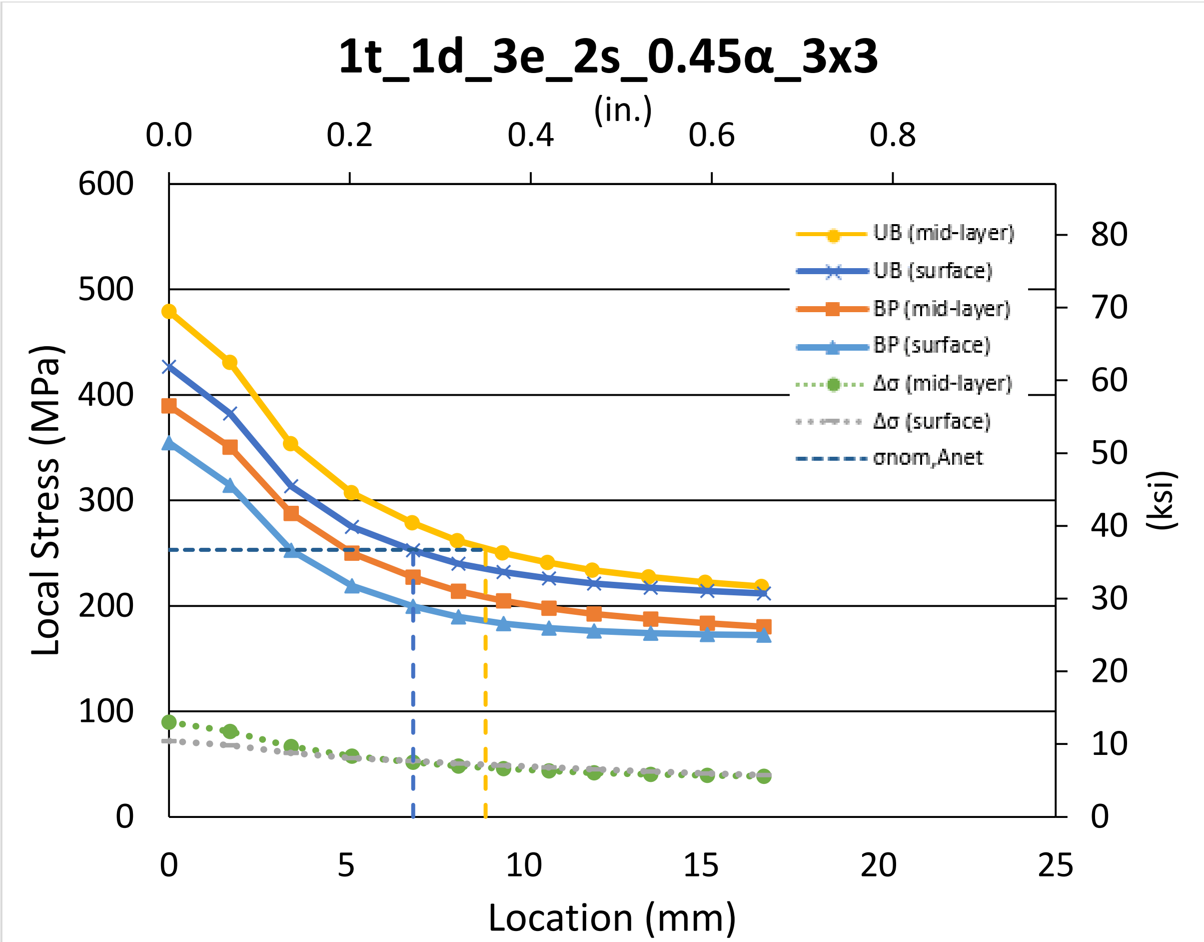

(a)Stress Distributions

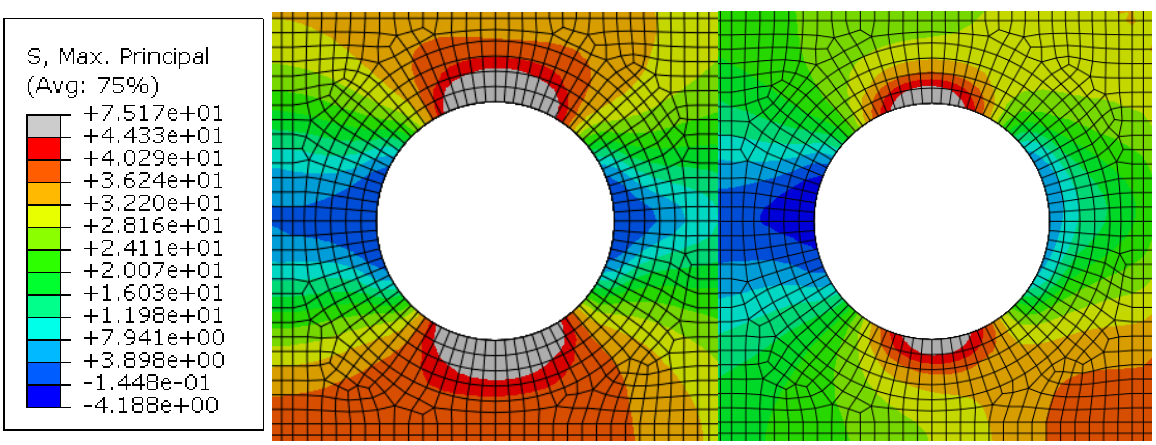

Unbolted Plate Bolted Plate

$\sigma_{nom,Anet}$ = 36.70ksi

(b) FEM screenshots

Figure D. 33: 1t_1d_3e_2s_0.45α_3x3

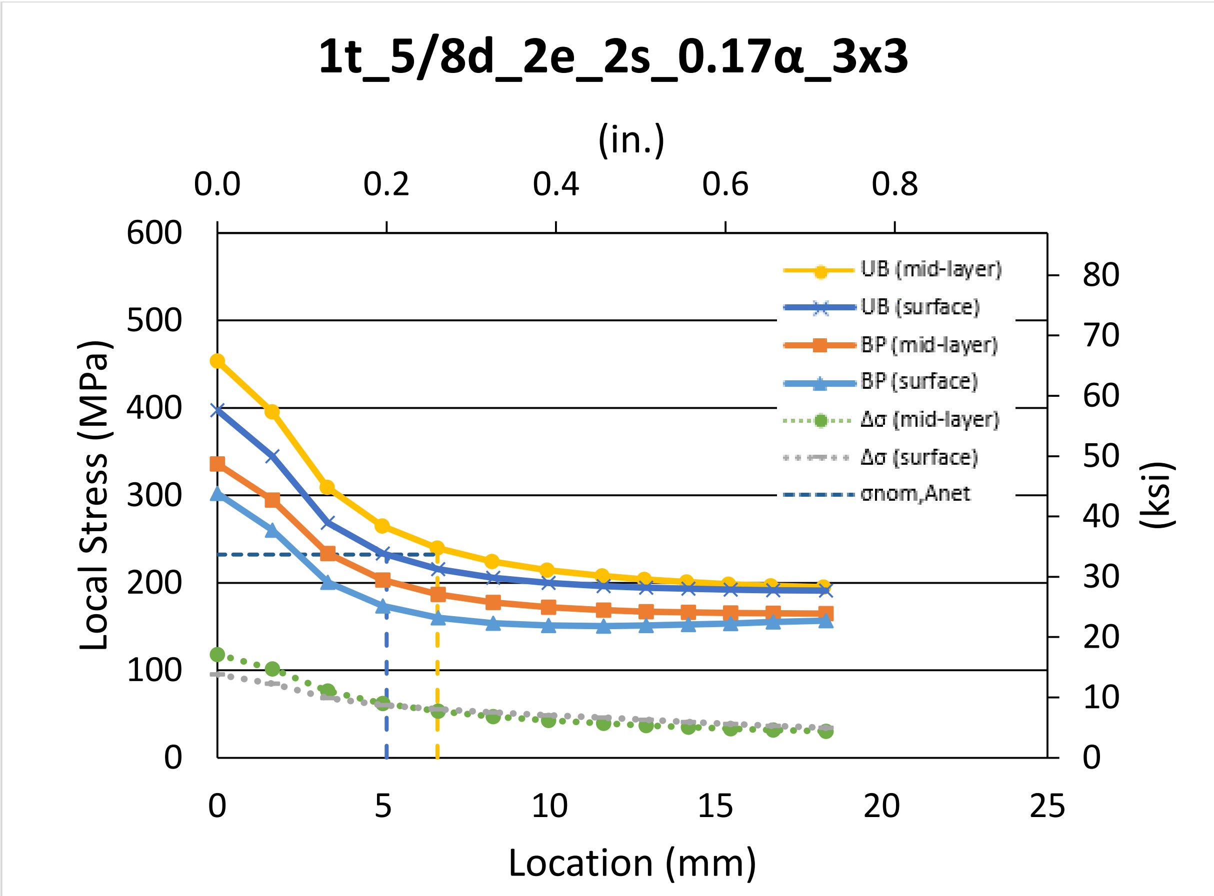

(a)Stress Distributions

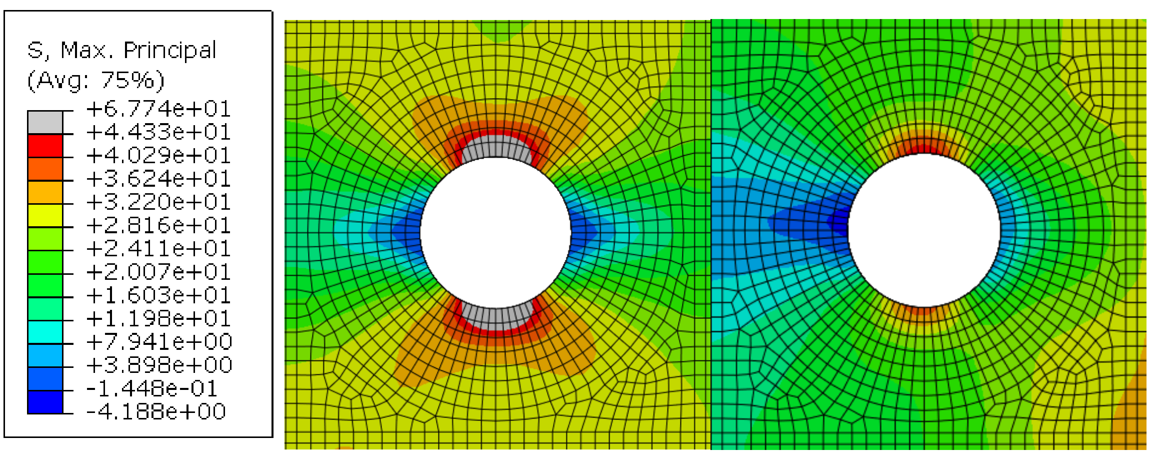

Unbolted Plate Bolted Plate

$\sigma_{nom,Anet}$ = 33.68 ksi

(b) FEM screenshots

Figure D. 34: 1t_5/8d_2e_2s_0.17α_3x3

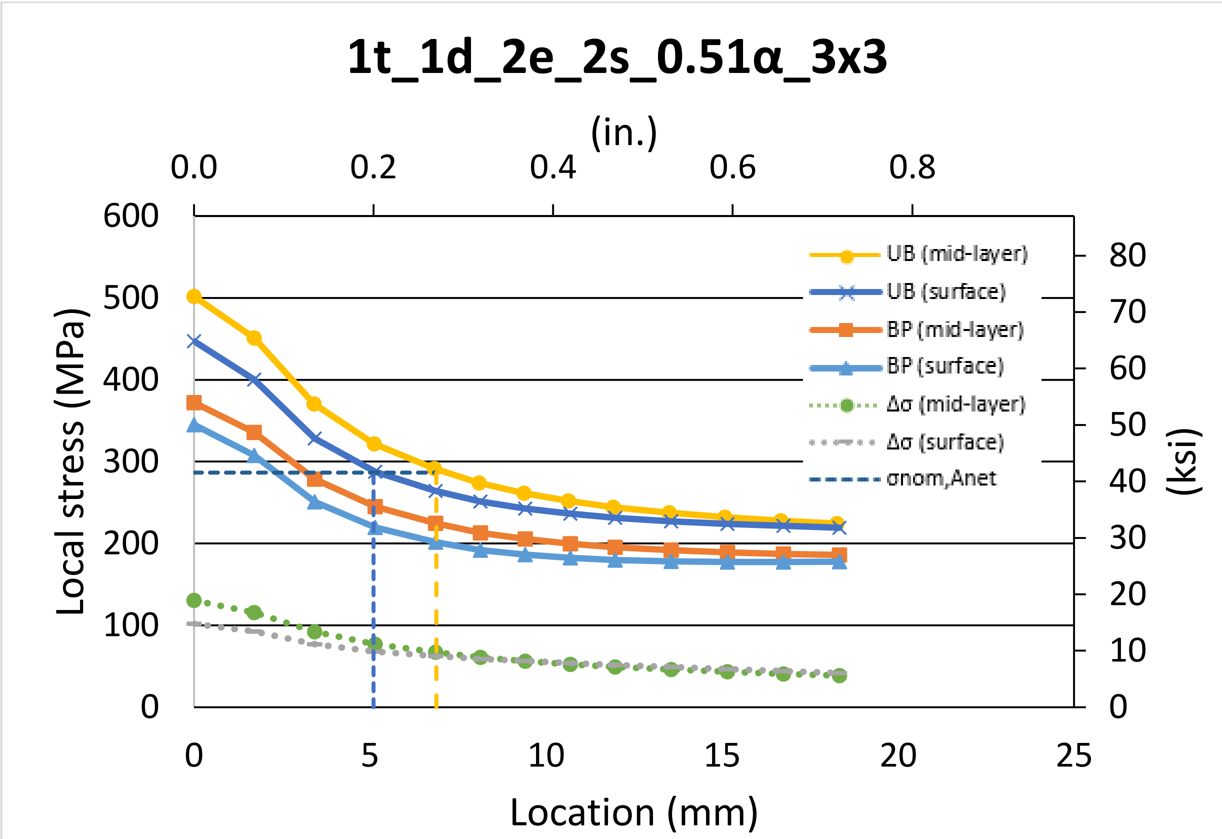

(a)Stress Distributions

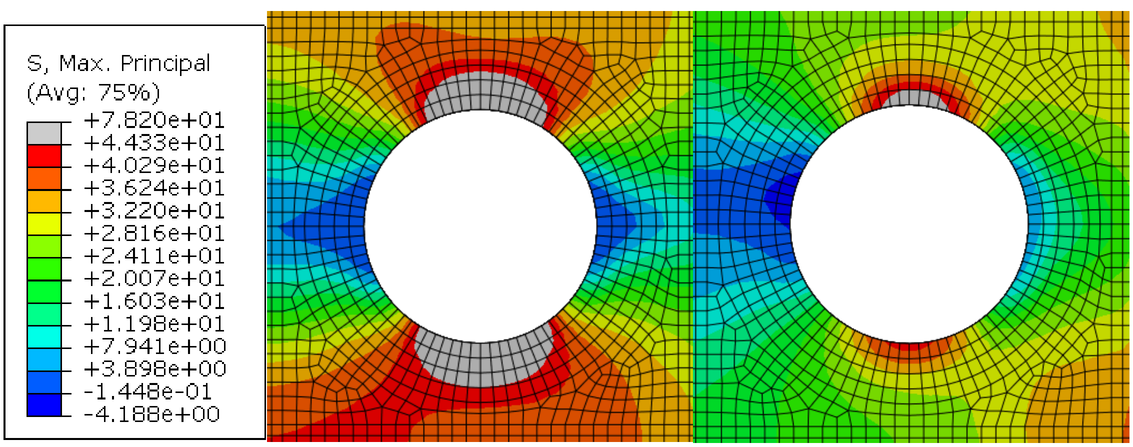

Unbolted Plate | Bolted Plate

$\sigma_{nom,Anet}$ = 41.56 ksi

(b) FEM screenshots

Figure D. 35: 1t_1d_2e_2s_0.51α_3x3

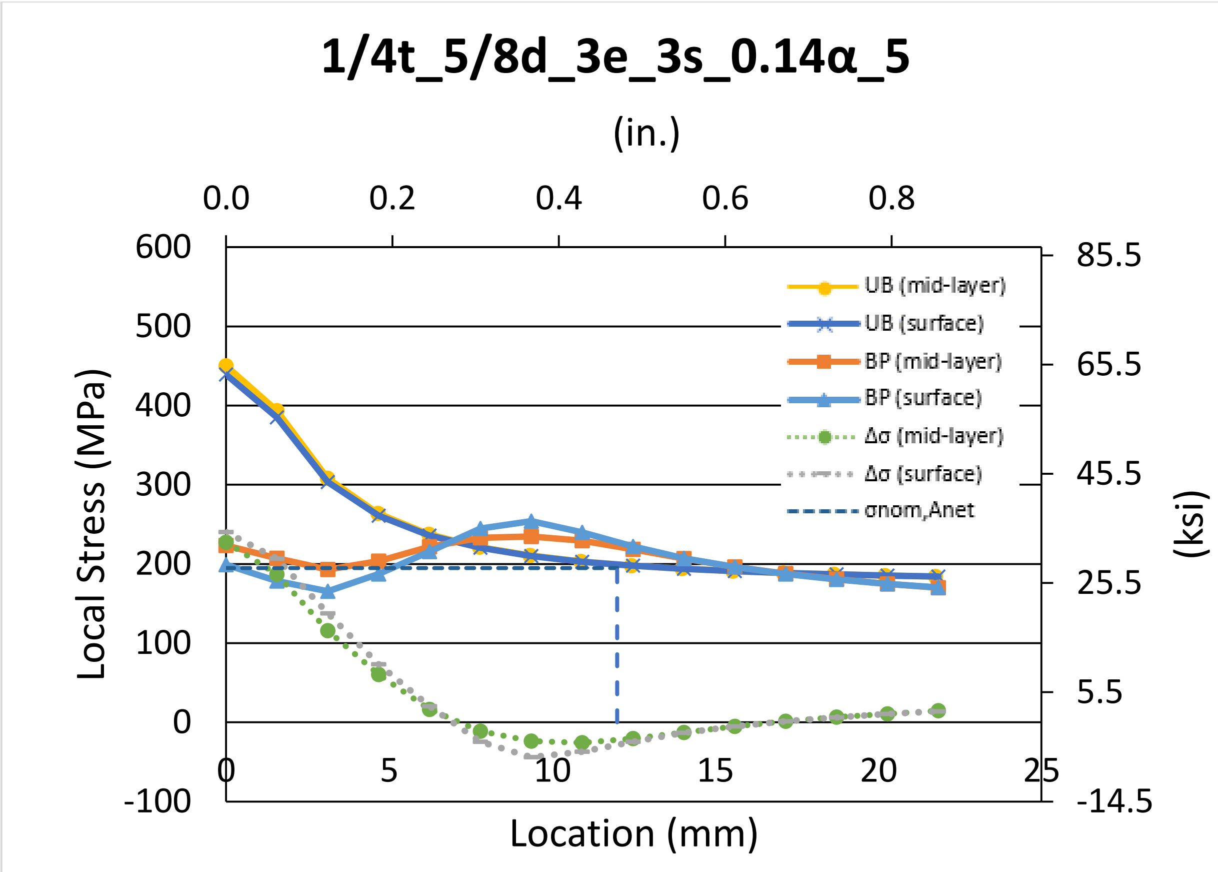

(a)Stress Distributions

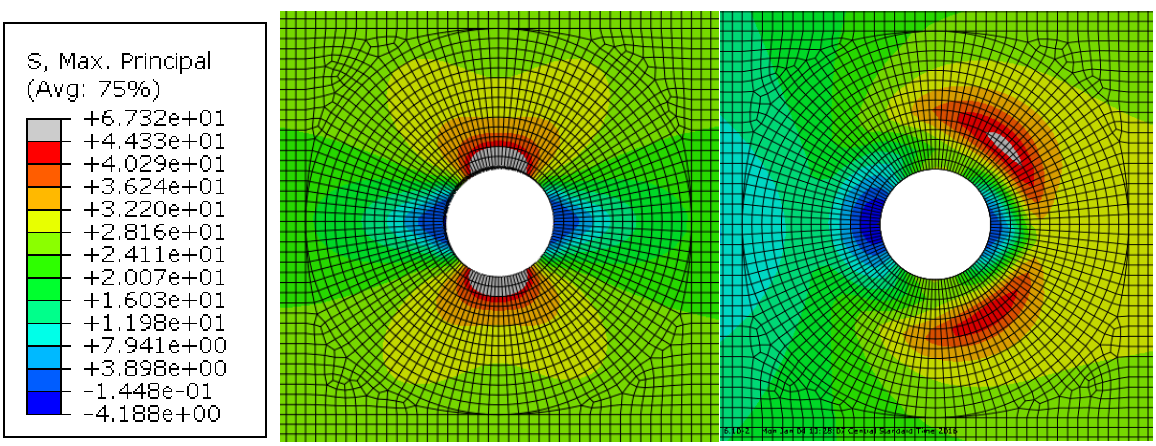

Unbolted Plate Bolted Plate

$\sigma_{nom,Anet}$ = 28.24 ksi

(b) FEM screenshots

Figure D. 36: 1/4t_5/8d_3e_3s_0.14α_5

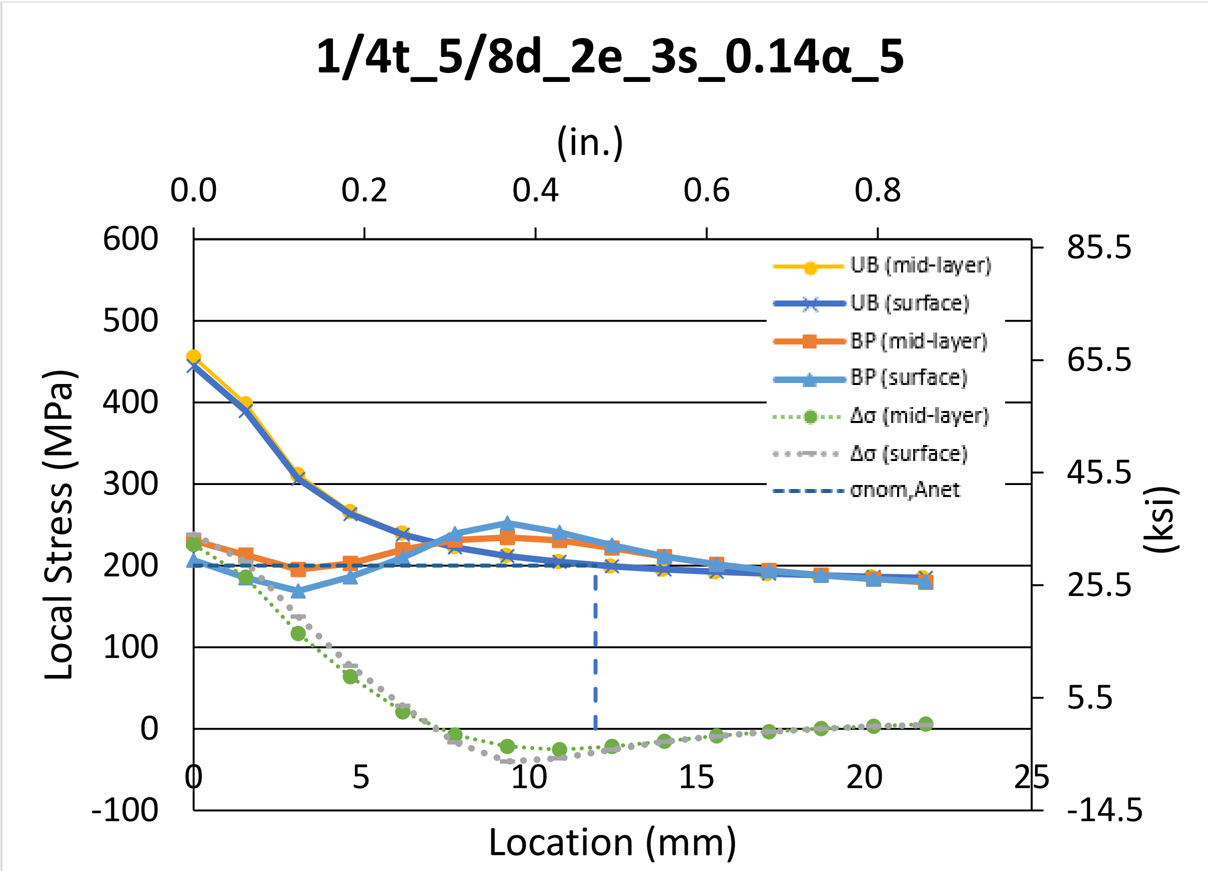

(a)Stress Distributions

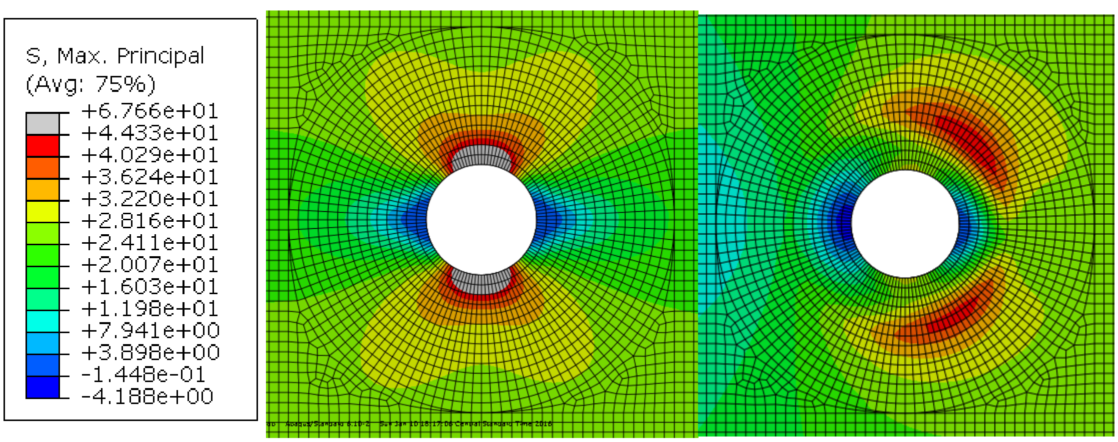

Unbolted Plate　　　　Bolted Plate

$\sigma_{nom,Anet}$ = 28.99 ksi

(b) FEM screenshots

Figure D. 37: 1/4t_5/8d_2e_3s_0.14α_5

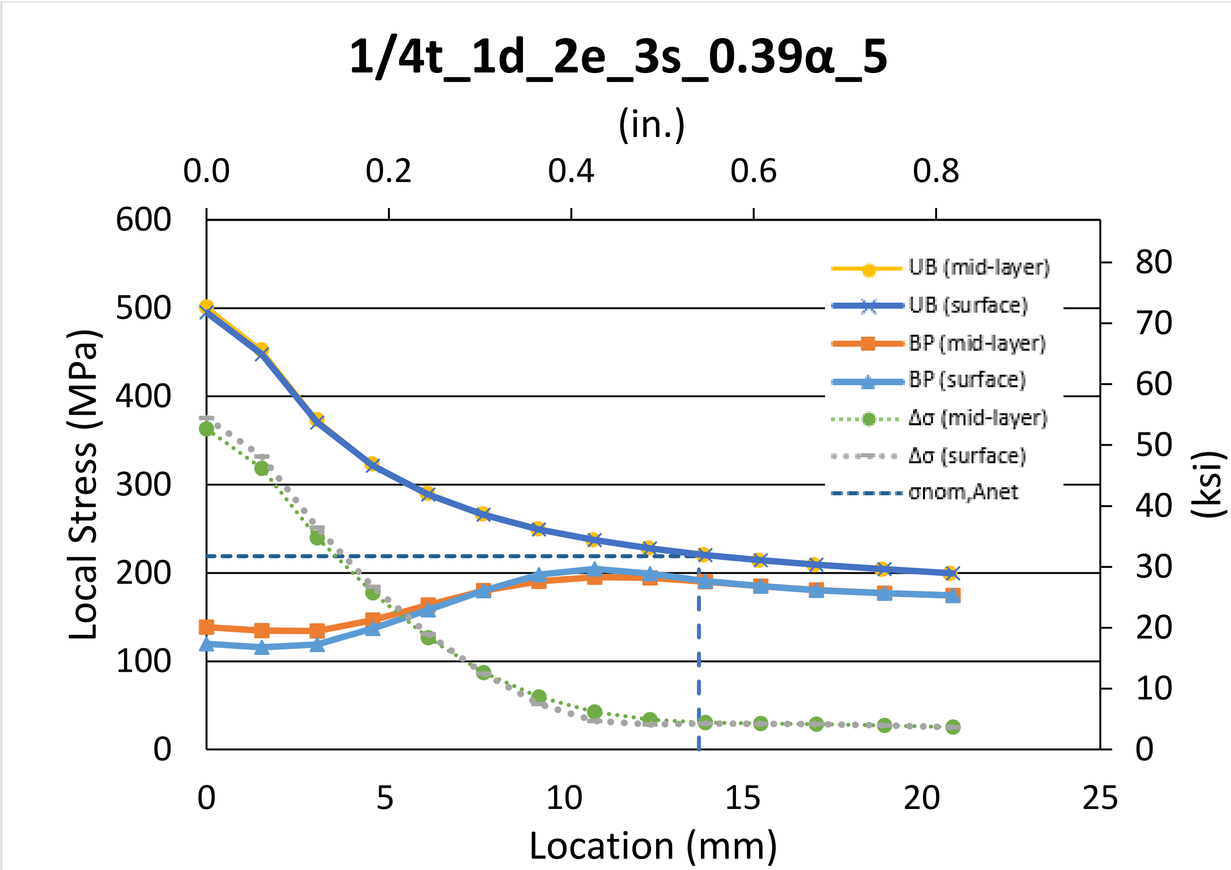

(a)Stress Distributions

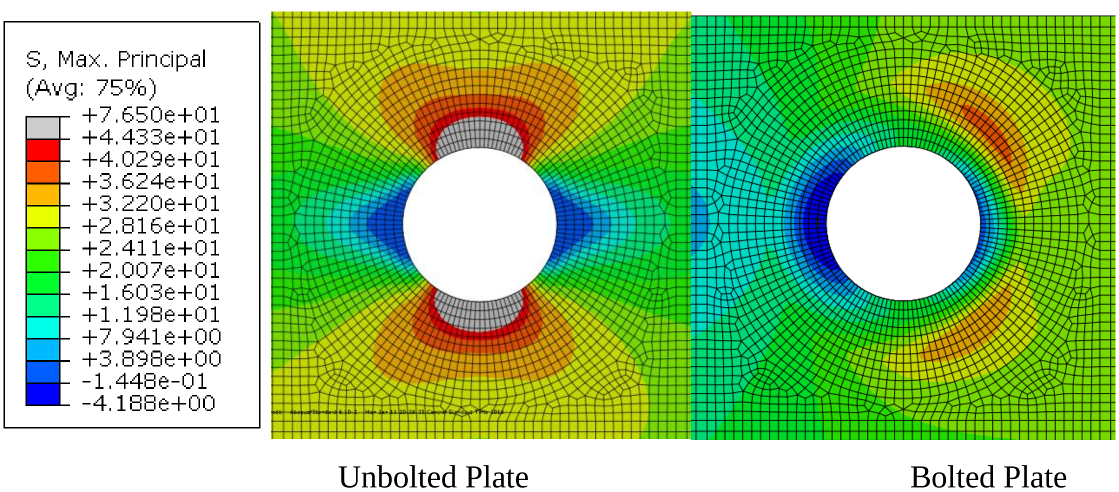

$\sigma_{nom,Anet}$ = 31.75 ksi

(b) FEM screenshots

Figure D. 38: 1/4t_1d_2e_3s_0.39α_5

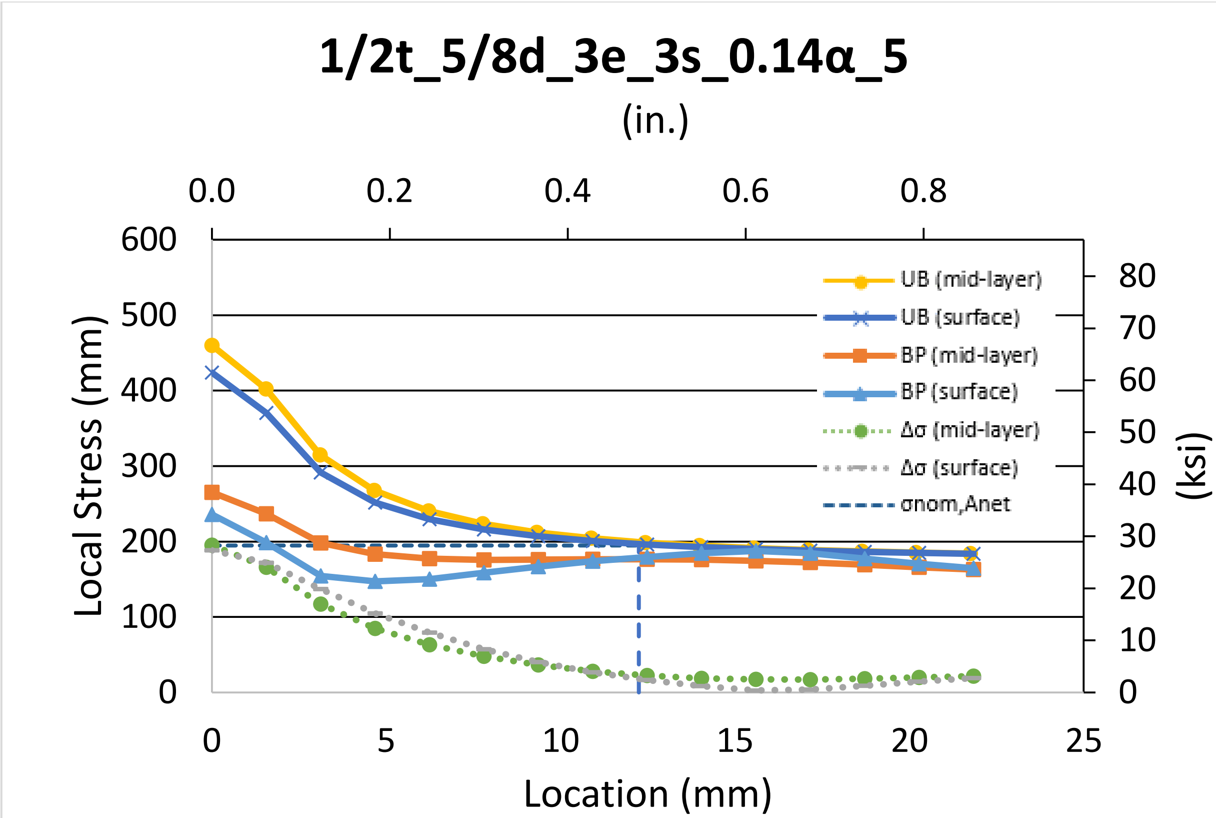

(a)Stress Distributions

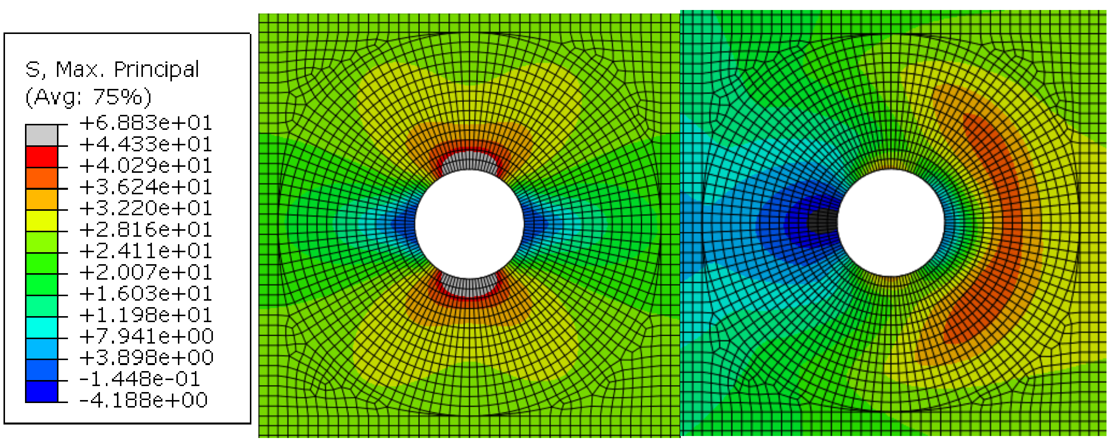

Unbolted Plate Bolted Plate

$\sigma_{nom,Anet}$ = 28.24 ksi

(b) FEM screenshots

Figure D. 39: 1/2t_5/8d_3e_3s_0.14α_5

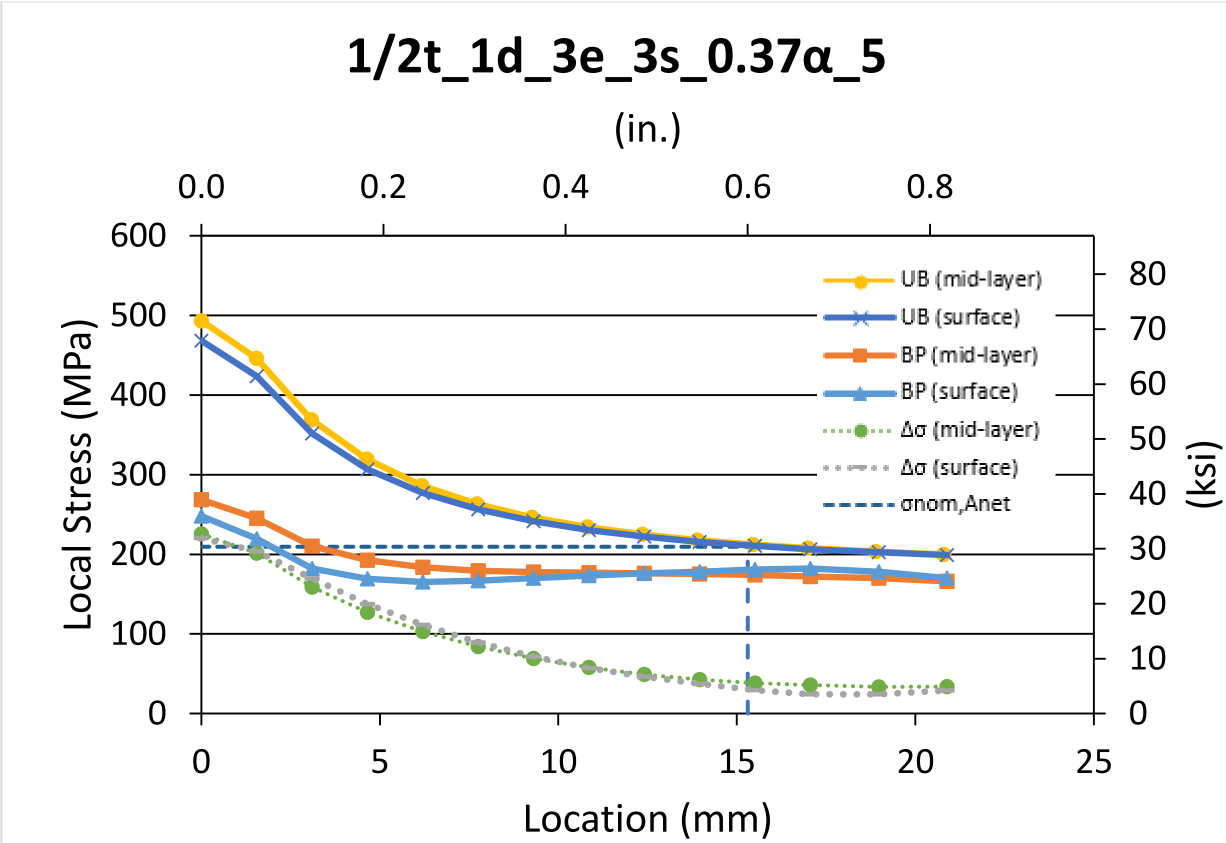

(a)Stress Distributions

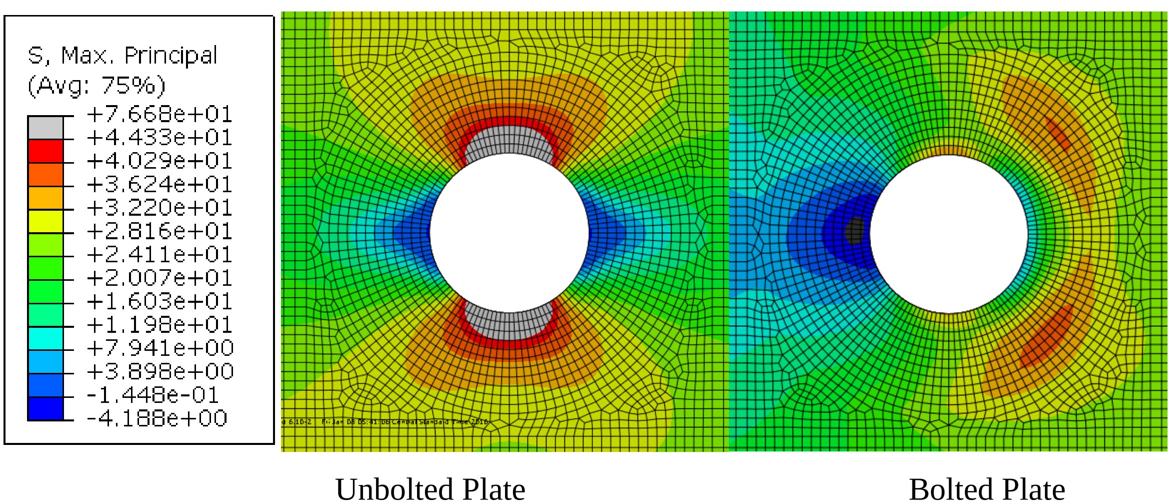

$\sigma_{nom,Anet}$ = 30.38 ksi

(b) FEM screenshots

Figure D. 40: 1/2t_1d_3e_3s_0.37α_5

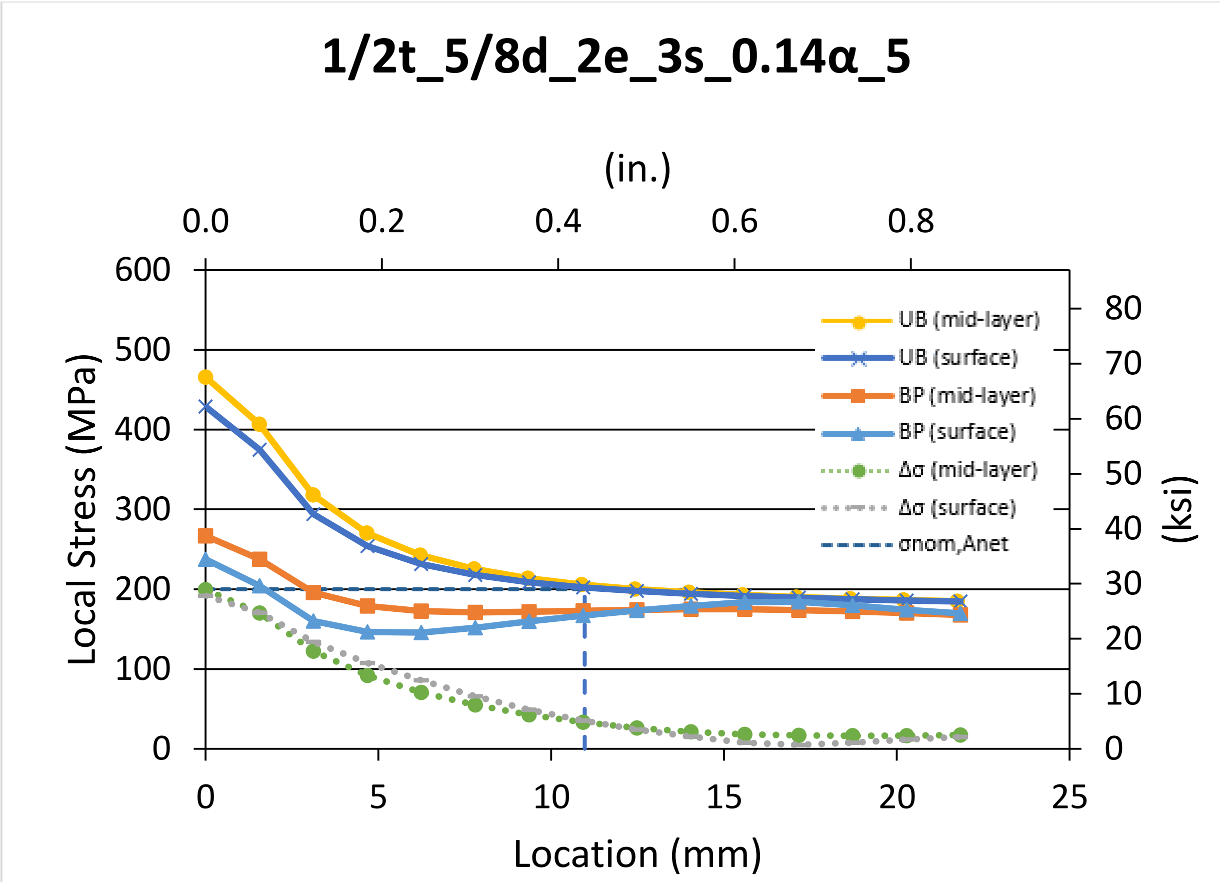

(a)Stress Distributions

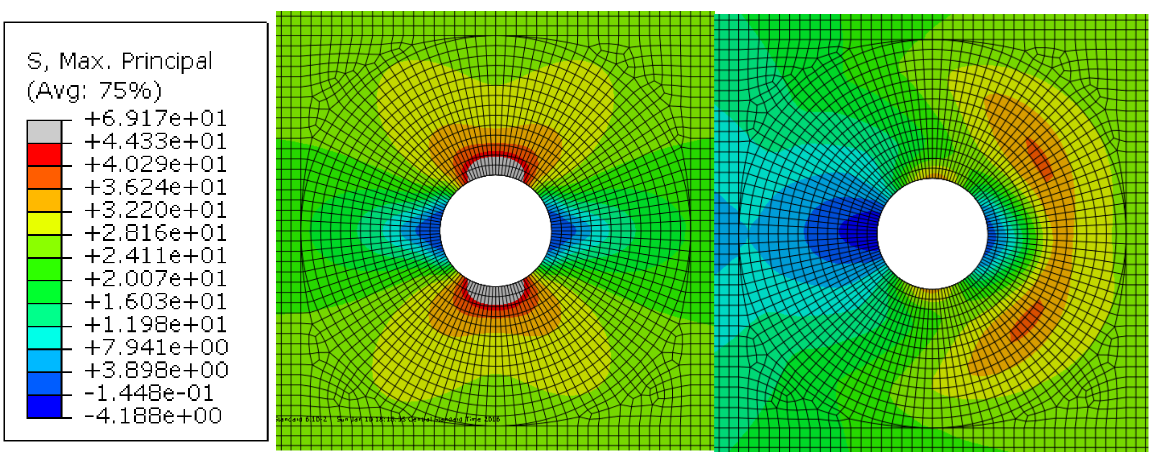

Unbolted Plate

Bolted Plate

$\sigma_{nom,Anet}$ = 28.99 ksi

(b) FEM screenshots

Figure D. 41: 1/2t_5/8d_2e_3s_0.14α_5

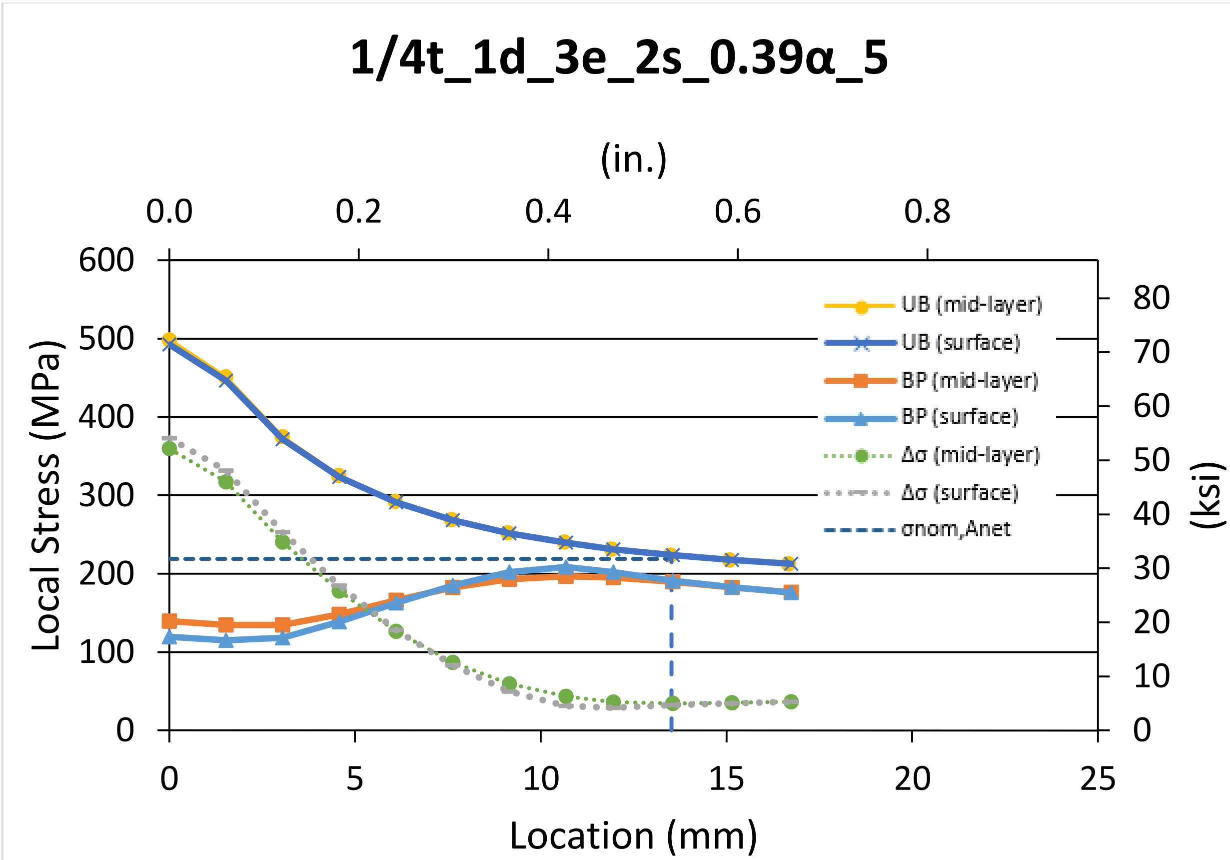

(a)Stress Distributions

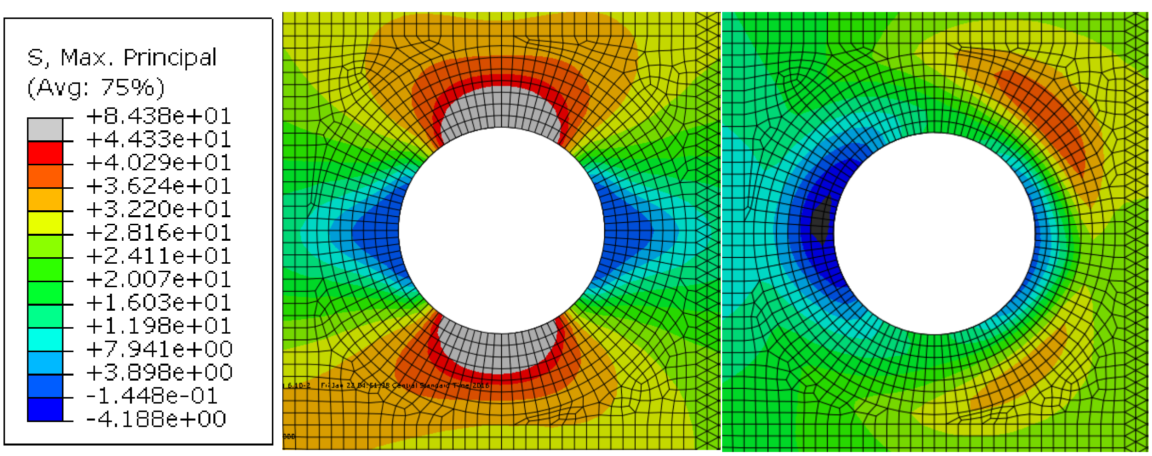

Unbolted Plate Bolted Plate

$\sigma_{nom,Anet}$ = 31.75 ksi

(b) FEM screenshots

Figure D. 42: 1/4t_1d_3e_2s_0.39α_5

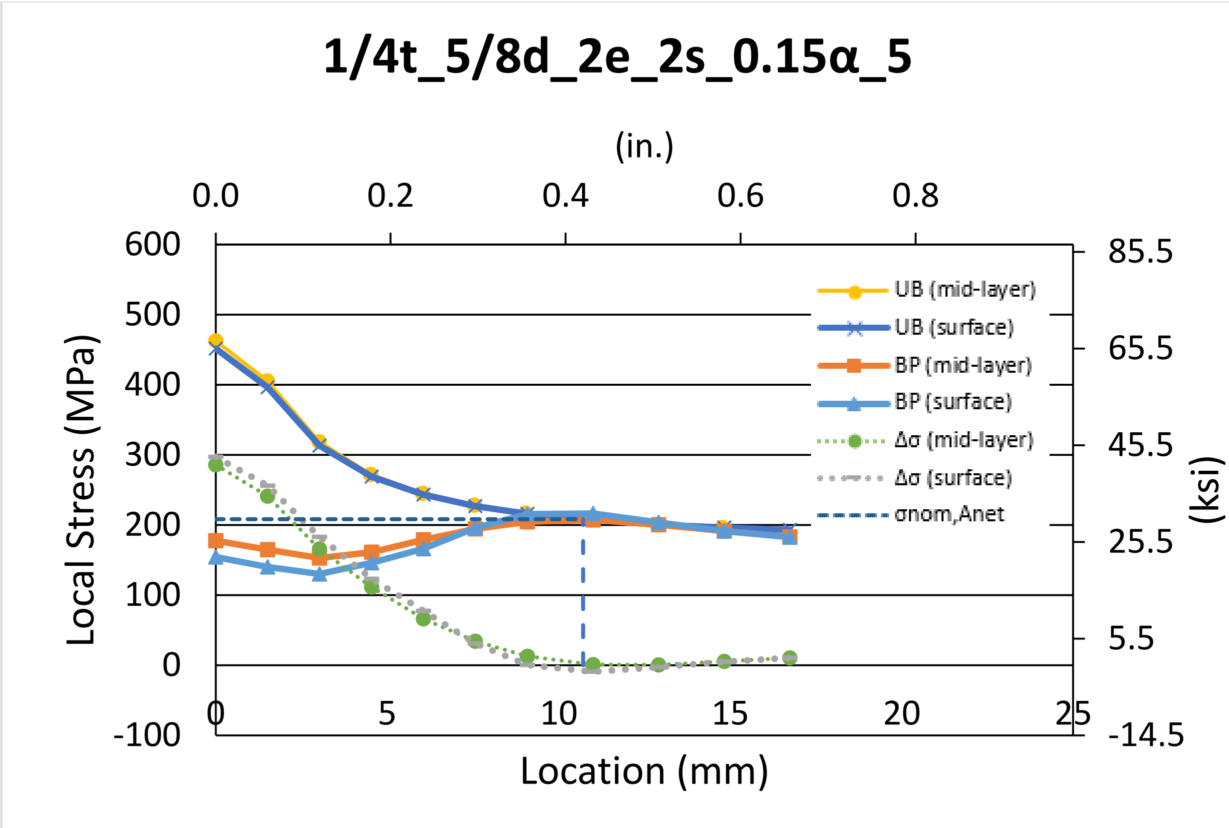

(a)Stress Distributions

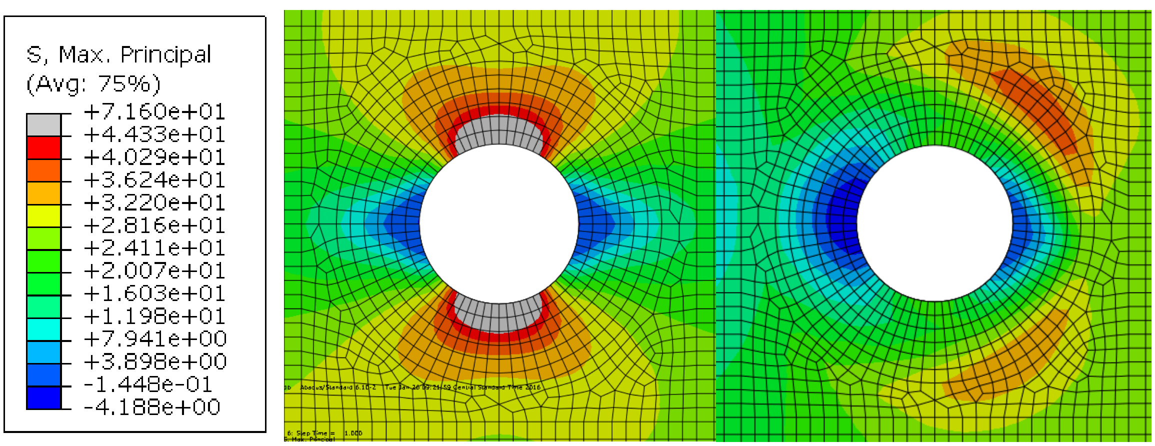

Unbolted Plate Bolted Plate

$\sigma_{nom,Anet}$ = 30.19 ksi

(b) FEM screenshots

Figure D. 43: 1/4t_5/8d_2e_2s_0.15α_5

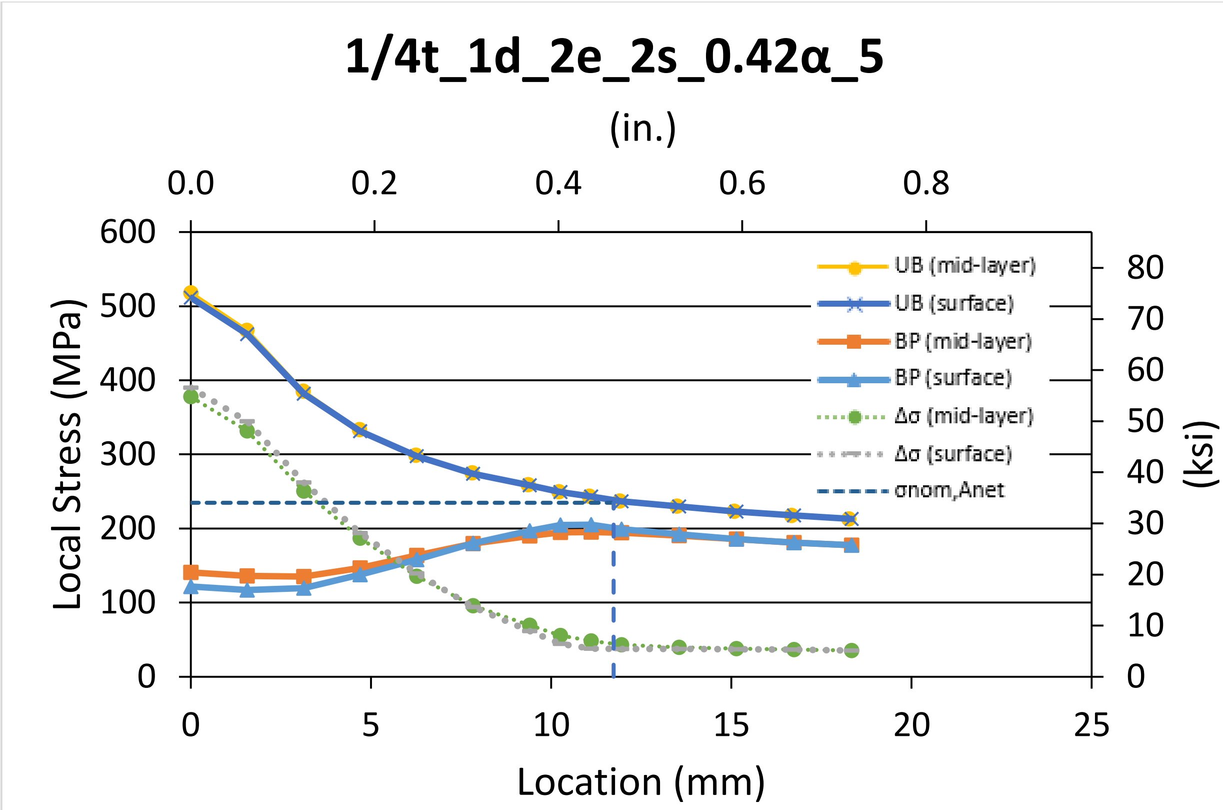

(a)Stress Distributions

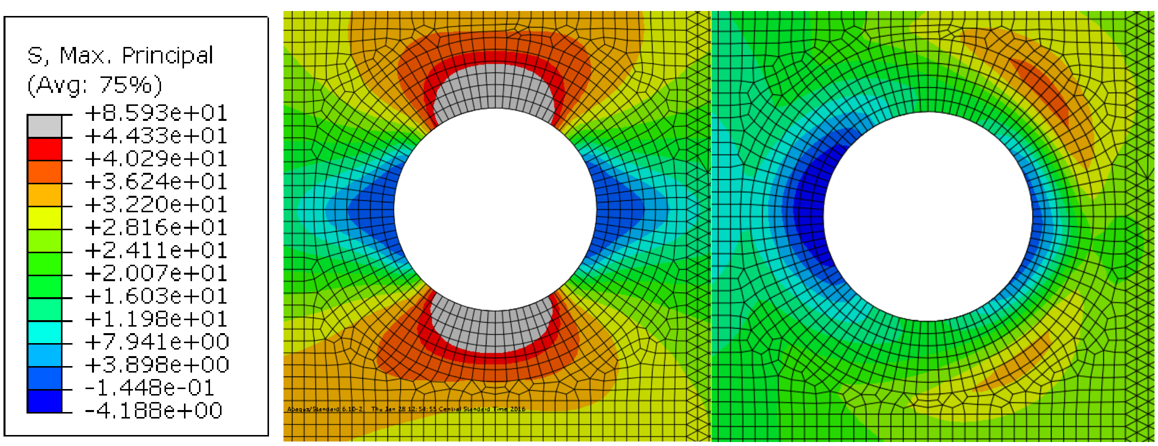

Unbolted Plate Bolted Plate

$\sigma_{nom,Anet}$ = 34.04 ksi

(b) FEM screenshots

Figure D. 44: 1/4t_1d_2e_2s_0.42α_5

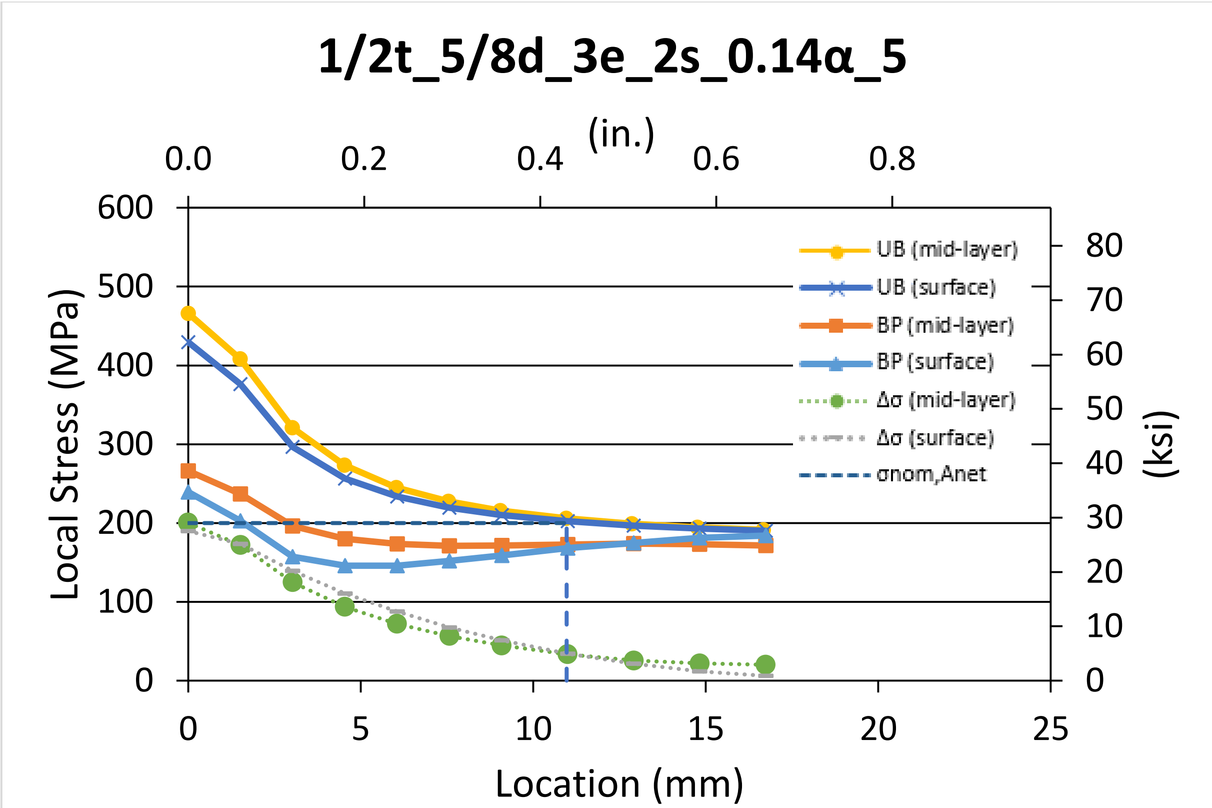

(a)Stress Distributions

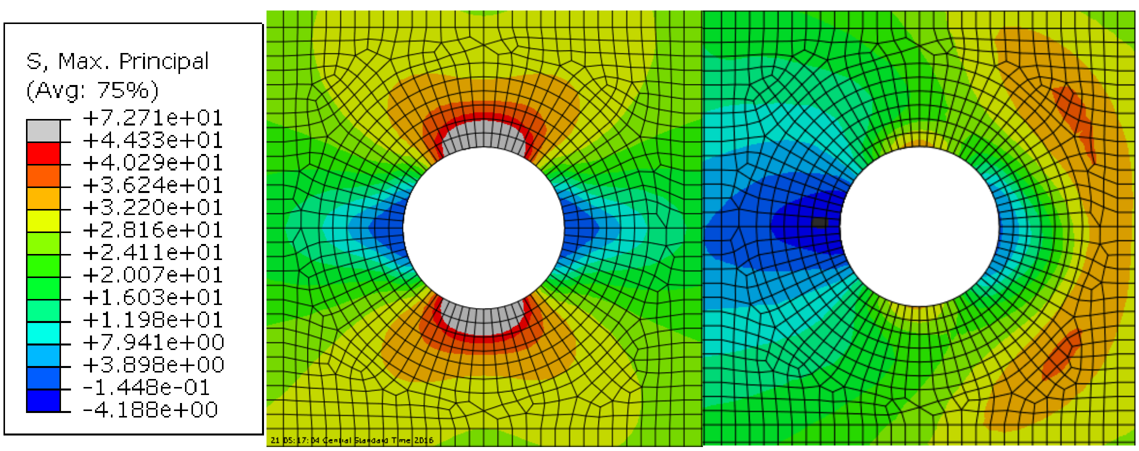

Unbolted Plate Bolted Plate

$\sigma_{nom,Anet}$ = 28.99 ksi

(b) FEM screenshots

Figure D. 45: 1/2t_5/8d_3e_2s_0.14α_5

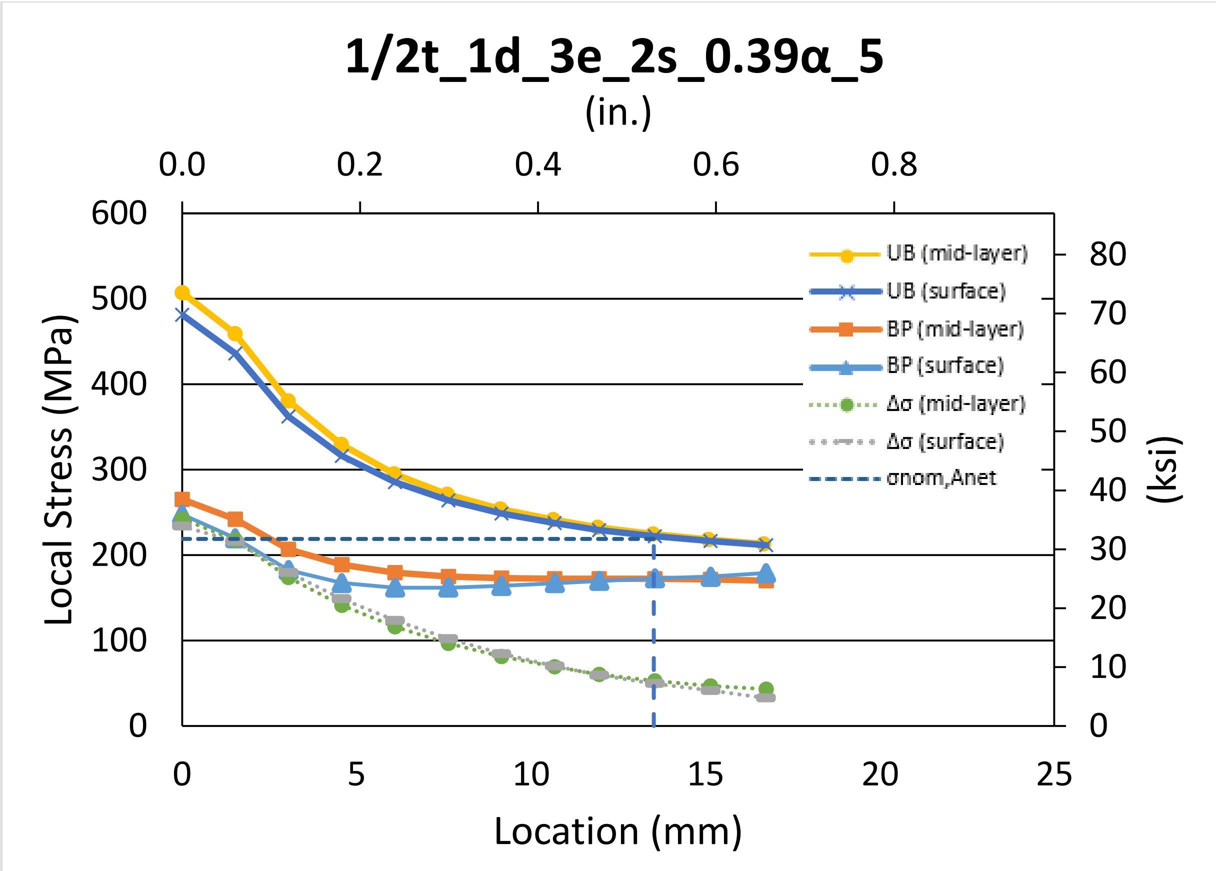

(a)Stress Distributions

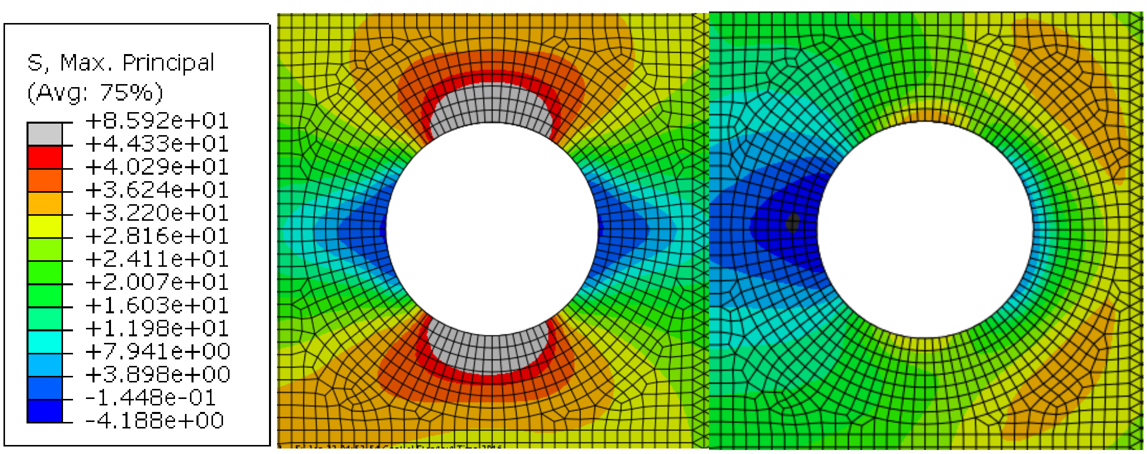

Unbolted Plate

Bolted Plate

$\sigma_{nom,Anet}$ = 31.75ksi

(b) FEM screenshots

Figure D. 46: 1/2t_1d_3e_2s_0.39α_5

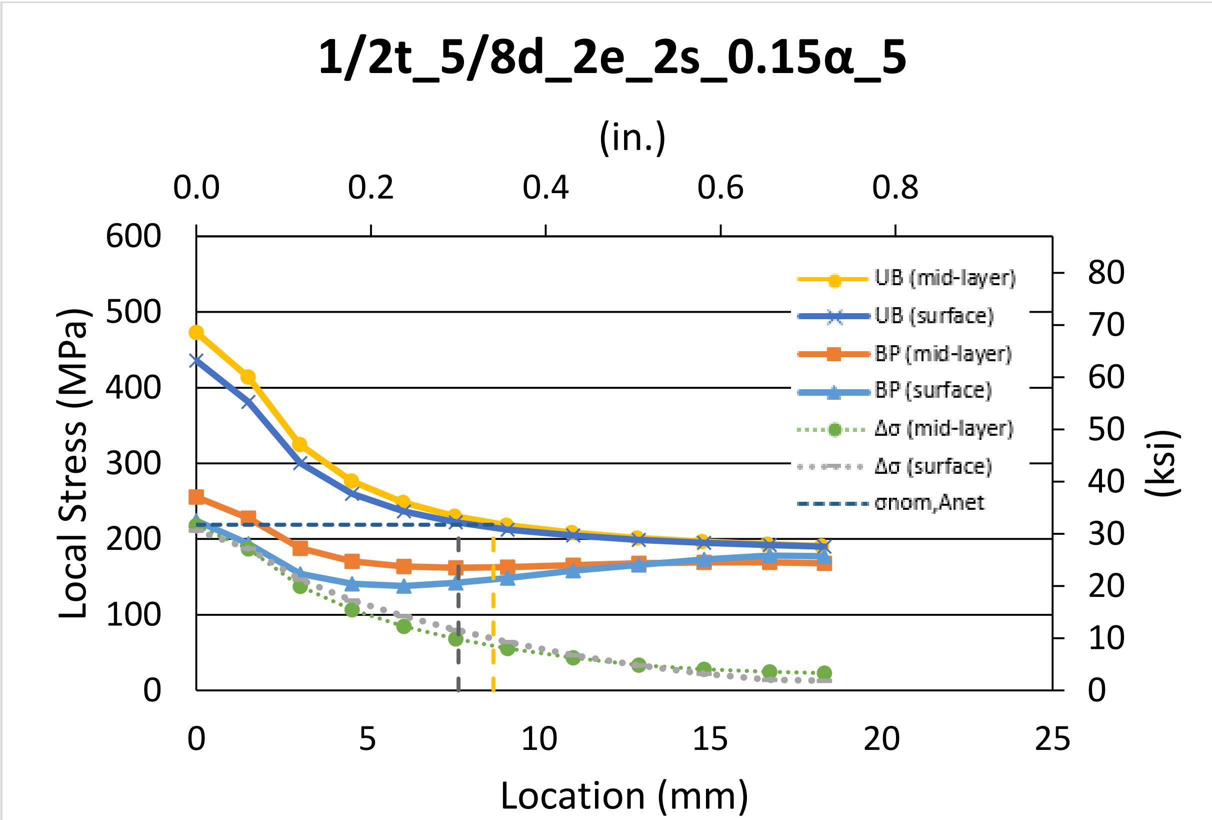

(a)Stress Distributions

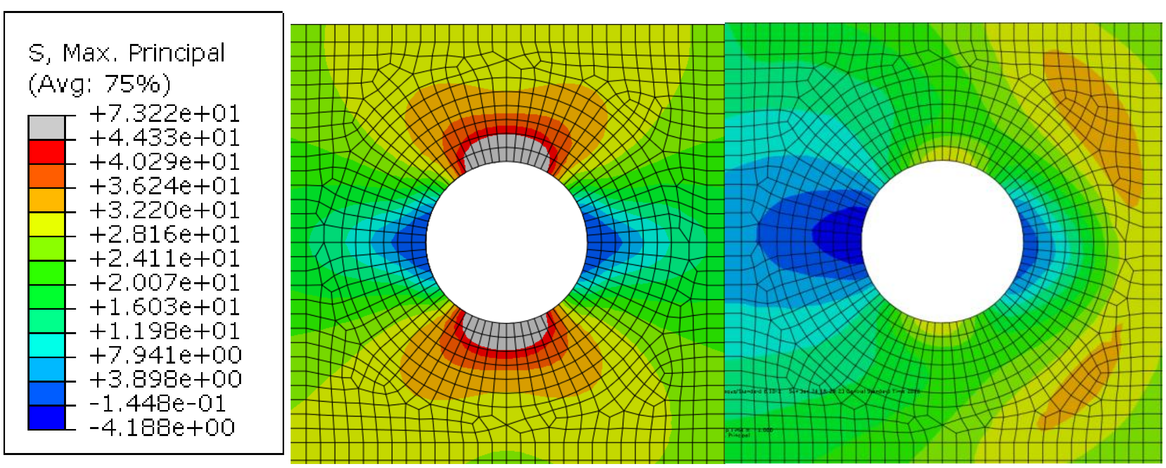

Unbolted Plate Bolted Plate

$\sigma_{nom,Anet}$ = 30.19 ksi

(b) FEM screenshots

Figure D. 47: 1/2t_5/8d_2e_2s_0.15α_5

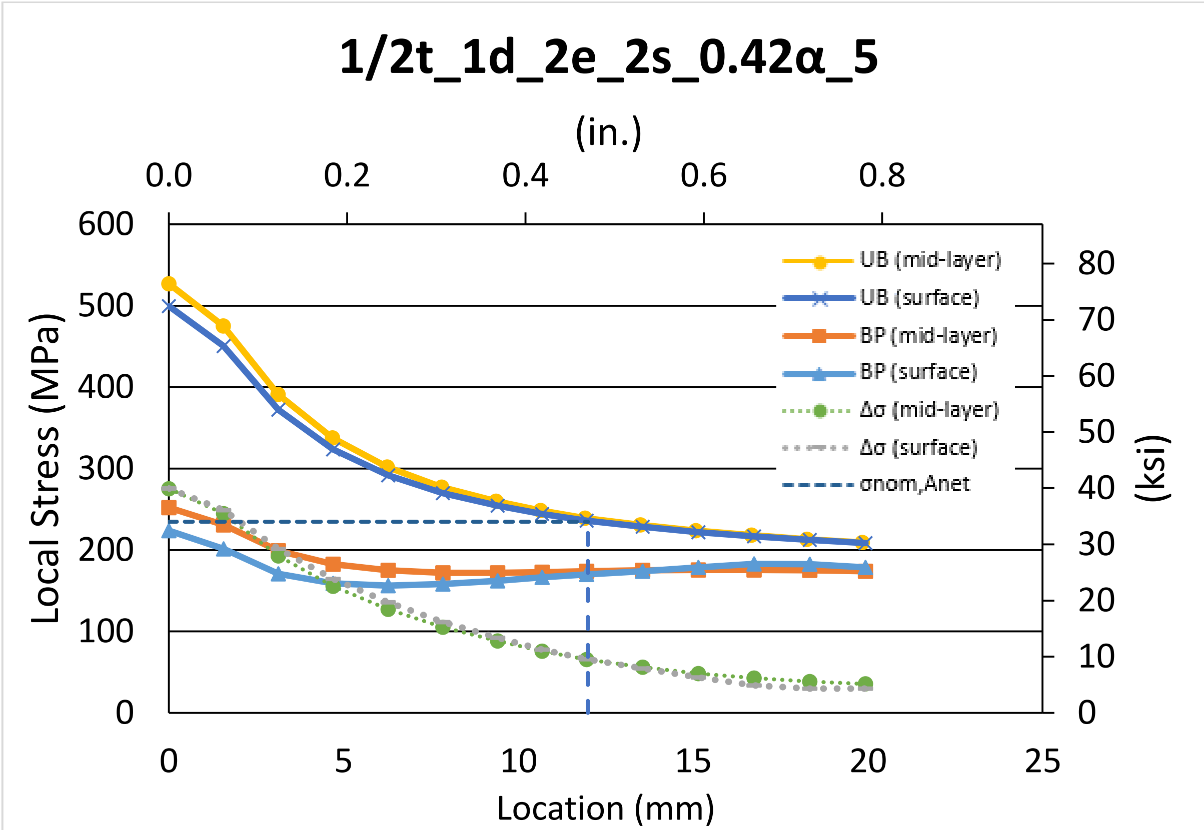

(a)Stress Distributions

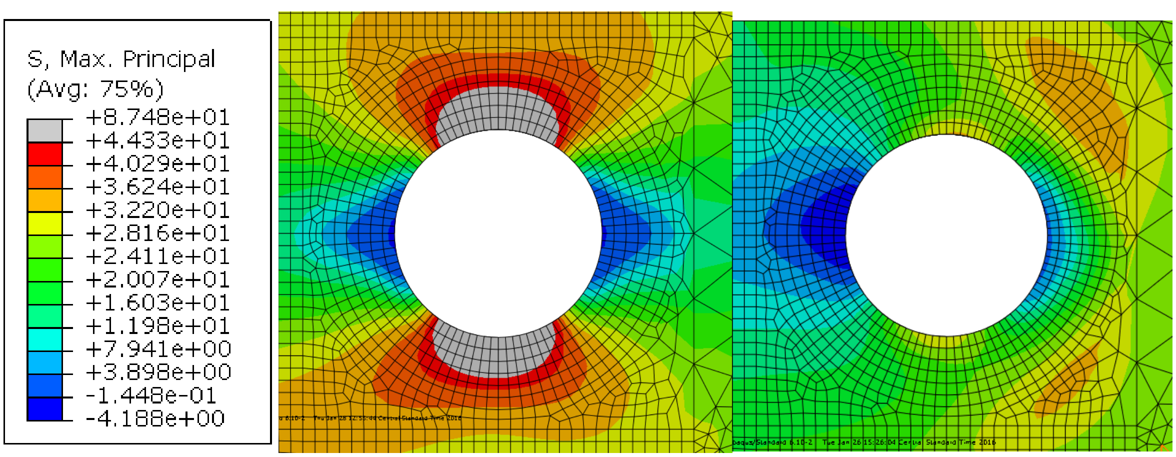

Unbolted Plate

Bolted Plate

$\sigma_{nom,Anet}$ = 34.04 ksi

(b) FEM screenshots

Figure D. 48: 1/2t_1d_2e_2s_0.42α_5

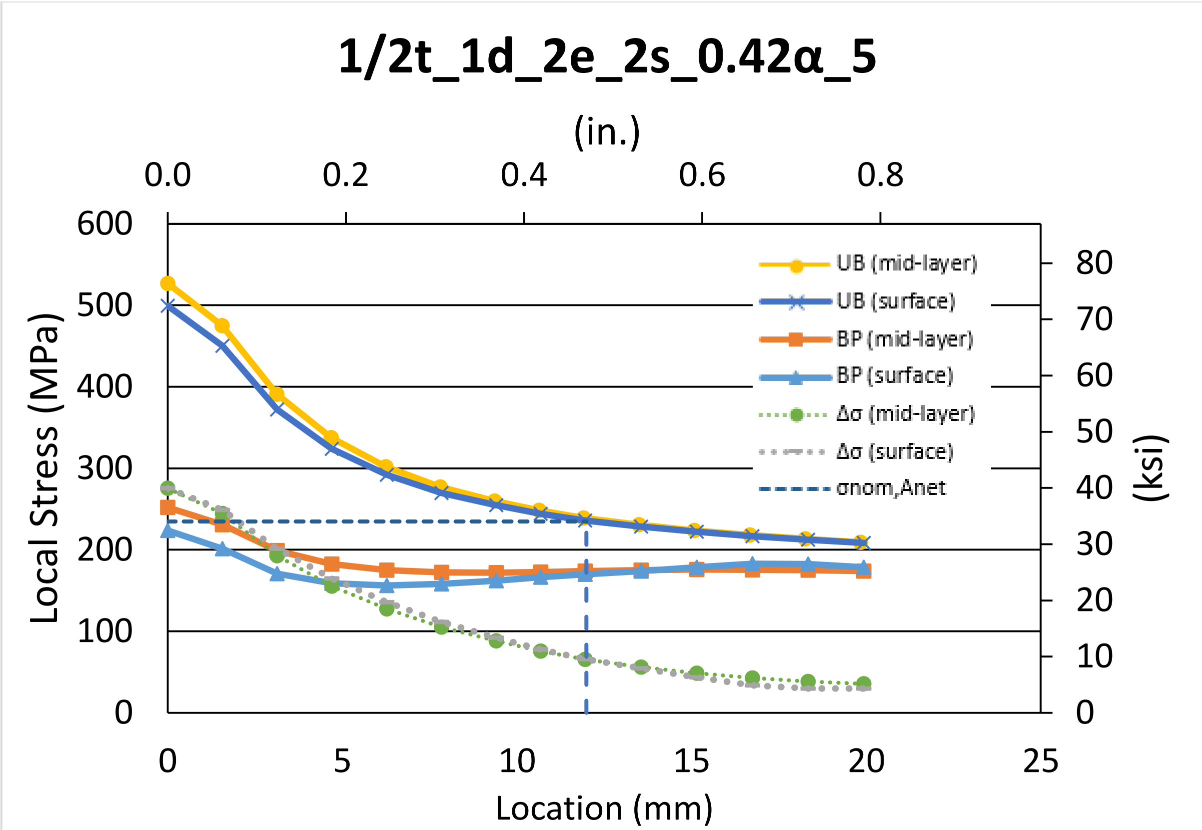

(a)Stress Distributions

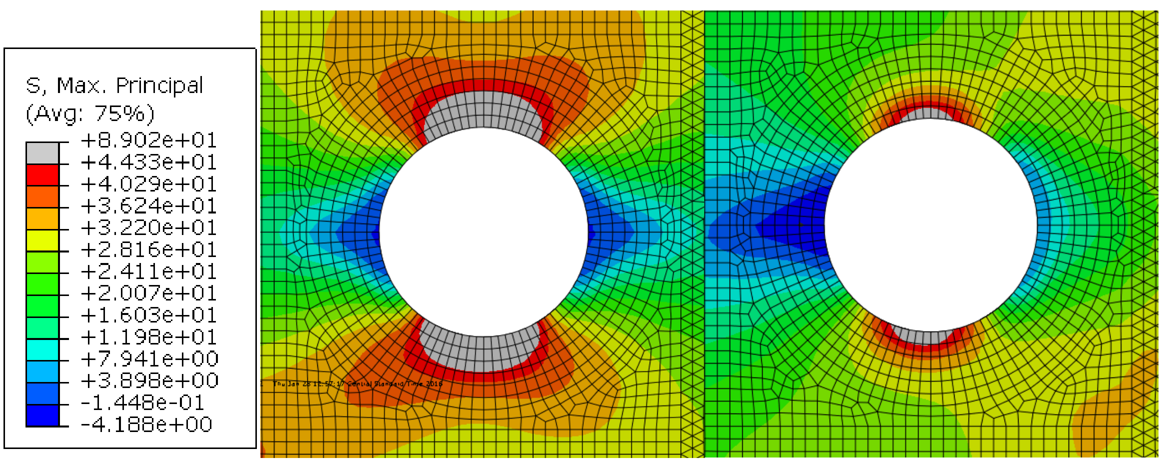

Unbolted Plate

Bolted Plate

$\sigma_{nom,Anet}$ = 34.04 ksi

(b) FEM screenshots

Figure D. 49: 1/2t_1d_2e_2s_0.42α_5

APPENDIX E COMPARISON OF STRESS DISTRIBUTIONS OF EDGE DISTANCES AND BOLT SPACING

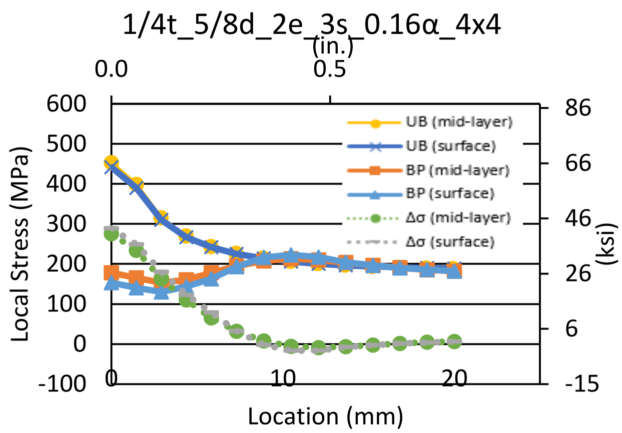

(a) 50.8mm [2 in.] edge distance

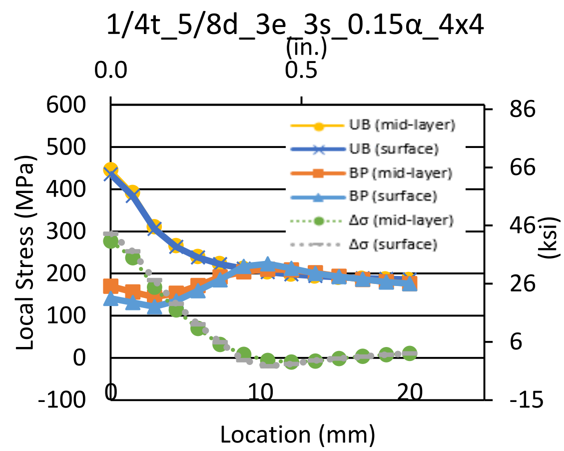

(b) 76.2 mm [3 in.] edge distance

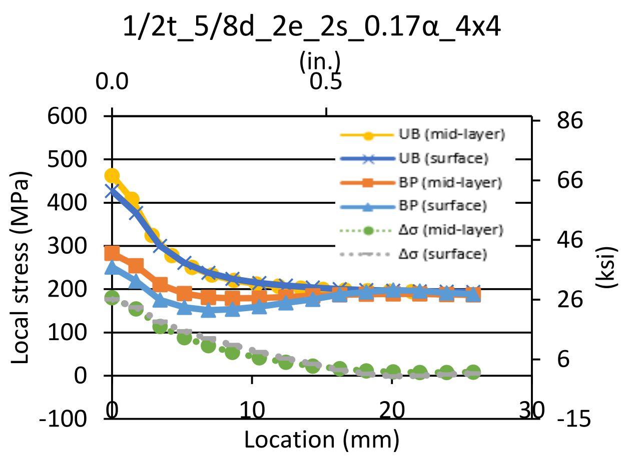

(c) 50.8mm [2 in.] edge distance

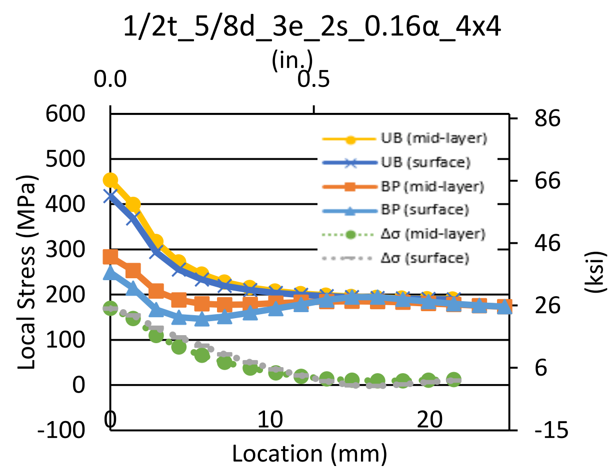

(d) 76.2 mm [3 in.] edge distance

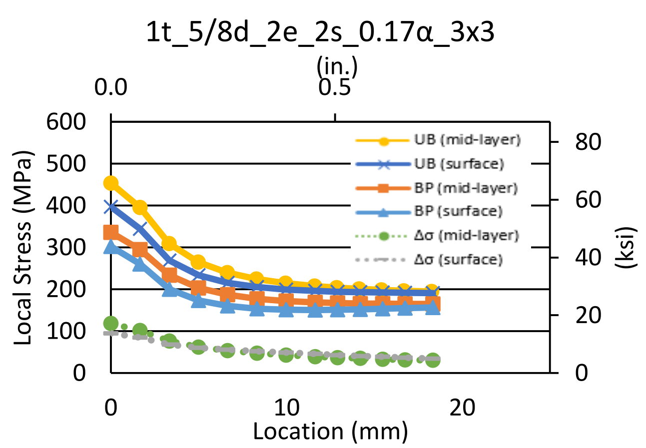

(e) 50.8mm [2 in.] edge distance

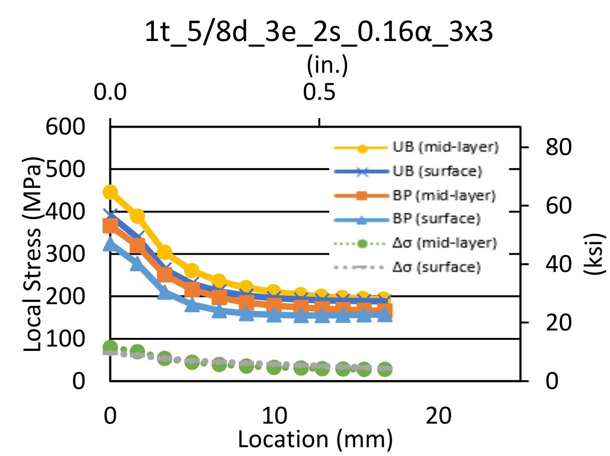

(f) 76.2 mm [3 in.] edge distance

Figure E. 1 Comparison of Stress Distribution with Different Edge Distances

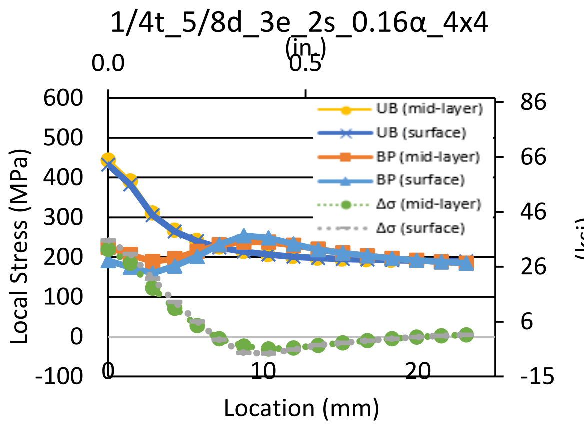

(a) 50.8mm [2 in.] bolt spacing

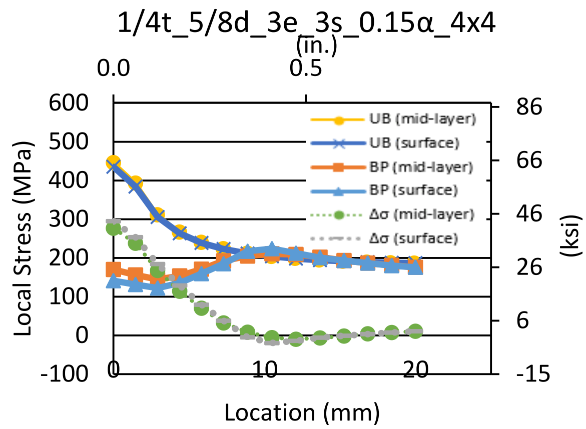

(b) 76.2 mm [3 in.] bolt spacing

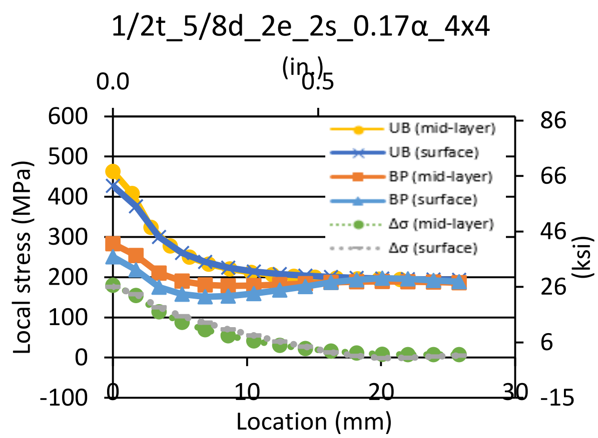

(c) 50.8mm [2 in.] bolt spacing

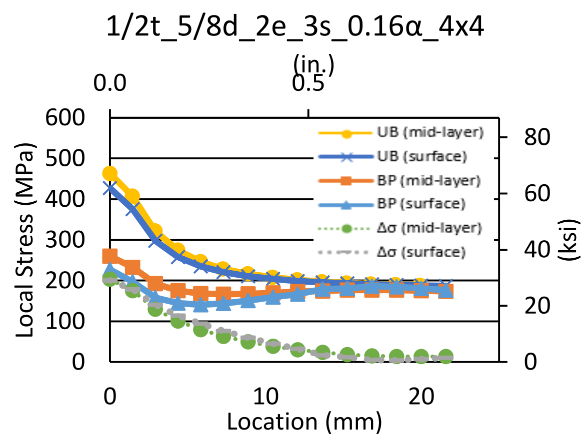

(d) 76.2 mm [3 in.] bolt spacing

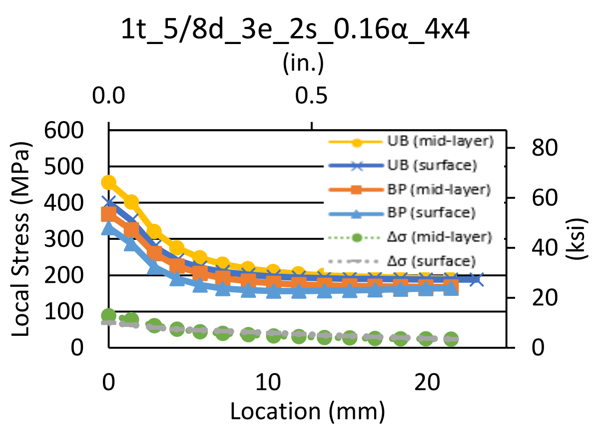

(e) 50.8mm [2 in.] bolt spacing

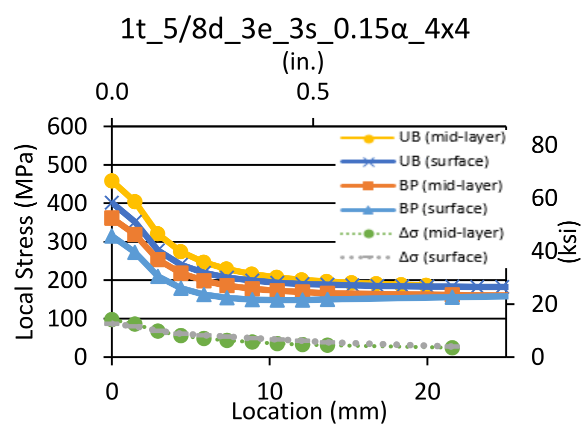

(f) 76.2 mm [3 in.] bolt spacing

Figure E. 2: Comparison of Stress Distribution with Different Bolt Spacing

APPENDIX F CHANGE IN STRESS VS. VARIABLES

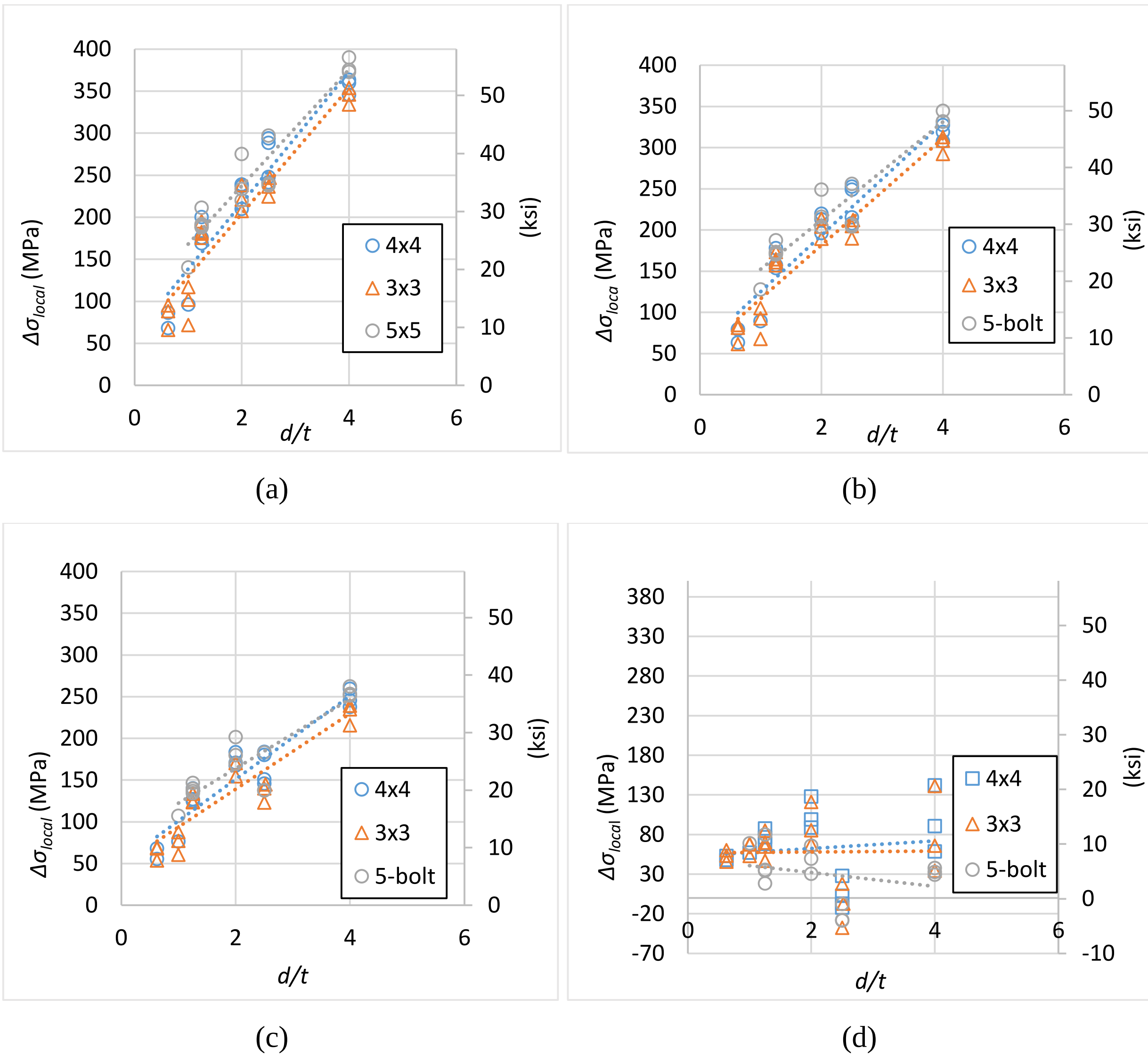

Figure F. 1 The $\Delta\sigma_{local}$ versus *d/t* at different distances away from bolt hole: (a) distance = at hole edge; (b) distance = one element from hole edge; (c) distance = two elements from hole edge; (d) σ_{local} = σ_{nom}

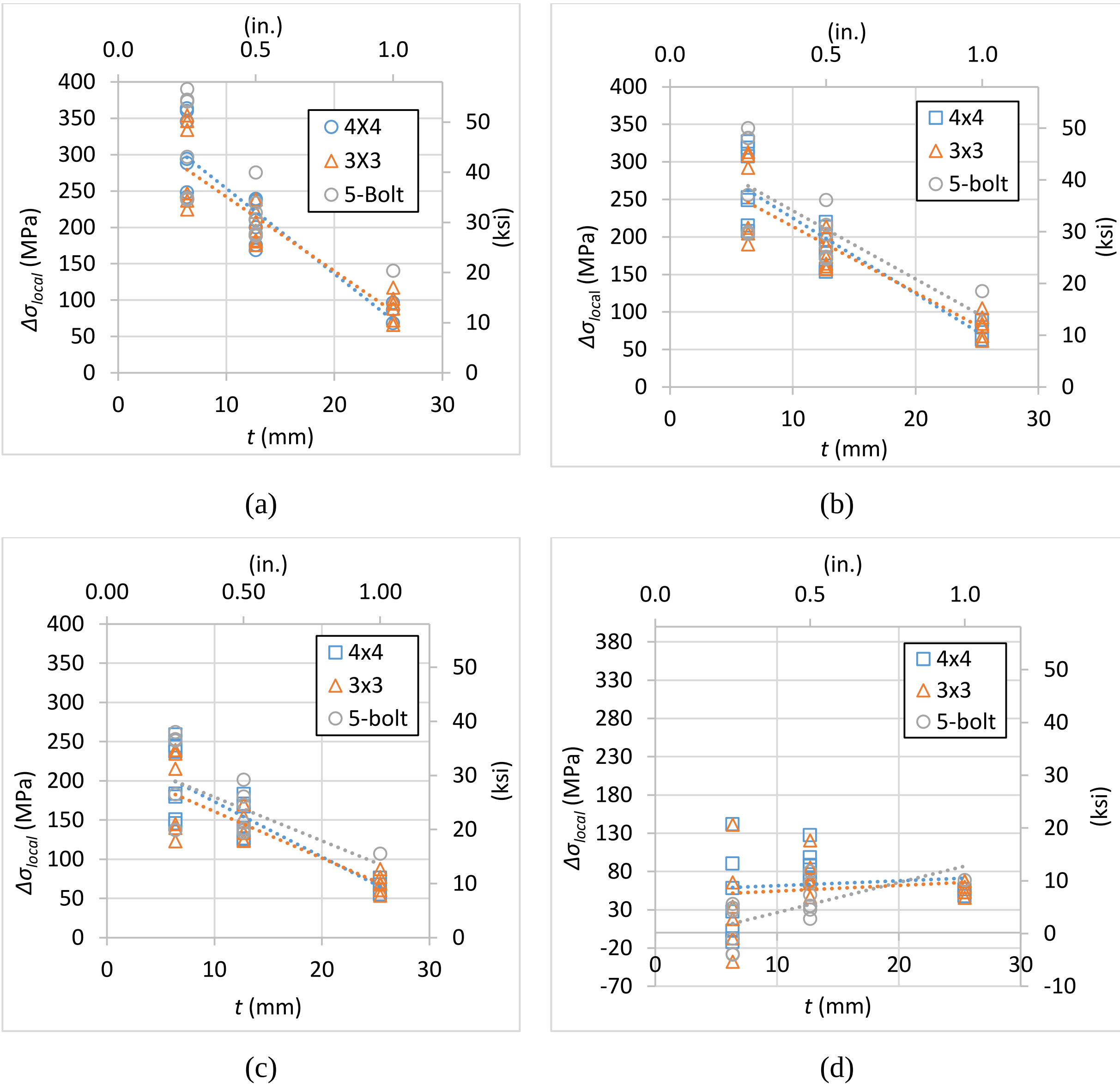

Figure F. 2: The $\Delta\sigma_{local}$ versus t at different distances away from bolt hole: (a) distance = at hole edge; (b) distance = one element from hole edge; (c) distance = two elements from hole edge; (d) σ_{local} = σ_{nom}

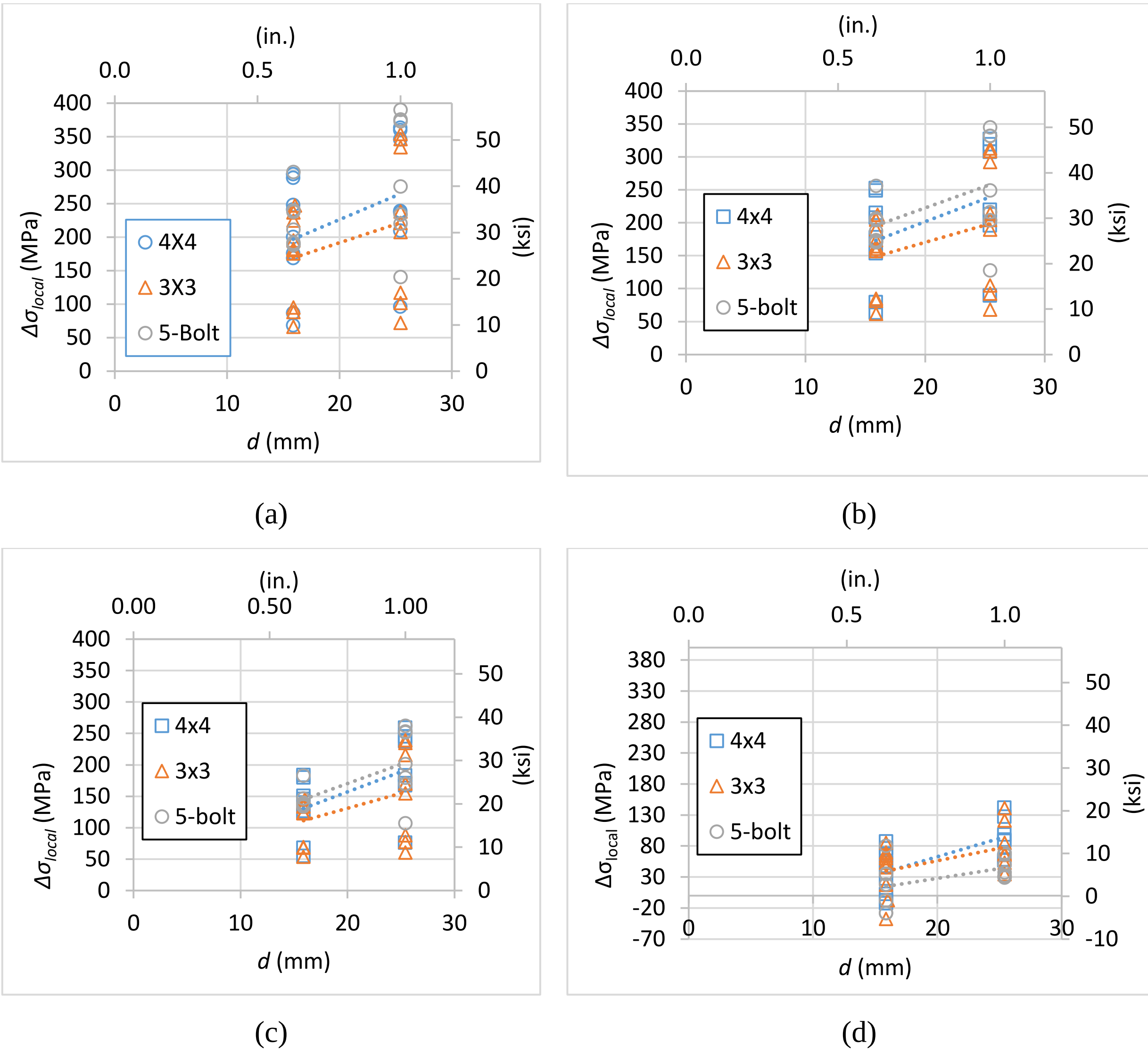

Figure F. 3: The $\Delta\sigma_{local}$ versus d at different distances away from bolt hole: (a) distance = at hole edge; (b) distance = one element from hole edge; (c) distance = two elements from hole edge; (d) σ_{local} = σ_{nom}

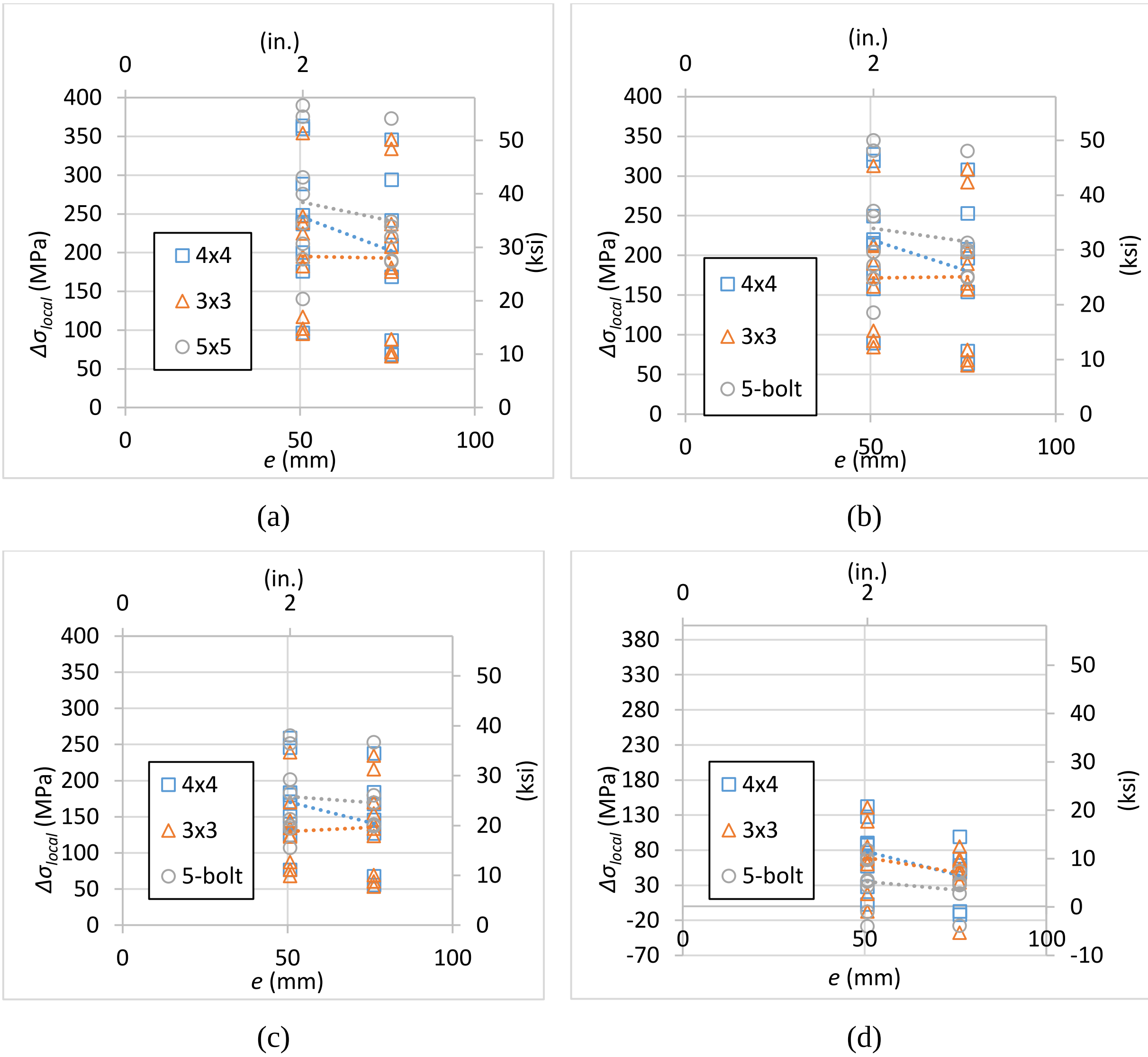

Figure F. 4: The $\Delta\sigma_{local}$ versus e at different distances away from bolt hole: (a) distance = at hole edge; (b) distance = one element from hole edge; (c) distance = two elements from hole edge; (d) σ_{local} = σ_{nom}

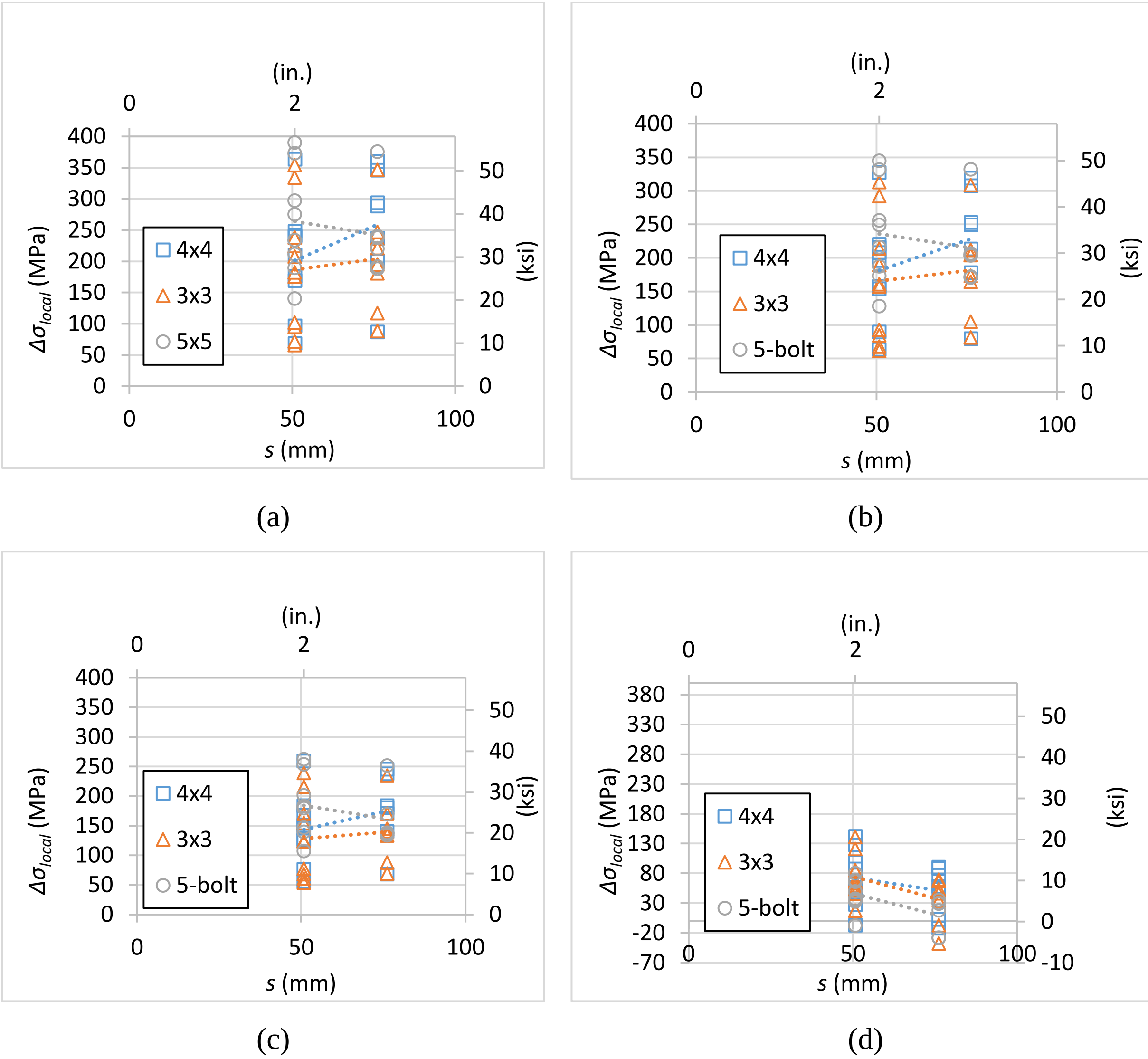

Figure F. 5: The $\Delta\sigma_{local}$ versus s at different distances away from bolt hole: (a) distance = at hole edge; (b) distance = one element from hole edge; (c) distance = two elements from hole edge; (d) σ_{local} = σ_{nom}

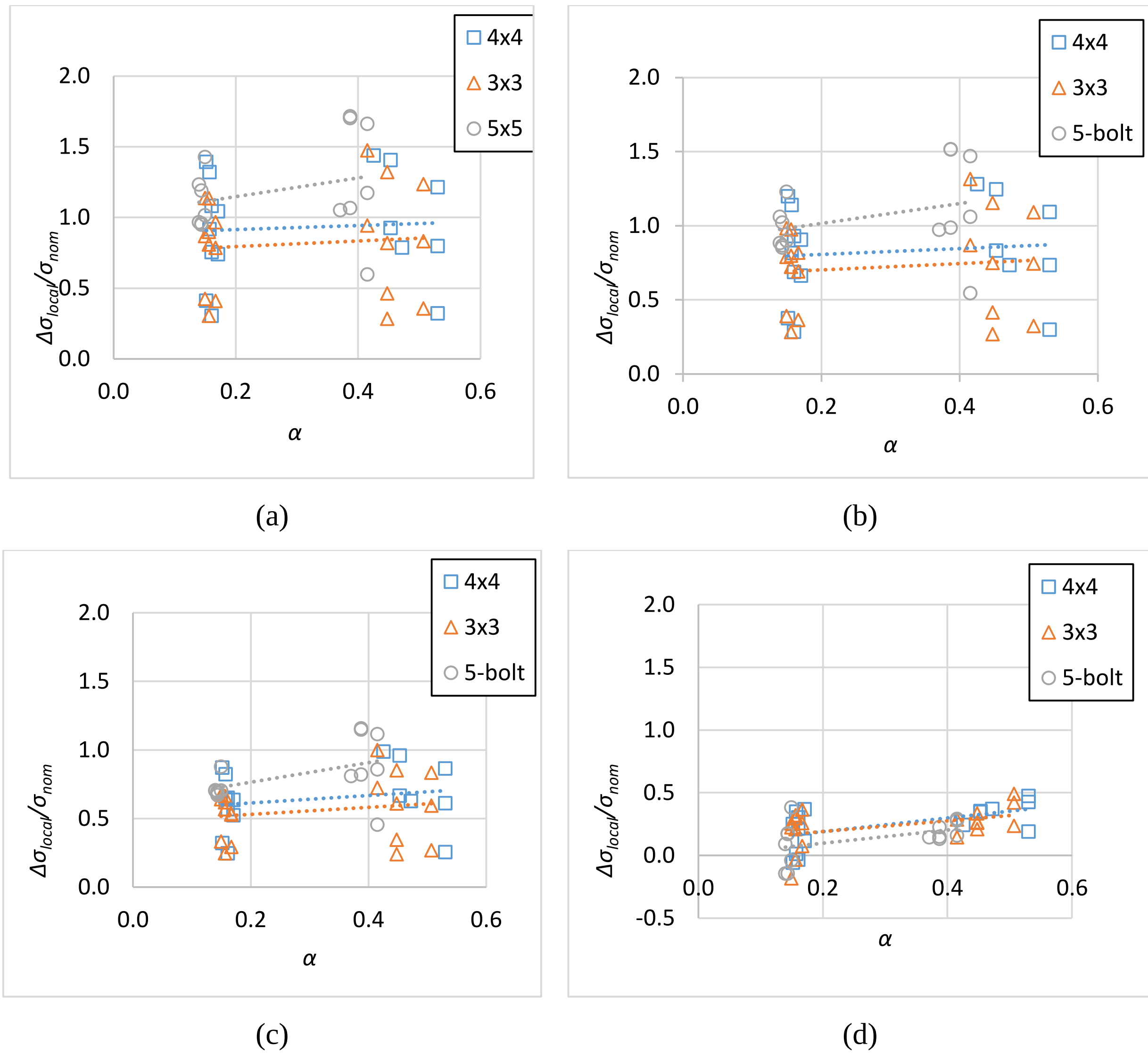

Figure F. 6: The $\Delta\sigma_{local}/\sigma_{nom}$ versus α at different distances away from bolt hole: (a) distance = at hole edge; (b) distance = one element from hole edge; (c) distance = two elements from hole edge; (d) $\sigma_{local} = \sigma_{nom}$

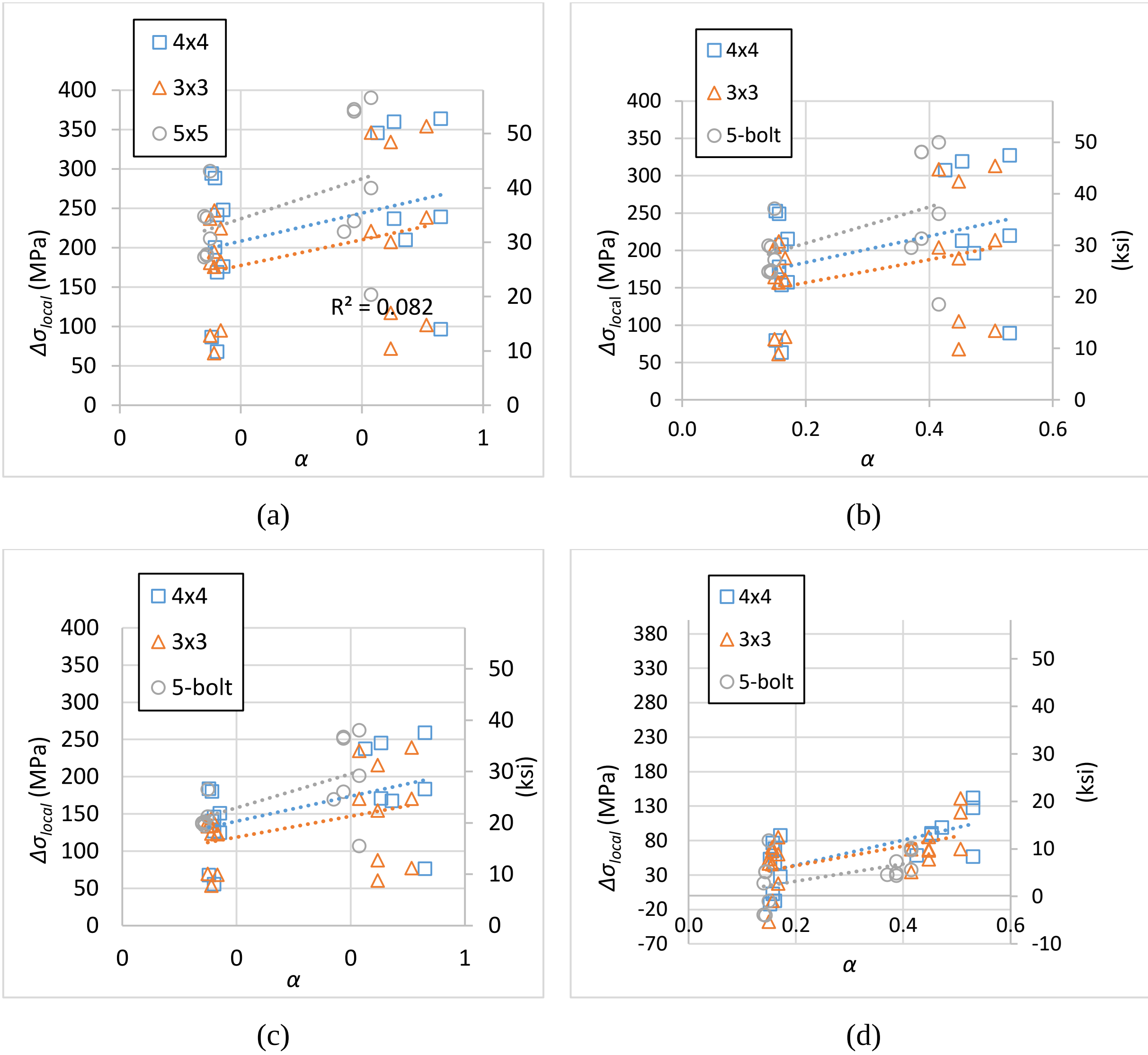

Figure F. 7: The $\Delta\sigma_{local}$ versus α at different distances away from bolt hole: (a) distance = at hole edge; (b) distance = one element from hole edge; (c) distance = two elements from hole edge; (d) σ_{local} = σ_{nom}

APPENDIX G SPSS OUTPUT

The column highlighted in green show the independent variables: *t* (plate thickness), *d* (bolt diameter), *e* (edge distance) and *s* (bolt spacing), and the dependent stress variable, $\Delta\sigma_{local}/\sigma_{nom}$. The goal of the statistical analysis was to determine which independent variables had the greatest influence on $\Delta\sigma_{local}/\sigma_{nom}$.

Table G. 1: SPSS output: relative influence on $\Delta\sigma_{local}/\sigma_{nom}$

Model	Unstandardized Coefficients		Standardized Coefficients	t	Sig.	Correlations		
	B	Std. Error	Beta			Zero-order	Partial	Part
(Constant)	1.059	0.193		5.483	0			
t	-1.221	0.08	-0.89	-15.277	0	-0.901	-0.917	-0.87
d	0.403	0.118	0.20	3.405	0.001	0.162	0.457	0.19
e	-0.007	0.044	-0.01	-0.156	0.877	-0.062	-0.024	-0.01
s	0.087	0.045	0.11	1.938	0.059	0.23	0.28	0.11

a. Dependent Variable: Δσ/σnom

Table G. 2. SPSS Output: relative influence on $\Delta\sigma_{local}/\sigma_{nom}$

Model		Unstandardized Coefficients		Standardized Coefficients	t	Sig.	Correlations		
		B	Std. Error	Beta			Zero-order	Partial	Part
1	(Constant)	0.274	0.055		5.008	0			
	d/t	0.191	0.038	0.56	5.047	0	0.873	0.601	0.32
	e/t	0.01	0.015	0.09	0.674	0.503	0.8	0.1	0.04
	s/t	0.035	0.014	0.32	2.606	0.012	0.824	0.362	0.17

a. Dependent Variable: $\Delta\sigma/\sigma_{nom}$

Table G. 3. SPSS Output: relative influence on $\Delta\sigma_{local}/\sigma_{nom}$ with normalized independent variables

Model		Unstandardized Coefficients		Standardized Coefficients	t	Sig.	Correlations		
		B	Std. Error	Beta			Zero-order	Partial	Part
1	(Constant)	1.284	0.098		13.077	0			
	t/d	-0.878	0.073	-0.91	-11.954	0	-0.859	-0.872	-0.84
	e/d	0.019	0.035	0.05	0.545	0.589	-0.181	0.081	0.04
	s/d	0.061	0.032	0.17	1.874	0.068	0.03	0.269	0.13

a. Dependent Variable: $\Delta\sigma/\sigma_{nom}$

Table G. 4: SPSS Output: relative influence on $\Delta\sigma_{local}$ vs. independent variables normalized by *d*

Model		Unstandardized Coefficients		Standardized Coefficients	t	Sig.	Correlations		
		B	Std. Error	Beta			Zero-order	Partial	Part
1	(Constant)	52.244	3.125		16.716	.000			
	t/d	-28.821	2.338	-.881	-12.328	.000	-.895	-.878	-.818
	e/d	-.637	1.120	-.051	-.569	.573	-.359	-.084	-.038
	s/d	.331	1.030	.027	.322	.749	-.168	.048	.021

a. Dependent Variable: $\Delta\sigma$

Table G. 5: SPSS Output: relative influence on $\Delta\sigma_{local}$ vs. independent variables normalized by *t*

Model		Unstandardized Coefficients		Standardized Coefficients	t	Sig.	Correlations		
		B	Std. Error	Beta			Zero-order	Partial	Part
1	(Constant)	9.278	1.366		6.793	.000			
	d/t	10.831	.946	.928	11.446	.000	.948	.863	.534
	e/t	-.344	.386	-.085	-.892	.377	.749	-.132	-.042
	s/t	.427	.339	.114	1.257	.215	.759	.184	.059

a. Dependent Variable: $\Delta\sigma$

Table G. 6: SPSS Output: relative influence on $\Delta\sigma_{local}$ vs. independent variables normalized by *e*

Model		Unstandardized Coefficients		Standardized Coefficients	t	Sig.	Correlations		
		B	Std. Error	Beta			Zero-order	Partial	Part
1	(Constant)	27.760	2.668		10.403	.000			
	t/e	-97.447	5.193	-.929	-18.765	.000	-.761	-.942	-.889
	d/e	69.099	6.371	.576	10.846	.000	.322	.850	.514
	s/e	1.580	2.350	.034	.672	.505	.185	.100	.032

a. Dependent Variable: Δσ

Table G. 7: SPSS Output: relative influence on $\Delta\sigma_{local}$ vs. independent variables normalized by *s*

Model		Unstandardized Coefficients		Standardized Coefficients	t	Sig.	Correlations		
		B	Std. Error	Beta			Zero-order	Partial	Part
1	(Constant)	35.876	2.662		13.480	.000			
	t/s	-91.198	5.132	-.957	-17.771	.000	-.816	-.936	-.879
	d/s	60.700	6.468	.528	9.385	.000	.170	.814	.464
	e/s	-4.405	2.547	-.098	-1.729	.091	-.194	-.250	-.086

a. Dependent Variable: Δσ

Table G. 8: SPSS Output: relative influence on $\Delta\sigma_{local}/\sigma_{nom}$ vs. independent variables normalized by *d*

Model		Unstandardized Coefficients		Standardized Coefficients	t	Sig.	Correlations		
		B	Std. Error	Beta			Zero-order	Partial	Part
1	(Constant)	1.284	.098		13.077	.000			
	t/d	-.878	.073	-.909	-11.954	.000	-.859	-.872	-.843
	e/d	.019	.035	.052	.545	.589	-.181	.081	.038
	s/d	.061	.032	.168	1.874	.068	.030	.269	.132

a. Dependent Variable: Δσ/σnom

Table G. 9: SPSS Output: relative influence on $\Delta\sigma_{local}/\sigma_{nom}$ vs. independent variables normalized by *t*

Model		Unstandardized Coefficients		Standardized Coefficients	t	Sig.	Correlations		
		B	Std. Error	Beta			Zero-order	Partial	Part
1	(Constant)	.274	.055		5.008	.000			
	d/t	.191	.038	.555	5.047	.000	.873	.601	.319
	e/t	.010	.015	.087	.674	.503	.800	.100	.043
	s/t	.035	.014	.322	2.606	.012	.824	.362	.165

a. Dependent Variable: $\Delta\sigma/\sigma_{nom}$

Table G. 10: SPSS Output: relative influence on $\Delta\sigma_{local}/\sigma_{nom}$ vs. independent variables normalized by *e*

Model		Unstandardized Coefficients		Standardized Coefficients	t	Sig.	Correlations		
		B	Std. Error	Beta			Zero-order	Partial	Part
1	(Constant)	.947	.103		9.169	.000			
	t/e	-2.854	.201	-.921	-14.195	.000	-.814	-.904	-.881
	d/e	1.194	.247	.337	4.842	.000	.129	.585	.301
	s/e	.209	.091	.153	2.295	.026	.216	.324	.143

a. Dependent Variable: Δσ/σnom

Table G. 11: SPSS Output: relative influence on $\Delta\sigma_{local}/\sigma_{nom}$ vs. independent variables normalized by *s*

Model		Unstandardized Coefficients		Standardized Coefficients	t	Sig.	Correlations		
		B	Std. Error	Beta			Zero-order	Partial	Part
1	(Constant)	1.231	.098		12.604	.000			
	t/s	-2.707	.188	-.962	-14.371	.000	-.870	-.906	-.884
	d/s	.984	.237	.290	4.145	.000	-.032	.526	.255
	e/s	-.014	.093	-.011	-.153	.879	-.212	-.023	-.009

a. Dependent Variable: Δσ/σnom

Table G. 12: SPSS Output: relative influence on $\Delta\sigma_{local}/\sigma_{nom\_Agro}$ vs. independent variables normalized by *d*

Model		Unstandardized Coefficients		Standardized Coefficients	t	Sig.	Correlations		
		B	Std. Error	Beta			Zero-order	Partial	Part
1	(Constant)	2.090	.125		16.725	.000			
	t/d	-1.153	.093	-.881	-12.338	.000	-.895	-.879	-.818
	e/d	-.026	.045	-.051	-.570	.571	-.360	-.085	-.038
	s/d	.013	.041	.027	.319	.751	-.169	.048	.021

a. Dependent Variable: $\Delta\sigma/\sigma_{nom\_Agro}$

Table G. 13: SPSS Output: relative influence on $\Delta\sigma_{local}/\sigma_{nom\_Agro}$ vs. independent variables normalized by *t*

Model		Unstandardized Coefficients		Standardized Coefficients	t	Sig.	Correlations		
		B	Std. Error	Beta			Zero-order	Partial	Part
1	(Constant)	.371	.055		6.770	.000			
	d/t	.433	.038	.927	11.423	.000	.948	.862	.534
	e/t	-.014	.015	-.086	-.899	.373	.749	-.133	-.042
	s/t	.017	.014	.115	1.265	.212	.759	.185	.059

a. Dependent Variable: $\Delta\sigma/\sigma_{nom\_Agro}$

Table G. 14: SPSS Output: relative influence on $\Delta\sigma_{local}/\sigma_{nom\_Agro}$ vs. independent variables normalized by *e*

Model		Unstandardized Coefficients		Standardized Coefficients	t	Sig.	Correlations		
		B	Std. Error	Beta			Zero-order	Partial	Part
1	(Constant)	1.110	.107		10.401	.000			
	t/e	-3.900	.208	-.929	-18.782	.000	-.761	-.942	-.889
	d/e	2.765	.255	.576	10.856	.000	.322	.851	.514
	s/e	.064	.094	.034	.676	.503	.185	.100	.032

a. Dependent Variable: Δσ/σnom_Agro

Table G. 15: SPSS Output: relative influence on $\Delta\sigma_{local/}\ \sigma_{nom\_Agro}$ vs. independent variables normalized by *s*

Model		Unstandardized Coefficients		Standardized Coefficients			Correlations		
		B	Std. Error	Beta	t	Sig.	Zero-order	Partial	Part
1	(Constant)	1.435	.107		13.453	.000			
	t/s	-3.649	.206	-.957	-17.746	.000	-.816	-.935	-.879
	d/s	2.429	.259	.528	9.372	.000	.170	.813	.464
	e/s	-.176	.102	-.098	-1.726	.091	-.194	-.249	-.085

a. Dependent Variable: $\Delta\sigma/\sigma_{nom\_Agro}$